



**EFFECT OF DIFFERENT SURFACTANT MIXTURES ON THE STABILISATION
MECHANISM OF HIGHLY CONCENTRATED WATER-IN-OIL EMULSIONS**

by

NEDA SANATKARAN

Thesis submitted in fulfilment of the requirements for the degree

Doctor of Technology: Chemical Engineering

in the Faculty of Engineering

at the Cape Peninsula University of Technology

Supervisor: Prof I. Masalova

Cape Town

November 2014

CPUT copyright information

The thesis may not be published either in part (in scholarly, scientific or technical journals), or as a whole (as a monograph), unless permission has been obtained from the University

CONFIDENTIALITY

All information presented in this thesis is classified as highly confidential and is prohibited for publishing without permission from AEL Mining Services.

DECLARATION

I, Neda Sanatkaran, declare that the contents of this thesis represent my own unaided work, and that the thesis has not previously been submitted for academic examination towards any qualification. Furthermore, it represents my own opinions and not necessarily those of the Cape Peninsula University of Technology.

**08/12/2014**

Signed

Date

ABSTRACT

The subject of this investigation was a highly concentrated water-in-oil emulsion (HCE), explosive grade, with volume fraction of approximately 88 vol%, wherein the dispersed phase was comprised of a super-cooled solution of inorganic salts. Explosive emulsions are thermodynamically unstable compounds and this instability is related to crystallisation in the dispersed phase, which is a supersaturated solution (>75 wt%) of an oxidiser (e.g. ammonium nitrate salt (AN) in water). Slow crystallisation of droplets can occur during shelf life storage, transportation and application, thereby suppressing the sensitivity of the emulsion to detonation. The structure of these emulsions with respect to their stability has been studied and their rheological properties have been well described.

Explosive emulsions are commonly stabilised by poly (isobutylene) succinic anhydride (PIBSA)-based surfactants that provide optimal shelf life stability, but become unstable during high shear conditions. This adversely affects the quality of these emulsions during their transportation through long hosepipes, as occurs in the relevant industry. Other issues associated with the use of PIBSA surfactants include long refinement times required, which increase the energy costs to form stable explosive emulsion.

The trend of using surfactant mixtures to provide overall stability, both during shelf life and high shear, has grown in recent years. Among other advantages of this approach are associated economic benefits, and improved safety and technological properties of emulsions. The choice of co-surfactants depends on the nature of the components of the emulsion and is mainly empirically-based. The key concept is using synergetic binary surfactant systems, which may impact on the stability and properties of the emulsions. This study presents results from such an investigation, bearing in mind that the emulsion performance depends on the fundamental physicochemical properties of the mixed surfactants. Initially, two groups of surfactants (block copolymers named Pluronics and water soluble surfactants named Tweens), as well as their combination with a PIBSA-based surfactant (PIBSA-Mea) and sorbitan monooleate (SMO) were selected to stabilise HCEs. Pluronics, when combined with PIBSA-Mea and SMO, were unsuccessful in forming stable emulsions, while the emulsions consisting of PIBSA-Mea/water soluble surfactants showed acceptable stability. Attempts at dissolving water-soluble surfactants in the aqueous phase were unsuccessful. This was attributed to the salting-out effect of Tweens in the presence of large quantities of AN in the water phase. In the current study, the water soluble surfactants were successfully dissolved in the oil phase containing industrial grade oil (Ash-H).

The stability and interfacial behaviour of one the most stable novel emulsions, stabilised by PIBSA-Mea/water soluble surfactants (Tween 80), and developed during this study, was then compared to the current standard industrial explosive formulation (PIBSA/SMO). Results showed an acceptable stability of the new emulsion formulation in both shelf life and under high shear. More interestingly, it was observed that there were markedly different interfacial behaviours of PIBSA-Mea/water soluble Tween 80 and PIBSA-Mea/oil soluble SMO at the water-oil interface over a wide range of surfactant/co-surfactant ratios.

Based on the results obtained from the aforementioned comparative studies, a series of non-ionic oil-soluble (Spans) and water-soluble (Tweens) compounds with systematically varying structure (length, presence of double bonds and number) of hydrophobic tails were identified and subsequently mixed with PIBSA-Mea. This was done in order to elucidate the effect of compatibility and synergism between PIBSA and co-surfactant, with particular reference to the interface to stability under shear and on-shelf of final explosive emulsions. An investigation of the effect/s of co-surfactant structure on interfacial properties at the water-oil interface was performed. The Rosen method was used to characterise synergism between the two surfactants. This was correlated with the stability on shelf and under shear as well as with the rheological properties/pumpability of the novel manufactured emulsions. The degree of synergism (interaction parameter) for PIBSA-Mea/Spans decreased, with a corresponding decrease in the length of alkyl tails, as well as the presence of a double bond in tail. There was a major antagonism noted for PIBSA-Mea/multi tails Span mixtures. In all the PIBSA-Mea/Tweens mixtures the opposite effect of tail length on interaction parameter was observed. However, the effect of tail structure on synergism was less pronounced for the Tweens group than it was for Spans.

Emulsification was markedly more rapid for the PIBSA-Mea/water soluble Tweens mixtures, and an improved stability on shelf and under high shear was recorded for this group when compared to PIBSA-Mea/Span mixtures. In the current study, depending on the structure of the surfactant, it was shown that synergism between the surfactant and co-surfactant is one of the major factors in determining stability of the emulsions. In addition, the influence of the chemical structure of co-surfactants on the rheological properties of the emulsions was studied. Higher pumpability of the explosive emulsions stabilised with water soluble Tween is attributed to a lower yield stress of the PIBSA-Mea/Tweens emulsions, compared to the PIBSA-Mea/Spans emulsions.

Finally, the partial replacement of PIBSA by certain suitable water-soluble Tweens offers a cost-effective, easily available and environmentally friendly alternate. Additionally, such a system could provide acceptable stability for different technological applications associated with emulsions, including droplet refinement during emulsion production, adequate long-term storage and acceptable pumping characteristics of these mixtures. Overall, this would reduce the cost of the final product on an industrial scale.

PUBLICATIONS

- Sanatkaran, N. & Masalova, I. 2015. Interfacial behavior of oil/oil and oil/water soluble binary surfactants and their effect on stability of highly concentrated W/O emulsions, *Colloid Journal*, 77:77-81.
- Sanatkaran, N., Masalova, I. & Malkin, A. 2014. Effect of surfactant on interfacial film and stability of highly concentrated emulsions stabilized by various binary surfactant mixtures, *Colloids and Surfaces A: Physicochemical and Engineering Aspects*, 461:77-81.
- Sanatkaran, N. & Masalova, I. 2014. Effect of surfactant structure on interfacial film and stability of highly concentrated emulsions with supersaturated dispersed phase, *Proceedings of the 5th South African Society of rheology Cconference (SASOR 2014)*, Stellenbosch, South Africa. 7-12.
- Sanatkaran, N. & Masalova, I. 2013. Synergism between a polymeric surfactant and various nonionic sorbitan and polyoxyethylene derivatives of fatty acid ester surfactants at the water-oil interface, *Proceedings (peer-reviewed) of the 13th Chemical Engineering and Technology Cconference (CHEMTECh'13)*, Istanbul, Turkey. 17-24.

ACKNOWLEDGEMENTS

Undertaking this PhD has been a truly life-changing experience for me and it would not have been possible without the support and guidance received from many people, to whom I am greatly indebted.

- I express my sincere gratitude to my advisor, Prof. Irina Masalova, for the continuous support of my PhD studies and research, for her patience, motivation, enthusiasm, and immense knowledge. Her guidance helped me throughout both the research for, and writing of, this thesis.
- I extend my gratitude to AEL Mining Services for providing the materials used to manufacture emulsions for the investigation. Furthermore, the research reported on here would have not been possible without financial support received from AEL.
- Thanks are due to Prof. Alexander Yakovlevich Malkin for his professional and useful comments with regard to my research.
- I am sincerely appreciative of my laboratory supervisor, Mr Nazeem George, for his assistance and for providing a pleasant and safe environment in which to conduct my research.
- I am indebted to my former colleague, Dr Reza Foudazi, and my fellow laboratory colleagues of the Rheology Research Group, Steve Tshilumbu and Emil Mamedov, for their stimulating discussions and support throughout my work. I am grateful to the Flow Process Research Centre at the Cape Peninsula University of Technology for providing me with the opportunity to participate in this internationally-recognised research unit. Their support is gratefully acknowledged.
- Special thanks go to my Uncle Mahdi and my Auntie Hamideh. Without them I would never have started this wonderful experience in South Africa.
- Last but not least, I would like to thank my family: my respective parents and my lovely brothers, Emad and Foad, for supporting me spiritually throughout my life and always believing in me and encouraging me to follow my dreams.

DEDICATION

This thesis is dedicated to my parents for their love, endless support and encouragement.

TABLE OF CONTENTS

CONFIDENTIALITY	i
ABSTRACT	iii
PUBLICATIONS.....	vi
TABLE OF CONTENTS.....	ix
LIST OF FIGURES.....	xii
LIST OF TABLES	xxi
GLOSSARY	xxiii
NOMENCLATURE	xxvi
ACRONYMS.....	xxviii
CHAPTER ONE: INTRODUCTION.....	1
CHAPTER TWO: THEORY AND LITERATURE REVIEW	10
2.1 INTRODUCTION	10
2.2 EMULSIONS.....	10
2.2.1 General definition.....	10
2.3 HIGHLY CONCENTRATED W/O EMULSIONS (EXPLOSIVE GRADE).....	12
2.4 STABILITY OF EMULSIONS.....	12
2.4.1 Instability aspects.....	12
2.4.2 Factors affecting emulsion stability	13
2.4.3 Instability of explosive emulsions	15
2.5 EMULSIFYING AGENTS.....	16
2.5.1 Solid particles	16
2.5.2 Ionic materials	17
2.5.3 Surfactants	17
2.5.4 Surfactants used to stabilise explosive emulsions	20
2.6 INTERFACIAL PROPERTIES OF EMULSIONS	25
2.6.1 Interfacial tension	26
2.6.2 Measuring interfacial tension: Wilhelmy plate method	27
2.6.3 Laplace pressure.....	27
2.6.4 Contact angle	28
2.6.5 Film thickness and disjoining pressure.....	28
2.6.6 Interaction energies (forces) between droplets	29
2.6.7 Molecular interactions in binary surfactant systems.....	32
2.7 EMULSIFICATION.....	36
2.7.1 Effect of surfactant structure on emulsification.....	39

2.7.2	Droplet size and droplet size distribution.....	41
2.7.3	Evolution of droplet size and droplet size distribution in highly concentrated emulsions (HCEs).....	42
2.8	RHEOLOGICAL PROPERTIES.....	44
2.8.1	Viscoelasticity.....	46
2.8.2	Flow properties.....	48
2.8.3	Effect of surfactant structure on rheological properties of HCEs.....	50
2.9	SUMMARY.....	51
	CHAPTER THREE: MATERIALS AND METHODS	53
3.1	INTRODUCTION	53
3.2	MATERIALS AND MATRIX OF SAMPLES	53
3.2.1	Material and Matrix of Samples Used for Feasibility Study.....	53
3.2.2	Material and matrix of samples used for the main core of the study.....	58
3.3	METHODS	65
3.3.1	Interfacial tension measurements	65
3.3.2	Interfacial elasticity measurements	66
3.3.3	Droplet size analysis	67
3.3.4	Microscopic observation.....	67
3.3.5	Rheological analysis.....	68
3.3.6	Pumping of mixtures.....	69
	CHAPTER FOUR: FEASIBILITY STUDY.....	71
4.1	INTRODUCTION	71
4.2	BACKGROUND	71
4.3	INTRODUCTION OF VARIOUS SURFACTANT TYPES TO STABILISE HIGHLY CONCENTRATED W/O EMULSIONS.....	74
4.3.1	Experiments and Results	75
4.4	COMPARISON OF THE STABILITY OF EXPLOSIVE EMULSIONS STABILISED WITH PIBSA-MEA/TWEEN 80 and PIBSA-MEA/SPAN 80	81
4.4.1	Emulsification	81
4.4.2	High Shear Condition	82
4.4.3	Ageing.....	83
4.4.4	Interfacial study	84
4.5	SUMMARY.....	86
	CHAPTER FIVE: EFFECT OF CO-SURFACTANT STRUCTURE ON THE EMULSIFICATION PROCESS, INTERFACIAL AND RHEOLOGICAL PROPERTIES, SHELF LIFE AND STABILITY UNDER HIGH SHEAR OF EXPLOSIVE EMULSIONS.....	87

5.1	INTRODUCTION	87
5.2	EXPERIMENTS AND RESULTS	87
5.2.1	Interfacial Properties	87
5.2.2	Emulsification	99
5.2.3	Rheological properties.....	107
5.2.4	Stability under high shear.....	121
5.2.5	Ageing	125
	CHAPTER SIX: SUMMARY AND CONCLUSION.....	132
▪	Recommendations for future research.....	137
	BIBLIOGRAPHY	138
	APPENDIX A: CHOICE OF SURFACTANT	156
	Interfacial Tension	156
	Evolution of droplet size over time.....	160
	APPENDIX B: EFFECT OF SURFACTANT STRUCTURE ON INTERFACIAL PROPERTIES.....	162
	APPENDIX C: EFFECT OF SURFACTANT STRUCTURE ON REFINEMENT TIME	167
	APPENDIX D: EFFECT OF SURFACTANT STRUCTURE ON RHEOLOGICAL PROPERTIES OF THE EMULSIONS	171
	Determination of yield stress of the fresh emulsions using Foudazi model	171
	Viscoelasticity	176
	APPENDIX E: EFFECT OF SURFACTANT STRUCTURE ON SHERA STABILITY OF THE EMULSIONS UNDER HIGH SHEAR CONDITION.....	180
	Droplet size distribution (DSD) as a function of pumping cycles (NP).....	180
	Evolution of droplet size under high shear (pumping) with pumping cycles (NP).....	183

LIST OF FIGURES

Figure 1.1: Photomicrographs of freshly prepared liquid explosive (left) and crystallised liquid explosive (right). Scale bar, 50 μm = 6 mm.	2
Figure 1.2: Application of explosive emulsions underground	2
Figure 2.1: Different types of emulsions a) O/W, b) W/O, c) W/O/W, d) O/W/O (Bouyer <i>et al.</i> , 2012).....	11
Figure 2.2: Microscopic images of dilute (a) and highly concentrated (b) emulsions (Foudazi <i>et al.</i> , 2011).....	11
Figure 2.3: Instabilities of emulsions (Bouyer <i>et al.</i> , 2012).....	13
Figure 2.4: Microscopic images of a concentrated emulsion where the droplet deformation at compression is shown. Taken in the Rheology laboratories at the Cape Peninsula University of Technology	15
Figure 2.5: The typical structure of a surfactant (aceyourchemistry.blogspot.com)	17
Figure 2.6: Schematic of monomeric and polymeric surfactants films (www.skin-care-forum.basf.com).....	18
Figure 2.7: The aggregation of the surfactants controlled by critical packing parameter (McClements, 2005)	19
Figure 2.8: Oleic acid.....	20
Figure 2.9: Sorbitan monooleate	21
Figure 2.10: Substituted oxazoline (R represents an unsaturated hydrocarbon tail derived from unsaturated fatty acid, preferably oleic acid) (Sudweeks & Jessop, 1979)	22
Figure 2.11: Hydrocarbyl polyamine (PIB) (Cechanski, 1997).....	22
Figure 2.12: A conjugated diene wherein R ⁱ is either a hydrogen or hydrocarbyl group (Coolbaugh and Mahamat, 2003).....	23
Figure 2.13: Variation of interfacial tension versus log concentration of surfactant in bulk at the water-oil interface (www.particlesciences.com).....	26
Figure 2.14: Schematic of contact angles formed by oil drops on a solid surface (Yuan & Lee, 2013).....	28
Figure 2.15: Liquid film between two neighbouring liquid drops	29
Figure 2.16: A schematic representation of the electrically charged double layer of a charged particle (Substech.com).....	31
Figure 2.17: A schematic representation of steric stabilization (R=radius) (home.unist.ac.kr)	32

Figure 2.18: A schematic diagram of droplet break-up and re-coalescence during the emulsification process (Walstra, 1993).....	37
Figure 2.19: Grace curve (1982) showing the influence of the viscosity ratio on the capillary number in shear flow (Tropea <i>et al.</i> , 2007).....	38
Figure 2.20: Droplet disruption and stabilisation in emulsification with and without surfactant (Brösel & Schubert, 1999)	39
Figure 2.21: Typical Gauss for explosive emulsions with different sauter droplet sizes and stabilised by PIBSA-Mea (Mudeme <i>et al.</i> , 2010).....	43
Figure 2.22: Evolution of the average diameter of droplets during prolonged shearing for EEs stabilised with 8 and 14% PIBSA-Mea. The same trend can be observed for the range of droplet size distribution (Mudeme <i>et al.</i> , 2010).....	43
Figure 2.23: Schematic diagram of the structure of droplets in emulsions within in a range of 0 to 1 volume fractions (Mason, 1999)	44
Figure 2.24: Schematic logarithmic diagram of the steady shear stress, τ , versus shear rate for HCEs (solid line). By increasing the shear rate, τ exceeds the yield stress value where viscous behaviour is dominant. As soon as τ attains the Laplace pressure scale (σ/a) the droplets deform, stretch and rupture (dashed line) and depending on interfacial properties may also re-coalesce (Mason, 1999).....	45
Figure 2.25: Typical frequency sweep results obtained for different droplet sizes of HCEs (Masalova <i>et al.</i> , 2011a)	46
Figure 2.26: Typical HCEs flow curve fitted by the Herschel-Bulkley model with two sets of model coefficients (τ_{y0} , K) and constant $n=0.5$ for emulsions with variable droplet size/diameter (Foudazi <i>et al.</i> , 2011)	49
Figure 2.27: Highly concentrated explosive emulsions flow curves fitted by the Foudazi model with different droplet sizes (Foudazi <i>et al.</i> , 2011)	50
Figure 2.28: Elastic modulus (left) and flow curves (right) of highly concentrated explosive emulsions of different surfactant types with similar droplet size variation (Masalova <i>et al.</i> , 2011a).....	51
Figure 3.1: Silverson L4RT dispergator	57
Figure 3.2: Schematic structure of the sorbitan ring with different acids attached, forming Span surfactants. Structures of the various R groups are indicated.....	58
Figure 3.3: Three-dimensional structures of Span surfactants (hydrogen atoms: white, carbon atoms: blue, oxygen atoms: red)	59
Figure 3.4: Schematic structures of the ethoxylated sorbitan ring with different acids attached, forming Tween surfactants ($a+b+c+d=20$).....	60

Figure 3.5: Three-dimensional structures of Tween surfactants (hydrogen atoms: white, carbon atoms: blue, oxygen atoms: red)	61
Figure 3.6: Hobart N50 mixer	64
Figure 3.7: Kruss K 100 Tensiometer	66
Figure 3.8: The PAT1 Tensiometer	66
Figure 3.9: Mastersizer-2000 instrument	67
Figure 3.10: The Leica optical microscope	68
Figure 3.11: Rotational Rheometer MCR-301 (Paar Physica).....	68
Figure 3.12: Function control and components of the pumping instrument used: (a) overall pumping device; (b) schematic representation of pressure control panel; and (c) schematic representation of the piston movement whilst under compressor pressure inside the pump chamber	70
Figure 4.1: Possible structures of asphaltenes in W/O emulsions.....	72
Figure 4.2: General structure of polyether-modified silicone	73
Figure 4.3: General formula of Pluronic (left), and the structural layer produced by Pluronic at a water-oil interface (right).....	73
Figure 4.4: An AN solution (60 wt%) containing 1 wt% Tween 80 surfactant, (left) and dispersing of Tween 80 in pure Ash-H oil (right). Squares in left picture indicate the formation of Tween 80 agglomerates in the aqueous phase.....	76
Figure 4.5: Determination of the interfacial tension for Span 80 (blue), Pluronic PE 6100 (red) and Span 80/PE 6100 (10/1) mixture (green).....	77
Figure 4.6: The average droplet size of the HCES stabilised by the PIBSA-Mea/Tween 20 (red), PIBSA-Mea/Tween 80 (green), Span 80/PE3100 (blue), Span 80/PE6100 (navy), Span 80/Tween 20 (purple) and Span 80/Tween 80 (yellow) surfactant mixtures.....	78
Figure 4.7: Emulsion preparations of different surfactant systems prepared by using the Silverson mixer	79
Figure 4.8: Emulsion preparation using Silverson mixer and different surfactant systems. Scale bar, 50 μm = 6 mm	79
Figure 4.9: Photomicrographs of pumped emulsions stabilised by the PIBSA-Mea only (left), PIBSA-Mea/Span 80 (middle) and PIBSA-Mea/Tween 80 (right). Scale bar, 50 μm = 6 mm	82
Figure 4.10: Optical microscopic pictures of the fresh and aged un-pumped PIBSA-Mea/Span 80 (top) and PIBSA-Mea/Tween 80 (bottom) emulsions over time, showing higher stability on shelf for the PIBSA-Mea/Tween 80 emulsion. Scale bar, 50 μm = 6 mm.....	83
Figure 4.11: The interfacial tension of individual PIBSA-Mea and Span 80 as well as PIBSA-Mea/Span 80 mixtures below and above the CMC of PIBSA-Mea.....	85

Figure 4.12: The interfacial tension of individual PIBSA-Mea and Tween 80 as well as PIBSA-Mea/Tween 80 mixtures below (○) and above (●) the CMC of PIBSA-Mea.....	85
Figure 5.1: Determination of CMC value of the PIBSA-Mea surfactant.....	88
Figure 5.2: Experimental evaluation of the interaction parameter β between PIBSA-MEA and Tween 20 surfactants, based on interfacial tension measurements.....	91
Figure 5.3: Schematic diagram of the interfacial layer in the presence of a) PIBSA-Mea/Span 60 and b) PIBSA-Mea/Span 80 surfactant mixtures.....	95
Figure 5.4: The histogram of drop size distribution of the explosive emulsion (EE) stabilised with PIBSA-Mea (PI-M) surfactant at different refining times.....	99
Figure 5.5: Droplet size evolution as a function of refining time for emulsions with different emulsion formulations under investigation (P-M for PIBSA-Mea, T for Tween and S for Spans).....	100
Figure 5.6: Droplet size evolution as a function of refining time for the PIBSA-Mea/Span 80 emulsion (red dots) fitted by model (line).....	101
Figure 5.7: Droplet size distribution of the explosive emulsions stabilised with the employed surfactant mixtures.....	101
Figure 5.8: Photomicrographs depicting explosive emulsions stabilised with different surfactant types - no crystallisation occurred after manufacturing of the emulsions. Scale bar, 50 μm = 6 mm.....	102
Figure 5.9: The interaction parameter (β) between (a) the PIBSA-Mea/Spans mixtures and (b) the PIBSA-Mea/Tweens, versus the characteristic refinement time (θ) of the emulsions.....	106
Figure 5.10: Rheological behaviour of the oil phases containing Ash-H oil and surfactant mixtures where P-M stands for PIBSA-Mea, S for Spans and T for Tweens.....	108
Figure 5.11: Two different mechanisms of flow occur during low and high shear rates for the EEs. At high shear rates, a more regular structure is accompanied by plastic deformations (right) and under conditions of low shear, drops maintain their shape and resist the stress elastically (left).....	109
Figure 5.12: Flow curves for the explosive emulsions stabilised with PIBSA-Mea/Span mixtures.....	109
Figure 5.13: Flow curves for the explosive emulsions stabilised with PIBSA-Mea/Tween mixtures.....	110
Figure 5.14: Fittings of Foudazi model (dash) on the flow curve of the PIBSA-Mea/Span 20 stabilised emulsion (dots).....	111

Figure 5.15: Fittings of Foudazi model (dash) on the flow curve of the PIBSA-Mea/Tween 20 stabilised emulsion (dots)	111
Figure 5.16: Flow curve of an EE fitted by Herschel-Bulkley model (left) and comparison between the experimental (dots) and calculated (line) pressure drop as a function of flow rate	114
Figure 5.17: Flow curve of the PIBSA-Mea/Span 20 emulsion (dots) fitted by Herschel-Bulkley model (line)	115
Figure 5.18: Flow curve of the PIBSA-Mea/Tween 20 emulsion (dots) fitted by Herschel-Bulkley model (line)	115
Figure 5.19: Storage modulus as a function of strain for the emulsions stabilised by PIBSA-Mea/Span mixtures ($D_{32} = 10 \mu\text{m}$)	117
Figure 5.20: Storage modulus as a function of strain for the emulsions stabilised by PIBSA-Mea/Tween mixtures ($D_{32} = 10 \mu\text{m}$)	117
Figure 5.21: Storage modulus, G' (open) and loss modulus, G'' (filled) of the PIBSA-Mea/Span 80 emulsion as a function of strain amplitude	118
Figure 5.22: Storage modulus, G' (open) and loss modulus, G'' (filled) of the PIBSA-Mea/Tween 80 emulsion as a function of strain amplitude	118
Figure 5.23: Storage modulus, G' (open) and loss modulus, G'' (fill) as a function of frequency for the emulsions stabilised by PIBSA-Mea/Span mixtures ($D_{32} = 10 \mu\text{m}$)	119
Figure 5.24: Storage modulus, G' (open) and loss modulus, G'' (fill) as a function of frequency for the emulsions stabilised by PIBSA-Mea/Tween mixtures ($D_{32} = 10 \mu\text{m}$)	119
Figure 5.25: CMC value for the Pibsa-Mea/Span (orange pattern) and Pibsa-Mea/Tween (blue fill) surfactant mixtures	120
Figure 5.26: Histogram of drop size distribution of pumped emulsions stabilised by PIBSA-Mea/Span 20 mixture when NP =0 (red), 3 (green), 5 (blue), 7 (navy) and 10 (purple)	121
Figure 5.27: Droplet size (D_{32}) evolution as a function of pumping cycles (NP) for the PIBSA-Mea/Span 40 emulsion (orange circle) fitted by model (orange line) and the PIBSA-Mea/Tween 40 emulsion (blue square) fitted by model (blue line)	122
Figure 5.28: Photomicrographs of the PIBSA-Mea and PIBSA-Mea/Spans stabilised emulsions under different shear conditions. NP indicates the number of pumping cycles. Scale bar, $50 \mu\text{m} = 4 \text{ mm}$	124
Figure 5.29: Photomicrographs of the PIBSA-Mea/Tweens stabilised emulsions under different shear conditions. NP indicates the number of pumping cycles. Scale bar, $50 \mu\text{m} = 4 \text{ mm}$	124
Figure 5.30: Droplet size distributions of PIBSA-Mea/Span 40 emulsion fresh (blue), after 10 days (green) and 20 days (red)	126

Figure 5.31: Droplet size distributions of PIBSA-Mea/Tween 40 emulsion fresh (green), after 10 days (red), 20 days (blue) and 30 days (navy)	126
Figure 5.32: Photomicrographs of ageing in un-pumped emulsions samples containing different surfactant mixtures at t_{cr} . Scale bar, 50 μm = 6 mm	127
Figure 5.33: Time period required for commencement of crystallisation in different un-pumped emulsions (P-M denotes PIBSA-Mea and P-M/co denotes the mixtures of PIBSA-Mea/ co-surfactants - Spans or Tweens).....	128
Figure 5.34: Photomicrographs of ageing in the un-pumped emulsions samples after 45 days. Scale bar, 50 μm = 6 mm	129
Figure 5.35: The white creamy paste structure of fully crystallised PIBSA-Mea/Spans emulsions (right) and the phase separated structure including AN agglomerates of the fully crystallised PIBSA-Mea/Tweens emulsions (left)	130
Figure 5.36: Photomicrographs showing the appearance of various pumped emulsions (NP=5) after ageing 10 days. Scale bar, 50 μm = 6 mm	131
Figure 5.37: Photomicrographs showing the appearance of various pumped emulsions (NP=5) after ageing 20 days. Scale bar, 50 μm = 6mm	131
Figure A.1: Determination of the interfacial tension for PIBSA-Mea (blue), Pluronic PE 3100 (red) and PIBSA-Mea/PE 3100 (10/1) mixture (green).....	156
Figure A.2: Determination of the interfacial tension for PIBSA-Mea (blue), Pluronic PE 6100 (red) and PIBSA-Mea/PE 6100 (10/1) mixture (green).....	156
Figure A.3: Determination of the interfacial tension for PIBSA-Mea (blue), Tween20 (red) and PIBSA-Mea/Tween 20 (10/1) mixture (green)	157
Figure A.4: Determination of the interfacial tension for PIBSA-Mea (blue), Tween80 (red) and PIBSA-Mea/Tween 80 (10/1) mixture (green)	157
Figure A.5: Determination of the interfacial tension for SMO (blue), Pluronic PE 3100 (red) and Span 80/PE 3100 (10/1) mixture (green).....	158
Figure A.6: Determination of the interfacial tension for SMO (blue), Tween20 (red) and Span 80/Tween 20 (10/1) mixture (green)	158
Figure A.7: Determination of the interfacial tension for SMO (blue), Tween80 (red) and Span 80/Tween 80 (10/1) mixture (green)	159
Figure A.8: Evolution of droplet size with time for the PIBSA-Mea/Tween 20 emulsion fresh (red), after three days (green) and after 10 days (blue).....	160
Figure A.9: Evolution of droplet size with time for the PIBSA-Mea/Tween 80 emulsion fresh (red), after 3 days (green) and after 10 days (blue).....	160

Figure A.10: Evolution of droplet size with time for the SMO/Pluronic PE3100 emulsion fresh (red), after 3 days (green) and after 10 days (blue).....	160
Figure A.11: Evolution of droplet size with time for the SMO/Tween 20 emulsion fresh (red), after three days (green) and after 10 days (blue)	161
Figure A.12: Evolution of droplet size with time for the SMO/Tween 80 emulsion fresh (red), after three days (green) and after 10 days (blue)	161
Figure B.1: Determination of CMC value of Span 20 surfactant and PIBSA-Mea/Span 20 mixture	162
Figure B.2: Determination of CMC value of Span 40 surfactant and PIBSA-Mea/Span 40 mixture	162
Figure B.3: Determination of CMC value of Span 60 surfactant and PIBSA-Mea/Span 60 mixture	163
Figure B.4: Determination of CMC value of Span 80 surfactant and PIBSA-Mea/Span 80 mixture	163
Figure B.5: Determination of CMC value of Span 85 surfactant and PIBSA-Mea/Span 85 mixture	164
Figure B.6: Determination of CMC value of Tween 40 surfactant and PIBSA-Mea/Tween 40 mixture	164
Figure B.7: Determination of CMC value of Tween 60 surfactant and PIBSA-Mea/Tween 60 mixture	165
Figure B.8: Determination of CMC value of Tween 80 surfactant and PIBSA-Mea/Tween 80 mixture	165
Figure B.9: Determination of CMC value of Tween 85 surfactant and PIBSA-Mea/Tween 85 mixture	166
Figure C.1: Droplet size evolution as a function of refining time for the pure PIBSA-Mea emulsion (dots) fitted by model (line).....	167
Figure C.2: Droplet size evolution as a function of refining time for the PIBSA-Mea/Span 20 emulsion (dots) fitted by model (line).....	167
Figure C.3: Droplet size evolution as a function of refining time for the PIBSA-Mea/Span 40 emulsion (dots) fitted by model (line).....	167
Figure C.4: Droplet size evolution as a function of refining time for the PIBSA-Mea/Span 60 emulsion (dots) fitted by model (line).....	168
Figure C.5: Droplet size evolution as a function of refining time for the PIBSA-Mea/Span 85 emulsion (dots) fitted by model (line).....	168

Figure C.6: Droplet size evolution as a function of refining time for the PIBSA-Mea/Tween 20 emulsion (dots) fitted by model (line).....	168
Figure C.7: Droplet size evolution as a function of refining time for the PIBSA-Mea/Tween 40 emulsion (dots) fitted by model (line).....	169
Figure C.8: Droplet size evolution as a function of refining time for the PIBSA-Mea/Tween 60 emulsion (dots) fitted by model (line).....	169
Figure C.9: Droplet size evolution as a function of refining time for the PIBSA-Mea/Tween 80 emulsion (dots) fitted by model (line).....	169
Figure C.10: Droplet size evolution as a function of refining time for the PIBSA-Mea/Tween 85 emulsion (dots) fitted by model (line).....	170
Figure D.1: Fittings of Foudazi model (dash) on the flow curve of the PIBSA-Mea stabilised emulsion (dots)	171
Figure D.2: Fittings of Foudazi model (dash) on the flow curve of the PIBSA-Mea/Span 40 stabilised emulsion (dots)	171
Figure D.3: Fittings of Foudazi model (dash) on the flow curve of the PIBSA-Mea/Span 60 stabilised emulsion (dots)	172
Figure D.4: Fittings of Foudazi model (dash) on the flow curve of the PIBSA-Mea/Span 80 stabilised emulsion (dots)	172
Figure D.5: Fittings of Foudazi model (dash) on the flow curve of the PIBSA-Mea/Span 85 stabilised emulsion (dots)	173
Figure D.6: Fittings of Foudazi model (dash) on the flow curve of the PIBSA-Mea/Tween 40 stabilised emulsion (dots)	173
Figure D.7: Fittings of Foudazi model (dash) on the flow curve of the PIBSA-Mea/Tween 60 stabilised emulsion (dots)	174
Figure D.8: Fittings of Foudazi model (dash) on the flow curve of the PIBSA-Mea/Tween 80 stabilised emulsion (dots)	174
Figure D.9: Fittings of Foudazi model (dash) on the flow curve of the PIBSA-Mea/Tween 85 stabilised emulsion (dots)	175
Figure D.10: Storage modulus (open) and loss modulus (filled) of the PIBSA-Mea/Span 20 emulsion	176
Figure D.11: Storage modulus (open) and loss modulus (filled) of the PIBSA-Mea/Span 40 emulsion	176
Figure D.12: Storage modulus (open) and loss modulus (filled) of the PIBSA-Mea/Span 60 emulsion	177

Figure D.13: Storage modulus (open) and loss modulus (filled) of the PIBSA-Mea/Span 85 emulsion	177
Figure D.14: Storage modulus (open) and loss modulus (filled) of the PIBSA-Mea/Tween 20 emulsion	178
Figure D.15: Storage modulus (open) and loss modulus (filled) of the PIBSA-Mea/Tween 40 emulsion	178
Figure D.16: Storage modulus (open) and loss modulus (filled) of the PIBSA-Mea/Tween 60 emulsion	179
Figure D.17: Storage modulus (open) and loss modulus (filled) of the PIBSA-Mea/Tween 85 emulsion	179
Figure E.1: Droplet size distributions of PIBSA-Mea/Span 40 emulsion under 0 (red), 3 (green), 5 (blue), 7 (navy), 10 (violet) pumping cycles	180
Figure E.2: Droplet size distributions of PIBSA-Mea/Span 60 emulsion under 0 (red), 3 (green), 5 (blue), 7 (navy), 10 (violet) pumping cycles	180
Figure E.3: Droplet size distributions of PIBSA-Mea/Span 80 emulsion under 0 (red), 3 (green), 5 (blue), 7 (navy), 10 (violet) pumping cycles	181
Figure E.4: Droplet size distributions of PIBSA-Mea/Tween 20 emulsion under 0 (red), 3 (green), 5 (blue), 7 (navy), 10 (violet) pumping cycles	181
Figure E.5: Droplet size distributions of PIBSA-Mea/Tween 40 emulsion under 0 (red), 3 (green), 5 (blue), 7 (navy), 10 (violet) pumping cycles	181
Figure E.6: Droplet size distributions of PIBSA-Mea/Tween 60 emulsion under 0 (red), 3 (green), 5 (blue), 7 (navy), 10 (violet) pumping cycles	181
Figure E.7: Droplet size distributions of PIBSA-Mea/Tween 80 emulsion under 0 (red), 3 (green), 5 (blue), 7 (navy), 10 (violet) pumping cycles	182
Figure E.8: Droplet size evolution as a function of pumping cycles for the PIBSA-Mea/Span 20 emulsion (orange circle) fitted by model (orange line) and the PIBSA-Mea/Tween 20 emulsion (blue square) fitted by model (blue line)	183
Figure E.9: Droplet size evolution as a function of pumping cycles for the PIBSA-Mea/Span 60 emulsion (orange circle) fitted by model (orange line) and the PIBSA-Mea/Tween 60 emulsion (blue square) fitted by model (blue line)	183
Figure E.10: Droplet size evolution as a function of pumping cycles for the PIBSA-Mea/Span 80 emulsion (orange circle) fitted by model (orange line) and the PIBSA-Mea/Tween 80 emulsion (blue square) fitted by model (blue line)	184

LIST OF TABLES

Table 3.1: Surfactants used for feasibility study (a+b+c+d=20).....	55
Table 3.2: Matrix of samples for feasibility study	56
Table 3.3: Matrix of samples selected for comparison between PIBSA-Mea/Tween 80 emulsion formulations and PIBSA-Mea/Span 80 standard industrial formulation	57
Table 3.4: Summary of surfactant properties (a+b+c+d=20)	62
Table 3.5: Matrix of samples used during the second stage of the study.....	64
Table 4.1: Summary of surfactant properties for feasibility study	75
Table 4.2: Summary of interfacial tensions of water-oil interfaces (σ) in the presence of selected surfactant systems	76
Table 4.3: Emulsification analyses of the selected matrix of surfactants.....	78
Table 4.4: Emulsification analyses of the selected matrix of surfactants.....	80
Table 4.5: Matrix of mixtures for comparison study	81
Table 4.6: Refinement time of the manufactured emulsions	81
Table 4.7: Droplet size of the pumped emulsions after five pumping cycles	82
Table 4.8: Ageing of the un-pumped and pumped emulsions under investigation	83
Table 4.9: The CMC values and interfacial tensions at CMC of individual surfactants under investigation.....	84
Table 5.1: Interfacial properties of individual PIBSA-Mea and Spans	91
Table 5.2: Interfacial properties of PIBSA-Mea/Spans mixtures.....	93
Table 5.3: Interfacial properties of individual PIBSA-Mea and Tweens.....	96
Table 5.4: Interfacial properties of PIBSA-Mea/Tween mixtures	97
Table 5.5: Matrix of samples used in the emulsification process.....	99
Table 5.6: Summary of refinement times for the emulsions under investigation	102
Table 5.7: A Summary of the minimum concentration of surfactant required to cover the emulsion droplets ($D_{32}=10 \mu\text{m}$).....	104
Table 5.8: The adsorption efficiency of surfactant mixtures required to decrease the interfacial tension of the water-oil interface to 10 mN/m.....	105
Table 5.9: Summary of the viscosity values for the oil phases used in the emulsions under investigation.....	108
Table 5.10: Summary of the coefficients obtained by fitting Foudazi equation on flow curve of the emulsion under investigation	112

Table 5.11: Summary of yield stresses and co-efficient calculated for the emulsion formulations under investigation using Herschel-Bulkley equation.....	116
Table 5.12: Summary of equilibrium storage modulus (G_0) of the emulsion formulations under investigation obtained from amplitude sweep (AS) and frequency sweep (FS) tests.....	120
Table 5.13: Summary of critical droplet diameters of the explosive emulsions under investigation during the shearing process (D_0 , the initial droplet size of the emulsions equal to $10\ \mu\text{m}$)	123

GLOSSARY

Terms	Explanation
Aggregation number	The number of molecules present in a micelle once the critical micelle concentration (CMC) has been reached.
Capillary number	Ratio between the viscous stress which acts to deform the droplet and stabilising Laplace pressure.
Coalescence	Spontaneous joining of smaller droplets in an emulsion system to form larger droplets.
Crystallisation	Destabilisation mechanism due to a change in the physical state of the emulsion dispersed phase – change from liquid state to crystal state.
Disjoining pressure	The short-range interaction force of an area situated between the water-oil interface.
Elastic	A conservative property in which part of the mechanical energy used to produce deformation is stored in the material and recovered on release of stress.
Emulsion	Two immiscible liquids (usually oil and water), with one of the liquids dispersed as small spherical droplets in the other.
Explosive emulsion	High internal phase water-in-oil emulsion of a concentrated solution of nitrate salts in water emulsified in an oil base.
Flow curve	Curve presenting the variation of shear stress versus shear rate.

Interfacial tension	Measurement of cohesive (excess) energy present at an interface arising from the imbalance of forces between molecules at an interface (gas/liquid, liquid/liquid, gas/solid, liquid/solid).
Interaction parameter	An indicator which compares the molecular interaction of surfactant mixtures with the self-interactions of surfactants individually before mixing.
Laplace pressure	The pressure difference between fluids separated by an interface resulting from the interfacial tension and the curvature of the interface.
Non-Newtonian fluid	A fluid in which flow behaviour does not obey the Newtonian's law, i.e. viscosity is dependent on the stress or shear rate.
Osmotic pressure	The equilibrium energy density required to confine the dispersed phase droplets to a finite volume fraction of continuous phase.
Rheology	Science of deformation and flow of matter, relevant to the deformation of materials resulting from an applied stress.
Storage modulus	A measure of the deformation energy stored in a sample during the shear process. After the load is removed, this energy is available and acts as the driving force for reformation, which partially or completely compensates the previous deformation.
Surfactant	An amphiphilic (amphipathic) molecule that has a hydrophilic head group (polar region), with a high affinity for water, and a lipophilic tail group (non-polar region), with a high affinity for oil.

Viscoelastic material	A time-dependent material exhibiting both viscous and elastic effects under the action of outside stresses in the absence of time dependence.
Viscosity	The property of a material to increasingly resist deformation as the shear rate increases; a measure of this property is defined as the quotient of shear stress divided by the shear rate in steady flow.
Yield stress	A critical shear stress value below which an ideal plastic or viscoplastic material behaves as a solid (no flow). Once the yield stress is exceeded, a plastic material yields (deforms plastically) while a viscoelastic material flows as a liquid.

NOMENCLATURE

Symbol	Description	Unit
a_s, A_I	The cross-sectional area of one surfactant	m^2
a_0	The area occupied by the head group	m^2
A_N	The average surface area of droplets	m^2
A	Hamaker constant	-
C	Concentration	mol/L
Ca	Capillary number	-
D or d	Diameter of droplet (particle)	m
D_{crit}	Critical droplet size	m
D_0	Initial droplet size	m
D_{32}	Surface-volume mean drop diameter	m
F	Force	N
f	Activity coefficient of a surfactant	-
G_A	Van der Waals energy between two drops	J
G_T	Interaction energy between in interfacial film	J
G'	Storage modulus	Pa
G''	Loss modulus	Pa
ΔG^{exc}	The excess energy of mixing	J
h	Film thickness	m
h_{max}	Maximum film thickness	m
ΔH^M	Heat of mixing	J
k	Boltzmann constant	$J/^\circ k$
L	Length	m
l_c	The length of hydrophobic tail	m
N	Aggregation number	-
NP	Number of the passes through an orifice	-
P_v	Critical packing parameter	-
pC_{half}	Efficiency of the surfactant mixtures	-
R, a	Droplet radius	m
R_{32}	Surface-volume mean drop radius	m

R	Universal gas constant	J/mole ^o k
T	Absolute temperature	^o k
t	Time	s
t _{cr}	The time required for crystallisation to initiate	days
V _{DPh}	Total volume of emulsion droplets	m ³
V _E	Total volume of the emulsion	m ³
V _{mic}	Core volume of micelles	m ³
v	The volume of hydrophobic portion of surfactant	m ³
W _{ii}	Self-interaction energy of the surfactant	J
X _{1, α}	Mole fraction	-
\bar{x}	Mean particle size	m
Γ	Gibbs surface excess concentration	mol/m ²
Π _L	Laplace pressure	Pa
Π _{dis}	Disjoining pressure	Pa
β	Interaction parameter	-
γ'	Shear rate	1/s
φ	Dispersed phase volume fraction	%
φ*	Volume fraction corresponding to the hexagonal close packing of undistorted spheres	%
η	Viscosity	Pa.s/cP
θ	Characteristic time	min
θ	Contact angle	grad
μ	Chemical potential of a surfactant	J/Kg
π	Surface pressure	Pa
σ	Interfacial tension	N/m
τ	Shear stress	Pa
τ _y	Yield stress	Pa
ω	Width of droplet size distribution (standard deviation)	-

ACRONYMS

AN	Ammonium nitrate
CMC	Critical micelle concentration
DSD	Droplet size distribution
EE	Explosive emulsion
FT-IR	Fourier transform Infrared
HCEs	Highly concentrated emulsions
HLB	Hydrophilic-lipophilic balance
IT	Interfacial tension
O/W	Oil-in-water
O/W/O	Oil-in-water-in-oil
PIBSA	Poly(isobutylene succinic) anhydride
SANS	Small angle neutron scattering
SMO	Sorbitan monooleate
MEA	Monoethanolamine, i.e. 2-aminoethanol
W/O	Water-in-oil
W/O/W	Water-in-oil-in-water

CHAPTER ONE: INTRODUCTION

The manufacturing of emulsions is of increasing interest in consumer-orientated chemical industries. In practice, the development of emulsions is based on trial and error or modelling approaches. The trial and error method is slow and tedious, while results obtained from a modelling approach may not necessarily work in practical application. Hence, it would be preferable to develop a systematic procedure to design emulsions with higher performance and enhanced qualities. Such an approach would stimulate a rapid development of emulsion-based products and also reduce manufacturing costs for the retail market. To achieve this goal, an understanding of the characteristic behaviour of an emulsion and its particular components is necessary.

Highly concentrated emulsions (HCEs) comprise one of the most common categories of emulsions used by various industries. The latter include the pharmaceutical and food sectors, refineries and others. The HCEs are classified as having a high volume fraction of the dispersed phase (in excess of 74 vol%, up to a maximum of 98 vol%) in which the dispersed phase droplets are arranged in a closely packed hexagonal configuration. The hexagonal close-packing configuration creates a robust hydrodynamic interaction between adjoining droplets. This induces a mechanical barrier between the droplets and thereby prevents their free movement, resulting in a stable, gel-like, particulate network (Becher, 1988; Grassi *et al.*, 1996; Masalova & Malkin, 2007a). A unique type of highly concentrated water-in-oil (W/O) emulsion is the “liquid explosive” category used for mining applications (Cooper & Baker, 1989).

Explosive emulsions (EE) are comprised of a thermodynamically-unstable solution of a supersaturated aqueous solution of inorganic salt, dispersed in an oil continuous phase. The stability of such emulsion could be evaluated in terms of coalescence and/or crystallisation of overcooled aqueous phase with time or under high shear conditions (Boyd *et al.*, 1972; Masalova *et al.*, 2006). Crystallisation may result in a loss of both performance and functionality of explosive emulsions (Cooper & Baker, 1989; McKenzie & Lawrence, 1990; McKenzie, 1991; Boer, 2003). Pictorial representations of stable and crystallised emulsions are shown in Figure 1.1.

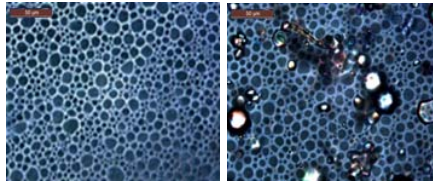


Figure 1.1: Photomicrographs of freshly prepared liquid explosive (left) and crystallised liquid explosive (right). Taken in the Rheology laboratories at the Cape Peninsula University of Technology

In their final applications, these emulsions need to be transferred over long distances to fill holes with various diameters. Some mines extend down to 4-6 km below ground surface, and working conditions are harsh due to the high temperature and space limitations. Therefore, the success of emulsion transportation becomes vital. In addition, the emulsion needs to retain its stability during and after the pumping process. Figure 1.2 illustrates underground applications of explosive emulsions.



Figure 1.2: Application of explosive emulsions underground ()

A number of studies have shown that the crystallisation of emulsion explosives depends on the emulsion formulation and the ratio of the various compounds used (Ganguly *et al.*, 1992; Aronson & Petko, 1993; Villamagna *et al.*, 1995a; Masalova *et al.*, 2006). These exert a marked effect on the different aspects of the emulsions, including interfacial and rheological properties, transportability and stability with regard to crystallisation (Coolbaugh & Mahamat, 2003; Kovalchuk & Masalova, 2012). The challenge for the industries manufacturing this kind of emulsion is to develop formulations which provide acceptable stability throughout shelf life and when subjected to intense shear (Masalova & Malkin, 2013).

The formulation of an emulsion generally consists of two immiscible liquids, an active-agent (normally a surfactant) and further additives. The active agents of an emulsion formulation define the quality and stability of the product with respect to a desired application (Binet *et*

al., 1982; Cooper & Baker, 1989). Many patents have been granted for explosive emulsion composition and particularly for the selection of suitable emulsifiers, or blends thereof. These are designed to suppress coalescence and crystallisation of the supersaturated droplets of the oxidiser solution (Tomic, 1973; Chattopadhyay, 1996a; Cechanski, 1997; Hobson *et al.*, 2007). During the past decade, most researches have been focused on achieving the desirable aforementioned emulsion characteristics by using combinations of two different surfactants, including those of polymeric and conventional nature. Polymeric surfactants provide long-term stability due to steric effect, while conventional surfactants maintain the stability of explosive emulsions under high shear conditions due to their high mobility. The stabilising system currently most commonly in use by the mining industry is a binary mixture of two surfactants; polymeric polyisobutylene succinic anhydride (PIBSA)- based surfactant, in combination with the conventional oil soluble surfactant, sorbitan monooleate, under the trade name of Span 80.

The application of PIBSA-based surfactants in emulsions is supported by the fact that these surfactants provide long-term on shelf stability. The PIBSA molecules tend to form micelles in the oil phase, creating a steric barrier between drops and thus improving the stability of such an emulsion (Shen & Duhamel, 2008; Reynolds *et al.*, 2010). The drawback of this mechanism of operation is that high volumes of the surfactant are required. In addition, the manufacturing of an emulsion containing PIBSA requires relatively long emulsification time to reach a desirable droplet size. This directly translates to high energy consumption in terms of industrial scale production. Another disadvantage of PIBSA surfactants is their low mobility (Mw 1100-1300) to cover the surfaces of newly-formed droplets when EE is subject to high shear during transportation process. Furthermore, PIBSA is regarded as an environmentally-unfriendly, compound according to the provided MSDS by the PIBSA supplier.

In order to improve the stability of the emulsion under high shear, manufacturers introduced mobile surfactants; mainly Span 80 (Mw 429) from the family of Spans, to the emulsion formulation, in combination with PIBSA (Masalova *et al.*, 2011b). However, the presence of Span 80 in the emulsion formulation reduces the shelf life stability of liquid explosives when compared with PIBSA-based emulsions (Mudeme *et al.*, 2010). This could be attributed to the following:

- The incompatibility between the hydrophobic tail of PIBSA (38 carbon atoms) and Span 80 (17 carbon atoms) reduces their molecular interaction at the interface, thereby disrupting the interfacial film packing (Shiao *et al.*, 1998) and destabilising the PIBSA micelles, which has a negative effect on the steric barrier between drops (Reynolds *et al.*,

2009b).

- Span 80 molecules occupy the interface over a relatively short time. The Span 80 surfactant is much more mobile and has a stronger interaction with oxidiser molecules when compared with PIBSA molecules. Therefore it is difficult for PIBSA molecules to replace Span 80 at interface to provide the optimal stability of the emulsion (Masalova *et al.*, 2011b; Kovalchuk & Masalova, 2012; Campana *et al.*, 2013).
- In addition, Span 80 molecules tend to develop an opaque structured multilayer at the interface, which could initiate the crystallisation (Opawale & Burgess, 1998; Drelich *et al.*, 2010).

In spite of these limitations, the binary mixture of PIBSA-based surfactant and Span 80 is used widely by mining industries to stabilise explosive emulsions with acceptable stability for specific applications. However, the question remains:

- How to improve stability of such emulsion systems under high shear without compromising their stability on shelf?

In recent years there has been considerable research devoted towards developing new formulations to stabilise such systems (Ghosh & Rousseau, 2011; Zank, *et al.*, 2006; Yaron *et al.*, 2011; Tshilumbu *et al.*, 2013). However, unsatisfactory results were obtained from those studies with regards to shear stability of the explosive emulsions.

Other studies related to these types of emulsions have concentrated on the rheological properties of the emulsions (Masalova *et al.*, 2006; Masalova & Malkin, 2007a; Masalova & Malkin, 2008; Masalova *et al.*, 2011b), as well as small angle neutron scattering (SANS) study of the emulsions structure (Reynolds *et al.*, 2000; Reynolds *et al.*, 2002). However, formulations used in these studies were limited only to PIBSA-based emulsions and/or their mixture with Span 80.

To date, from the literature surveyed, there is very limited information published with regards to using other types of surfactants, in addition to PIBSA-based surfactant and Span 80 to stabilise highly concentrated emulsions with a super-cooled dispersed phase.

A review of recent studies on stability of W/O emulsions, stabilised by either polymeric surfactants or mixtures of water/oil soluble surfactants, revealed that most of the studies

were focused on dilute emulsion systems (Wu *et al.*, 1999, Khristov *et al.*, 2000; Zank, *et al.* 2006; Kang *et al.*, 2011; Yaron *et al.*, 2011).

Hence, a feasibility study was conducted in order to find out whether various surfactants are able to stabilise HCEs with a super-cooled dispersed phase.

Block copolymer surfactants (known as Pluronics) and water-soluble surfactants (known as Tweens) were chosen and used individually and/or in combination with PIBSA and Span 80 for the feasibility study. The following results were obtained:

- It was impractical to add Tween molecules in aqueous medium, due to the salting-out effect of Tweens in presence of electrolytes. Alternatively, it was found that Tween surfactants can be dispersed in oil phase and utilised in this medium.
- Use of only Pluronics and water-soluble surfactants and mixtures of PIBSA/Pluronics to stabilise HCE was unsuccessful.
- Use of binary mixtures of Span 80/Pluronics and Span 80/Tweens to stabilise HCE was successful; however, the emulsions coalesced in the within 10 days after preparation.
- Stable emulsions were produced by the use of binary mixtures of PIBSA/Tweens.

A mixture of PIBSA with one of the Tweens (Tween 80) with similar hydrophobic structure of Span 80 was selected and used to stabilise HCE with a super-cooled dispersed phase as the result of above discussed study. Its properties were compared to the standard industrial formulation of PIBSA/Span 80. Satisfactory results were obtained when Span 80 was replaced with Tween 80, with a similar tail structure. The time to reach a certain droplet size of the emulsion (refinement time) was substantially reduced (from 29 min to 8 min) and the emulsion was more stable (increased by about 100%). But, this led to another question:

- Why did replacing of Span 80 (a mobile oil soluble surfactant) with bulky water-soluble Tween 80 ease the emulsion formation and produce more stable emulsion both under high shear and on shelf?

Interfacial behaviour of the PIBSA/Span 80 and PIBSA/Tween 80 binary mixtures was investigated in order to answer the aforementioned question. This was performed over a wide range of the surfactants' concentrations/ratio. The rate of interfacial tension reduction was strongly influenced by the type of co-surfactants employed. It was observed that the

interfacial tension decreased quicker when using a mixture of PIBSA/Tween 80 than it did when using the individual surfactants themselves. For the mixture of PIBSA/Span 80, interfacial behaviour of the mixture was similar to Span 80 itself. This may result from different type of interaction (synergetic, ideal or antagonistic) between the surfactants in these two mixtures (Sanatkaran & Masalova, 2015, *Colloid Journal*, accepted paper). This finding further raised the following questions:

- Is it possible to use other surfactants from the Spans and Tweens family, with different tail molecular structures, to stabilise HCEs with a super-cooled dispersed phase?
- Is Span 80 from the series of Span surfactants or Tween 80 from the series of Tween surfactants the best option to use in combination with PIBSA to provide optimal stability of such emulsion systems?

A range of Span and Tween surfactants with various hydrophobic tail structures were chosen as co-surfactant and mixed with a PIBSA-based surfactant, in order to obtain answers to these questions. The following objectives of this study were formulated:

- To investigate the synergetic compatibility between the defined binary surfactant mixtures as a function of co-surfactant structure.
- To investigate the effect of synergetic compatibility of the surfactant mixtures on the emulsification process.
- To gain a better understanding of the effect of synergetic compatibility between surfactant mixtures on storage stability of the HCEs with a super-cooled disperse phase.
- To gain a better understanding of the effect of synergetic compatibility between surfactant mixtures on stability of the HCEs with a super-cooled disperse phase under high shear conditions.
- To investigate the effect of defined surfactant systems on rheological properties of the manufactured emulsions. This gives good grounds for estimation of the pumping characteristics of new formulations of explosive emulsions during transportation.

The methods used to accomplish the objectives of this study are presented below:

a) Interfacial properties:

- A Kruss K100 tensiometer was used to measure the interfacial tension (IT) of the water-oil interface in the presence of the employed binary surfactant mixtures.
- Critical micelles concentration (CMC) value of the surfactant systems was obtained using the interfacial tension method.
- Gibbs' series of equations were used to calculate the Gibbs free energy of micellisation (ΔG_{mic}), the transfer of the surfactant molecules from the interface to the micelles (ΔG_{min}) and the average minimum area per surfactant molecule (A_{min}).
- Rosen's (2003) model was used to obtain the extent of synergism or antagonism (synergetic compatibility) in a binary mixture of surfactants, as well as the mole fraction of each surfactant at interface.

b) Emulsion manufacturing:

- A Hobart N50 mixer was used to manufacture the emulsions, in 1 kg batches.
- A Malvern Mastersizer 2000 instrument was used to measure the droplet size and droplet size distribution during emulsification process.
- The characteristic refinement time of the manufactured emulsions was obtained by fitting the droplet sizes data during emulsification with an exponential model.

c) Rheological properties:

- An MCR301 rheometer was used in both rotational and oscillation modes to determine the flow and viscoelastic characteristics of the fresh emulsions respectively.
- Storage modulus G' was determined as the value at the plateau region from the amplitude and frequency sweep measurements.
- Flow curves of the emulsions were fitted by the Herschel-Bulkley model to obtain characteristic rheological parameters of the emulsions, particularly yield stress.

d) High shear condition:

- A locally-designed and manufactured double piston pump was used to investigate stability of manufactured emulsions under high shear conditions.
- The critical droplet size of the pumped emulsions was obtained by fitting the droplet sizes data after different pumping cycles with an exponential model .

e) Ageing:

- A Leica optical microscope equipped with a digital camera was used to track the start and crystallisation kinetics of the emulsions visually. This was followed up by daily observations of the manufactured emulsions.

Finally, the effect of compatibility between surfactants and co-surfactants is discussed in relation with the following:

- characteristic refinement time;
- rheological characteristic parameters; and
- stability on shelf and under high shear conditions.

The findings of this study provide valuable information about the effect of synergetic compatibility of surfactant mixtures within the HCEs. It assists the manufacturers to improve the emulsion stability in storage, transportation and high shear conditions. Also, it aids to reduce energy consumption during the manufacturing process and pumping. Moreover, knowledge gained from these results could provide a sound basis for future studies regarding the modification of surfactant structures and assist in developing a better understanding of the mechanism of stability in emulsion explosives.

This thesis presents the research study carried out over a period of three years. It consists of six chapters, as follows:

- **Chapter One** is an introduction to the current study.
- **Chapter Two** presents general definitions of emulsion, emulsification, microscopic and macroscopic properties of emulsions and a relevant literature review of HCEs is included, with emphasis on liquid explosives.

-
- **Chapter Three** provides a description of materials and methods relating to emulsion preparation and analytical procedures used in the present study.
 - **Chapter Four** presents a feasibility study on the design of the sample matrix.
 - **Chapter Five** provides a discussion of the analysis of the results obtained from a comprehensive study of processing, pumpability and stability of explosive emulsions affected by synergetic compatibility between the defined surfactant mixtures.
 - **Chapter Six** presents both a summary and the overall conclusions of the study.

CHAPTER TWO: THEORY AND LITERATURE REVIEW

2.1 INTRODUCTION

Highly concentrated water-in-oil emulsions (HCEs) with an oversaturated dispersed phase are uniquely complex systems, playing an important role in many industries, including explosives, nutritious foods, and drug delivery systems. This chapter aims at introducing emulsions and HCEs in general and providing a more detailed discussion of HCEs as liquid explosives. Interfacial and rheological properties, emulsification, stability and their interrelationships are further discussed. The effect of emulsifier (surfactant) structure on the properties of emulsions is emphasised. The structure of the chapter is as follows:

- definition of emulsions;
- emulsion explosives;
- stability of emulsions and explosives;
- history of surfactants used in explosive emulsions;
- interfacial properties and theories;
- emulsification; and
- rheological properties.

2.2 EMULSIONS

2.2.1 General definition

Emulsions are a combination of two immiscible or partially-immiscible liquids, most commonly oil and water, in which one of the liquids (the dispersed or internal phase) is dispersed in the other (the continuous or external phase). As shown in Figure 2.1, when the two liquids are mixed, different types of emulsions are produced:

- simple emulsions: water-in-oil (W/O) and oil-in-water (O/W)
- multiple emulsions: water-in-oil-in-water (W/O/W) and oil-in-water-in-oil (O/W/O)

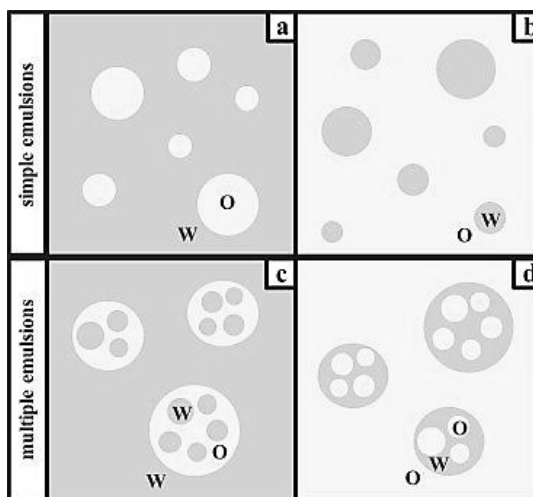


Figure 2.1: Different types of emulsions a) O/W, b) W/O, c) W/O/W, d) O/W/O (Bouyer et al., 2012)

Depending on the concentration of the dispersed phase, emulsions are classified as dilute, concentrated or highly concentrated (Figure 2.2).

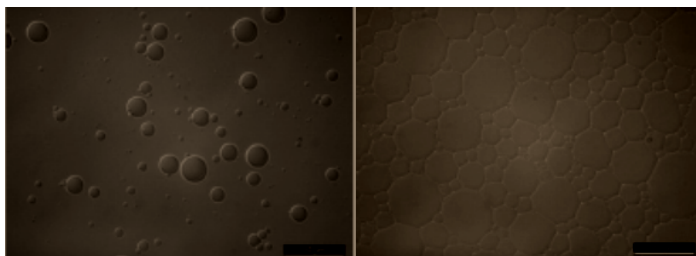


Figure 2.2: Microscopic images of dilute (a) and highly concentrated (b) emulsions (Foudazi et al, 2011)

The concentration of droplets in an emulsion is determined in terms of the dispersed phase volume fraction (ϕ), as:

$$\phi = \frac{V_{Dph}}{V_E}$$

Equation 2.1

where V_{Dph} is the total volume of the emulsion droplets and V_E the total volume of the emulsion (McClements, 2005).

Highly concentrated emulsions are classified as high internal phase ratio (>74%) emulsions. The stable spherical shape of droplets cannot be maintained in these systems and they

consequently deform to form a closely-packed hexagonal configuration (Webber & Engineers, 1999). The droplets are in contact with each other and therefore the mobility of the droplets is restricted.

2.3 HIGHLY CONCENTRATED W/O EMULSIONS (EXPLOSIVE GRADE)

One class of highly concentrated W/O emulsions with a large internal phase volume fraction (>80%) of an oversaturated inorganic salt solution, such as ammonium nitrate (AN), is the class of explosive emulsions (liquid explosives). Internationally, explosive emulsions are the most commonly used industrial explosive. They are widely used in coal mining, metal and non-metal mining, quarrying and construction. These emulsions offer safety, storage stability and cost advantages over other industrial explosives, such as dynamite (Clay, 1978; Sudweeks & Jessop, 1980). Explosive emulsions were first introduced by Richard Egly and Albert Neckar (Egly & Neckar, 1964). They offer the advantages of high bulk density, effective blasting energy, and water resistance. They are also cost-effective, as AN is inexpensive. Among the problems that are associated with the use of these blends, however, are their pumpability and the stability of their explosive properties. These disadvantages are related to the specific oversaturated dispersed phase of the given blend.

2.4 STABILITY OF EMULSIONS

2.4.1 Instability aspects

Different types of instabilities are possible in emulsions. During emulsification, the interfacial area between the droplets and continuous phase increases. This results in a higher interfacial free energy, contrary to the thermodynamic concept that all systems tend to remain in their globally minimum energy state (Bouyer *et al.*, 2012). Thus, as soon as shear forces are absent, an emulsion will separate into two phases, a process which is initiated by various mechanisms (Figure 2.3). Important instability mechanisms are the

- aggregation of dispersed phase droplets (flocculation);
- combination of two droplets to form a larger droplet (coalescence);
- separation of an emulsion into two phases, where one phase contains a greater number of droplets when compared to the other (creaming in O/W emulsions or sedimentation in W/O emulsions); and
 - diffusion of smaller droplets through the continuous phase and the subsequent adherence of these to larger droplets (Ostwald ripening) (Fennema, 1996).

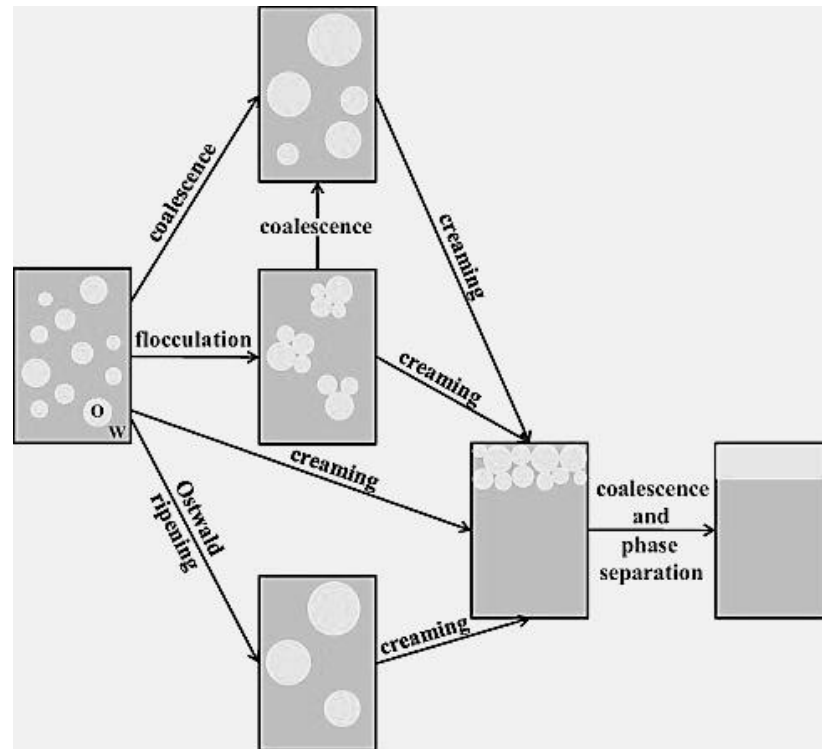


Figure 2.3: Instabilities of emulsions (Bouyer et al., 2012)

Normally, all types of instability mechanisms occur concurrently. However, flocculation and creaming are considered as necessary precursor mechanisms for coalescence to occur, as the latter process is a result of the short-range attractive interactions (forces) between droplets. Thus, for coalescence to materialise, droplets must be close enough for these forces to exert their effect (Radeva, 2001).

2.4.2 Factors affecting emulsion stability

The stability of emulsions in general is influenced by a number of factors (Zhou & Rosen, 2003):

- physical properties of the interfacial film;
- existence of an electrical or steric barrier on the droplets;
- viscosity of the phases;
- droplet size distribution;
- temperature; and
- ratio between the two phases.

Highly orientated adsorbed molecules create a closely-packed interfacial layer with low mobility at the interface (Myers, 2005). The condensed interfacial film can increase the

mechanical strength of the interface and this has a profound effect on emulsion stability (Rosen & Kunjappu, 2012). Furthermore, the conformational rearrangement of active agents, such as particles and proteins at the interface, creates a robust steric barrier between droplets and stabilises the system against flocculation (McClements, 2005).

The rate of coalescence in an emulsion system is influenced by the frequency of collisions among the dispersed phase droplets. These collisions could be reduced by increasing the viscosity of the continuous phase. Addition of a thickening agent can increase the viscosity of the continuous phase and thereby improve the stability of the emulsion (Rosen & Kunjappu, 2012). Another factor which affects the rate of collision is temperature. Temperature has an impact on the emulsion components, such as interfacial tension and the solubility of the emulsifiers and also viscosity of the system (Rosen & Kunjappu, 2012).

Emulsions comprised of a uniform droplet size are more stable than those where there is a variable droplet size distribution. Thermodynamically, larger droplets with less interfacial area per unit volume are more stable than smaller droplets. Hence, smaller droplets combine to create larger ones. This thermodynamic phenomenon can be controlled by manufacturing an emulsion with a narrow size distribution of dispersed phase droplets (Rosen & Kunjappu, 2012).

A further important factor which affects the appearance, stability and cost of the final emulsion is the concentration of droplets. This concentration depends on the nature of the emulsion compounds used: at a certain concentration of the dispersed phase an emulsion either splits into two phases or inverts to the other type (Becher, 1988). It has even been reported that emulsions containing 0.99% volume fraction of the dispersed phase were synthesised in the absence of a centrifugal force (Lissant, 1966; Nixon & Beerbower, 1969; Lissant *et al.*, 1974; Mittal, 1975; Princen, 1979; Princen *et al.*, 1980). However, as HCEs form a class of emulsions wherein the volume fraction exceeds 74% of the internal phase, they exhibit a closely-packed hexagonal configuration of droplets (Figure 2.4) (Princen, 1979).

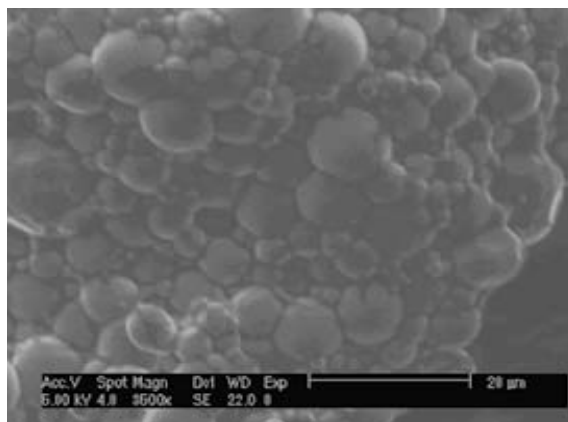


Figure 2.4: Microscopic images of a concentrated emulsion where the droplet deformation at compression is shown. Taken in the Rheology laboratories at the Cape Peninsula University of Technology

2.4.3 Instability of explosive emulsions

Due to their unique composition, the HCEs with a super-cooled dispersed phase show behaviour different from that recorded for other types of emulsions. Firstly, the hexagonal close packing configuration forms a marked hydrodynamic interaction between adjoining droplets. This induces a mechanical obstacle between droplets, thus preventing their free movement. As a result, a stable, gel-like particulate network is formed. Therefore, in these systems, aggregation or flocculation instabilities cannot occur. In HCEs, coalescence is the most common type of emulsion instability (Masalova & Malkin, 2007a; Masalova & Malkin, 2008; Reynolds *et al.*, 2010). Additionally, for emulsions with a supersaturated dispersed phase, as is associated with explosive emulsions, instability is also caused by the crystallisation of the supersaturated inorganic salt solution. This occurs prior to the coalescence of drops (Masalova *et al.*, 2006; Masalova & Malkin, 2007b). Overall, therefore, controlling the droplet size distribution of the dispersed phase during ageing is not essential, as the alteration in droplet size prior to crystallisation is not significant (Kharatiyan, 2005; Masalova *et al.*, 2006).

Crystallised explosive emulsions have a low detonation sensitivity for final applications (Coolbaugh & Mahamat, 2003). A number of studies show that the crystallisation phenomenon in explosives depends on the formulation and ratio of the various components (Ganguly *et al.*, 1992; Aronson & Petko, 1993; Villamagna *et al.*, 1993; Villamagna *et al.*, 1995b; Masalova *et al.*, 2006). This exerts a major influence on the emulsion, and affects, among other characteristics, its rheological properties/pumpability, portability, and detonatibility (Coolbaugh & Mahamat, 2003; Kovalchuk & Masalova, 2012). A number of factors affect the crystallisation process, including the following:

- oil type;
- oxidiser concentration (Ganguly *et al.*, 1992);
- impurities such as dust and ions (Becher, 1988; Adya & Neilson, 1991);
- dispersed phase volume fraction (Kharatiyan, 2005; Masalova *et al.*, 2006); and
- surfactant concentration, type and behaviour at the droplet interfaces (Ganguly *et al.*, 1992; Ghaicha *et al.*, 1995 Maheshwari & Dhathathreyan, 2004).

The crystallisation process might be initiated within the droplets, depending on the purity of the oxidiser (homogenous crystallisation) (Becher, 1988; Adya & Neilson, 1991), or at the droplet surfaces, depending on the properties of the interfacial layer (heterogeneous crystallisation) (Somasundaran, 2006; Tshilumbu *et al.*, 2010). As the crystals increase in size, they emerge from the layer separating the droplets and spread throughout the emulsion bulk phase (Becher, 1988; Kharatiyan, 2005; Masalova *et al.*, 2006). The commencement and crystallisation kinetics depend on the rigidity of the interface layer and the concentration of micelles (White *et al.*, 2004; Kharatiyan, 2005). Reverse micelle and/or multi-layers created by the surfactant prevent the propagation and spreading of crystallisation originating from aqueous droplets, throughout the remaining emulsion (Reynolds *et al.*, 2009a) by creating a steric barrier within inter-droplet layers (Prieve *et al.*, 2008; Roberts *et al.*, 2008). In addition, instability of emulsions has been observed when the micelle volume fraction in the system is critically low (Reynolds *et al.*, 2010).

2.5 EMULSIFYING AGENTS

Emulsions are inherently unstable. Thus, to ensure a stable shelf-life of an emulsion, emulsifier agents are often required. There are three general types of emulsifying agents. These include ionic materials, colloidal solids, and surfactants. The various types of emulsifying agents provide the stability of emulsions using inherently different mechanisms (Myers, 2005).

2.5.1 Solid particles

This category of emulsifying agent consists of fine solid particles with colloidal dimensions, normally less than 1 μm diameter, and is commonly used to stabilise "Pickering emulsions" (Pickering, 1907; Schlaepfer, 1918; Finkle *et al.*, 1923). The stability of such emulsions relies on the presence of a robust physical barrier produced by the particles, which itself depends on the nature of the particles and occurs either at a specific point of the interface and/or within the external phase (Myers, 2005).

2.5.2 Ionic materials

Adsorbed non-surfactant ions constitute a further category of emulsifying agent, with a minimal influence on interfacial tension. Stabilisation of the emulsion system by ionic materials is achieved by varying mechanisms. For example, these ions can impose a weak electrostatic barrier between drops and/or enable orientation of the solvent molecules at the interface, thereby creating the physical conditions required to stabilise the emulsion.

2.5.3 Surfactants

Surfactants, as shown in Figure 2.5, are usually comprised of a hydrophilic head group (water-soluble) and a hydrophobic (lipophilic) tail (oil-soluble).

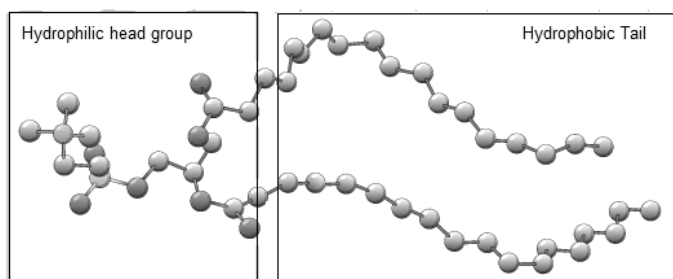


Figure 2.5: The typical structure of a surfactant (aceyourchemistry.blogspot.com)

Based on the nature of the hydrophilic group, the surfactant could be categorised as cationic, anionic, zwitterionic or nonionic.

A surfactant increases the stability of an emulsion by providing repulsive forces between droplet interfaces. This occurs by accumulation of the surfactant at the interface and/or micellisation in the solution. After mixing two phases of the emulsion, the surfactant molecules occupy the interface and orientate such that either end can interact with the preferred liquid phase. This decreases the free energy of the surface of the emulsion. Typical surfactants adsorb at the interface and prevent droplets from coalescing by producing electrical, mechanical, and steric barriers. These also reduce the interfacial free energy between the two phases (Myers, 2005). On the other hand, polymeric surfactants such as proteins, unlike monomeric surfactants, have a limited ability to orientate at the interface (Figure 2.6), which decreases their ability to reduce interfacial tension when compared with monomeric surfactants, due to varying functional groups (multiple anchoring points) in their structure. However, they provide excellent stability against coalescence and agglomeration, mainly by steric stabilisation (McClements, 2005). Moreover, using the polymeric molecules

to stabilise an emulsion increases the viscosity of the continuous phase and can retard creaming and reduce flocculation (Myers, 2005).

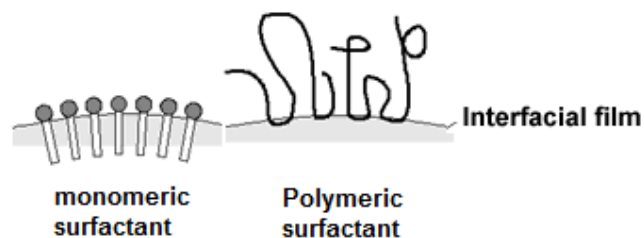


Figure 2.6: Schematic of monomeric and polymeric surfactants films (www.skin-care-forum.basf.com)

Griffin (1954) proposed the hydrophilic-lipophilic balance (HLB) number (0-20) of a surfactant as a tool to characterise the type of final emulsion. Surfactants with an HLB number in the range of 3 - 6 are expected to form W/O emulsions, whilst higher HLB numbers, between 8-18, form O/W emulsions. Different equations are formulated to calculate HLB numbers. Davies (2012) proposed the following formula:

$$HLB = 7 + (\text{hydrophilic group number}) - 0.475n_c \quad \text{Equation 2.2}$$

where n_c is the number of $-CH_2-$ groups in the surfactant tail.

Further studies by Shinoda and Friberg (1975) showed that taking only the HLB number of a surfactant into account did not entirely represent the behaviour of the surfactant molecules. Other parameters also exert an influence. These include the temperature (for non-ionic surfactants), type of oil and nature and concentration of electrolytes. A new method, “phase inversion temperature” (PIT), was proposed to assist in the selection of a suitable surfactant required for stabilisation of a specific emulsion. The HLB of nonionic surfactants alters appreciably with temperature (Kunieda *et al.*, 1987). The hydration forces between the hydrophilic head group of a surfactant and the water are more pronounced at lower temperatures. Under these conditions, the surfactant becomes increasingly hydrophilic and forms an O/W emulsion. At higher temperatures, the hydration force is minimal and the surfactant assumes a more lipophilic character. As such, it forms a W/O emulsion (Shinoda, 1969). Therefore, the PIT is a temperature at which the hydrophilic and hydrophobic properties of the surfactant are in equilibrium.

A theoretical feature of the surfactants established by Israelachvili *et al.* (1976) is based on the influence that the molecular geometry of surfactants has on controlling the thermodynamics and architecture of the micellisation process, and is independent of a detailed knowledge of molecular interaction energies. Briefly, the aggregation of the surfactants can be controlled by the “critical packing parameter” (CPP), P_v which is shown in Equation 2.3 (Myers, 2005):

$$P_v = v/a_0 l_c \quad \text{Equation 2.3}$$

where v is the volume of the hydrophobic portion of surfactant, a_0 the area occupied by the head group and l_c the length of hydrophobic tail.

The P_v value is a useful tool for predicting the shape and size of a surfactant aggregate (Figure 2.7) and therefore, the efficiency of packing of the molecules.

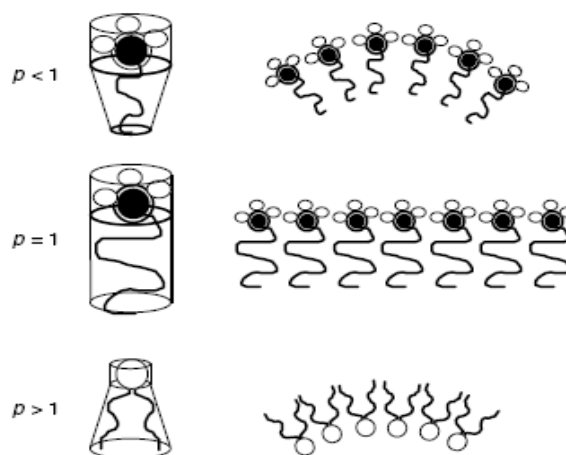


Figure 2.7: The aggregation of the surfactants controlled by critical packing parameter (McClements, 2005)

Under certain thermodynamic conditions in an emulsion, surfactant molecules can create self-assembled structures known as micelles. Typically these micelles exist in spherical form. The CPP was developed to relate the surfactant molecular structure to the expected aggregate shape (Nagarajan & Ruckenstein, 1991) and is used “to interpret the influence of the dynamic surfactant structure on the size and shape of the resulting micelles” (Liu, 2008, 267; Nagarajan, 2001).

2.5.4 Surfactants used to stabilise explosive emulsions

Selecting a suitable surfactant to prepare a stable explosive emulsion is crucial (Binet *et al.*, 1982; Cooper & Baker, 1989; Swarbrick & Boylan, 1991). The first requirement of a suitable surfactant is to lower interfacial tension such that new surfaces are stabilised as the emulsion forms. This property is known as the emulsifying capacity. The second requirement is the ability of an emulsion at rest to prevent both the coalescence of droplets and the crystallisation of salts from spreading from nucleated droplets to their dormant neighbours (Takamura *et al.*, 1979). A third desired feature, related to the first but seemingly at odds with the second, is the ability to preserve the interfacial layer dynamically when an emulsion explosive is sheared (Chattopadhyay, 1996b). To date, the surfactant systems (surfactant and co-surfactant) employed have been somewhat successful in meeting one or two of the above requirements. However, improvements in the combination of properties exhibited by emulsion systems are still sought, particularly for the successful combination of all three requirements in a single surfactant system.

The first explosive emulsions were prepared using oxazolines as surfactants. These are salts complexed to long tail fatty acids (Figure 2.8). They included calcium, magnesium and aluminium oleates, calcium stearate, sorbitan esters and an ethylene oxide condensate of fatty acids. It was found that approximately 1-5% w/w of surfactants with a solubility below 5% in water provided suitably stable emulsions (Egly & Neckar, 1964).

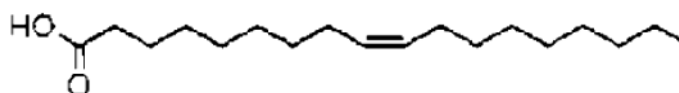


Figure 2.8: Oleic acid

Sorbitan fatty acid esters are particularly suitable emulsifiers. For example, a final emulsion prepared by using sorbitan monooleate (SMO) is claimed to be stable for a minimum of 28 days at a storage temperature of 21 °C (Figure 2.9). Emulsions prepared by using sorbitan monostearate, and sorbitan monopalmitate as emulsifiers had a similar stability (Bluhm, 1969). Moreover, when these emulsifiers were blended into the oil before the addition of the aqueous phase, this reduced both the amounts of emulsifier and energy required for mixing to produce a stable emulsion (Clay, 1978).

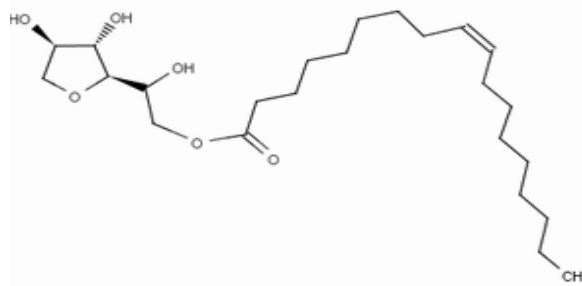


Figure 2.9: Sorbitan monooleate

SMO is a common emulsifier used in the explosives industry, due to cost-effectiveness and ready availability when a short storage time (shelf life) is not an issue (Egly & Neckar, 1964; Bluhm, 1969; Wade, 1973; Clay, 1978; Cescon & Millet, 1985; Edamura *et al.*, 1988).

Wade (1978) described a small-diameter cap-sensitive emulsion type explosive comprised of a mixture of carbonaceous fuel, water, inorganic salts, gas bubbles, a detonation catalyst, SMO, polyoxyethylene derivatives and diglycerides as emulsifiers. However, the disadvantages of Wade's compositions were that they exhibited limited stability; and became dehydrated and hardened during ageing. This adversely affected both the handling characteristics and explosive performance of these particular emulsions.

Patents relevant to the aforementioned emulsions did not address stability pertaining to the condition of the emulsion for several days or weeks before or after packaging, or before delivery in bulk form to a borehole. Various attempts to improve the storage characteristics of emulsion explosives have concentrated on the emulsifier component, and particularly on the selection of suitable emulsifiers, or blends thereof (Aronson & Petko, 1993; Aronson *et al.*, 1994; Ghosh & Rousseau, 2011). These blends are designed to suppress coalescence of the supersaturated droplets of the oxidizing salts present in the discontinuous phase (Cooper and Baker, 1989). Research was conducted using aliphatic amines (fatty acid amines) which were between 14 - 22 carbon atoms in tail length to stabilize EEs. Such emulsions showed acceptable shelf life length (Sudweeks & Jessop, 1979). Cationic emulsifiers with unsaturated hydrophobic tails, such as fatty acid amines which include substituted oxazoline (Figure 2.10), were claimed to have superior stability with regard to both detonability and inhibiting crystal growth (Sudweeks & Jessop, 1979).

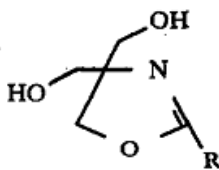


Figure 2.10: Substituted oxazoline (R represents an unsaturated hydrocarbon tail derived from unsaturated fatty acid, preferably oleic acid) (Sudweeks & Jessop, 1979)

Such features were not observed for emulsifiers with saturated hydrocarbon tails. It has also been noted that various combinations of unsaturated cationic emulsifiers, when used with selected liquid organic fuels, such as refined mineral oil, were effective in providing stability and detonability (Sudweeks & Jessop, 1980). Further, it is claimed that the use of soya lecithin as an emulsifying agent produces a stable explosive emulsion (Barnhard & Bahr, 1983).

A hydrocarbyl polyamine emulsifier (Figure 2.11) was introduced to provide improved stability and compatibility in an emulsion. Here, the ingredients were dissolved in oxidizing aqueous solutions (Cechanski, 1997). The resulting emulsion showed satisfactory long term shelf stability but was unstable when shear conditions were imposed.

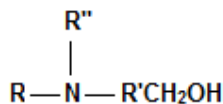


Figure 2.11: Hydrocarbyl polyamine (PIB) (Cechanski, 1997)

The use of the polyisobutylene (PIB) lipophilic group with a (M_w 400 - 5000) to stabilise EES has been emphasised by some research groups (Binet *et al.*, 1982; McKenzie & Lawrence, 1990; Venter & Kruger, 1996; Hales *et al.*, 2004). A bis derivative (with additional polymer tail) has been shown to improve both emulsion stability and detonation properties (McKenzie & Lawrence, 1990).

It has been suggested that the use of ammonium and alkali metal stearate, either individually or as a combination, as emulsifying agents provide improved stability under shearing conditions (Tomic, 1973). In 2003, explosive emulsifiers containing functional diene polymers such as isoprene, butadiene, and styrene (Figure 2.12) were invented, and emulsions prepared using these polymers showed an improved stability when subjected to shear conditions (Coolbaugh and Mahamat, 2003).

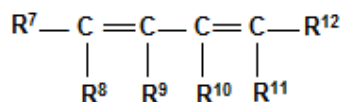


Figure 2.12: A conjugated diene wherein Rⁱ is either a hydrogen or hydrocarbonyl group (Coolbaugh and Mahamat, 2003)

The presence of amine groups in surfactant structures is claimed in many patents (Forsberg, 1989; McKenzie, 1991; Chattopadhyay, 1996a; Boer, 2003; Hales *et al.*, 2004). These surfactants act as a “crystal habit modifier” in an oxidising salt solution to control and limit the crystallisation nucleation, crystallisation growth and size of any salts that may precipitate. They may further enhance adsorption of hydrocarbon oils to microscopic salt crystals.

The presence of carboxylic and hydroxyl groups in surfactant structures has been claimed by various research groups (Yates & Dack, 1987; Chattopadhyay, 1996a; McKenzie, 1991; Venter & Kruger, 1996). Those carboxylic groups which can hydrolyze to form a carboxylic acid reduce deterioration to a minimum during storage (Yates & Dack, 1987).

Branched polyalkyl hydrocarbons such as polyolefins, including those derived from olefins containing from 2 - 6 carbon atoms, are present in some emulsifiers. Most common amongst these are ethylene propylene butane-1 and isoprene and isobutene (Cooper & Baker, 1989). It has been stated that copolymers containing oxygen and nitrogen atoms such as polyoxyethylene and polyethylene-imine (replacing the oxygen atom by N-H), can be used as emulsifiers (Binet *et al.*, 1982). The use of branched polyalkylene polyamines in EE formulation has also been reported (Forsberg, 1989).

The polymeric surfactants are expected to stabilise an emulsion during storage. Some commercial examples of these emulsifiers used in the explosive industry are PIBSA, and PIBSA combined with an amine (Reynolds *et al.*, 2002). Explosive emulsions stabilised by PIBSA-based surfactants are resistant to crystallisation for months (Masalova *et al.*, 2006). In PIBSA-based stabilised emulsions, a small portion of the surfactant forms a monolayer at the water-oil interface. Most of the surfactant molecules (~88%) form reverse micelles which are dissolved in the oil phase (Reynolds *et al.*, 2000; Reynolds *et al.*, 2001; Reynolds *et al.*, 2002; Reynolds *et al.*, 2010). Reynolds *et al.* (2001 & 2002) proposed that the film quality of the monolayer and the reverse micelle structure are dependent on the nature and polydispersity of the PIBSA tail length. The head group and ionic strength of PIBSA surfactant used are also important. The PIBSA-based emulsifiers with higher molecular

weight tend to enhance the formation of micelles more than PIBSA-based emulsifiers with low molecular weight and are least flexible and are associated with poorest coverage (Reynolds *et al.*, 2002; Reynolds *et al.*, 2010). However, the film quality of the monolayer and the reverse micelle structure are independent of the PIBSA surfactant concentration. Overall, the sole use of PIBSA-based emulsifiers provides long shelf life stability for explosive emulsions, but these same emulsions exhibit a tendency to destabilise under high shear conditions. PIBSA micelles in the oil phase are highly stable and cannot rapidly provide surfactant monomers to the newly formed surfaces which are created under high shearing conditions.

Addition of conventional emulsifiers to polymeric surfactants is claimed to stabilise emulsions (Binet *et al.*, 1982; Yates & Dack, 1987; Chattopadhyay, 1996b; Hales *et al.*, 2004). The addition of non-polymeric emulsifiers to the polymeric surfactants provides superior homogenisation of emulsions. Homogenisation additives are effective as they are more mobile (diffuse or migrate easily) than are the bulky polymeric emulsifiers. Thus, when new interfaces are formed under the high shear conditions, more mobile molecules (animal oils, fatty acid additives and common emulsifiers) migrate to the interface and provide stability by promoting the formation of smaller droplets and also by preventing crystallisation of the internal phase. Using a mixture of SMO, soya lecithin and polymeric surfactants such as poly-12-hydroxy steric acid and polyethylene glycol was reported to improve the stability of an emulsion against phase separation over a wide range of temperatures, i.e. -6 - +50°C (Bhattacharyya *et al.*, 1983). A mixed emulsifier system comprised of a derivative of PIBSA in combination with a co-surfactant such as SMO has been studied (Yates & Dack, 1987). This investigation on stability of emulsions prepared by a PIBSA/SMO mixture revealed that by using paraffin oil which compensates for the tail length difference between SMO and PIBSA, the destabilizing effect of SMO is suppressed (Chattopadhyay, 1996b). Adding a mixture of PIBSA-based surfactant with 1:4 sorbitan:oleic acid ratio to the emulsion system produced a fluid of vigorous explosive strength and excellent stability (Nguyen, 1991). Furthermore, mixtures of a PIBSA-based surfactant with vegetable oils and PIBSA combined with sorbitan sesquioxide demonstrated an improved performance with respect to crystallisation stability during both shelf life and under high shear when compared with a PIBSA/SMO mixture (Atkins, 1994; Shiao *et al.*, 1998). However, the mixture of PIBSA/sorbitan sesquioxide required the use of polar oil such as nitroalkane (Shiao *et al.*, 1998).

Chattopadhyay (1996a) demonstrated that the notable synergy in a mixture of low molecular weight PIBSA/high molecular weight PIBSA explained the improved performance with

respect to a tenacious resistance to shear-induced crystallisation and an increased stability during storage. The same author also claimed that the addition of animal oil or fatty acids to PIBSA-derived surfactants improved the long term stability of the homogenised emulsion phase (Chattopadhyay, 1996a). Hales *et al.* (2004) established that the improved stability was superior to that provided by an organic vegetable oil phase. Hobson *et al.* (2007) described a W/O emulsion obtained using a surfactant mixture comprised of a PIBSA-derived surfactant with a molecular weight range of 300 - 3000 together with an ethoxylated alkylamine. Among the aforementioned blends, a mixture of PIBSA/SMO is most commonly used by the explosive industries, as it yields a satisfactory performance during application. However, the long term stability of emulsions is reduced by addition of SMO to the system when compared to emulsions produced by use of solely PIBSA-based surfactants (Mudeme *et al.*, 2010). This can be explained by different hypotheses:

- The extensive difference between surfactant and co-surfactant tail length (the PIBSA tail has 38 carbon atoms and SMO tail has 18 carbon atoms) is responsible for destabilisation of emulsions under zero shear (shelf life). This is a result of decreased interaction energy caused by disruption in the molecular packing around the droplets. However, this decreased energy does improve stability under shear conditions (Shiao *et al.*, 1998);
- Greater attractive forces occurring between SMO and water molecules may suppress the interaction between PIBSA-Mea and the oxidiser in the emulsion. Thus PIBSA molecules are gradually replaced by SMO molecules at the interface (Kovalchuk *et al.*, 2010; Kovalchuk & Masalova, 2012). Over time, SMO molecules develop an opaque structure at the interface which may influence the mechanism of crystallisation (Drelich *et al.*, 2010).
- Reynolds, *et al.* (2009b) suggests that the explanation for the destabilisation mechanism of SMO is related to the destabilisation of PIBSA micelles by SMO molecules.

2.6 INTERFACIAL PROPERTIES OF EMULSIONS

The interactions among the molecular constituents of the two immiscible liquid phases and the surfactant of an emulsion control the interfacial properties of the system. Interfacial properties include the interfacial tension, disjoining pressure, Laplace pressure, contact angle and film thickness, all of which influence emulsion behaviour at both microscopic and colloidal levels. This enables the numerous macroscopic phenomena which occur in emulsions.

2.6.1 Interfacial tension

The differences in the various forces between molecules at a liquid/liquid interface create an excess energy known as “interfacial tension (σ)”. The excess energy or surface free energy tends to minimise the surface area of the droplets, and is responsible for the shape of dispersed phase drops. Interfacial tension can be formulated as a force/length expressed by using the SI unit of mN/m. Adding surfactant to the emulsion decreases the interfacial tension of the system. Increasing the concentration (C) of surfactants further decreases σ . However, once a certain critical mass of surfactant is reached, the concentration at the interface attains equilibrium with both free molecules and micelles of the surfactant in bulk. This concentration is known as the “critical micelles concentration” (CMC) (Figure 2.13). Adding more surfactant to the system beyond the CMC point has no effect on interface and the interfacial tension remains relatively constant.

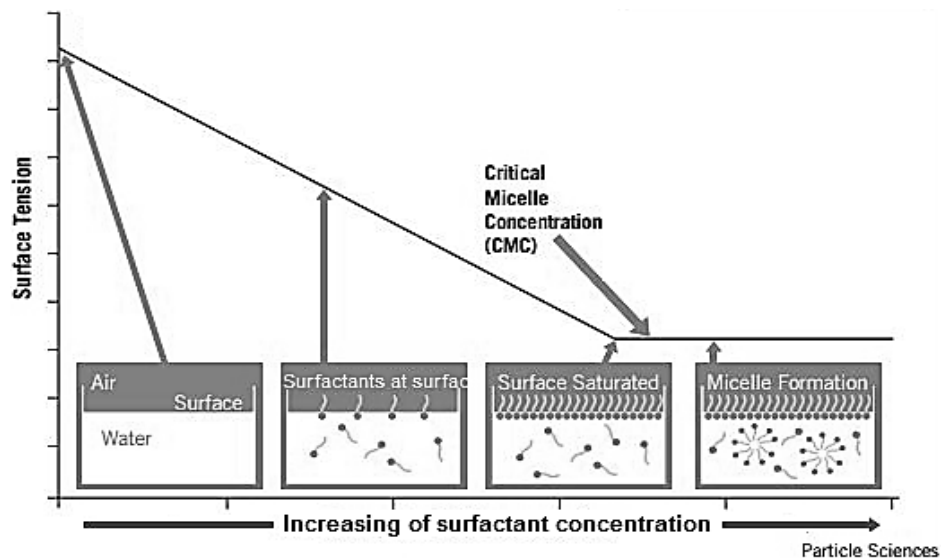


Figure 2.13: Variation of interfacial tension versus log concentration of surfactant in bulk at the water-oil interface (www.particlesciences.com)

Co-existence of micelles and surfactant disassociated in a system wherein the CMC point is exceeded was proposed by McBain (1913). Different properties of micelles are as follows (Adam, 1924; Hartley, 1936):

- When micelles occur as spheres, their radius is approximately equal to the length of hydrophobic tail.

- Micelles typically consist of 50 - 100 surfactant molecules (aggregation number). The aggregation number increases as the alkyl tail lengths of the surfactant increases.
- Micellisation occurs within a narrow concentration range, due to the high association of surfactants.
- Micelle properties are similar to those of a hydrophobic liquid. Thus they are highly mobile and often solubilise organic molecules. The aggregation number refers to the ratio between the core volume of micelles (V_{mic}) and volume of one tail (v) which can be calculated as (Tadros, 2006):

$$N = \frac{V_{mic}}{v} = \frac{4\pi R_{mic}^2}{a_s} \quad \text{Equation 2.4}$$

where a_s is the cross-sectional area of one surfactant and R_{mic} is the radius of a micelle.

2.6.2 Measuring interfacial tension: Wilhelmy plate method

Different methods are used to measure interfacial tension. These include the pendant drop, Wilhelmy Plate, and Du Noüy Ring methods (Klbron: *Measurement of surface tension*, n.d.). For the Wilhelmy plate method, a thin plate is used as the substrate and is attached to an electrobalance to measure the force (F) acting vertically on the plate. The plate is immersed at the water-oil interface and the interfacial tension can be calculated by using Equation 2.5.

$$\sigma = F / L \cos \theta \quad \text{Equation 2.5}$$

where L is the plate length and θ is the contact angle.

2.6.3 Laplace pressure

The Laplace pressure (Π_L) represents the pressure difference measured between the inner and outer curved surfaces of droplets. For the dispersed phase droplets in an emulsion, the Π_L is:

$$\Pi_L = 2\sigma / R \quad \text{Equation 2.6}$$

where σ is the interfacial tension and R is the droplet (curve) radius (de Gennes *et al.*, 2004, 9).

2.6.4 Contact angle

The contact angle (θ) is the angle formed by the intersection of the two liquids, liquid-vapour or liquid-solid interface (Yuan & Lee, 2013). For liquid beads on a solid surface, the contact angle is equal or higher than 90° . However, the contact angle associated with liquid spreading on a solid surface is much less ($\theta < 90^\circ$). The shape of a liquid droplet and its contact angle is determined by the interfacial tension of the liquid.

Young (1804) first described the contact angle of a liquid drop on a solid surface. According to Young, the mechanical equilibrium of the drop is influenced by three interfacial tensions (Figure 2.14).

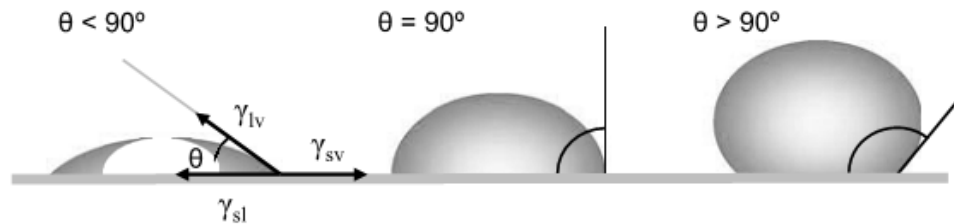


Figure 2.14: Schematic of contact angles formed by oil drops on a solid surface (Yuan & Lee, 2013)

This is expressed by Young's equation:

$$\sigma_{lv} \cos \theta = \sigma_{sv} - \sigma_{sl} \quad \text{Equation 2.7}$$

where σ_{lv} , σ_{sv} and σ_{sl} represent the liquid-vapour, solid-vapour, and solid-liquid interfacial tensions, respectively, and θ is the contact angle. Where there are two liquids, the σ_{lv} is replaced by σ_{l1v} which represents the liquid1-vapor, the σ_{sl} to σ_{l1l2} for liquid1-liquid2, and σ_{sv} to σ_{l2v} for liquid2-vapor interfacial tension.

2.6.5 Film thickness and disjoining pressure

When two drops are pressed together in an emulsion, their interfaces begin to deform due to short-range repulsion. This results in the creation of a thin film (h) of the continuous phase (Figure 2.15).

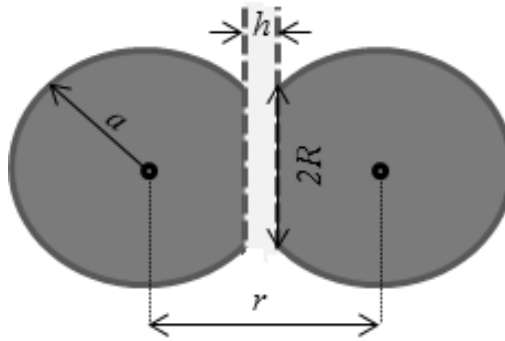


Figure 2.15: Liquid film between two neighbouring liquid drops

The nature of repulsion between droplet interfaces influences the thickness of this film. When droplets are highly compressed, the thickness of the film decreases. Derjaguin (1934) initially introduced a thermodynamic parameter, “disjoining pressure”, Π_{dis} to characterise the film thickness. This pressure is described as the net force (energy) per unit area that acts across the film:

$$\Pi_{dis} = -\frac{dG_T}{dh} \quad \text{Equation 2.8}$$

where G_T is the total interaction energy in the film. The G_T is dependent on the nature of the surfactant and the type of repulsion it creates in the film (or interfacial layer).

The disjoining pressure is the difference between the thermodynamic equilibrium state pressures on surfaces. It is caused by a thin interfacial region, and the pressure in the bulk phase which results from the interaction between the surfaces of droplets (Bergeron, 1999; Sadoc & Rivier, 1999). The maximum film thickness (h_{max}) of neighbouring droplets can be determined as (Foudazi *et al.*, 2010b):

$$h_{max} = D_{32} \phi^{*1/3} (\phi^{-1/3} - 1) \quad \text{Equation 2.9}$$

where ϕ^* represents the maximum closest packing of droplets.

2.6.6 Interaction energies (forces) between droplets

Different types of intermolecular forces or interactions in the interfacial thin film affect the stability of an emulsion. These are summarised below. Van der Waals forces of attraction

tend to destabilise the emulsion, whereas electrostatic and steric repulsions provide stability within the emulsion (Tadros, 2006).

2.6.6.1 Van der Waals forces

Van der Waal's forces are weak attractive interactions between molecules and are the result of London (dispersion interaction), Debye (dipole-induced dipole interaction) and Keesom (dipole–dipole interaction) forces. The dipole interactions are a product of the chemical nature of molecules involved. Generally, their contribution to the total energy is not as significant as that associated with the energy originating from London forces (Myers, 2005; Tadros, 2006). Hamaker (1937) suggested that the presence of London dispersion between the emulsion droplets species results in a marked attraction, particularly between closely-packed neighbouring droplets. The total van der Waals attraction (G_A) between two spherical droplets with equal radius (a) separated by a distance (h) is determined by using the following equation (Tadros, 2006):

$$G_A = -\frac{A_H a}{12h} \quad \text{Equation 2.10}$$

where A_H is the effective Hamaker constant, a droplet radius and h is film thickness .

For HCEs the droplets are deformed and G_A is determined as follows (Petsev, 2004, 328):

$$G_A = -\frac{A_H}{12} \left\{ \begin{aligned} & \frac{2aL}{(L+h)^2} + \frac{2aL}{h(2L+h)} + 2 \ln \left[\frac{h(2L+h)}{(L+h)^2} \right] + \frac{R^2}{h^2} - \frac{2R^2}{h(L+h)} \\ & - \frac{2R^2}{(L+h)[2(L-a)+h]} + \frac{(h^2 + 4R^2)(\sqrt{h^2 + 4R^2 - h})}{2h[2(L-a)+h]} \\ & - \frac{2R^2(2L^2 + Lh + 2ah)}{h(L+h)^2[2(L-a)+h]} \end{aligned} \right\} \quad \text{Equation 2.11}$$

Where $L = a + \sqrt{a^2 - R^2}$ and $2R$ is the diameter of deformed droplet (Figure 2.15).

Several factors, as defined by McClements (2005), can exert an effect on van der Waals interactions:

- size of droplets (interactions between bigger droplets are greater);
- physical properties of both dispersed and continuous phases;

- distance between droplets (the closer the droplets are together, the more the interaction increases, whereas when this distance increases, the interaction becomes negligible);
- thickness and composition of the adsorbed emulsifier layer; and
- presence and concentration of electrolyte (interaction is weaker as the concentration of the electrolyte increases in the emulsion).

2.6.6.2 Electrostatic forces

Electrostatic forces result from the interpenetration of a layer (Figure 2.16) which is surrounded by ionized emulsifiers. If two electrically charged droplets approach one another, and the distance between them becomes less than the thickness of the double electric layer, the overlapping of the layers creates repulsion. The degree and charge of the electrical force on an emulsion droplet depend on the following:

- type and concentration of emulsifier at the interface; and
- environmental conditions, such as pH, temperature and ionic strength (McClements, 2005).

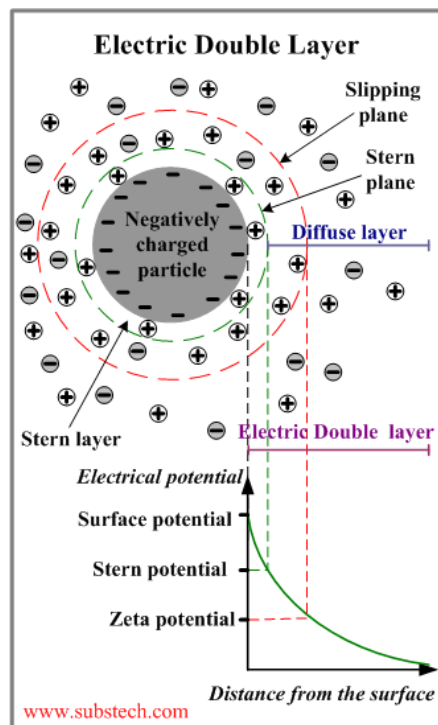


Figure 2.16: A schematic representation of the electrically charged double layer of a charged particle (Substech.com)

Three types of ions influence the surface charge of a particle. These are the potential-determining, indifferent electrolyte and adsorbed ions (McClements, 2005). The first type is responsible for the association-dissociation of the charged groups, the second type accumulates around the charged groups, creating an electrostatic interaction, and the third originates from the alteration of ionized surfactants. To stabilise the emulsion in absence of steric repulsions, the energy of the attractive forces must be less than that of the double layer repulsion (McClements, 2005).

2.6.6.3 Steric repulsion

Steric stabilisation arises from the presence of a mechanical barrier which prevents the coalescence of dispersed phase drops, when the droplets approach each other and become too close. A steric repulsion between droplets results as the surfaces are surrounded by an adsorbed high-molecular-weight polymer, or surface-active solid particles or long-tail non-ionic surfactants. This barrier effectively separates the droplets.

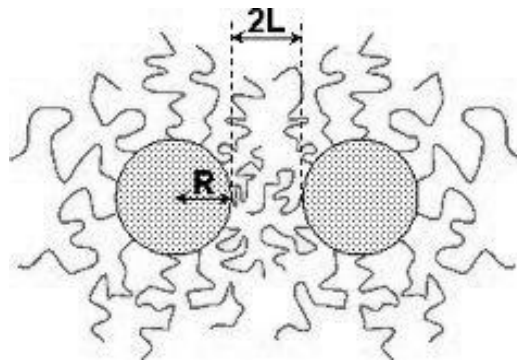


Figure 2.17: A schematic representation of steric stabilization (R =radius) (home.unist.ac.kr)

As shown in Figure 2.17, steric interaction occurs between two approaching surfaces when the film thickness between these surfaces is of the order of, or less than, $2L$, where L is the mean-square end-to-end distance of the hydrophilic portion of the emulsifier tail (Russel *et al.*, 1989).

Other types of short-range interactions include oscillatory structural, hydrophobic attraction, repulsive hydration, fluctuation wave and protrusion.

2.6.7 Molecular interactions in binary surfactant systems

Surfactant mixtures are commonly used in many emulsion formulations, principally due to the superior properties these mixtures have when compared to single surfactants (Scamehorn,

1986; Holland & Rubingh, 1992; Huibers & Shah, 1997; Zhou & Rosen, 2003; Szymczyk, 2012). It is well known that different compounds in a mixture interact with each other and create either favourable or unfavourable conditions for a specific application. Interaction between binary surfactants results in an altered equilibrium composition at the interface or in the micelles from the bulk (Szymczyk & Jańczuk, 2007).

Generally, four types of behaviour are possible in mixed systems, i.e. synergetic, antagonistic, additive or indifferent (ideal). The first two are caused by the molecular interaction between different surfactants (ideality deviation) and are relevant to different industrial applications (Dynarowicz-Łątka & Kita, 1999). The nature and strength of interaction in the interfacial monolayer depends on the chemical structure of surfactants (hydrophobic tail and head group). Attractive forces between the hydrophobic tails of surfactant result in an aggregation in the form of micelles or multilayers. Whether repulsive or attractive interaction occurs will depend on the electrostatic charges of the head group (non-ionic, cationic or anionic). The interaction between head groups is normally greater than that between the tails. Hence, head groups are generally responsible for the non-ideality of the system (Holland & Rubingh, 1992). Over decades, many investigators have discussed these mixtures in terms of different concepts and have proposed different empirical (Talmon & Prager, 1978) and semi-empirical models (Zana, 1995; Rosen & Gu, 1987).

Some research groups have determined interactions in mixed insoluble monolayers using additivity rules, similar to the manner in which binary volume mixtures are interpreted (Goodrich, 1957; Gaines & George, 1966). These thermodynamic approaches have considered the monolayer of only two surfactants and ignored the presence of a solvent in the system (Langmuir films). Conversely, some investigations into the adsorbed monolayer of a single surfactant showed that the non-ideality behaviour originates from an interaction between surfactant and solvent (Butler, 1932; Defay & Prigogine, 1951; Fowkes, 1962). One of the most salient points among different research approaches is the definition of ideal behaviour i.e. absence of interactions. Experimental data show that the non-ideality of one approach might fall into the ideal range of a different approach (Dynarowicz-Łątka & Kita, 1999).

The following thermodynamic approach has been used as a fundamental method to study the interactions in an adsorbed monolayer in a system comprised of two surfactants (1 and 2) which are dissolved in a solvent such as water. The chemical potential of surfactant 1 in the bulk (μ_1^b) is given in Equation 2.12:

$$\mu_1^b = \mu_1^{0,b} + RT \ln f_1^b c_1 \quad \text{Equation 2.12}$$

where f_1^b is the activity coefficient and c_1 is the concentration of surfactant 1 in the bulk solution. The $\mu_1^{0,b}$ is the reference state of chemical potential of a 1 M solution of pure surfactant 1.

The chemical potential of a surfactant at the interface, which is in equilibrium with the bulk, is related to the surface tension (σ) and area per molecule of the surfactant 1 (A_1) (Butler, 1932; Frumkin, 1925):

$$\mu_1^s = \mu_1^{0,s} + RT \ln f_1^s X_1 + (\sigma^0 - \sigma) A_1 \quad \text{Equation 2.13}$$

$$X_1 = \frac{\Gamma_1}{\Gamma_1 + \Gamma_2 + \Gamma_0} \quad \text{Equation 2.14}$$

where σ^0 is the initial surface tension, $\mu_1^{0,s}$ is the standard chemical potential of a pure surfactant layer at the surface and $\sigma = 0$; X_1 is the molar fraction of surfactant 1 at the interface and Γ_i is the molar Gibbs surface excess of surfactants 1, 2 and solvent (0), respectively.

In the case of an ideal mixture, when there is no interaction between molecules, the second term on the right hand side in Equation 2.13 is equal to zero, whilst in a non-ideal system the activity coefficient differs from unity. For the dilute system of surfactants (low concentration), the chemical potential of the solvent in the bulk and at the interface are similar ($\mu_0^b = \mu_0^s$). The interaction coefficient of solvent (f_0^s) is expressed by Equation 2.15 (Butler, 1932):

$$\pi = (\sigma_0 - \sigma) = -\frac{RT}{A_0} \ln f_0^s X_0^s \quad \text{Equation 2.15}$$

where surface pressure (π) is considered as an osmotic pressure.

Replacing the molar Gibbs surface excess of solvent with $\sum \Gamma_i A_i = 1$ will yield Equation 2.16, which can be regarded as a general surface equation state. This can be used for both single and binary mixtures of surfactants (Dynarowicz-Łątka & Kita, 1999).

$$\pi = -\frac{RT}{A_0} \left[\ln \left(1 + \frac{A_0(\Gamma_1 + \Gamma_2)}{1 - A_1\Gamma_1 - A_2\Gamma_2} \right) \right] - \ln f_0^s \quad \text{Equation 2.16}$$

By using Equation 2.16, different models with variable assumptions are derived. For example, considering identical surface areas of surfactants and the activity coefficient of a solvent equal to one, this equation will be similar to the Frumkin isotherm (Frumkin, 1925) and Szyszkowski-Langmuir adsorption equation. Lucassen-Reynders (1973) suggested that the interactions between components in a monolayer can be estimated by defining a mean molar area ($\bar{A} = \frac{1}{\Gamma_1 + \Gamma_2}$). This approach also takes into account the solvent effect and can be used for both soluble and insoluble monolayers (Lucassen-Reynders, 1973). Under equilibrium conditions ($\mu_i^b = \mu_i^s$) the interaction of surfactants molecules can be calculated assuming an ideal entropy of final mixing and by using the activity coefficient obtained from the second term of the Margules expansion approximations (first term=0) (Fried *et al.*, 1975):

$$\begin{aligned} \ln f_1^s &= \beta(1 - X_1)^2; \\ \ln f_2^s &= \beta X_1^2 \end{aligned} \quad \text{Equation 2.17}$$

where β is a dimensionless interfacial parameter indicating the degree of non-ideality of the system (Rosen & Gu, 1987). The β parameter is an indicator used to compare the molecular interaction of surfactant mixtures with the self-interactions of individual surfactants before mixing, as is shown in Equation 2.18 (Rubingh, 1979).

$$\beta = [W_{12} - (W_{11} + W_{22}) / 2] / RT \quad \text{Equation 2.18}$$

where W_{11} and W_{22} represent the molar self-interaction energy of surfactants 1 and 2, respectively. The W_{12} is the molar interaction energy between the mixed surfactants at a water-oil interface.

Non-ideality can be expressed by using the heat of mixing (ΔH^M):

$$\Delta H^M = \Delta G^{exc} = \beta X_1(1 - X_1) / RT \quad \text{Equation 2.19}$$

where ΔG^{exc} is the excess energy of the mixing. The resulting equations are summarised in the following model developed by Rosen (Rosen & Kunjappu, 2012).

$$\frac{X_1^2 \ln(\alpha C_{12} / X_1 C_1)}{(1 - X_1)^2 \ln[(1 - \alpha) C_{12} / (1 - X_1) C_2]} = 1 \quad \text{Equation 2.20}$$

$$\beta = \frac{\ln(\alpha C_{12} / X_1 C_1)}{(1 - X_1)^2} \quad \text{Equation 2.21}$$

where α is the molar fraction of surfactant 1 in the total surfactant mixture in solvent. Values C_1 , C_2 and C_{12} are the molar concentrations of the individual surfactants 1, 2 and as a mixture, respectively, which are required to produce a given interfacial tension before CMC.

A negative value for β implies more attractive or less repulsive interaction between two surfactants at interface. This is known as “synergism” which increases the packing efficiency in the interfacial monolayer. A positive value of β indicates additional repulsive or less attractive interaction, and is known as “antagonism”. The β value can also be used for interaction in binary micelles by replacing concentrations in Equation 2.20 and 2.21 with the CMC values of the pure surfactants and the CMC of the surfactant mixture (Rosen & Kunjappu, 2012). Other micellisation models can be found elsewhere (Clint, 1975; Motomura *et al.*, 1984; Maeda, 1995).

Synergism in binary surfactant mixtures has been the focus of many studies, due to the wide range of applications in the food and cosmetic industries (Chow & Ho, 1996; Lu & Rhodes, 2000; Campana *et al.*, 2013). Few studies report on synergism of mixed monolayers in HCEs with an oversaturated dispersed phase. Here, the stability is related to the crystallisation phenomenon, rather than to the coalescence of droplets (Ghaicha *et al.*, 1995; Masalova *et al.*, 2011b). Using the Langmuir method, Ghaicha *et al.* (1995) examined various surfactant mixtures of several surfactants used in explosive emulsion formulations. The packing efficiency of these binary systems was markedly affected by the tail length of the oil when the latter was used as the solvent. Under conditions of tail length compatibility and high synergism, HCEs with maximum stability were produced. The interfacial interactions and elasticity behaviour of surfactants with different head groups and identical hydrophobic tails in liquid explosives were studied. These were related to the rheological properties of the resultant emulsions (Masalova *et al.*, 2011a).

2.7 EMULSIFICATION

The aim of emulsification is to produce a desirable size of dispersed phase droplets for a certain application. When two immiscible liquids are placed in the same container, the most

thermodynamically stable state is that which creates one layer above the other. This depends on the respective liquid viscosities. To produce an emulsion, either a surfactant or a considerable amount of energy, or both, are required (McKenna, 2003). The emulsification process consists of two steps (Figure 2.18).

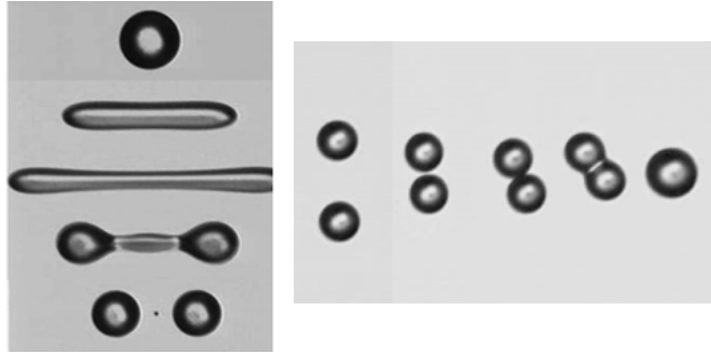


Figure 2.18: A schematic diagram of droplet break-up and re-coalescence during the emulsification process (Walstra, 1993)

During the first step, one phase of the emulsion is disrupted to form droplets. These droplets further deform and thereby produce smaller droplets. This increases the emulsion specific surface area. During the disruption phase, two types of forces act against each other. These antagonistic forces are the interfacial forces characterised by Laplace pressure, which tends to hold droplets in shape, and the disruptive forces (shear) which result from mixing. These latter forces tend to pull the droplets apart (Walstra, 1993).

Depending on which force is dominant, the emulsification separates into:

- a *stability zone*, where the Laplace pressure is higher ; and
- a *breaking zone*, where shearing forces are breaking droplets (Jackson & Tucker, 2003).

To establish the break-up criterion, the capillary number (Ca) has been defined as the ratio between the two opposite forces:

$$Ca = \frac{\eta_e \dot{\gamma}_{av} R}{\sigma} \quad \text{Equation 2.22}$$

where η_e is the viscosity of continuous phase, $\dot{\gamma}_{av}$ is the average shear rate in the mixer, R is droplet radius ($R = D_{32}/2$), and σ is the interfacial tension.

A small capillary number represents the stability zone when the interfacial stress dominates, and once a critical value (Ca_{crit}) is exceeded, droplets become unstable and disintegrate. The dependence of the critical capillary number on the viscosity ratio ($p = \eta_i/\eta_e$) was demonstrated by Grace (1982) where η_i is the internal (dispersed) phase viscosity and η_e is the external (continuous) phase viscosity (Figure 2.19). If the viscosity ratio < 1 , the effect of interfacial tension on break-up is significant, while for higher viscosity ratios, the internal circulation within the drops is the dominant factor. Relatively high viscous stress of internal circulation in the drops decreases the viscous forces of the external phase, which favours smaller deformation. It has been found for highly concentrated emulsions that the viscosity of the external phase must be replaced with the viscosity of the emulsion (η_{em}) in Equation 2.22 and the viscosity ratio (p) formula (Mudeme *et al.*, 2010).

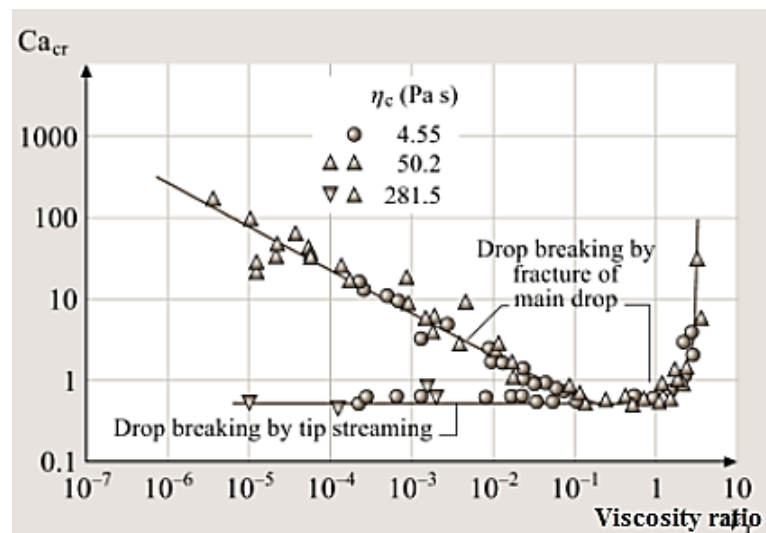


Figure 2.19: Grace curve (1982) showing the influence of the viscosity ratio on the capillary number in shear flow (Tropea *et al.*, 2007)

During the second step of emulsification, the newly formed small droplets must be stabilised by a suitable quantity of surfactant. This prevents re-coalescence and the droplets remain kinetically stable for a reasonable time period (Walstra & Smulders, 1998). Emulsion droplets have a tendency to re-coalescence. The reason for this is twofold. The droplets are thermodynamically unstable and they may not be completely covered by surfactant molecules. The droplets undergo relative motions which lead to collisions among them. The collisions, together with drainage of the continuous phase between neighbouring droplets can cause re-coalescence (Mohan & Narsimhan, 1997). To prevent re-coalescence, the rate of surfactant adsorption to interface must occur more rapidly than do the collisions (Jafari *et al.*, 2008).

2.7.1 Effect of surfactant structure on emulsification

Many factors influence the size and re-coalescence of droplets. These include surfactant type and concentration, surfactant adsorption rate, emulsion composition and formulation and energy input. Two important roles of a surfactant during the emulsification process are (Brösel and Schubert, 1999):

- decreasing the interfacial tension at the water-oil interface, thereby decreasing the amount of energy required for the disintegration of a droplet; and
- creating a layer which surrounds newly formed droplets, thus preventing re-coalescence (Figure 2.20).

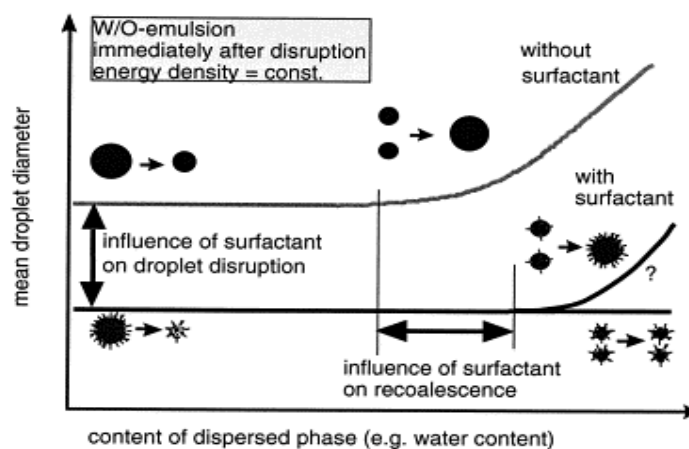


Figure 2.20: Droplet disruption and stabilisation in emulsification with and without surfactant (Brösel & Schubert, 1999)

The final droplet size, or the refining period required to reach a desired droplet size, therefore depends on different characteristics of the surfactant, according to McClements (2005):

- Surfactant concentration - sufficient surfactant must be available to completely surround the droplet surfaces.
- Rate of adsorption - the time needed for the surfactant to diffuse through the continuous phase and adsorb to the droplet surface.
- Adsorption efficiency - the probability that the surfactant can adsorb at interface which causes a marked decrease in interfacial tension.
- Effectiveness of surfactant layer - an efficient dense layer decreases the probability of droplet re-coalescing.

- Interfacial rheology - the viscoelastic interfacial layer created by the surfactant provides a resistance to the deformation of droplets, thus making the disintegration process difficult but decreasing the possibility of re-coalescence.

The amount of surfactant required to produce the desired small droplets depends on its activity (f_s) in the bulk. Activity of surfactant determines the reduction in interfacial tension, as formalised by the Gibbs adsorption equation:

$$-d\sigma = RT\Gamma \ln f_s \quad \text{Equation 2.23}$$

where R is the gas constant, T absolute temperature and Γ the surface excess (number of moles of surfactant adsorbed per unit area of interface).

The reduction of interfacial tension is influenced by the nature of the surfactant and oil in the emulsion formulation. Some systematic research has investigated the effect of surfactant type on emulsification (Narsimhan & Goel, 2001; Lobo & Svereika, 2003; Tcholakova *et al.*, 2004). Based on these studies, there are two regimes for discussion:

- *Surfactant-rich regime*: Here, the droplet size depends on interfacial tension of the surfactant and the extent of the forces applied during mixing and is not affected by the surfactant concentration.
- *Surfactant-poor regime*: Here the droplet size is markedly influenced by the surfactant concentration (McClements, 2005):

$$D_{\min} = \frac{6\Gamma\phi}{c_{surf}} \quad \text{Equation 2.24}$$

where ϕ is the dispersed phase volume fraction, C_{surf} is the surfactant concentration and D_{min} is the sauter diameter (D_{32}) in the case of a polydispersed emulsion.

Interfacial adsorption of a surfactant is an important factor which determines the degree of stabilisation in the re-coalescence process (Karbstein & Schubert, 1995; Schulz & Daniels, 2000; Stang *et al.*, 2001; Schultz *et al.*, 2004). The newly formed interface around the droplets must be coated rapidly. High molecular weight surfactants such as polymers show slow molecular movement and increase the re-coalescence rate. Thus they extend the time of emulsification (Jafari *et al.*, 2008). Linear and low molecular weight surfactants rapidly

occupy fresh interfaces. Therefore, re-coalescence of droplets is low (Schulz & Daniels, 2000). Another factor affecting emulsification time is the ability of surfactants to reduce the interfacial tension. The greater the reduction of the interfacial tension by a surfactant at a certain applied energy, the greater the decrease in the emulsification time (Kolb *et al.*, 2001). The kinetics of surfactant adsorption is discussed by several authors (Stang *et al.*, 2001; Brosel & Schubert, 1999; Schulz & Daniels, 2000; Flourey *et al.*, 2003). Where binary surfactants are concerned, the interaction of surfactants is one of the factors which may affect the emulsification process. The interaction between surfactants can cause ingredients to compete with respect to the occupation of the surfaces of newly formed drops. This alters the time required for emulsification (Jafari *et al.*, 2008).

2.7.2 Droplet size and droplet size distribution

The emulsification process normally consists of two events: 1) the creation of an emulsion from two immiscible liquids (pre-emulsion); and 2) the reduction of droplet size to a desired value in the existing emulsion (refining).

One of the important parameters used for determining emulsion properties, such as shelf life and appearance, is the magnitude of the individual dispersed phase droplets. The droplet size distribution is a result of equilibrium between two opposing processes which occur during emulsification (*viz.* break up and re-coalescence of droplets). Most commonly, the emulsion product contains droplets of variable sizes and these are known as polydispersed emulsions. Generally it is convenient to measure mean particle size (\bar{x}) and the standard deviation of particle size, (ω) (Hunter, 1986; Rawle, 2011). These can be calculated as indicated:

$$\bar{x} = \frac{\sum_{i=1} n_i x_i}{N} \quad \text{Equation 2.25}$$

$$\omega = \sqrt{\frac{\sum_{i=1} n_i (x_i - \bar{x})^2}{N}} \quad \text{Equation 2.26}$$

where n_i is the number of droplets in the size class i , N is the total number of droplets and x_i is the value of the particle size of class i . Different average droplet sizes (x_{ab}) can be defined based on frequency of distribution (S_n):

$$S_n = \int_0^{\infty} x^n F(x) dx \approx \sum_{i=1}^n n_i D_i^n \quad \text{Equation 2.27}$$

$$x_{ab} = \left(\frac{S_a}{S_b} \right)^{1/(a-b)} \quad \text{Equation 2.28}$$

where a and b are integers normally between 0-6 and S_n is the n^{th} moment of distribution. The D_{32} (x_{32}) is the area-volume average diameter which is related to the average surface area of internal phase (A_N) exposed to continuous phase per unit per volume of emulsion (Walstra, 2002):

$$A_N = \frac{6\phi}{D_{32}} \quad \text{Equation 2.29}$$

2.7.3 Evolution of droplet size and droplet size distribution in highly concentrated emulsions (HCEs)

Droplet size distribution can be described by the Gauss function (f) for explosive emulsions (Figure 2.21):

$$f = \frac{A}{\omega\sqrt{\pi/2}} e^{-2(d-d_{50})^2/\omega^2} \quad \text{Equation 2.30}$$

where ω is the width and d_{50} is the maximum value of the distribution curve, A is the fitting parameter and d is the experimental droplet size distributed over the curve.

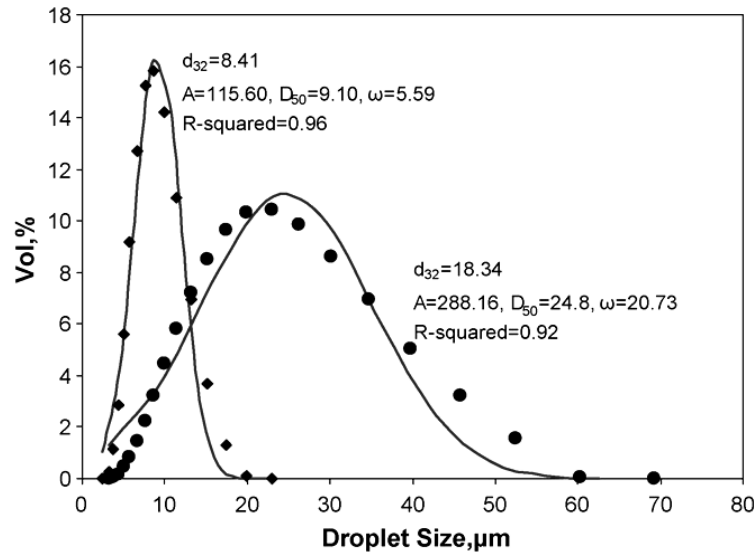


Figure 2.21: Typical Gauss for explosive emulsions with different sauter droplet sizes and stabilised by PIBSA-Mea (Mudeme *et al.*, 2010)

During emulsification of explosive emulsions, initially the sauter droplet size (D_{32}) decreases markedly with time and the range of droplet size distribution is narrow. As the time period increases, the reduction of droplet size becomes slower and it remains relatively constant (Figure 2.22).

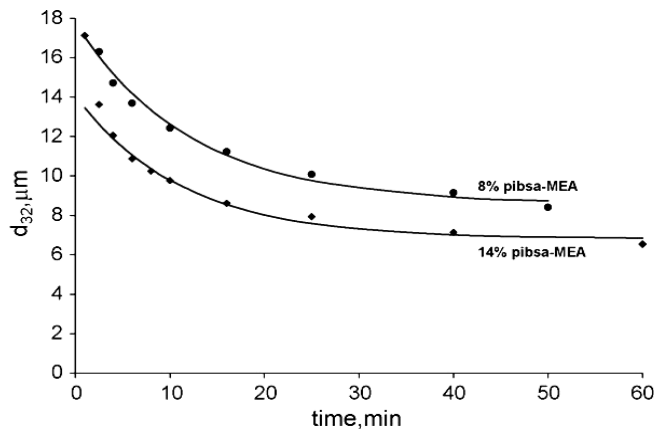


Figure 2.22: Evolution of the average diameter of droplets during prolonged shearing for EEs stabilised with 8 and 14% PIBSA-Mea. The same trend can be observed for the range of droplet size distribution (Mudeme *et al.*, 2010)

Thus it is possible to introduce a minimum value of ω and D_{32} (ω_{crit} and d_{crit}) at $t \rightarrow \infty$. Equation 2.31 can be used to accommodate the experimental results obtained from droplet size evolution over time (Mudeme *et al.*, 2010) :

$$D = D_{crit} + e^{-(t/\theta)} (D_0 - D_{crit}) \quad \text{Equation 2.31}$$

where D_0 and D_{crit} are fitting parameters, D_0 corresponds the initial time of refining and θ is the characteristic time of a certain formulation and process condition which is independent of D_0 . The same model is applicable for ω .

2.8 RHEOLOGICAL PROPERTIES

In addition to interfacial tension measurement (Takamura *et al.*, 1984; Ishii *et al.*, 1988; Krawczyk *et al.*, 1991), rheological measurements have also been used for the evaluation of emulsion stability (Zografi, 1982).

“Rheology is the science of deformation and flow of matter” (Fredrickson, 1964, 25). Depending on the nature of a solid, its response to an applied force varies from plastic, through viscoelastic to elastic. Elastic materials deform under an applied force and return reversibly to their original state as soon as the force is removed. However, a plastic deformation is irreversible and plastics flow as a fluid after a certain amount of force has been applied (Malkin *et al.*, 2006). The rheological properties of dilute, semi-dilute and highly concentrated emulsions have been reviewed in many studies (Oldroyd, 1955; Choi & Schowalter, 1975; Aomari *et al.*, 1998; Derkach, 2009). Investigations revealed that increasing an emulsion concentration in excess of a critical value could considerably modify its structural and rheological properties (Figure 2.23). This includes the yield stress appearance and a marked change in viscosity (Mason, 1996; Mason *et al.*, 1999).

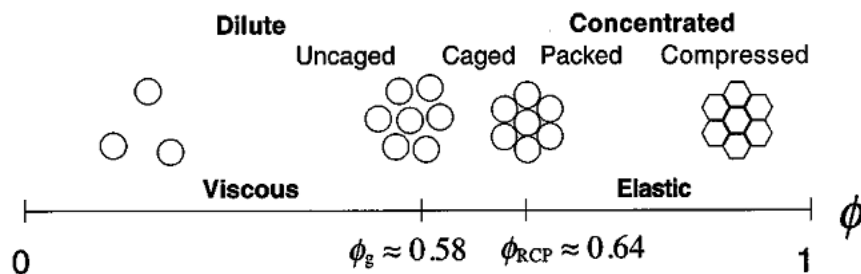


Figure 2.23: Schematic diagram of the structure of droplets in emulsions within a range of 0 to 1 volume fractions (Mason, 1999)

Droplets in HCEs exist as closely-packed connected polyhedrons, thus prohibiting free movement of droplets. When shear is applied to the HCEs, the hexagonally shaped droplets

deform to that of parallelogram and therefore the film area increases. When deformation is slight and stresses are minimal, HCEs behave as soft solid matter. Hence such emulsions cannot flow below the “yield stress” point value. The yield stress point (Figure 2.24) signals the departure of the structure in dispersed phase droplets from the initial unsheared polyhedral form. At this point, the assumed parallelogram-shaped droplets become unstable under shear and new smaller droplets are generated which invert to a hexagonal conformation. As soon as the shear applied increases beyond the yield stress point, the emulsion flows irreversibly. The HCEs therefore display the characteristics of a typical non-Newtonian fluid. Non-Newtonian fluids are characterised by a shear-rate dependent viscosity and/or elastic effects.

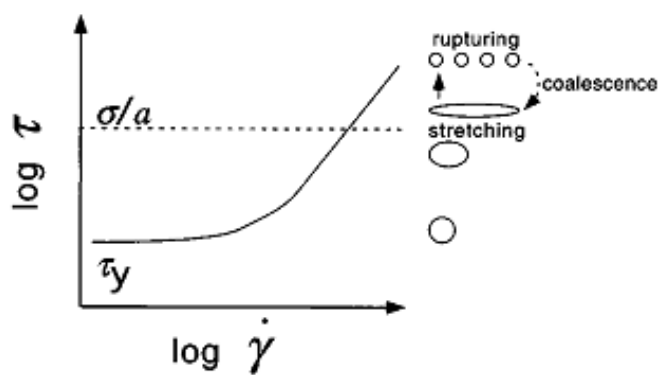


Figure 2.24: Schematic logarithmic diagram of the steady shear stress, τ , versus shear rate for HCEs (solid line). By increasing the shear rate, τ exceeds the yield stress value where viscous behaviour is dominant. As soon as τ attains the Laplace pressure scale (σ/a) the droplets deform, stretch and rupture (dashed line) and depending on interfacial properties may also re-coalesce (Mason, 1999)

Liquid explosives are a class of HCE containing an oversaturated solution comprised predominantly of AN or another oxidiser. Therefore, liquid explosives show complex non-Newtonian behaviour, as do the HCEs. This includes viscoelasticity, rheopectic properties, and yield stress. A remarkable amount of research has been dedicated to the rheological analysis of the explosive type HCEs, including steady flow, transient regimes of deformation and viscoelastic tests (Masalova *et al.*, 2003; Malkin *et al.*, 2004; Masalova *et al.*, 2005; Masalova & Malkin, 2007a; Masalova & Malkin, 2007b; Masalova & Malkin, 2007c; Masalova & Malkin, 2008; Foudazi *et al.*, 2010b; Masalova *et al.*, 2011a; Foudazi *et al.*, 2012; Masalova & Malkin, 2013). For this study, an overview of investigations into the rheology of HCEs, including the explosive emulsion type, was done. A summary of this follows.

2.8.1 Viscoelasticity

The elasticity of HCEs originates from an increase in the surface area of droplets associated with the transition from spherical to polyhedral form. This is balanced by the osmotic pressure of droplets and this, in turn, can be measured by using Laplace pressure. The elasticity behaviour of the HCEs can be identified by the independence of the elastic modulus over an extensive range of frequency sweep (Figure 2.25) (Lacasse *et al.*, 1996; Masalova *et al.*, 2005).

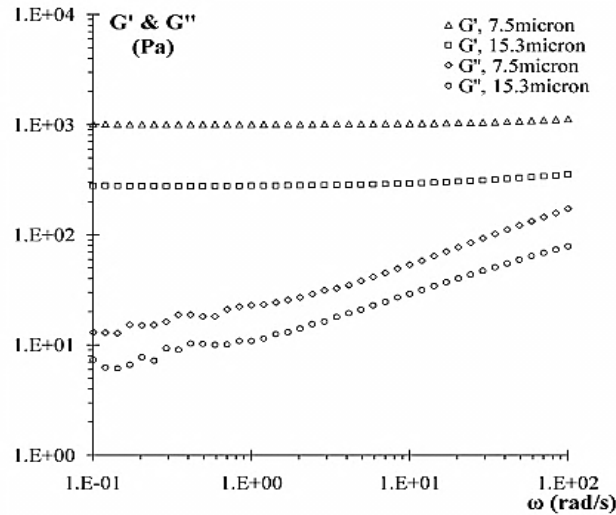


Figure 2.25: Typical frequency sweep results obtained for different droplet sizes of HCEs (Masalova *et al.*, 2011a)

In earlier work it was demonstrated that the viscoelastic behaviour of concentrated emulsions (ϕ to a maximum of 0.96 v%) could be described by the single-relaxation-time Maxwell model, and that the plateau region of the elastic modulus was considered to be a static modulus (G_0) (Pons *et al.*, 1992; Pons *et al.*, 1993; Langenfeld *et al.*, 1999). However, due to the complexity of the system, more advanced models (Equations 2.32 and 2.33), proposed by Princen and Kiss (1986), have been applied to predict the existence of elasticity and yield stress in HCEs (Lacasse *et al.*, 1996; Mason *et al.*, 1996; Babak *et al.*, 2001; Ponton *et al.*, 2001). According to the Princen model, interfacial tension (σ), the dispersed phase volume fraction (ϕ) and droplet size simultaneously dominate the rheological properties of HCEs. The elastic region before yield stress point ($\tau < \tau_c$) is calculated as:

$$G' = A \frac{\sigma}{R_{32}} \phi^{1/3} (\phi - \phi_c)$$

Equation 2.32

where G' is the elastic modulus, ϕ_c the critical volume fraction, R_{32} the surface-volume mean drop radius and A is the adjustable parameter of an individual system.

Some studies disagree with the Princen model (Lacasse *et al.*, 1996; Malkin *et al.*, 2004; Masalova *et al.*, 2006; Mason, 1999). Lacasse *et al.* (1996) show the dependence of the elastic modulus to ϕ ($\phi - \phi_c$) by using surface evolver software. Malkin *et al.* (2004) observe that the dependency of the elastic modulus to $(R_{32})^{-1}$ does not agree with their experimental data. However, they report a more noticeable effect of droplet size on elasticity of the system where there was a linear dependence of elastic modulus to $(R_{32})^{-2}$.

Some studies show that dilatational rheology and the shear of the thin film (interfacial layer) contributes to the overall elasticity of the emulsion as the principal source of elasticity, when the interfacial tension is minimal (Buzza & Cates, 1994; Hemar *et al.*, 1995; Bressy *et al.*, 2003). Bengoechea *et al.* (2006) suggest the existence of additional sources of elasticity in the system.

There are three types of interaction among the deformable interfaces of droplets when at a high concentration of internal phase:

- firstly, a depletion attraction;
- secondly, a short-range repulsive interaction which prevents droplets re-coalescing (disjoining pressure); and
- thirdly, a repulsive interaction caused by the energy required to overcome interfacial tension and deform two neighbouring droplets (Mason, 1999).

The third interaction is considered as Laplace pressure in Princen's model. Thus, the remaining two could be responsible for the additional source of elasticity in the system. While attractive forces can be found in adhesive emulsions (Mason, 1999) the repulsive interaction (disjoining pressure) of interface layers has been considered as an additional source of stored energy in HCEs (Foudazi *et al.*, 2010a; Foudazi *et al.*, 2010b). Foudazi *et al.* (2010b) suggested that the electrostatic repulsion enhanced by the presence of reversed micelles, could be the reason that the elastic modulus of explosive emulsions is not scaled by Laplace pressure.

2.8.2 Flow properties

The flow properties of HCEs depend on the packing, deformation and intrinsic elasticity of the emulsion droplets. By extending their earlier model to include three dimensions, Princen and Kiss (1989) derived an equation (Equation 2.33) to calculate the yield stress of HCEs. This relates the flow behaviour of the emulsion to inherent microstructural variables such as R , σ , μ_e (viscosity of continuous phase), and ϕ :

$$\tau = \tau_o + C(\phi) \frac{\sigma}{R_{32}} \left(\mu_e \frac{R_{32} \dot{\gamma}}{\sigma} \right)^{2/3} \quad \text{Equation 2.33}$$

where τ_o is the yield stress of the system and $C(\phi)$ is a numerical factor that may depend on ϕ .

There are several articles in which the rheological properties of HCEs based on Princen's model are in agreement (Reinelt & Kraynik, 1990; Aronson & Petko, 1993; Kraynik & Reinelt, 1996; Babak *et al.*, 2001). However, some disagreement with this model is noted in other publications (Pons *et al.*, 1992; Otsubo & Prud'homme, 1994; Pons *et al.*, 1995; Dimitrova & Leal-Calderon, 2004; Masalova *et al.*, 2006). The effect of interfacial tension on the steady-flow of emulsions was studied by Otsubo and Prud'homme (1994). These authors stress that the interfacial energy associated with droplet deformation resulted in a marked elasticity. Hence the viscosity of the fluid is proportional to the interfacial tension.

Calculating the flow curve for HCEs explosive types after exposure to low and high stresses revealed the presence of a Newtonian plateau at low shear rate (Masalova *et al.*, 2005; Masalova & Malkin, 2007b). The use of a microscope to observe the structure of the highly concentrated explosive emulsion structure showed that two different mechanisms of flow occurred. Under low shear conditions, large droplets were seen to roll over smaller ones. When shearing conditions were high, deformation of drops was noted, whilst at an intermediate shear rate, the low curve showed a hump. This hump represented a transient point between the observed flow mechanisms in low and high shear regions. The flow curves were fitted by implementing the Herschel-Bulkley model using different sets of coefficients which were measured when the yield stresses were below and above the hump point (Figure 2.26) (Malkin & Masalova, 2007). The Herschel-Bulkley model is presented in Equation 2.34:

$$\tau = \tau_{y0} + K \dot{\gamma}^n \quad \text{Equation 2.34}$$

where τ is shear stress, and model coefficients include τ_{y0} as yield stress, K consistency and n as the power law exponent.

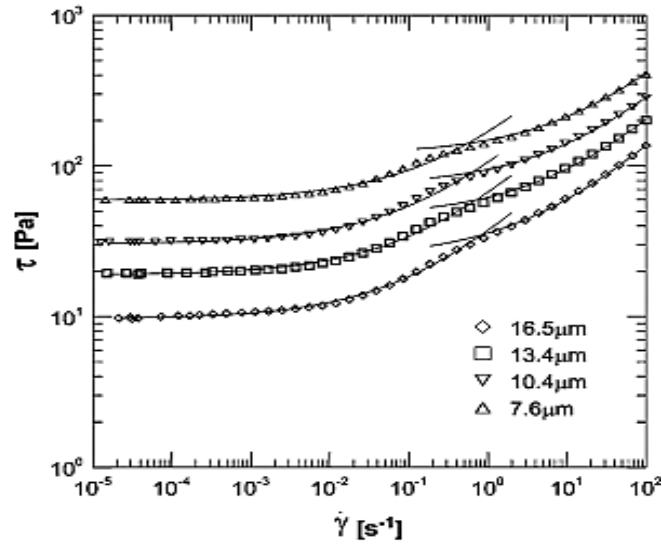


Figure 2.26: Typical HCEs flow curve fitted by the Herschel-Bulkley model with two sets of model coefficients (τ_{y0} , K) and constant $n=0.5$ for emulsions with variable droplet size/diameter (Foudazi *et al.*, 2011)

Windhab (1993) proposed the following model to fit a similar flow curve for dispersions which included directly measured yield stress (τ_{y0}), the hump point ($\tau_{y1}, \dot{\gamma}^*$) and high shear viscosity (μ_∞):

$$\tau = \tau_{y0} + \eta_\infty \dot{\gamma} + (\tau_{y1} - \tau_{y0}) [1 - \exp(-\dot{\gamma} / \dot{\gamma}^*)] \quad \text{Equation 2.35}$$

Recently, Foudazi *et al.* (2011) developed a new model to predict the entire range of flow curves for HCEs and included the hump points. This showed excellent fitting of the experimental data obtained from the emulsions (Figure 2.27):

$$\tau = \tau_{y0} + K \dot{\gamma}^{0.5} + (\tau_{y1} - \tau_{y0}) [1 - \exp(-\dot{\gamma} / \dot{\gamma}^*)] \quad \text{Equation 2.36}$$

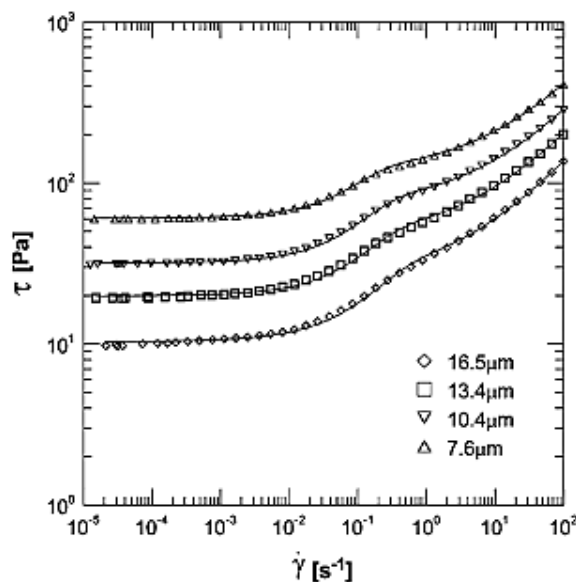


Figure 2.27: Highly concentrated explosive emulsions flow curves fitted by the Foudazi model with different droplet sizes (Foudazi *et al.*, 2011)

Data collected from the flow curve measurement can also be used to predict transport characteristic, such as pressure drop versus flow rate, of the emulsions. However, some models, such as Foudazi and Windhab, are not practical to estimate pumping characteristics of EEs, due to their complexity. Masalova (2003) discovered that the Herschel-Bulkley model can accurately describe the pipe flow behaviour of EEs for industrial practical applications. Results obtained from that study were supported by experimental data collected by measuring pressure drop against flow rate of different EE formulations through pipelines with different diameters.

2.8.3 Effect of surfactant structure on rheological properties of HCEs

During the formation of an emulsion, factors such as continuous phase viscosity, internal volume fraction, droplet size and interfacial tension all determine the rheological properties of the final product. Moreover, the interrelationship of these factors and the rheological properties of the individual phases of the emulsion, together with the processing procedure, further determine the final rheological properties of HCEs (Welch *et al.*, 2006).

Many investigators have discussed the effect of surfactant type on the rheological properties of emulsions (Jiao & Burgess, 2003; Leal-Calderon *et al.*, 2007; Santana *et al.*, 2012). However, few works have been published on the effect of surfactant structure on rheological behaviour of HCEs. For an emulsion system to flow, deformation of droplets and shearing of the inter-droplet layer are important, and both of these are markedly influenced by the

surfactant type and its concentration (Foudazi *et al.*, 2011). Becher (1988) observes that the viscosity of emulsions decreased when sorbitan derivative surfactants were replaced by oxazoline and amine surfactants. Bampfield and Cooper (1988) observe a noticeable increase in the viscosity of explosive emulsions when these were stabilised by various polymeric surfactants. The presence of surface active agents such as polymers in continuous phase can exert an effect on the rheology of emulsions by altering the viscosity of the continuous phase, or by creating a steric barrier between drops which have not coalesced (Meller & Stavans, 1996). The effect of surfactant type on rheological parameters of HCEs has been investigated by Masalova *et al.* (2011a) (Figure 2.28).

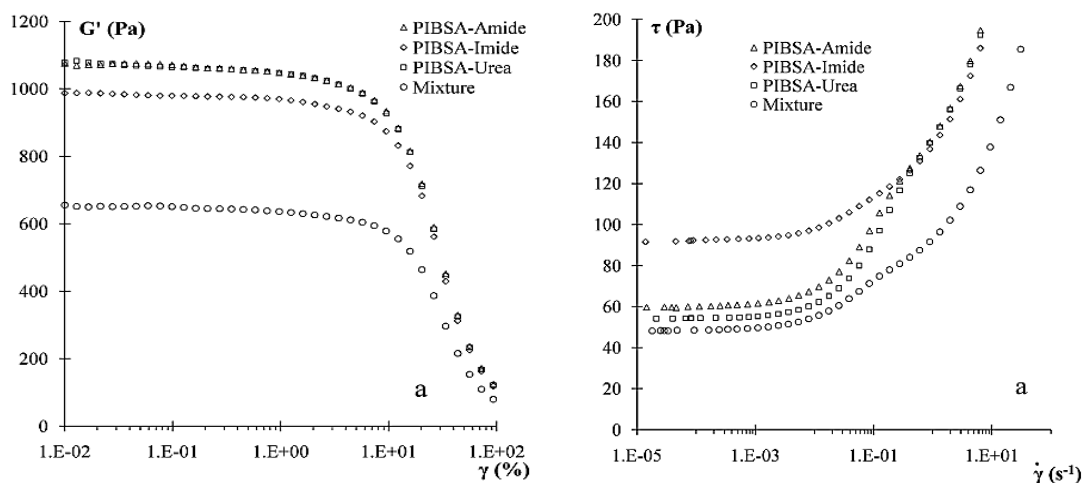


Figure 2.28: Elastic modulus (left) and flow curves (right) of highly concentrated explosive emulsions of different surfactant types with similar droplet size variation (Masalova *et al.*, 2011a)

From the investigations on the influence of surfactant type on the rheological properties of HCEs it can be concluded that the role of surfactant structure is very important, particularly as droplet size decreases in the emulsions.

2.9 SUMMARY

The scope of the present study is focused on highly concentrated emulsions (HCEs) in which the internal phase is formed by a super-cooled water solution of inorganic salts. Instability of such emulsions arises from crystallisation of the dispersed phase in the system as time progresses (ageing), or under conditions of high shear. These systems attract high interest due to numerous potential technological applications in cosmetics, mining, food and explosives.

Many systematic studies have been conducted over the past decade related to highly concentrated emulsions (HCEs), with a significant number of publications covering all aspects of those systems. However, few have focused on HCEs with a super-cooled internal phase, where instability is related to crystallisation of metastable dispersed phase. The majority of research in this field is conducted by only a few groups. Masalova *et al.* (from 2003 to date) have made significant contributions to the study of rheological properties, manufacturing processes and stability of such emulsion systems, while White *et al.* (2000-2011) have investigated the microscopic properties of emulsions by small angle neutron scattering. The majority of these studies focused on the use of PIBSA-based surfactants and/or their blending with SMO. Except for a small number of patents, hardly any systematic studies have been conducted on the implementation of other types of surfactant and/or surfactant mixtures.

The present state of knowledge concerning interfacial properties of highly concentrated W/O emulsions reveals an absence of systematic experimental data, especially concerning the effect of interactions between surfactant mixtures at interface as one of the factors affecting the emulsification process, the rheological properties and stability of the emulsion.

The focus of this thesis is to investigate and understand the effect of synergetic compatibility of various binary surfactant mixtures on manufacturing processes, stability on shelf and under high shear, as well as rheological properties of HCEs. This is achieved by investigating the interfacial films and the surfactant molecular structure of the different binary surfactant systems of oil/oil and oil/water surfactants with various chemical structures.

CHAPTER THREE: MATERIALS AND METHODS

3.1 INTRODUCTION

This chapter provides a description of materials and general methodology used during the present study. The study consisted of two phases:

- *Feasibility study*: this stage involved manufacturing of highly concentrated W/O emulsions using different polymeric and water-and oil-soluble conventional surfactants and their mixtures, as selected from related literature. Findings from this step of the study were used to define the final matrix of samples. The first section of this chapter lists details of materials as well as the emulsification procedure used in the feasibility study.
- *Main study*: a group of fatty acid based surfactants with systematic variation in head and tail groups were selected from the family of Spans and Tweens, in combination with PIBSA-based surfactant. This enabled a study of the effects of the synergetic compatibility between surfactants at interface, associated with their chemical structure, on the stability and pumpability of HCEs with super-cooled dispersed phase. In the second section of this chapter, a full description of materials and emulsion preparation for the main core of the study is presented.

The last section of this chapter includes the description of the instruments used for analysis of the manufactured emulsions.

3.2 MATERIALS AND MATRIX OF SAMPLES

3.2.1 Material and Matrix of Samples Used for Feasibility Study

To manufacture highly concentrated W/O emulsions, two phases are generally required, the oil phase and the aqueous phase. For the feasibility stage of the current study in order to manufacture HCEs, the following materials and matrix of samples were chosen:

- *Aqueous phase*: an oxidiser solution consisting of 60 wt% of ammonium nitrate (AN) in water.
- *Fuel (oil) phase*: different type of surfactants, individually or as mixtures, dissolved in industrial grade oil (Ash-H).
- *Surfactants*: two types of block copolymers (Pluronics), two types of water-soluble surfactants (Tweens), a PIBSA-based surfactant (PIBSA-Mea) and Span 80 (SMO).

Ash-H contained iso-paraffins (80% – 90%), n-paraffins and cycloparaffins (10% – 15%), and aromatics (less than 0.1%), with an average carbon number of 14. The interfacial tension of

Ash-H/60% AN aqueous solution was equal to 19 mN/m, and the density was 794 kg/m³ at 20 °C.

PIBSA-Mea has an overall molecular weight of approximately 1109 and is produced by a chemical reaction between polyisobutylene succinic anhydride (PIBSA) and monoethanolamine (Mea) components. The schematic structure of PIBSA-Mea is illustrated in Table 3.1, where R represents a polyisobutylene backbone with 19 repeat units of –(CH₃)₂-CH₂-. There is no precise HLB number available for this surfactant, but the supplier states that it is below four.

Pluronics are non-ionic triblock copolymers composed of hydrophobic segments of polyoxypropylene (polypropylene oxide) and hydrophilic segments of polyoxyethylene (polyethylene oxide). Two Pluronic surfactants with the commercial names PE3100 and PE6100, with a hydrophilic lipophilic balance (HLB) equal to three and molecular weights of 1000 and 2000, were purchased from BASF, South Africa. The general structure of Pluronics is depicted in Table 3.1.

Sorbitan monooleate (SMO), available under the commercial name of Span 80, is an ester formed between sorbitan and oleate fatty acid, with HLB equal to 4.3. Tween 20 and 80 are nonionic surfactants derived from polyethoxylated (20 segments) sorbitan and monolaurate and oleate fatty acids with HLB equal to 16.7 and 15 respectively. The chemical structures of Span 80 and tweens are depicted in Table 3.1

Table 3.1: Surfactants used for feasibility study (a+b+c+d=20)

Material	HLB	M _w	Structure
PIBSA-MEA	<4	1109	
Pluronic PE3100	3	1000	<p>x, y and z are not provided by supplier.</p>
Pluronic PE6100	3	2000	<p>x, y and z are not provided by supplier.</p>
Span 80	4.3	429	
Tween 20	16.7	1228	<p>n = a + b + c + d</p>
Tween 80	15	1228	<p>a+b+c+d = 20</p>

**for all Tweens a+b+c+d=20*

Formulations used to form HCEs were then separated into the following groups:

- emulsions stabilised by selected single surfactants only;
- emulsions prepared by mixing Pluronics with selected surfactants;
- emulsions stabilised by mixing PIBSA-Mea with selected surfactants; and
- emulsions prepared by mixing SMO with selected surfactants.

The matrix of samples is presented in Table 3.2. The ratio between oil: aqueous phase was 1:9 by mass for all the emulsions.

Table 3.2: Matrix of samples for feasibility study

Type of surfactant	Type of co-surfactant	Ratio of surf/co-surf	AN emulsions	
			C_{AN} (%) [*]	C_{SURF} (%) [*]
Pluronic PE3100	-----	-----	60	8, 15 and 20
Pluronic PE6100	-----	-----	60	8, 15 and 20
Pluronic PE3100	SMO (Span 80)	10/1	60	8
Pluronic PE3100	Tween 20	10/1	60	8
Pluronic PE3100	Tween 80	10/1	60	8
Pluronic PE6100	SMO (Span 80)	10/1	60	8
Pluronic PE6100	Tween 20	10/1	60	8
Pluronic PE6100	Tween 80	10/1	60	8
PIBSA-MEA	Pluronic PE3100	10/1	60	8
PIBSA-MEA	Pluronic PE6100	10/1	60	8
PIBSA-MEA	Tween 20	10/1	60	8
PIBSA-MEA	Tween 80	10/1	60	8
SMO (Span 80)	Pluronic PE3100	10/1	60	5
SMO (Span 80)	Pluronic PE6100	10/1	60	5
SMO (Span 80)	Tween 20	10/1	60	5
SMO (Span 80)	Tween 80	10/1	60	5

^{*} C_{AN} : concentration of AN in the aqueous phase; C_{SURF} : total concentration of surfactants in the oil phase

During the first stage of the investigation, all of the samples were manufactured using a Silverson L4RT dispergator (Figure 3.1). Agitation was performed at different speeds. Pre-emulsions were prepared at 500 rpm and refined to a smaller droplet size at 2500 rpm. Throughout this stage, a lower concentration of AN (60 wt%) was gradually added to the oil phase by a pipette. The aqueous phase was stable at ambient temperature and therefore the instability in samples was controlled solely by the means of coalescence and not as a result of crystallisation of dispersed phase. To control the rate of coalescence in prepared emulsion samples, droplet size analyses were performed (Section 3.3.3).



Figure 3.1: Silverson L4RT disperser

The PIBSA-Mea/Tweens mixtures were found to be the most promising formulations. One of the water-soluble Tween surfactants (Tween 80) with similar hydrophobic tail (oleate tail) to Span 80 was selected as the co-surfactant and added to explosive emulsion formulation in combination with PIBSA-Mea. This section of the research can be found in detail in Chapter Four (Section 4.4). The stability of the prepared emulsion was then compared to a standard industrial formulation of PIBSA-Mea/Span 80. The matrix of samples for this part of the feasibility study is as follows (Table 3.3):

- Aqueous phase: 80 wt% ammonium nitrate (AN) in water; and
- Fuel (oil) phase: binary mixture of PIBSA-Mea/Tween 80 and PIBSA-Mea/Span 80 in Ash-H oil.

To prepare the emulsions, a Hobart mixer was used. The detail of the mixing process can be found in Section 3.2.2.

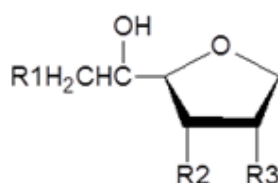
Table 3.3: Matrix of samples selected for comparison between PIBSA-Mea/Tween 80 emulsion formulations and PIBSA-Mea/Span 80 standard industrial formulation

Type of surfactant	Type of co-surfactant	Sur/co-sur ratio (wt)	C _{AN} (wt %) in AqPh	Aqu/oil phase ratio (wt)
PIBSA-Mea	Span 80	10:1	80	92.4:7.6
PIBSA-Mea	Tween 80	10:1	80	92.4:7.6

3.2.2 Material and matrix of samples used for the main core of the study

This section of the research is reported in detail in Chapter Five. Using the results obtained from the feasibility study (see Chapter Four), ten binary surfactant mixtures were selected for final analyses. A PIBSA-Mea surfactant was chosen as the principal surfactant in combination with fatty acid-based surfactants (Spans and Tweens) as co-surfactants.

Sorbitan fatty acid esters, available under the commercial name of Spans, are esters formed between sorbitan and differing fatty acids (viz. lauric, palmitic, stearic and oleate). The structure of Span surfactants is given below in Figure 3.2. Three-dimensional structures of Spans are illustrated in Figure 3.3.



Surfactant	Schematic structure	R1	R2	R3
Span 20		OOC(C11H23)	OH	OH
Span 40		OOC(C15H31)	OH	OH
Span 60		OOC(C17H35)	OH	OH
Span 80		OOC(C17H33)	OH	OH
Span 85		OOC(C17H33)	OOC(C17H33)	OOC(C17H33)

Figure 3.2: Schematic structure of the sorbitan ring with different acids attached, forming Span surfactants. Structures of the various R groups are indicated

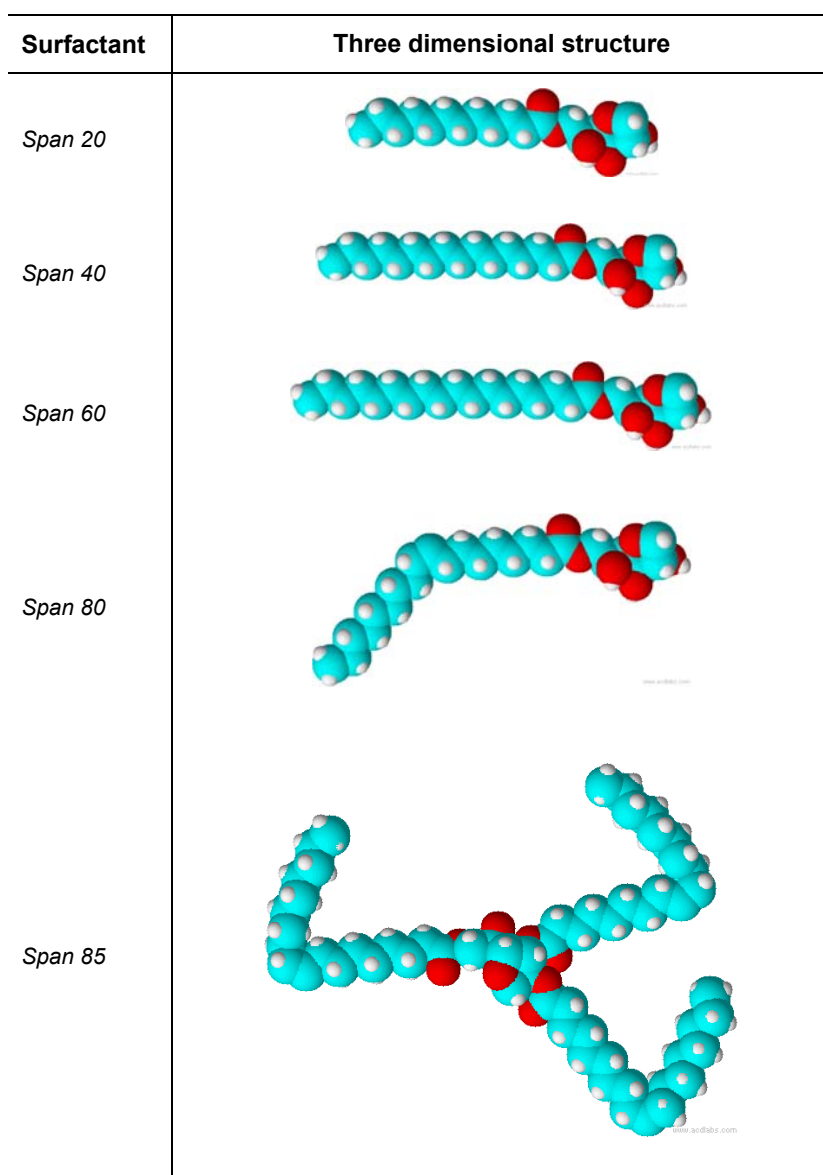
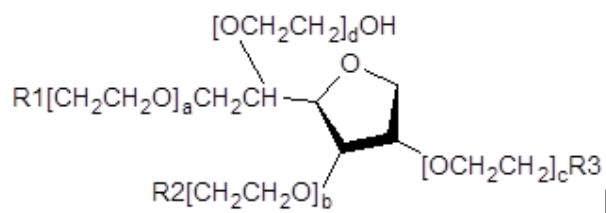


Figure 3.3: Three-dimensional structures of Span surfactants (hydrogen atoms: white, carbon atoms: blue, oxygen atoms: red)

Tweens are nonionic surfactants derived from polyethoxylated sorbitan and variable fatty acids, similar to Spans. The structure of Tween surfactants is given in Figure 3.4. Three dimensional structures of Tweens are illustrated in Figure 3.5.



Surfactant	Schematic structure	R1	R2	R3
Tween 20		OOC(C11H23)	OH	OH
Tween 40		OOC(C15H31)	OH	OH
Tween 60		OOC(C17H35)	OH	OH
Tween 80		OOC(C17H33)	OH	OH
Tween 85		OOC(C17H33)	OOC(C17H33)	OOC(C17H33)

Figure 3.4: Schematic structures of the ethoxylated sorbitan ring with different acids attached, forming Tween surfactants ($a+b+c+d=20$)

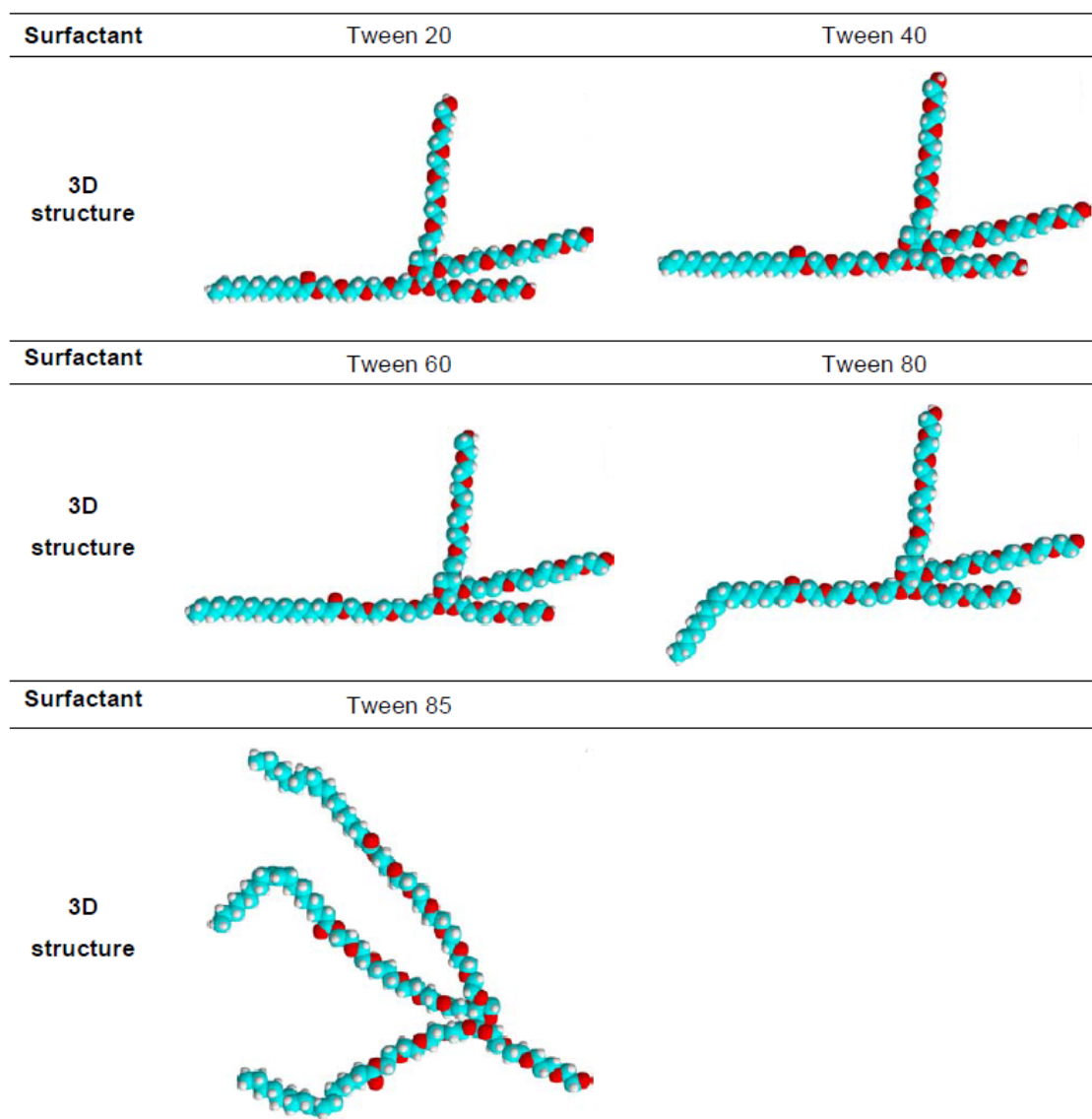
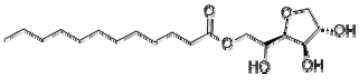
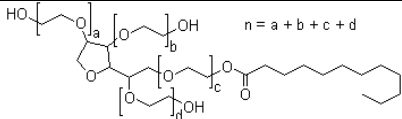
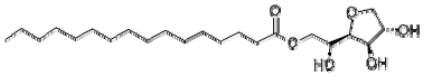
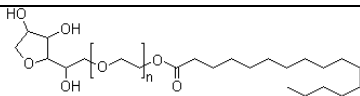
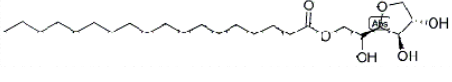
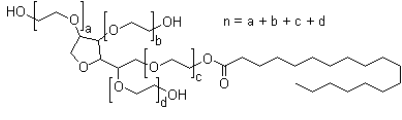
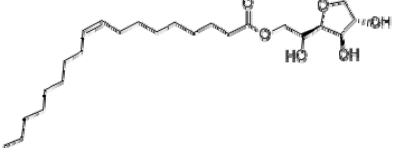
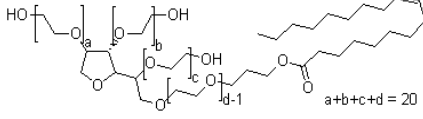
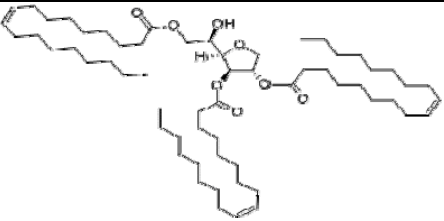
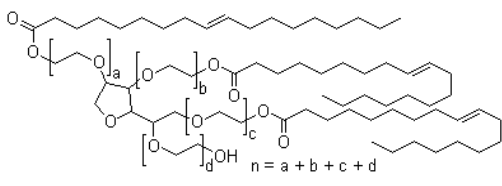


Figure 3.5: Three-dimensional structures of Tween surfactants (hydrogen atoms: white, carbon atoms: blue, oxygen atoms: red)

The summary of co-surfactant properties is presented in Table 3.4.

Table 3.4: Summary of surfactant properties (a+b+c+d=20)

Material	HLB	M _w	Structure	Material	HLB	M _w	Structure
Span 20	8.6	346		Tween 20	16.7	1228	
Span 40	6.7	403		Tween 40	15.6	1277	
Span 60	4.7	430		Tween 60	14.9	1312	
Span 80	4.3	429		Tween 80	15	1228	
Span 85	1.8	957		Tween 85	11	≈1870	

Ammonium nitrate (AN), industrial Ash-H oil and a concentrated polyisobutylene succinic anhydride (PIBSA)-based surfactant (PIBSA-Mea) solution in Ash-H oil (50 wt%) were produced and supplied by Lake International Technologies (South Africa). Span 40 was purchased from Aldrich, and Span 20, Span 60, Span 80 (SMO), Span 85, Tween 20 and Tween 60 were obtained from Merck. Tween 40 and Tween 85 were supplied by Sigma, and Tween 80 was purchased from Sigma Aldrich. All surfactants were used without further purification.

These ten co-surfactants were separated into two groups based on head group structure (Spans and Tweens). Head group structures were clustered into three major categories (a-c) based on hydrophobic tail structure, as indicated below:

a. *Length of hydrophobic tail:*

- Sorbitan monolaurate (Span 20), sorbitan monopalmitate (Span 40) and sorbitan monostearate (Span 60) with 11, 15 and 17 carbons in the tail, respectively.
- Polyoxyethylene sorbitan monolaurate (Tween 20), polyoxyethylene sorbitan monopalmitate (Tween 40) and polyoxyethylene sorbitan monostearate (Tween 60) with 11, 15 and 17 carbons in tail, respectively.

b. *Unsaturated and saturated hydrophobic tail:*

- Sorbitan monostearate (Span 60,) with 17 carbons as a saturated tail, and sorbitan monooleate (Span 80), with 17 carbons as an unsaturated oleate tail (C8=C9).
- Polyoxyethylene sorbitan monostearate (Tween 60), with 17 carbons as a saturated tail and polyoxyethylene sorbitan monooleate (Tween 80), with 17 carbons as an unsaturated oleate tail (C8=C9).

c. *Number of hydrophobic tails attached to the head group:*

- Sorbitan monooleate (Span 80), with a single oleate tail and sorbitan trioleate (Span 85), with three oleate tails.
- Polyoxyethylene sorbitan monooleate (Tween 80), with a single oleate tail and polyoxyethylene sorbitan trioleate (Tween 85), with three oleate tails.

The ratio of PIBSA-Mea/co-surfactants was maintained at 10:1 w/w as the standard formulation for explosive emulsions. A total of 8 wt% surfactant mixtures were added to Ash-

H oil, as this was the minimum concentration required to stabilise an explosive emulsion containing only PIBSA-Mea. An oversaturated AN solution (80 wt%) with a density of approximately 1.4 -1.5 g/L was used as the aqueous phase. The AN solution was prepared at 80 °C by using a heating plate. The temperature of equilibrium crystallisation (fudge point) of this AN solution was approximately 59±1 °C. The ratio of oil/aqueous phases was maintained at 7.6/92.4 w/w (88/12 v/v %). The matrix of samples is presented in Table 3.5.

Table 3.5: Matrix of samples used during the second stage of the study

Type of surfactant	Type of co-surfactant	Ratio of surf/co-surf	AN emulsions	
			C _{AN} (%)	C _{SURF} (%)
PIBSA-Mea	-----	-----	80	8
PIBSA-Mea	Span 20	-----	80	8
PIBSA-Mea	Span 40	10:1	80	8
PIBSA-Mea	Span 60	10:1	80	8
PIBSA-Mea	Span 80	10:1	80	8
PIBSA-Mea	Span 85	10:1	80	8
PIBSA-Mea	Tween 20	10:1	80	8
PIBSA-Mea	Tween 40	10:1	80	8
PIBSA-Mea	Tween 60	10:1	80	8
PIBSA-Mea	Tween 80	10:1	80	8
PIBSA-Mea	Tween 85	10:1	80	8

*C_{AN}: concentration of AN in the aqueous phase; C_{SURF}: total concentration of surfactants in the oil phase

Emulsion samples to be investigated were manufactured using a Hobart N50 mixer (Figure 3.6).



Figure 3.6: Hobart N50 mixer

Emulsions were prepared as follows:

- The oil phase was transferred to a pre-warmed mixer bowl and heated for four to five minutes (80 °C).
- The Hobart was operated at speed 1 and the AN solution was slowly added to the oil phase in the mixing bowl.
- The pre-emulsion was refined at a mixer speed of 3, equivalent to a shear rate of approximately 380/s. To avoid splashing, the Hobart was covered by a plastic bag during the refinement period.
- Several emulsion properties such as stability, rheology, appearance and shelf-life depend on droplet size and droplet size distribution (McClements, 2005). In all samples investigated, in order to minimise the effects of droplet size, emulsification was performed until a D_{32} equal to 10 μm was achieved. To determine the manner in which target droplet size of 10 μm could be controlled, several samples were collected during refining. The droplet size of the samples collected was determined (Section 3.3.3).

3.3 METHODS

3.3.1 Interfacial tension measurements

The Wilhelmy plate method was used to determine the interfacial tension of the water-oil interface in the presence of the surfactants, with a Kruss K100 tensiometer supplied by Krüss GmbH, Germany (Figure 3.7). The tests were done under atmospheric pressure conditions. Approximately 12 cm^3 of AN-*analytical grade* in water solution (60 wt%) was placed in a glass dish. A hydrophilic platinum (Wilhelmy) plate was suspended vertically, such that the lower edge was immersed below the surface of the AN solution. Approximately 40 cm^3 of the oil phase was added, in order that the plate was fully submerged. The samples were placed in a jacketed chamber maintained at 25 ± 0.1 °C by circulating cooling water. Measurements were taken until equilibrium was reached. The interfacial tension was calculated by using Equation 3.1:

$$\sigma = F / L \cos\theta \quad \text{Equation 3.1}$$

where F (mN), is the vertical force acting on the plate, after a correction was made for the plate buoyancy, L (m) is the moist plate length, and θ is the contact angle. The measuring range of the device was from 1 -100 mN/m with a resolution of 0.001 mN/m.



Figure 3.7: Kruss K 100 Tensiometer

The contact angle was considered to be zero due to the hydrophilic nature of the plate. All the samples were analysed twice and the mean values were reported within an accuracy of 0.1.

3.3.2 Interfacial elasticity measurements

A PAT1 Tensiometer (Figure 3.8) supplied by Sinterface Technologies (Germany) was used to calculate the interfacial elasticity of the systems. The Tensiometer operates based on the Young-Laplace equation. This describes the profile of a pendant drop formed by the high density phase (e.g. 40% AN solution) suspended in the low density phase (e.g. oil phase containing surfactant) (Fainerman *et al.*, 2013). The Sinterface functions over a range of 0.01 -1 Hz frequencies, and the data from oscillation are processed using Equation 3.2 to obtain the interfacial elasticity (E'):

$$E' = (\Delta\sigma/\Delta A_0) \cos\delta$$

Equation 3.2

where ΔA_0 is the amplitude of oscillation of the droplet area and δ is the phase lag between the interfacial tension and the area, derived from Fourier transformation.

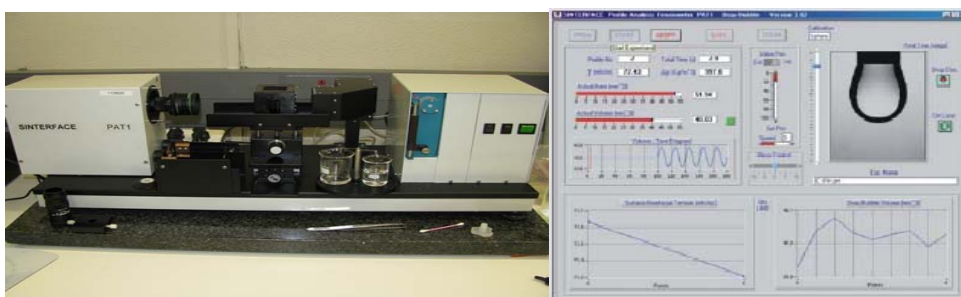


Figure 3.8: The PAT1 Tensiometer

NOTE: In spite of all attempts made, it was not possible to calculate the interfacial elasticity for the oil phases used in this study. This was due to the inability of the oil phase to maintain the droplet during the experiment. As a result, this interfacial elasticity was excluded from the study.

3.3.3 Droplet size analysis

To measure the dispersed phase droplet size, a laser diffraction technique was performed using a Malvern Mastersizer-2000 (Figure 3.9).

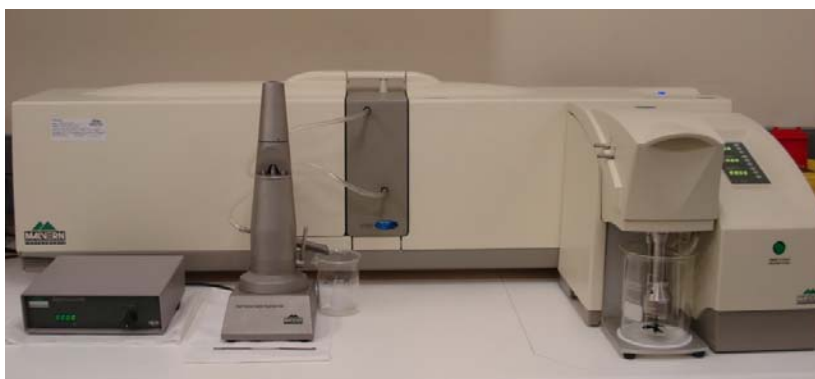


Figure 3.9: Mastersizer-2000 instrument

The Mastersizer measures the intensity of light scattered from a collimated He-Ne laser as it travels through a dilute dispersed sample, over a wide range of angles. Particle size within the range of 0.26 - 1500 μm can be measured. This size range was adequate for measuring the droplet sizes in all samples under investigation. The software designed for the Mastersizer 2000 controls the system during measurement and collects the scattering data. The analysis uses the rigorous Mie theory to calculate droplet size distribution. In the current study, a minimal quantity/volume of each emulsion sample was diluted by volumes of oil sufficient to avoid any agglomeration. An average value of $D_{32} \pm 1\%$ was calculated after repeating five assays for each sample.

3.3.4 Microscopic observation

The stability of samples to crystallisation was tracked by using a Leica optical microscope (GmbH, Germany) equipped with a digital camera. The magnification used was x 40 (Figure 3.10).



Figure 3.10: The Leica optical microscope

Since the aqueous phase consisted of a supersaturated AN solution, the stability was measured by determining the crystallisation of the dispersed phase.

The stability of the emulsions was measured by removing six different samples from each emulsion. The commencement of crystallisation was considered to have started when samples collected from any emulsion were observed to contain an average of five to 10 crystals in a very thin layer of sample over a slide. The crystallisation kinetics was subsequently followed by regular microscopic observations of a crystallised emulsion during certain days of ageing.

3.3.5 Rheological analysis

Rheological experiments were conducted using a rotational stress rheometer MCR 301 (Paar Physica, Figure 3.11).

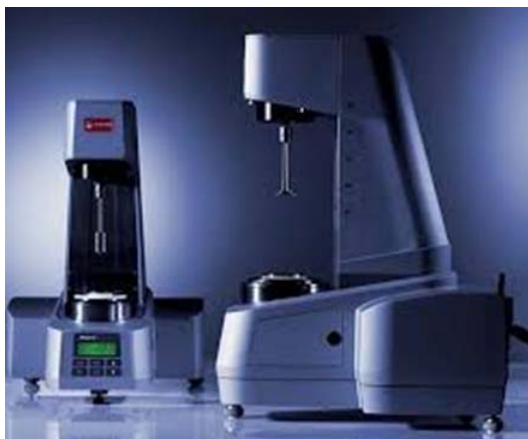


Figure 3.11: Rotational Rheometer MCR-301 (Paar Physica)

The geometry which was used for the material under investigation was a bob-in-cup with a sandblasted surface. Dimensions were a 1.13 mm gap and a 26.66 mm bob diameter at 30 ± 0.1 °C. The following tests performed were as follows:

- Oscillatory test at a constant frequency of 1 Hz in a range of 0.01- 200% of strain amplitude.
- Frequency sweep at a constant strain of 0.1% (from pre-determined linear viscoelastic region) in a descending range from 100 - 0.1 rad/s of angular frequency.
- Flow curve in a descending range from 10^3 to 10^{-4} s⁻¹ of shear rate.

Results from previous studies done elsewhere revealed that by using a sandblasted cup the likelihood of a slip can be disregarded in explosive emulsions (Masalova *et al.*, 2006). Torque and angular resolutions were 0.1 nNm and 0.01 rad, respectively. To ensure that the structure of the emulsions was not changing during the rheological measurements, each test was repeated twice.

3.3.6 Pumping of mixtures

High shearing forces, such as those exerted during pumping, were simulated by home-made equipment, shown in Figure 3.12.

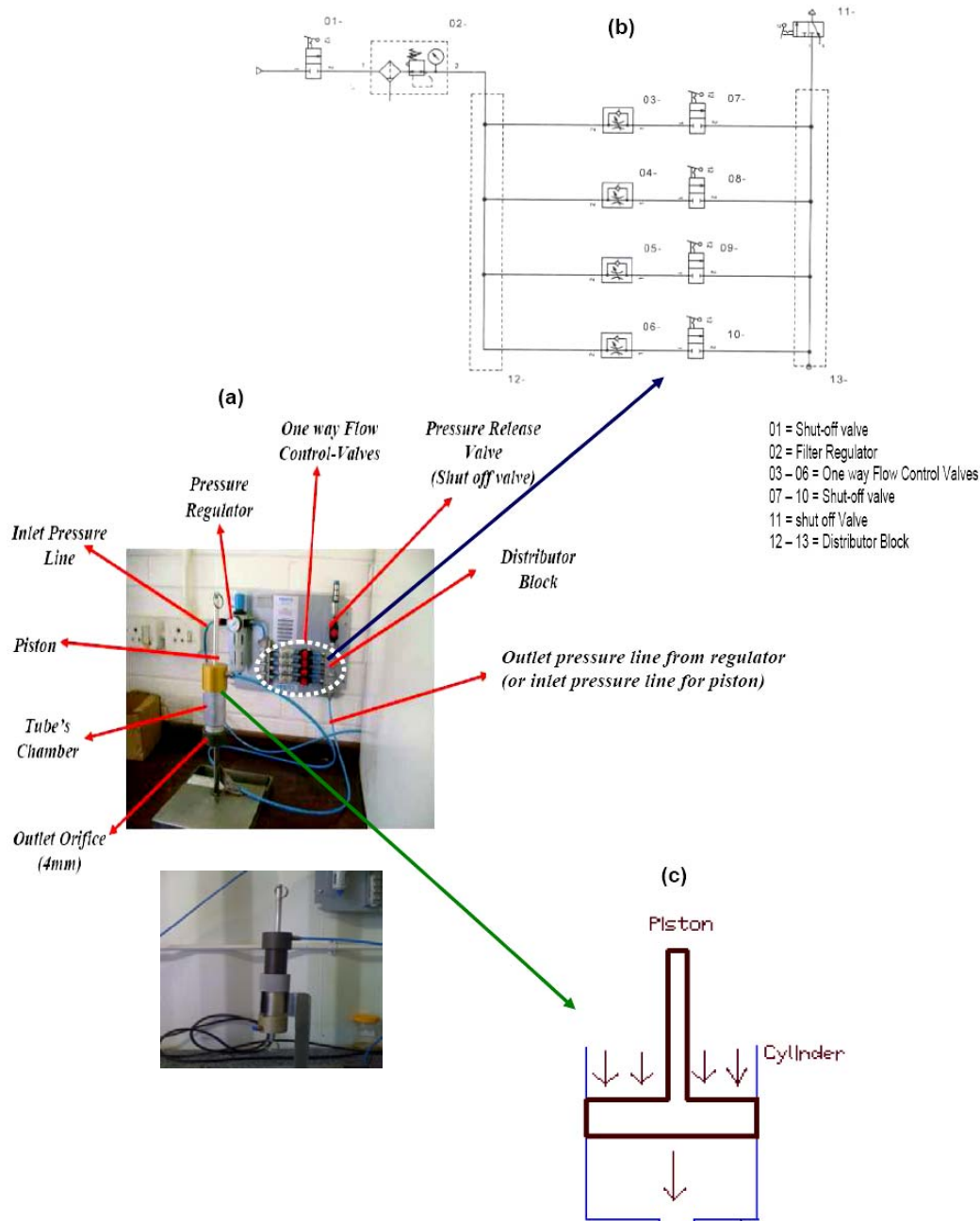


Figure 3.12: Function control and components of the pumping instrument used: (a) overall pumping device; (b) schematic representation of pressure control panel; and (c) schematic representation of the piston movement whilst under compressor pressure inside the pump chamber

The equipment includes two double cylindrical chambers connected by a $\varnothing 4$ mm orifice hole with a length of 3mm in a chamber cover plate. Each chamber has the cap end and the piston head end. The test was performed by loading one of the chambers with the emulsions and extruding them under a pressure of four bars (supplied by a compressor) through the orifice hole. Each emulsion was extruded in 3, 5, 7 and 10 passing cycles.

CHAPTER FOUR: FEASIBILITY STUDY

4.1 INTRODUCTION

A feasibility study was conducted to identify the matrix of samples for the main core of the work. The following results from the feasibility study are presented in this chapter:

- A review of recent publications related to the study of various surfactants used to stabilise W/O emulsion systems.
- Various polymeric and water-soluble surfactants were selected and used individually and in combination with a PIBSA-based surfactant and Span 80 to stabilise highly concentrated W/O emulsions. Then, stability of the manufactured emulsions to coalescence was examined.
- One of the most promising surfactant systems (PIBSA-Mea/Tween 80) was added to an explosive emulsion formulation and the stability to crystallisation of the manufactured emulsion was compared to the standard formulation of PIBSA-Mea/Span 80.
- Finally, the interfacial behaviour of both PIBSA-Mea/Span 80 and PIBSA-Mea/Tween 80 in a wide range of concentrations/ratios of surfactant/co-surfactants was investigated.

4.2 BACKGROUND

The choice of a practical emulsification system for an application depends upon several factors, such as optimum Hydrophilic Lipophilic Balance (HLB), Phase Inversion Temperature (PIT), Critical Packing Parameter (CPP), molecular weight, structural compatibility within the system, as well as economics, environmental and aesthetic factors (Griffin, 1954; Shinoda, 1967; Shinoda, 1969; Becher, 1988; Myers, 2005). Water-in-oil explosive emulsions are comprised of a large volume of nitrate salt aqueous solution dispersed in a small volume of hydrocarbon oil. Stabilisation is normally achieved by using surfactants with low HLB (Schick, 1987; Ghaicha *et al.*, 1995; Tadros, 2006) and these surfactants should provide emulsion stability at low pH (3 -5) (Binet *et al.*, 1982, Cooper and Baker, 1989, McKenzie, 1991, Boer, 2003). With regard to molecular weight, high molecular weight surfactants may provide better long term stability than do low molecular weight surfactants. However, the latter may show acceptable stability under shear, due to higher mobility in the emulsion bulk (Tadros, 2006).

To improve the stability of explosive emulsions, two key developments are emphasised in the published literature regarding emulsifiers. These are the development of new surfactant structures as well as the use of surfactant blends.

It would be favourable to develop an explosive emulsion that contains a mixture of surfactants with improved properties. These improvements would provide firstly an effective emulsifier capable of resisting the tendency for the oxidising phase of the explosive to crystallise and/or coalesce at rest. Secondly, there should be stability under high shearing conditions (Shinoda *et al.*, 1971; Chattopadhyay, 1996a; Gullapalli & Sheth, 1999).

It has been found that an exceptional shelf-life stability of emulsion explosives is possible, due to enhanced steric stabilisation, as influenced by the hydrophobic portion of polymeric molecules (Hales *et al.*, 2004, Zank *et al.*, 2006). It is preferable to have a highly branched unsaturated tail, as this provides good stability against coalescence due to the creation of a more structured interface (Cooper & Baker, 1989; Perrin *et al.*, 1999).

One of the famous classes of polymeric surfactants, which are present in water-in-crude-oil emulsions, is the asphaltenes. Asphaltene molecules are large polycyclic aromatic hydrocarbons with molecular weights ranging from 1000 - 10,000 g/mol, having hydrophilic functional groups attached to the hydrophobic backbone of asphaltene. In a hydrocarbon mixture, asphaltene can be present in the form of colloidal particles, as a precipitate, or as molecular surfactants (Figure 4.1).

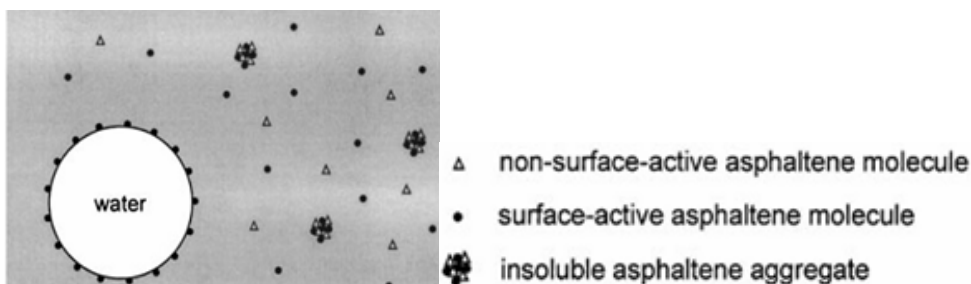


Figure 4.1: Possible structures of asphaltenes in W/O emulsions

Some publications show that in application only soluble and surface-active asphaltenes can adsorb on the interface and sterically stabilise W/O emulsions (Wu *et al.*, 1999; Khristov *et al.*, 2000).

Another example of polymeric surfactants which is widely used in highly concentrated water-in-oil cosmetic emulsions is polyether-modified silicone (Figure 4.2). Good stability of emulsions prepared using polyether-modified silicone as a surfactant is claimed by Omura and Nunba (2003), in terms of both shelf life and behaviour under shear.

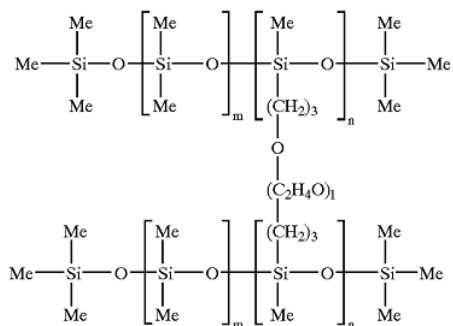


Figure 4.2: General structure of polyether-modified silicone

Zank, *et al.* (2006) prepared an emulsion consisting of a high volume fraction of saturated ammonium nitrate dispersed as droplets in hexadecane, and stabilised by the surfactant Pluronics (Figure 4.3).

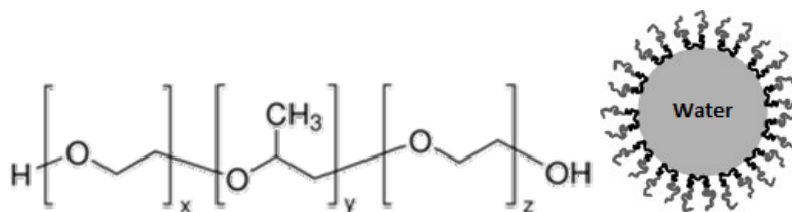


Figure 4.3: General formula of Pluronics (left), and the structural layer produced by Pluronic at a water-oil interface (right)

The resulting emulsion, using Pluronic L92, was stable to phase separation at rest, but unstable when subjected to shear. Shearing caused rapid breakdown and no aggregation of surfactant was observed in either the oil or aqueous phases. Shear stability of the Pluronic emulsion was attributed to the hydrophilic nature of the surfactant. This caused depletion between reverse micelles in the oil phase, as well as aggregation into blocks in the lamellar phase.

Some reports have been published on the influence of the addition of binary mixtures of surfactants on the stability and properties of water-in-oil emulsions. A synergistic effect was observed due to the compatibility between Span 80 and polyethylene glycol sorbitan monooleate surfactants. This was caused by an identical hydrophobic monooleate tail size and a narrower droplet size distribution of the aqueous phase. As a dilute W/O emulsion, the mixture was stable for more than a month and was also satisfactorily stable under shear (Fu *et al.*, 2010). It has been reported that emulsions prepared by adding a mixture of petroleum sulphonate surfactant and partly hydrolysed polyacrylamide (HPAM) resulted in improved stability. This was due to a decrease in the water-oil interfacial tension caused by the

petroleum sulphonate surfactant, as well as to an increase in interfacial elasticity introduced by the HPAM (Kang *et al.*, 2011).

To prepare a stable emulsion, water-soluble co-surfactants have been added to polymeric oil soluble emulsifiers (Perrin *et al.*, 1999; Fu *et al.*, 2010; Kang *et al.*, 2011; Yaron *et al.*, 2011). Addition of water-soluble polyamide-based co-surfactants (PAM) to PIBSA was reported to improve stability of a highly concentrated W/O emulsion (Yaron *et al.*, 2011). Adding PAM to the formulation caused a marked collapse in both the observed emulsion yield stress and the aqueous water-oil interfacial tension (approximately by a factor of 10). The PAMs showed negligible influence on viscosity at higher shear rates but caused changes in both micellar radii and the volume fraction of the surfactant micelles in the continuous oil phase. Finally, micelles became more hydrophilic (Yaron *et al.*, 2011).

4.3 INTRODUCTION OF VARIOUS SURFACTANT TYPES TO STABILISE HIGHLY CONCENTRATED W/O EMULSIONS

Surfactant selection and evaluation can be a bewildering adventure. It can be somewhat demystified by taking advantage of information developed for products that have proven valuable under certain circumstances. In the current study, within the surfactants which have been used to manufacture water-in-oil emulsions, two groups of surfactants are selected to determine whether these could stabilise highly concentrated water-in-oil emulsions. Those two groups of surfactants consist of the following:

- block copolymer surfactants known as Pluronics; and
- water-soluble surfactants known as Tweens.

Asphaltenes and polyether-modified silicone were not included in the current research. Asphaltenes were not available for large scale usage and polyether-modified silicone use was restricted due to mandatory regulations regarding the supply of explosive products.

The list of commercial surfactants selected for the feasibility study is presented in Table 4.1.

Table 4.1: Summary of surfactant properties for feasibility study

Material	HLB	M_w
PIBSA-MEA	<4	1109
Span 80	4.3	429
Pluronic PE3100	3	1000
Pluronic PE6100	3	2000
Tween 80	15	1310
Tween 20	16.7	1228

The two Pluronic surfactants used were the commercially-named PE3100 and PE6100, with a hydrophilic lipophilic balance (HLB) equal to three and molecular weights of 1000 and 2000, respectively. The Pluronics were supplied by BASF, South Africa, after being recommended as suitable for use by the supplier.

4.3.1 Experiments and Results

4.3.1.1 Preparation of oil and aqueous phases

To prepare oil and aqueous phases, all oil soluble surfactants (Pluronics, SPAN 80 and PIBSA-Mea) were dispersed in Ash-H oil as oil phase, and the water-soluble (Tween 20 and Tween 80) surfactants in the 60% AN solution as aqueous phase. Tween surfactants have been developed to stabilise O/W or multiple emulsions by adding them to the water phase. However, in this present study, Tween molecules formed transparent gel-like aggregates in the aqueous phase, due to the salting-out effect of Tweens in the presence of large quantities of AN in the water phase.

An alternate procedure was adopted for adding water-soluble surfactants into the emulsion system. The water-soluble surfactant was added to the oil phase and successfully dispersed in the industrial Ash-H oil, which had short alkyl chains (average carbon number of 14) and an interfacial tension equal to 19 mN/m. Addition of Tween 80 molecules to organic solvents such as benzene and toluene has also been reported elsewhere (Santhanalakshimi & Maya, 1997). Furthermore, Jiao and Burgess (2003) discussed the diffusion of water-soluble surfactants from one water phase to a second water phase through the oil phase in W/O/W multiple emulsions. Because of the hydrophilic nature of Tween, the term 'water-soluble' was used, despite its addition in oil phase. Illustrations of the surfactant in the oil and the aqueous phases are shown in Figure 4.4.



Figure 4.4: An AN solution (60 wt%) containing 1 wt% Tween 80 surfactant, (left) and dispersing of Tween 80 in pure Ash-H oil (right). Squares in left picture indicate the formation of Tween 80 agglomerates in the aqueous phase

The oil phases containing water-soluble surfactants were slightly opaque when compared to the Ash-H at ambient temperature, but when heat was applied, the oil phase became transparent during the emulsification process. This was due to an alteration in surfactant properties when temperatures were in excess of the HLB temperature (Kunieda *et al.*, 1987). Polyoxyethylene chains of polyethoxylated surfactants such as Tweens dehydrate at higher temperatures and become hydrophobic (Solans *et al.*, 2004). Therefore, all the emulsion samples were prepared by adding all surfactants to the oil phase.

The interfacial tension of both single surfactants and their binary mixtures at 60% AN solution and oil interface were simultaneously measured by using a Kruss K100 tensiometer. The method used to measure interfacial tension is described in section 3.3. As the sensitivity range of the tensiometer was accurate to a minimum of 1 mN/m, all of the interfacial tensions recorded as less than this value are reported as <1. Results are presented in Table 4.2.

Table 4.2: Summary of interfacial tensions of water-oil interfaces (σ) in the presence of selected surfactant systems

Individual surfactant systems	σ (mN/m)	Surfactant binary systems	σ (mN/m)
PIBSA-Mea	9.8	PIBSA-Mea/Pluronic PE 6100	<1
Span 80	<1	PIBSA-Mea /Pluronic PE 3100	<1
Pluronic PE 3100	\approx 1	PIBSA-Mea /Tween 20	<1
Pluronic PE 6100	1.1	PIBSA-Mea /Tween 80	<1
Tween 20	<1	Span 80/Pluronic PE 6100	1.31
Tween 80	<1	Span 80/Tween 20	\approx 1
-----	-----	Span 80/Tween 80	<1

For the Pluronics and their combinations with Span 80 and PIBSA-Mea, a slight increase in the interfacial tension value was immediately observed as measurements were taken (e.g. PE 6100 and Span 80/PE 6100 in Figure 4.5). In the oil phase preparation step, tiny clusters of Pluronics in Ash-H oil were formed on the base of the glassware. However, these gradually disappeared after adding the oil phase to AN solution. This could be due to the rearrangement of Pluronic molecules at the water-oil interface over time. Thus this could explain similar behaviour observed during the interfacial tension test for these types of surfactants.

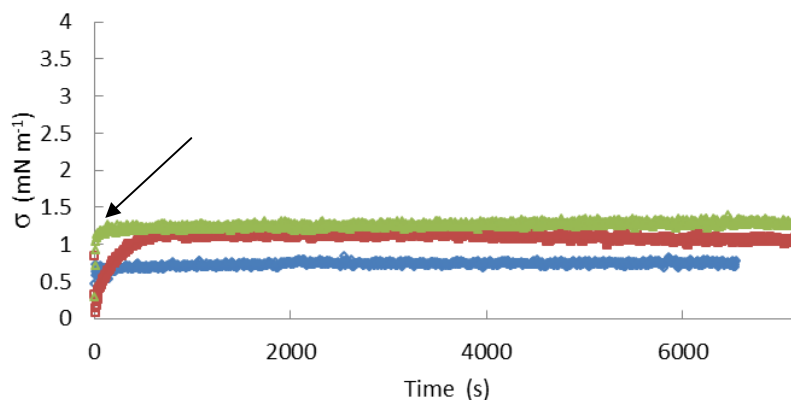


Figure 4.5: Determination of the interfacial tension for Span 80 (blue), Pluronic PE 6100 (red) and Span 80/PE 6100 (10/1) mixture (green)

Remaining graphs of the interfacial tension measurements for other samples as measured against time can be found in Appendix A.

4.3.1.2 Manufacturing of emulsions

To manufacture the emulsions (refer to methods described in Section 3.2.1), a Silverson L4RT dispergator was used. Different speeds of agitation were used. Pre-emulsions were prepared at 500 rpm. Subsequently, these were refined at 2500 rpm to produce smaller droplet sizes. Average droplet size (D_{32}) of the manufactured emulsions was measured by using Malvern mastersizer. The droplet size distribution for the freshly prepared emulsions is shown in Figure 4.6.

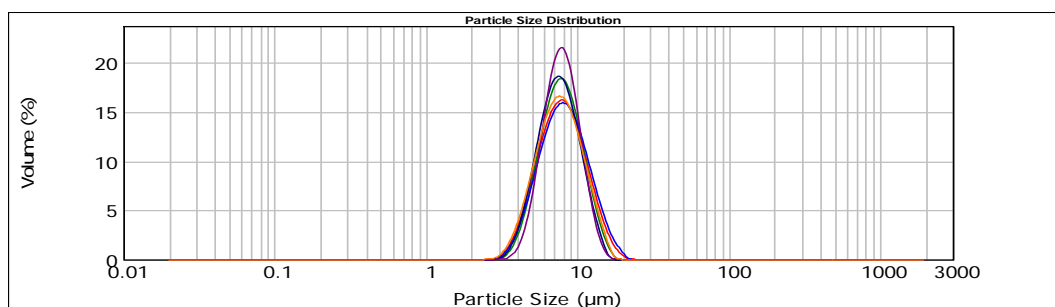


Figure 4.6: The average droplet size of the HCES stabilised by the PIBSA-Mea/Tween 20 (red), PIBSA-Mea/Tween 80 (green), Span 80/PE3100 (blue), Span 80/PE6100 (navy), Span 80/Tween 20 (purple) and Span 80/Tween 80 (yellow) surfactant mixtures

For the purposes of this study, the focus was solely on the formation of HCEs. Therefore, a lower concentration (60 wt%) of the AN solution, stable at ambient temperature, was mixed into the oil phase. The measurement of the inversion point (W/O to O/W emulsion) for the formulations was not considered during the course of the current study. Table 4.3 presents the results of the emulsification process.

Table 4.3: Emulsification analyses of the selected matrix of surfactants

Type of surfactant	Type of co-surfactant	Emulsion formation	D ₃₂ (µm)
Pluronic PE3100	----	Negative	----
Pluronic PE3100	Span 80	Negative	----
Pluronic PE3100	Tween 20	Negative	----
Pluronic PE3100	Tween 80	Negative	----
Pluronic PE6100	----	Negative	----
Pluronic PE6100	Span 80	Negative	----
Pluronic PE6100	Tween 20	Negative	----
Pluronic PE6100	Tween 80	Negative	----
PIBSA-MEA	Pluronic PE3100	Negative	----
PIBSA-MEA	Pluronic PE6100	Negative	----
PIBSA-MEA	Tween 20	Yes	7.3
PIBSA-MEA	Tween 80	Yes	7.2
Span 80	Pluronic PE3100	Yes	7.5
Span 80	Pluronic PE6100	Yes	7.1
Span 80	Tween 20	Yes	7.5
Span 80	Tween 80	Yes	7.0

The overall appearances of the emulsion formulations observed after manufacturing are shown in Figure 4.7.

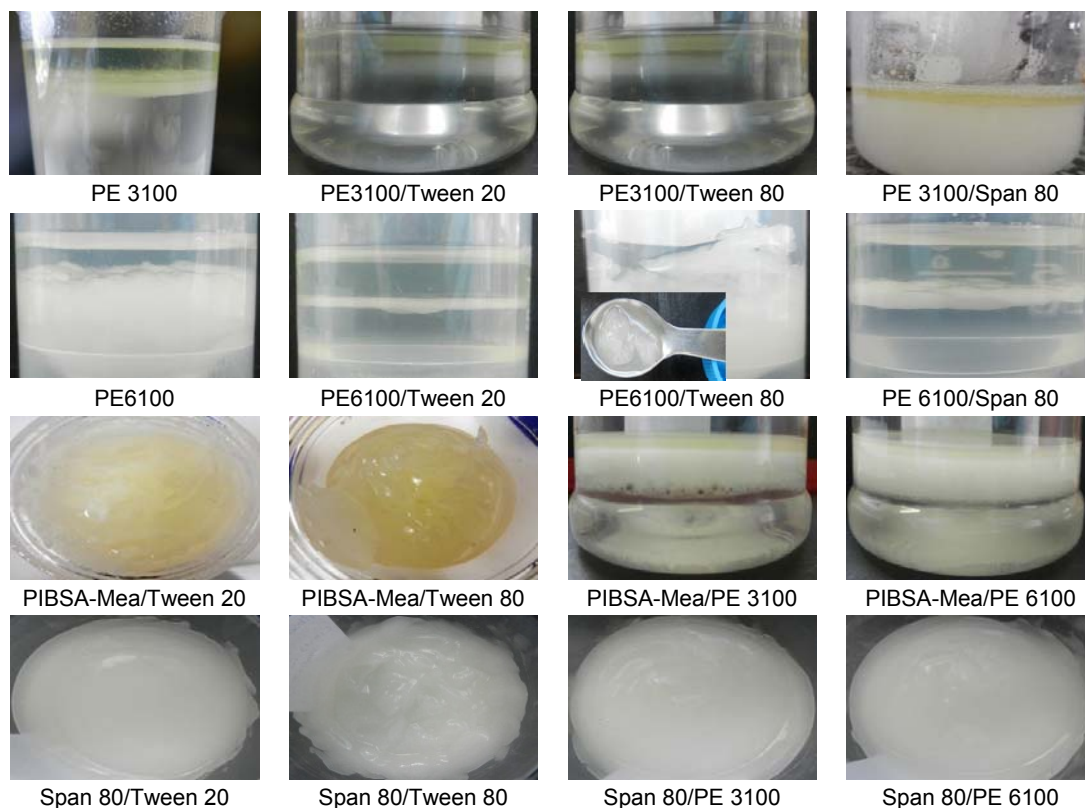


Figure 4.7: Emulsion preparations of different surfactant systems prepared by using the Silverson mixer

Microscopic observations of the emulsions structures are shown in Figure 4.8.

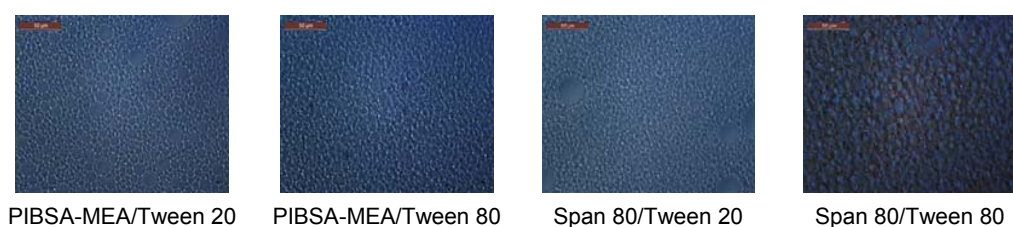


Figure 4.8: Emulsion preparation using Silverson mixer and different surfactant systems. Scale bar, 50 μm = 6 mm

The following resulted from the HCE manufacturing stage:

- *Pluronics*: When Pluronics were used alone, as well as in the mixtures with PIBSA and Tweens, no emulsion formation took place. However, combinations of Pluronics as co-surfactant with Span 80 could stabilise HCEs.

- *Tweens*: HCEs were produced by using the water-soluble Tweens as co-surfactants in combination with Span 80 and PIBSA-Mea.

4.3.1.3 Stability of emulsions against coalescence

Stability as regards coalescence of the manufactured emulsions was measured by measuring droplet size of the samples, using a Malvern Mastersizer-2000 (methods outlined in Section 3.3.3) during a period of 10 days. Results are presented in Table 4.4.

Table 4.4: Emulsification analyses of the selected matrix of surfactants

Type of surfactant	Type of co-surfactant	Stability against coalescence
PIBSA-MEA	Tween 20	<i>stable</i>
PIBSA-MEA	Tween 80	<i>stable</i>
Span 80	Pluronic PE3100	unstable
Span 80	Pluronic PE6100	separated
Span 80	Tween 20	unstable
Span 80	Tween 80	unstable

Only mixtures of PIBSA-Mea/Tweens provided acceptable stability against coalescence. Mixtures of Span 80 with other co-surfactants showed coalescence instability throughout the period of 10 days. Evolution of the droplet size distribution of the emulsions can be found in Appendix A.

The most stable HCEs were formed where the stabilising system consisted of PIBSA-Mea/water-soluble Tween mixtures. Therefore it would be reasonable to include this novel mixture to explosive emulsion formulation and subsequently compare its properties with those of the standard industrial formulation, consisting of PIBSA/Span 80. The aim was to establish whether the substitution of Span 80 for the water-soluble co-surfactants was advantageous to HCEs with a super-cooled dispersed phase. For this stage of the study, the mixture of PIBSA/Tween 80 was chosen. The reason for selecting Tween 80 rather than Tween 20 was due to the similarity in the hydrophobic oleate tail structure between Tween 80 and Span 80. This comparison included the refinement time as well as the stability with regard to crystallisation, both over time and under high shear conditions. Results from that investigation are discussed in the following section.

4.4 COMPARISON OF THE STABILITY OF EXPLOSIVE EMULSIONS STABILISED WITH PIBSA-MEA/TWEEN 80 and PIBSA-MEA/SPAN 80

All samples under investigation were manufactured using a Hobart N50 mixer, as outlined in Section 3.2.2. To prepare the oil phase, the surfactant mixtures of PIBSA-Mea/Span 80 and PIBSA-Mea/Tween 80 with a ratio of 10:1 (as the standard industrial ratio) were dissolved in Ash-H oil. A supersaturated AN solution (80 wt%) was used as the aqueous phase with a ratio of oil/aqueous phase of 7.6/92.4 w/w (Table 4.5).

Table 4.5: Matrix of mixtures for comparison study

Type of surfactant	Type of co-surfactant	Sur/co-sur ratio (wt)	AN con wt%	AqPh/OPh ratio (wt)
PIBSA-Mea	Span 80	10:1	80	92.4:7.6
PIBSA-Mea	Tween 80	10:1	80	92.4:7.6

*AN cons: concentration of AN in the aqueous phase; AqPh: aqueous phase; OPh: oil phase

After preparation of both mixtures, the stability was determined under shearing associated with both emulsification and pumping, as well as under the zero shear conditions associated with shelf life. A comparison was then made.

4.4.1 Emulsification

Refinement times, t_{ref} (manufacturing times to reach a dispersed phase droplet size of $D_{32} = 10 \mu\text{m}$) for the emulsion samples are presented in Table 4.6.

Table 4.6: Refinement time of the manufactured emulsions

Sample	Refinement time (min)
PIBSA-Mea	55'
PIBSA-Mea/Span 80	29'
PIBSA-Mea/Tween 80	8'15"

By adding co-surfactant to the emulsion formulations, the refinement time was decreased. Refinement time of the emulsion stabilised with PIBSA-Mea/Tween 80 was faster when compared to the emulsion stabilised with the PIBSA-Mea/Span 80 mixture.

4.4.2 High Shear Condition

When an emulsion is subjected to high shear, the droplets undergo severe deformation, which leads to disintegration into smaller droplets. Therefore, high shear can be considered as a second stage of refining, or cold refining. In the current study, high shear conditions were simulated by passing the emulsion, under pressure, through a small orifice five times (method outlined in Section 3.3.6).

The PIBSA-Mea emulsion crystallised under shear and measurement of droplet size was not possible for this sample. Previous studies done elsewhere stressed the instability of PIBSA-Mea emulsions under high shear (Reynolds *et al.*, 2002). Microscopic observations of the pumped emulsions structures are shown in Figure 4.9.



Figure 4.9: Photomicrographs of pumped emulsions stabilised by the PIBSA-Mea only (left), PIBSA-Mea/Span 80 (middle) and PIBSA-Mea/Tween 80 (right). Scale bar, 50 μm = 6 mm

Results of droplet size measurements for the pumped emulsions are presented in Table 4.7.

Table 4.7: Droplet size of the pumped emulsions after five pumping cycles

Sample	D_{32} after pumping (μm)
PIBSA-Mea	N/A
PIBSA-Mea/Span 80	5.5
PIBSA-Mea/Tween 80	6.0

The droplet size of the emulsions after high shear reduced to about 60% (D_{32} = 5.5 and 6 μm) of their initial droplet size (D_{32} = 10 μm). The size reduction of the droplets results in an increase of the emulsion viscosity. In addition, an increase in viscosity reduces the pumpability of the emulsion and increases flow line pressures. It was found that the D_{32} of the emulsion stabilised with PIBSA-Mea/Tween 80 was slightly larger than that of the D_{32} of PIBSA-Mea/Span 80 stabilised emulsions. Therefore, it can be said that the emulsion containing water-soluble Tween 80 performs better under high shear condition, as compared to the emulsion containing Span 80.

4.4.3 Ageing

Ageing instability of explosive emulsions is a consequence of slow crystallisation of the oversaturated inorganic salt solutions in the emulsion over time, and can be accelerated by high shear conditions (Masalova *et al.*, 2006).

Ageing results for the emulsions investigated in the current study were considered to be the number of days recorded before the commencement of crystallisation (the first day in which 5-10 crystals were observed in samples under the microscope). These time periods are presented in Tables 4.8 for un-pumped and pumped emulsions.

Table 4.8: Ageing of the un-pumped and pumped emulsions under investigation

Sample	Ageing of un-pumped samples (days)	Ageing of pumped samples (days)
PIBSA-Mea	45	0
PIBSA-Mea/Span 80	16	3
PIBSA-Mea/Tween 80	30	10

A binary mixture of PIBSA-Mea/Tween 80 markedly increased the ageing time of pumped samples and improved the stability of the un-pumped emulsion when compared to the PIBSA-Mea/Span 80 samples. Optical microscopic pictures of the fresh and aged un-pumped emulsions are shown in Figure 4.10. Slower crystallisation kinetics was observed for the PIBSA-Mea/Tween 80 emulsion compared to the one containing PIBSA-Mea/Span 80.

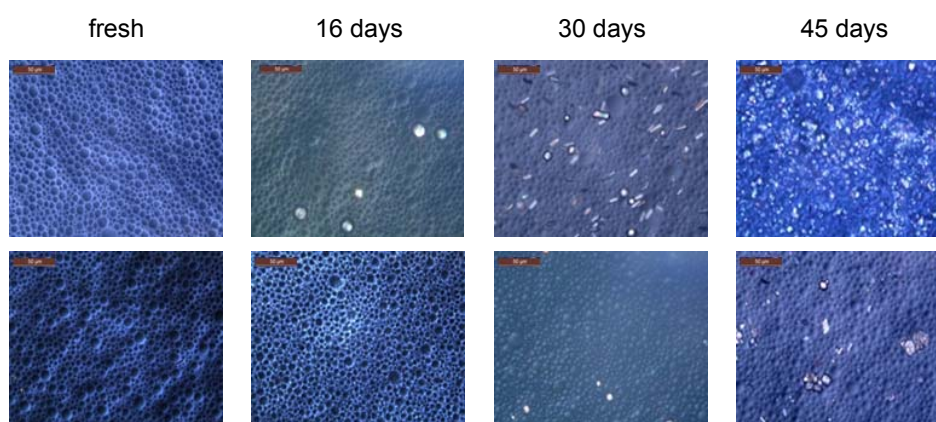


Figure 4.10: Optical microscopic pictures of the fresh and aged un-pumped PIBSA-Mea/Span 80 (top) and PIBSA-Mea/Tween 80 (bottom) emulsions over time, showing higher stability on shelf for the PIBSA-Mea/Tween 80 emulsion. Scale bar, 50 μm = 6 mm

Marked changes in the properties of the emulsion stabilised with PIBSA-Mea/Tween 80 were observed when compared to those of PIBSA-Mea/Span 80. It was therefore necessary to

examine the interfacial behaviour of the two formulations in order to find out why the replacement of Span 80 (a mobile oil soluble surfactant) with bulky water-soluble Tween 80 reduced the refinement time and produced more stable emulsion under high shear and on shelf.

4.4.4 Interfacial study

For interfacial studies, interfacial tensions between the aqueous and the oil phases were measured to determine the critical micelle concentration (CMC) of PIBSA-Mea, Tween 80 and Span 80 using the Wilhelmy plate method (Section 3.3.1). Following this, two sets of samples were prepared by adding variable amounts of PIBSA-Mea (below and above the CMC value) mixed with different concentrations of two co-surfactants in the oil. As discussed in Section 4.3.1, Tween 80 as a water-soluble surfactant was dispersed into the oil phase. The measured values for the CMC and minimum interfacial tension at CMC of PIBSA-Mea, Span 80 and Tween 80 are listed in Table 4.9.

Table 4.9: The CMC values and interfacial tensions at CMC of individual surfactants under investigation

Surfactant	CMC ($\mu\text{mol/L}$)	σ (mN/m)
PIBSA-Mea	76	9.5
Span 80	593	<1
Tween 80	13	<1

The lower CMC value of Tween 80 compared to Span 80 is due to higher hydrophobicity of Tween. However, the difference between CMC of PIBSA and Span 80 mostly arises from the difference between their hydrophobic tails.

The interfacial tensions of both binary surfactant systems as a function of co-surfactant concentration are represented in Figures 4.11 and 4.12 for PIBSA-Mea/Span 80 and PIBSA-Mea/Tween 80 respectively.

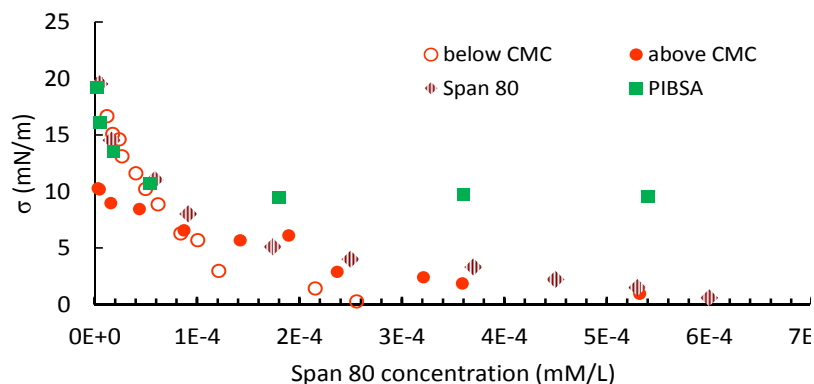


Figure 4.11: The interfacial tension of individual PIBSA-Mea and Span 80 as well as PIBSA-Mea/Span 80 mixtures below and above the CMC of PIBSA-Mea

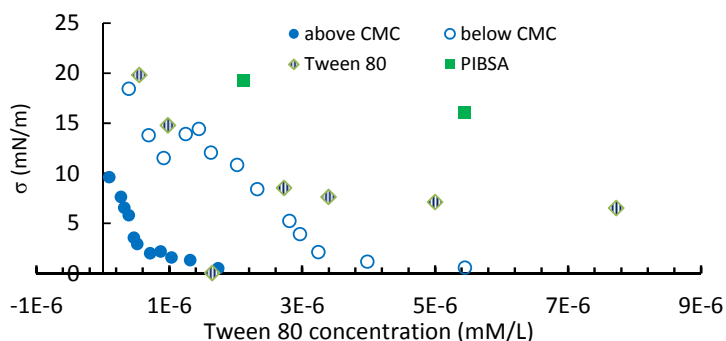


Figure 4.12: The interfacial tension of individual PIBSA-Mea and Tween 80 as well as PIBSA-Mea/Tween 80 mixtures below (○) and above (●) the CMC of PIBSA-Mea

There is a notable difference between the PIBSA-Mea/Span 80 and PIBSA-Mea/Tween 80 mixtures with regard to interfacial behaviour. In the PIBSA-Mea/Span 80 system, the rate of drop in interfacial tension increased when below the CMC of PIBSA-Mea compared to values obtained when the PIBSA's CMC value was exceeded (Figure 4.11). The reverse was recorded for the PIBSA-Mea/Tween 80 mixture (Figure 4.12).

It appeared that when there was insufficient polymeric surfactant to form micelles (below the CMC), Span 80 molecules covered the interface rapidly and decreased the interfacial tension. Above the CMC, when sufficient PIBSA-Mea was available to cover the interface and form micelles, the rate at which the addition of Span 80 lowered interfacial tension decreased, showing similar interfacial behaviour to Span 80 alone.

In the PIBSA-Mea/Tween 80 system, different behaviour was observed. Both below and above the CMC, the minimum interfacial tension ($\sigma < 1$) was reached far more rapidly than for Tween 80 alone.

This suggests that there is a different type of interactions (synergetic/ideal/antagonistic) between these two groups of surfactant mixtures at the interface (Holland & Rubingh, 1992). A strong synergism could exist between PIBSA-Mea and Tween 80, which accelerated the reduction of σ in both regions. In addition, the dramatic collapse of interfacial tension recorded when the CMC was exceeded could also possibly be due to Tween 80 molecules transporting PIBSA-Mea micelles to the interface, thereby increasing the adsorption rate (Jiao & Burgess, 2003).

4.5 SUMMARY

The feasibility study demonstrated promising results. A very significant improvement in all aspects of the emulsions under investigation was observed after replacing Span 80 with water-soluble Tween surfactant in the emulsion formulation. Water-oil interfacial properties of both PIBSA-Mea/Span 80 and PIBSA-Mea/Tween 80 mixtures were investigated in order to understand the reason behind this improvement. A remarkable difference in the interfacial behaviour of these mixtures could be related to different types of interactions (synergism/antagonism) between PIBSA-Mea and the two co-surfactants' molecules at the interface.

It was then decided to use various other combinations of surfactants from the Spans and Tweens family, with PIBSA to stabilise HCEs with super-cooled dispersed phases and find the best one among them to improve the stability of such emulsions, both on shelf and under high shear.

Ten surfactants from the family of Spans and Tweens, with varying tail structures, were selected to act as co-surfactants with the PIBSA-Mea main surfactant. The interfacial tension measurement was provided as an indirect method of deducing the type and degree of synergetic/antagonistic interaction (synergetic compatibility) between the binary mixtures, and related the latter to the stability and pumpability of the emulsions. Results from this investigation are discussed in the following chapter.

CHAPTER FIVE: EFFECT OF CO-SURFACTANT STRUCTURE ON THE EMULSIFICATION PROCESS, INTERFACIAL AND RHEOLOGICAL PROPERTIES, SHELF LIFE AND STABILITY UNDER HIGH SHEAR OF EXPLOSIVE EMULSIONS

5.1 INTRODUCTION

In this chapter, attention is focused on the interpretation of experimental results obtained from investigations into emulsification, interfacial and rheological properties/pumpability and stability during shelf life and under high shear conditions of HCEs with a super-cooled dispersed phase stabilised by different binary surfactant mixtures. In particular, results refer to the observation that the crystallisation of droplets was the main destabilisation factor encountered during the processing, storage and application of the emulsions.

The aim of this section of the research is to study the effect of co-surfactant chemical structure on interfacial films' properties and, in particular, of any synergetic/antagonistic interactions (synergetic compatibility) of surfactant and co-surfactant at the interface, as well as to relate this to other properties of the emulsions, such as stability and pumpability. For this purpose, ten binary mixtures of surfactants were chosen to stabilise emulsions under the investigation. The primary/main surfactant was PIBSA-Mea. Co-surfactants were selected from the family of Spans and Tweens. To conduct a systematic study on surfactant structure effect, the co-surfactants were divided into three different categories based on their hydrophobic tail structures. These consisted of the following:

- *Length of hydrophobic tail*: Span 20, Span 40 and Span 60 as well as Tween 20, Tween 40 and Tween 60 having 11, 15 and 17 carbons in the tail structure, respectively.
- *Unsaturated and saturated hydrophobic tail*: Span 60 and Span 80 as well as Tween 60 and Tween 80 with identical numbers of carbons in tail structure but, with a double bond (between C8 and C9) in Span 80 and Tween 80.
- *Number of hydrophobic tails attached to the head group*: Span 80 and Tween 80 with one oleate tail compared to Span 85 and Tween 85 with three oleate tails.

5.2 EXPERIMENTS AND RESULTS

5.2.1 Interfacial Properties

In order to develop a better understanding of surfactant structure effects on emulsion properties such as stability, the interfacial properties of surfactant mixtures under investigation were studied. This was conducted via the interfacial tension measurements at

the water-oil interface for the individual surfactants and their binary mixtures using a Kruss K100 tensiometer (Section 3.3.1).

The critical micelle concentrations (CMCs) were extrapolated from the intersection point of the straight lines of graphs depicting the variation of interfacial tension with the surfactant concentration, and the region in which the interfacial tension was in steady state (Figure 5.1).

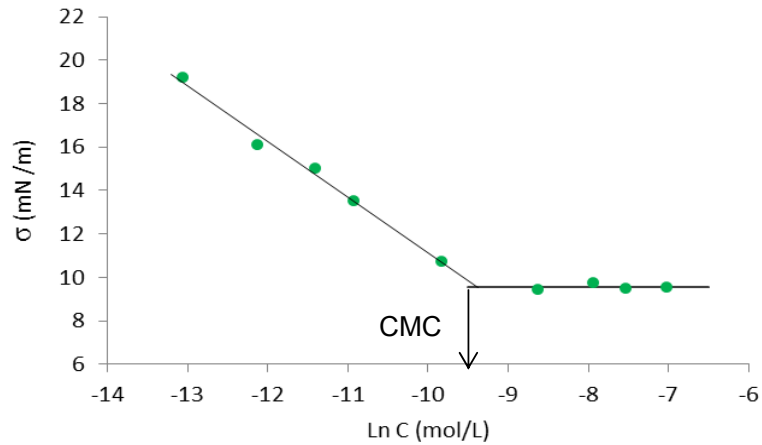


Figure 5.1: Determination of CMC value of the PIBSA-Mea surfactant

The Gibbs free energy of micellisation (ΔG_{mic}) and the transfer of the surfactant molecules from the interface to the micelle (ΔG_{min}) were calculated by using Equations 5.1 and 5.2, respectively (Crook *et al.*, 1963; Peltonen *et al.*, 2001; Szymczyk, 2012).

$$\Delta G_{mic} = RT \ln(cmc) \quad \text{Equation 5.1}$$

$$\Delta G_{min} = \Pi_{min} \times A_{min} \quad \text{Equation 5.2}$$

where R is the molar gas constant, T the absolute temperature and A_{min} is the average minimum area per surfactant molecule at interface.

The Π_{min} is the surface pressure at the CMCs, which is obtained by using Equation 5.3:

$$\Pi_{min} = \sigma_0 - \sigma_{cmc} \quad \text{Equation 5.3}$$

where, σ_0 is the interfacial tension between two immiscible liquids without surfactant, and σ_{cmc} is the interfacial tension of a water-oil interface containing surfactant at the CMC point.

The maximum surface excess concentration, Γ , at the water-oil interface was calculated based on the Gibbs adsorption equation (Equation 5.4):

$$\Gamma = -1/RT \times (d\sigma / d \ln C) \quad \text{Equation 5.4}$$

where $(d\sigma/d \ln C)$ is the maximal slope in the σ versus $\log C$ plot; and N is Avogadro's number. In addition, the average minimum area per molecule, A_{min} , at the water-oil interface for both individual surfactants and surfactant mixtures was obtained using Equation 5.5 (Myers, 2005):

$$A_{min} = 1/\Gamma N \quad \text{Equation 5.5}$$

The interfacial behaviour of PIBSA-Mea/Span 80 and PIBSA-Mea/Tween 80 reported in Chapter Four revealed that oil soluble co-surfactants (Span 80) and the water-soluble co-surfactant (Tween 80) acted in a markedly different manner at the interface. Thus, it was of interest to measure the degree of synergism between different surfactants of the mixtures at the interface and to compare the results obtained to other properties of the manufactured emulsions.

There are various empirical and semi-empirical models developed for the thermodynamic study of the interface. A well-known example of empirical models was developed by Tamlyn and Prager (1978). However, this model includes assumptions which do not apply to the current system, including the following:

- 1) the amount of surfactant is sufficient to cover only the interface;
- 2) the system is ideal; and
- 3) the molecular structure of the various emulsion components is not considered.

Semi-empirical models have been developed based on different experimental methods. For example, an approach suggested by Zana (1995) is based on light scattering and fluorescence quenching techniques. The monolayer behaviour of mixed surfactants can also be analysed, principally by using interfacial tension measurement such as the Rubingh or Motomura-based models (Elena & Emilio, 2007).

Motomura *et al.* (1984) showed that a model for a mixed micellar composition of surfactants can be derived from the excess thermodynamic functions, while the Rubingh model is based on regular solution theory. Although the thermodynamic basis of the Rubingh model is not as sound as is Motomura's model, it is the only model which gives a quantitative value for the

interaction between different surfactants at interface. Due to its simplicity, it is therefore used by many authors (Haque *et al.*, 1995; Chow & Ho, 1996; Lu & Rhodes, 2000; Campana *et al.*, 2013).

A useful non-ideal model to calculate the extent of synergism or antagonism in a binary mixture of surfactants was developed from the Rubingh theory by Zhou and Rosen (Zhou & Rosen, 2003). According to the Rosen model, if two surfactants, 1 and 2, create a structured layer at interface, the mole fraction of surfactant 1 (X_1) can be calculated from the experimental critical concentration of micelles (CMC) data by Equation 5.6:

$$\frac{X_1^2 \ln(\alpha C_{12} / X_1 C_1)}{(1 - X_1)^2 \ln[(1 - \alpha) C_{12} / (1 - X_1) C_2]} = 1 \quad \text{Equation 5.6}$$

where C_1 , C_2 and C_{12} are the concentrations of the individual surfactants and a mixture of them, at a certain interfacial tension below the CMC respectively, and α is the molar fraction of surfactant 1 in the mixture. Value X_1 is then substituted into Equation 5.7 to calculate the interaction parameter (β):

$$\beta = \frac{\ln(\alpha C_{12} / X_1 C_1)}{(1 - X_1)^2} \quad \text{Equation 5.7}$$

A negative value of β is interpreted as synergism, and shows a more attractive or less repulsive interaction between surfactants. For more repulsive or less attractive interaction, β becomes positive, and this is termed "antagonism". The experimental evaluation of the interaction parameter is shown in Figure 5.2.

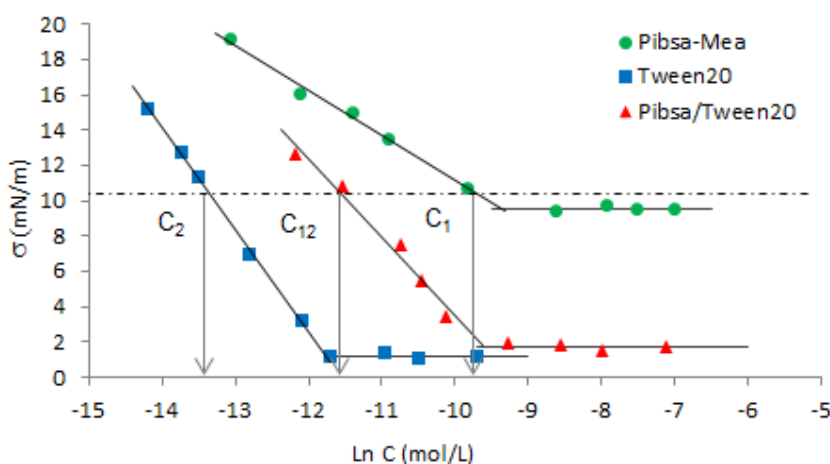


Figure 5.2: Experimental evaluation of the interaction parameter β between PIBSA-MEA and Tween 20 surfactants, based on interfacial tension measurements

5.2.1.1 PIBSA-Mea/Spans Group

▪ Individual surfactants

The calculated values of the critical micelle concentration (CMC), Gibbs free energy of micellisation (ΔG_{mic}) and the energy of transfer of the surfactant molecules from the interface to the micelle (ΔG_{min}), as well as the average minimum area per molecule (A_{min}) for PIBSA-Mea and Span surfactants, are introduced in Table 5.1. All interfacial tension measurements for both individual and mixtures of surfactants are included in Appendix B.

Table 5.1: Interfacial properties of individual PIBSA-Mea and Spans

Material	Tail structure	CMC ($\mu\text{mol/L}$)	A_{cmc} (\AA^2)	ΔG_{mic} (kJ)	ΔG_{min} (kJ)
PIBSA-Mea	19 x C(CH ₃) ₂ -CH ₂	76	155.9	-23.5	1.6
Span 20	11C	596	95.1	-18.4	1.8
Span 40	15 C	437	93.6	-19.2	1.9
Span 60	17 C	379	93.1	-19.5	1.8
Span 80	17 C (C8=C9)	593	121.6	-18.4	2.3
Span 85	3 x 17 C (C8=C9)	686	131.6	-18.1	2.6

It has been shown that the hydrophobic tail length exerts a major effect on the actual CMC value (Peltonen *et al.*, 2001, Rosen & Kunjappu, 2012). As presented in Table 5.1, PIBSA-Mea (with a long and bulky tail length) showed the lowest CMC when compared to Spans. The value recorded for the Spans with a longer hydrophobic tail length decreased slightly (Peltonen *et al.*, 2001; Rosen & Kunjappu, 2012).

CMC: Span 20-11C > Span 40-15C > Span 60-17C

In addition, it was found that the presence of a single double bond, viz., oleate, in the hydrophobic tail, increased the CMC when compared to values obtained for the saturated tail. This was due to the difficulty in packing imposed by the double-bond cis configuration (tail is bent) (Peltonen & Yliruusi, 2000; Peltonen *et al.*, 2001; Myers, 2005).

CMC: Span 80 (unsaturated tail) > Span 60 (saturated tail)

Moreover, the CMCs of the surfactants which displayed more than one hydrophobic tail in the structure occurred at higher concentrations (Varadaraj *et al.*, 1991). Increasing the number of tails in surfactant molecules reduces the effective tail length, which causes a steric inhibition of the micellisation process, and this causes the increased CMC noted for Span 85 when compared to that of Span 80.

The area per molecule of individual surfactants (A_{CMC}) is shown in Table 5.1. The area per molecule of PIBSA-Mea reported elsewhere in the literature supports this value (Ghaicha *et al.*, 1993; Reynolds *et al.*, 2001; Masalova *et al.*, 2011b). However, the area per molecule of Spans recorded during this study was higher than that reported by other publications. The type of oil used in an emulsion influences the value obtained for the area per molecule of surfactants (Peltonen *et al.*, 2001). Also, the short alkyl tails of Ash-H (average of 14 carbon atoms) could have been enclosed between aligned hydrophobic tails of Span molecules, thereby increasing the area per molecule of surfactant (Johnston *et al.*, 1984; Rosen *et al.*, 1988). The area per molecule was calculated to be greatest for PIBSA-Mea and least for Spans 40 and 60. Increasing the hydrophobic tail length reduced the area per molecule of surfactants, as there was a more efficient arrangement ability associated with longer linear hydrophilic tails (Peltonen & Yliruusi, 2000). The existence of a double bond in Span 80 and three hydrophobic tails in Span 85 increased the area per molecule of these surfactants. The cis unsaturated bond in the oleate tail of Span 80 interacts with water molecules, and therefore will be closer to the aqueous surface, thus increasing the tail disorder. In this manner, Span 80 molecules create an expanded film at the water-oil interface with a simultaneous increase in area per molecule (Elworthy & Florence, 1969; Boyd *et al.*, 1972; Lu & Rhodes, 2000). Furthermore, Span 85 has three oleate tails and therefore produces a wider configuration at the interface than do the other Spans.

The results calculated for the free energy of micellisation (ΔG_{mic}) and transfer energy (ΔG_{min}), listed in Table 5.1, indicate that micellisation is more favourable for PIBSA than for Spans.

This is probably due to the greater interaction of Span molecules with water molecules (Kovalchuk & Masalova, 2012). Hence, less energy is required to transfer PIBSA from the interface to micelle aggregates. Furthermore, it is easier for bulky PIBSA molecules to be accommodated in spherical micelles than at the interfacial layer (Zhou & Rosen, 2003). The ΔG_{mic} of Span 85 was less negative when compared to other Spans. The negativity of micellisation energy was reduced by increasing the number of tails, as well as decreasing the tail length. It is been claimed that the double bond effect was negligible (Peltonen *et al.*, 2001). In addition, results reported here indicate that the energy required to transfer Spans molecules from the adsorbed layer to micelles (ΔG_{min}) was lower for the shorter tail lengths. In addition, the unsaturated tail impact on increasing the ΔG_{min} value for Span 80 and 85 was marked.

▪ Mixture of surfactants

Table 5.2, lists the CMC, the area per molecule (A_{min}) and interaction parameter (β) recorded for the mixed monolayer of PIBSA-Mea/Spans mixtures at the water-oil interface. The values for β were calculated using Equations 5.6 and 5.7 at an interfacial tension = 10.5 (mN/m), where the interfacial tension slopes are almost linear.

Table 5.2: Interfacial properties of PIBSA-Mea/Spans mixtures

Material	Co-surfactant tail structure	CMC ($\mu\text{mol/L}$)	A_{min}^2 (\AA^2)	X_1	β
PIBSA-Mea/Span 20	11C	229	109.9	0.48	-3.0
PIBSA-Mea/Span 40	15 C	295	134.1	0.45	-2.6
PIBSA-Mea/Span 60	17 C	339	133.1	0.41	-1.5
PIBSA-Mea/Span 80	17 C (C8=C9)	415	155.5	0.42	-0.8
PIBSA-Mea/Span 85	3 X17 C (C8=C9)	1965	284.1	0.56	5.3

Effect of hydrophobic tail length - In all of the PIBSA-Mea/linear Spans mixtures, the interaction parameter (β) was negative. This indicated that the interactions between the two different surfactants after mixing were more attractive or less repulsive than was the case before mixing. Before mixing, there was a dipole-dipole interaction between head groups and a steric self-repulsion between the bulky branched hydrophobic tails of the polymeric PIBSA-Mea molecules. The latter was weakened by the dilution effect created by mixing with Spans (Zhou & Rosen, 2003).

On the other hand, the type of interaction between the nonionic surfactants, Span 20, 40 and 60, was a dipole-dipole interaction between the sorbitan head groups and van der Waals

self-attraction between linear hydrophobic tails (Pilpel & Rabbani, 1988; Szymczyk, 2012). After mixing, low molecular Span molecules occupied the spaces between the large polymeric molecules of PIBSA and formed a dense layer at the interface, resulting in negative values for β .

As Span tail length increased, synergism between PIBSA and Spans decreased (Table 5.2). This implies that the smaller Span molecules can be accommodated between PIBSA molecules more easily, while the stronger van der Waals attractive self-interaction in the longer hydrophobic tail decreases the magnitude of the β value for the PIBSA/Span 40 and 60 mixtures. Therefore, the reduction of repulsive interaction energy in the PIBSA/short tail Span mixture is greater than in the PIBSA/long tail Span mixture. Thus, the A_{\min} of the PIBSA/Span 20 mixture is less than that of the PIBSA/Span 40 and 60 mixtures. However, the molar fraction of the polymeric PIBSA-Mea surfactant at the interface is greater for PIBSA/Span 20, when compared with the other two mixtures.

Effect of unsaturated hydrophobic tail - The β value of PIBSA/Span with unsaturated tails (Span 80) mixture was less negative than that of PIBSA/Span with the saturated tail, Span 60. As illustrated in Table 5.2, the mixture of PIBSA/Span 80 showed an almost ideal mixture (β is very close to zero). However, the mixture of PIBSA/Span 60 showed synergism, although both Span 60 and 80 have the same number of carbon molecules, (17C), in the hydrophobic tail and the same molar fraction at interface. One explanation for such a result would be, as referred to in the foregoing, that the double bond in the oleate tail of Span 80 tends to interact with the aqueous phase and this creates an expanded film at the interface. Thus the surfactant molecules are unable to form a closely-packed interfacial layer (Figure 5.3).

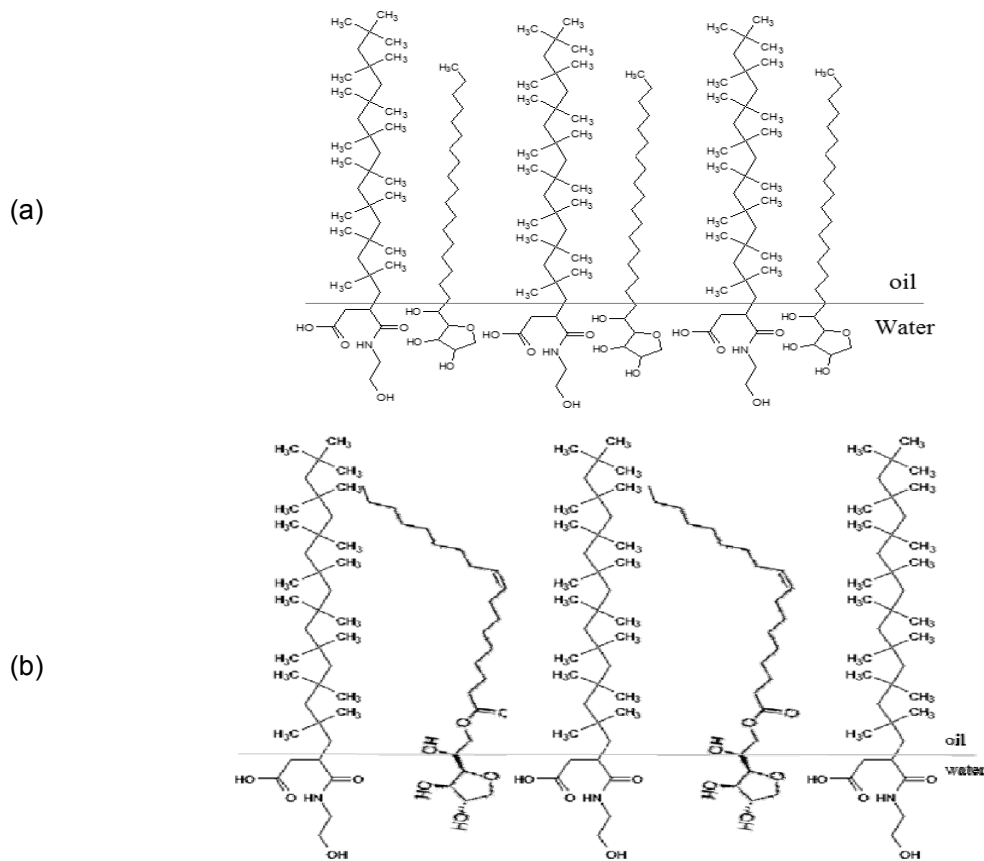


Figure 5.3: Schematic diagram of the interfacial layer in the presence of a) PIBSA-Mea/Span 60 and b) PIBSA-Mea/Span 80 surfactant mixtures

This could also be confirmed by comparisons between the A_{\min} value of the PIBSA/unsaturated Span mixture and individual surfactants. The A_{\min} of the PIBSA/Span 80 mixture is greater than that of Span 80 and more closely resembles the A_{\min} value of PIBSA-Mea. This suggests that Span 80 molecules were not homogeneously accommodated between the PIBSA surfactants and expanded on the aqueous surface by means of the unsaturated bonds.

Effect of the number of hydrophobic tails - The interaction value of PIBSA/Span 85 and PIBSA/Span 80 is presented in Table 5.2. It can be seen that the β value of the PIBSA-Mea/Span 85 mixture is positive, which means there is an antagonism between the two surfactants. The antagonism could be caused by the wide molecular structure of Span 85. The Span 85 surfactants, with three unsaturated oleate tails, occupy a large area at the interface and prevent the surfactants from forming a condensed associated structure with PIBSA-Mea at the interface, as was the case for linear Spans (Wan & Lee, 1974). Furthermore, owing to the bulky structure of Span 85 compared to the polymeric surfactants,

unlike other PIBSA-Mea/Span mixtures, PIBSA molecules compete with Span 85 molecules to occupy the interface, and as a result, PIBSA-Mea makes a greater contribution (higher X_1) at the interfacial layer in the PIBSA-Mea/Span 85 system.

5.2.1.2 PIBSA-Mea/Tweens group

▪ Individual surfactants

The experimental values of the critical micelle concentrations (CMCs), Gibbs free energy of micellisation (ΔG_{mic}) and transfer of the surfactant molecules from the interface to the micelle (ΔG_{min}) and average minimum area per molecule (A_{min}) of individual surfactants are presented in Table 5.3, where it must be taken into account that these surfactants have been dissolved in the oil as PIBSA-Mea and Spans, and not in the water. Thus, different interfacial behaviour was expected of Tweens when considering data from other publications.

Table 5.3: Interfacial properties of individual PIBSA-Mea and Tweens

Material	Tail structure	CMC ($\mu\text{mol/L}$)	A_{cmc} (\AA^2)	ΔG_{mic} (kJ)	ΔG_{min} (kJ)
PIBSA-Mea	19 x C(CH ₃) ₂ -CH ₂	76	155.9	-23.5	1.6
Tween 20	11C	8	70.9	-29.2	1.3
Tween 40	15 C	6	68.6	-29.9	1.3
Tween 60	17 C	5	58.8	-30.1	1.1
Tween 80	17 C (C8=C9)	13	84.5	-27.9	1.6
Tween 85	3 x17 C (C8=C9)	15	92.5	-27.7	1.8

In the current study for all Tweens, the CMCs were below the CMC value of PIBSA-Mea. The values were similar for Tween 20, 40 and 60. For Tween surfactants, the packing of the surfactant molecules is influenced principally by the bulkiness of the ethylene oxide segments, and not by the hydrophobic tail (Sarmoria *et al.*, 1992). A slight increase in the CMC for Tween 80 and Tween 85 could be caused by the presence of the double bond in the hydrophobic tails of these surfactants (Elworthy & Florence, 1969; Hua & Rosen, 1982; Siddiqui, 2014). Additionally, the greater molecular weight of Tween 85 could be responsible for an increase in the CMC (Varadaraj *et al.*, 1991).

On the other hand, the lower area per molecule of Tween molecules when compared with PIBSA-Mea indicates a closely-packed interfacial layer formed by Tween surfactants. The effect of tail length on the area per molecule of Tweens was negligible and regarded as irrelevant (Table 5.3). However, it has been reported that the effect of double-bonds and

multi-tails on the average area per molecule of Tween 80 and 85, respectively, has a more pronounced effect (Wan & Lee, 1974; Lu & Rhodes, 2000; Din *et al.*, 2010).

The Tweens showed less free energy of micellisation than did PIBSA-Mea. Tween molecules have a hydrophilic nature. Thus, as soon as the interface is occupied, it would be thermodynamically favourable for the residual Tween molecules to remain as aggregates in continuous phase, thus providing minimum interaction with the oil. Therefore, the energy required to transfer surfactant molecules from interface to micelles was similar for all Tweens. However, the notable tendency of double bonds in Tween 80 and 85 hydrophobic tails to interact with water molecules has been reported to increase the ΔG_{\min} slightly (Lu & Rhodes, 2000)

▪ Mixture of surfactants

The effect of various ethoxylated surfactant structures on the synergistic interaction between the surfactant mixtures is determined by using the Rosen theory, as referred to previously. The molar fraction of surfactants at interface (X_1), the interaction parameter of surfactant mixtures (β) and the average area per molecule (A_{\min}) are presented in Table 5.4. The interaction parameter obtained at interfacial tension=10.5 (mN/m).

Table 5.4: Interfacial properties of PIBSA-Mea/Tween mixtures

Material	Co-surfactant tail structure	CMC ($\mu\text{mol/L}$)	A_{\min} (\AA^2)	X_1	β
PIBSA-Mea/Tween 20	11C	67	92.5	0.45	-3.3
PIBSA-Mea/Tween 40	15 C	36	87.8	0.45	-5.6
PIBSA-Mea/ Tween 60	17 C	39	86.4	0.46	-5.8
PIBSA-Mea/ Tween 80	17 C (C8=C9)	91	103.4	0.46	-2.0
PIBSA-Mea/ Tween 85	3 x17 C (C8=C9)	111	116.4	0.41	-1.9

Effect of hydrophobic tail length - Calculated β values in the mixed monolayer for all the mixtures of PIBSA-Mea/Tweens with linear alkyl tails (Tween 20, 40 and 60) were negative, clearly indicating a synergism between this set of surfactant mixtures and the closely-packed interfacial film. When surfactants are mixed, the distances between the polar head groups of Tweens as well as PIBSA-Mea increase, and as a result the net short-range steric repulsion is reduced by mixing the surfactants (Kuhl *et al.*, 1994; Israelachvili, 2010). Another possible explanation is that when PIBSA-Mea and Tweens are used together, the ethoxylated sections of Tweens are squeezed into a sub-phase (Boyd *et al.*, 1972; Rakshit *et al.*, 1981;

Pilpel & Rabbani, 1988) and those areas of the hydrocarbon tails of Tween that are located in the oil phase penetrate between the adsorbed PIBSA molecules. The distance between neighbouring hydrocarbon tails is therefore reduced, so that the probability of substantial van der Waals attraction between surfactants tails increases.

As referred to previously, the Tweens and PIBSA molecules at the water-oil interfaces are likely to be located at different levels between the two phases, owing to their differing solubility in the oil and aqueous phases. Thus, the degree of interaction between the two surfactant hydrocarbon tails controls the amount of synergism in the mixture. It is known that stronger van der Waals attraction between the longer hydrophobic groups of two different surfactants occurs after mixing and that this causes greater negative β values (Xiao *et al.*, 1996; Zhou & Rosen, 2003). Synergism was more pronounced as the hydrophobic tail length increased in Tweens (Tween 40 and 60) when mixed with PIBSA-Mea (Table 5.4).

Effect of unsaturated hydrophobic tail - The presence of an unsaturated double bond in the hydrophobic tail of the ethoxylated surfactants markedly reduced the synergism between PIBSA-Mea and Tween 80 molecules, when compared to PIBSA/Tween 60 with saturated alkyl tails. The double bond of Tween 80 would interact with water molecules; thus the surfactant molecules created an expanded film at the water-oil interface. The expansion of Tween 80 at interface did not permit the surfactant molecules to form an efficient condensed layer at interface. This can be further confirmed from the experimental cross-sectional area (A_{\min}) of the PIBSA-Mea/Tween80 mixture. This was greater than the A_{\min} value observed for the PIBSA-Mea/Tween 60 mixture. However, the molar fraction of the polymeric surfactant PIBSA-Mea was almost identical in both mixtures.

Effect of the number of hydrophobic tails - Minimal synergism was attained by the mixing of Tween 85 surfactant with three oleate tails and the polymeric PIBSA-Mea surfactant in this group of samples (Table 5.4). Tween 85 molecules create an open conformation between PIBSA molecules at interface as a function of the three oleate tails. This is also inferred from the reported A_{\min} of the PIBSA-Mea/Tween 85 mixture (Boyd *et al.*, 1972). As a result, the decreased ability of Tween 85 to diffuse between PIBSA-Mea molecules yielded a less negative β value. Furthermore, greater amounts of surfactant would be required to cover the interface to reach a certain value of interfacial tension, and thus the CMC of the PIBSA-Mea/Tween 85 mixture is increased.

5.2.2 Emulsification

Highly concentrated water-in-oil emulsions were prepared using a Hobart N50 mixer (Section 3.2.2). Emulsions were stabilised using a defined matrix of surfactant mixtures (Table 5.5). Emulsions were manufactured in 1 kg batches. The target emulsion droplet size (D_{32}) for the final product was 10 μm .

Table 5.5: Matrix of samples used in the emulsification process

Type of surfactant	Type of co-surfactant	Sur/co-sur ratio (wt)	Sur total con wt%	AN con wt%	Aqueous/oil phase ratio (wt)
PIBSA-Mea	-----	-----	0.61	74	92.4:7.6
PIBSA-Mea	Span 20	10:1	0.61	74	92.4:7.6
PIBSA-Mea	Span 40	10:1	0.61	74	92.4:7.6
PIBSA-Mea	Span 60	10:1	0.61	74	92.4:7.6
PIBSA-Mea	Span 80 (SMO)	10:1	0.61	74	92.4:7.6
PIBSA-Mea	Span 85	10:1	0.61	74	92.4:7.6
PIBSA-Mea	Tween 20	10:1	0.61	74	92.4:7.6
PIBSA-Mea	Tween 40	10:1	0.61	74	92.4:7.6
PIBSA-Mea	Tween 60	10:1	0.61	74	92.4:7.6
PIBSA-Mea	Tween 80	10:1	0.61	74	92.4:7.6
PIBSA-Mea	Tween 85	10:1	0.61	74	92.4:7.6

*AN con: concentration of AN in the emulsion; sur: surfactant; co-sur: co-surfactant.

To determine when the target droplet size (t) was reached, several samples were taken from the emulsions at different refining times and the average droplet size (D_{32}) and droplet size distribution (DSD) of each sample was analysed by Malvern Mastersizer.

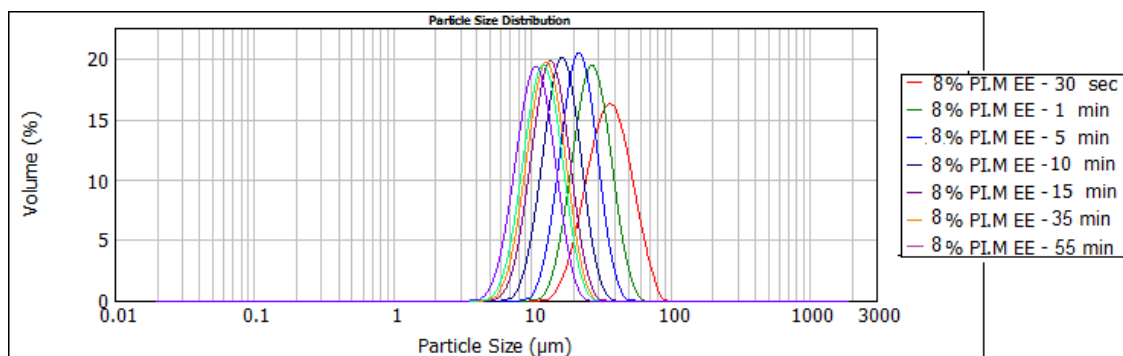


Figure 5.4: The histogram of drop size distribution of the explosive emulsion (EE) stabilised with PIBSA-Mea (PI-M) surfactant at different refining times

As shown in Figure 5.4, droplet size distribution was unimodal and unimodality became narrower as refinement time increased. The histograms shapes were similar for all emulsion formulations under investigation.

Droplet size evolution for the emulsions stabilised with different surfactant mixtures, as illustrated in Figure 5.5. The droplet disintegration rate recorded from samples containing only PIBSA-Mea and PIBSA-Mea/Span mixtures was rapid during the first 15 min of refining time and thereafter maintained a droplet size close to the required target size. In emulsions comprised of PIBSA-Mea/Tween mixtures, droplets showed a markedly rapid reduction in droplet size as refinement time progressed.

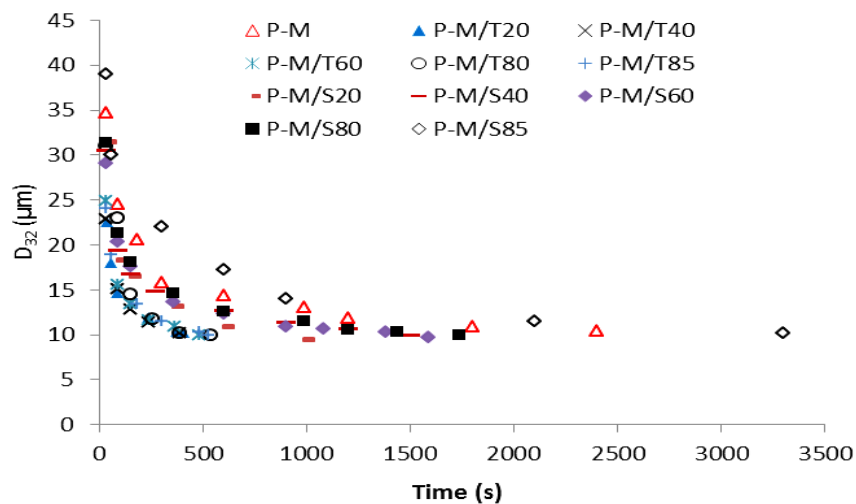


Figure 5.5: Droplet size evolution as a function of refining time for emulsions with different emulsion formulations under investigation (P-M for PIBSA-Mea, T for Tween and S for Spans)

Dynamic instability in emulsions is related to the disintegration of large droplets to smaller ones caused by mechanical forces. To estimate shear stability of emulsions during the emulsification procedure, first the characteristic refinement time (θ) was obtained using the following exponential equation:

$$D_{cal} = D_{crit} + e^{-(t/\theta)}(D_0 - D_{crit}) \quad \text{Equation 5.8}$$

where the critical diameter (D_{crit}) is defined as the diameter at which no change in droplet size (speed 3 of the mixer) is observed as mixing time increases. The D_0 represents the initial diameter of the droplets at the initial time of refining; t is refinement time in seconds and θ is a characteristic refinement time which is independent of D_0 .

The equation fitted all the experimental data satisfactorily. The fit of data of the emulsion stabilised with PIBSA-Mea/Span 80 mixture is presented in Figure 5.6. The data representing the fitting of other samples is given in Appendix C.

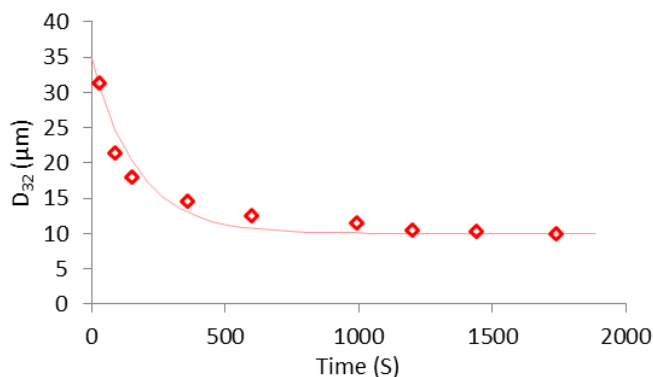


Figure 5.6: Droplet size evolution as a function of refining time for the PIBSA-Mea/Span 80 emulsion (red dots) fitted by model (line)

Qualitatively, it can be shown that the DSD of emulsions where the target droplet size ($D_{32} = 10 \pm 0.2 \mu\text{m}$) was stabilised by different water and oil soluble surfactant types was similar (Figure 5.7).

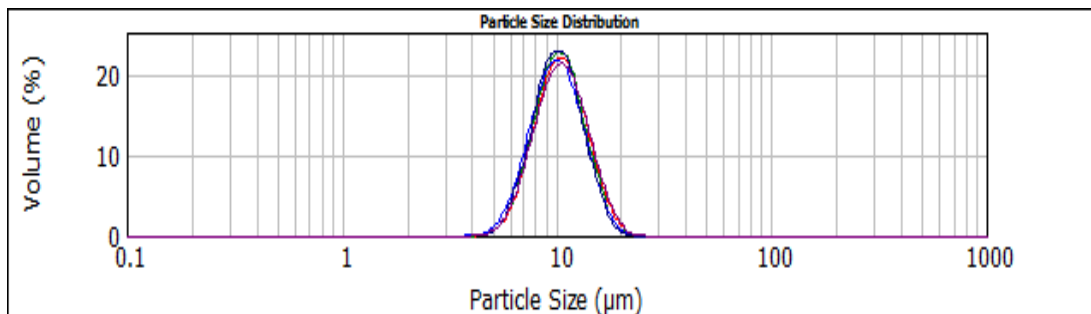


Figure 5.7: Droplet size distribution of the explosive emulsions stabilised with the employed surfactant mixtures

To avoid further errors in analyses caused by crystallisation of the oxidiser in the emulsion bulk during emulsification, all samples were examined under the optical microscope after the target droplet size was reached. Photomicrographs of representative samples are shown in Figure 5.8. These showed that for all formulations under study, un-crystallised emulsions were manufactured.

PIBSA-Mea

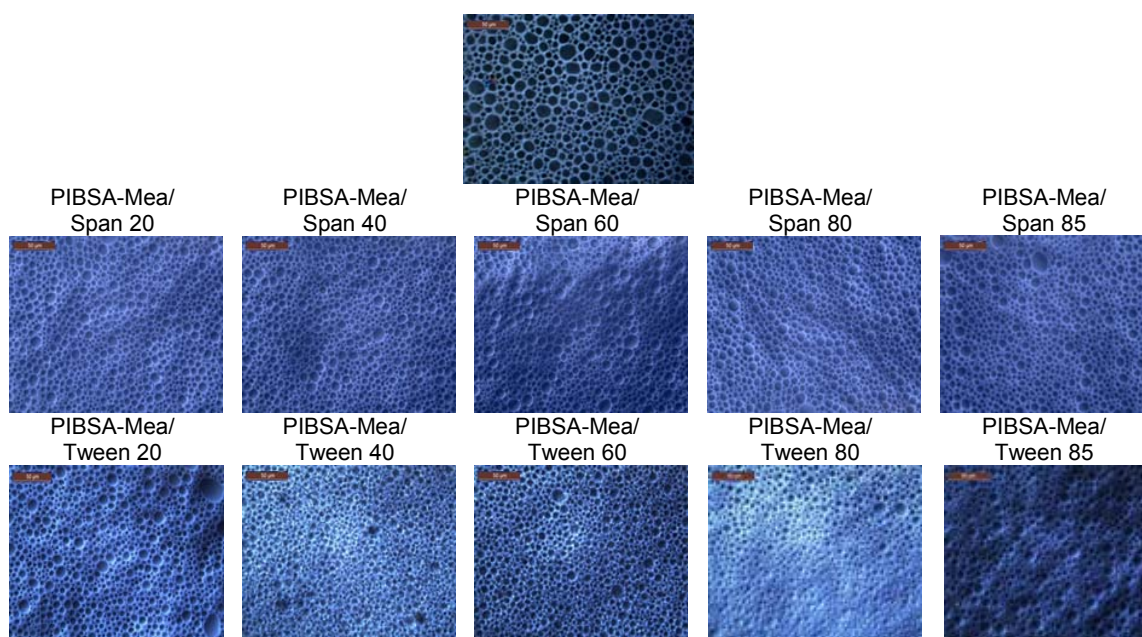


Figure 5.8: Photomicrographs depicting explosive emulsions stabilised with different surfactant types - no crystallisation occurred after manufacturing of the emulsions. Scale bar, 50 μm = 6 mm

Refinement times and characteristic refinement times (θ) for the emulsions are presented in Table 5.6. The D_{crit} for all samples was $10 \pm 0.2 \mu\text{m}$.

Table 5.6: Summary of refinement times for the emulsions under investigation

Surfactant mixture	Co-surfactant tail structure	Refinement time (min)	θ (sec)
PIBSA-Mea	$19 \times \text{C}(\text{CH}_3)_2\text{-CH}_2$	55'	290
PIBSA-Mea/ Span 20	11C	15'30"	115
PIBSA-Mea/ Span 40	15 C	25'	140
PIBSA-Mea/ Span 60	17 C	25'30"	155
PIBSA-Mea/ Span 80	17 C (C8=C9)	29'	170
PIBSA-Mea/ Span 85	3 x 17 C (C8=C9)	60'	300
PIBSA-Mea/ Tween 20	11C	7'	85
PIBSA-Mea/ Tween 40	15 C	6'45"	80
PIBSA-Mea/ Tween 60	17 C	7'45"	75
PIBSA-Mea/ Tween 80	17 C (C8=C9)	8'15"	90
PIBSA-Mea/ Tween 85	3 x 17 C (C8=C9)	8'45"	98

Refinement time was decreased by the addition of co-surfactants to the system when compared to emulsions stabilised with only PIBSA-Mea. An exception to this was Span 85. The influence of Tweens in refining is much greater than that associated with Spans. However, for both substances, the refinement time increased when emulsions contained co-surfactants with unsaturated (Span 80 and Tween 80) or multiple tails (Span 85 and Tween 85).

Other studies conducted on emulsification have shown that several parameters affect droplet break-up and re-coalescence during emulsification. These include temperature and energy input during emulsification, surfactant type and concentration, surfactant adsorption rate, and the viscosities of both continuous phase and emulsion (Karbstein & Schubert, 1995; Tesch & Schubert, 2002; Schultz *et al.*, 2004; McClements, 2005; Seekkuarachchi *et al.*, 2005; Jafari *et al.*, 2008). Surfactants can influence the result during both stages of emulsion manufacture. They can facilitate both droplet deformation and disruption, because they decrease the interfacial tension. On the other hand, they stabilise droplet interfaces and therefore avoid the occurrence of re-coalescence (Karbstein & Schubert, 1995).

The emulsification procedure was adopted from the standard industrial procedure for these types of emulsions and was identical for all manufactured emulsions in terms of energy input and temperature. Therefore, these variables can be disregarded in further discussion. In the current study, the effect of co-surfactants type and structure on the emulsification was the major focus. The break-up of droplets in the emulsification process can be determined by the capillary number, which depends on interfacial tension and the viscosity ratio between internal phase and emulsions (ρ). In this study, viscosity of the aqueous phase was approximately 41 mPa.s, and the viscosity of the emulsions was close to 640 cP at the emulsification condition. Therefore, the viscosity ratio (ρ) was small for the emulsions under investigation. This means that the emulsification process was affected mainly by the interfacial properties of the system. Thus, in the current study, surfactant characteristics in the emulsion formulations played a major role in emulsification. Minimum surfactant concentration required to entirely cover droplet surfaces of the emulsions (C_{surf}) was calculated using the Equation 5.9 (McClements, 2005). Results are shown in Table 5.7.

$$C_{surf} = \frac{6\Gamma\phi}{D_{32}}$$

Equation 5.9

where Γ is the maximum surface excess concentration, ϕ is the dispersed phase volume fraction and D_{32} is the average droplet size of final emulsions.

Table 5.7: A Summary of the minimum concentration of surfactant required to cover the emulsion droplets ($D_{32}=10 \mu\text{m}$)

Surfactant mixture	Total surfactant concentration (wt%)	Surfactant mixture	Total surfactant concentration (wt%)
PIBSA-Mea	0.043	----	---
PIBSA-Mea/Span 20	0.060	PIBSA-Mea/Tween 20	0.074
PIBSA-Mea/Span 40	0.052	PIBSA-Mea/Tween 40	0.079
PIBSA-Mea/Span 60	0.049	PIBSA-Mea/Tween 60	0.083
PIBSA-Mea/Span 80	0.045	PIBSA-Mea/Tween 80	0.070
PIBSA-Mea/Span 85	0.026	PIBSA-Mea/Tween 85	0.064

Total surfactant concentration in all the emulsion samples was 0.61 wt%. This was approximately 10 times in excess of the minimum requirement. Therefore, in all emulsions there was sufficient surfactant to cover the entire $10 \mu\text{m}$ droplet surfaces of the dispersed phase. This implies that most of the surfactants remained in the oil phase and formed reversed micelles in both single and mixed surfactant systems. This trend was previously shown by small-angle neutron scattering (Reynolds *et al.*, 2000; Reynolds *et al.*, 2001; Reynolds *et al.*, 2004).

According to Rosen and Kunjappu (2012, 238), the efficiency of a surfactant with regards to reducing the surface tension is defined as "the bulk concentration required to reduce the surface tension by 20 mN/m". The definition suggested by Rosen cannot be applied for systems where the interfacial tension reduction is less than 20 mN/m. This would include the systems investigated in the current study. To solve this difficulty, Pitt *et al.*'s (1996) suggestion was used as follows: efficiency is defined as "the concentration at which the surface or interfacial tension has reached a value half-way between the solvent value and the value at the CMC, C_{half} " (Pitt *et al.*, 1996, 322). Efficiencies of the surfactant mixtures (pC_{half}) were calculated using Equation 5.10.

$$pC_{\text{half}} = -\log(C_{\text{half}})$$

Equation 5.10

Results obtained from above equation, as well as the surface pressure (Π_{cmc}) for the surfactant systems, are given in Table 5.8.

Table 5.8: The adsorption efficiency of surfactant mixtures required to decrease the interfacial tension of the water-oil interface to 10 mN/m

Surfactant mixture	pC_{half}	π_{cmc} (mN/m)	Surfactant mixture	pC_{half}	π_{cmc} (mN/m)
PIBSA-Mea	5.0	9.5	----	---	---
PIBSA-Mea/Span 20	4.6	16.6	PIBSA-Mea/Tween 20	5.1	17.3
PIBSA-Mea/Span 40	4.7	15.5	PIBSA-Mea/Tween 40	5.2	>18
PIBSA-Mea/Span 60	4.7	15.8	PIBSA-Mea/Tween 60	5.4	>18
PIBSA-Mea/Span 80	4.8	14.5	PIBSA-Mea/Tween 80	5.1	17.9
PIBSA-Mea/Span 85	4.8	12.7	PIBSA-Mea/Tween 85	5.3	17.9

The efficiency of PIBSA-Mea/Tween mixtures was greater than that of PIBSA-Mea/Span mixtures. A higher efficiency accelerates the interfacial tension reduction and prevents the droplets coming closer by means of different repulsive forces. It also creates a resistant layer around the droplets, resulting in a reduced refinement time (Jafari *et al.*, 2008). Furthermore, the PIBSA-Mea/Tweens are more effective (improved π_{cmc}) than are the PIBSA-Mea/Spans. This higher surfactant efficiency accelerates the break-up of droplets and hence decreases refinement time. This was indeed observed with regard to PIBSA-Mea/Tweens.

The coverage efficiency of the surfactants was characterised by the interaction parameter (β) and could be related to the rate of re-coalescence. For high internal phase emulsions the disruption result is superimposed by coalescence and results in larger droplet sizes. Therefore, a more efficiently packed interface reduces the rate of coalescence (Karbstein & Schubert, 1995). A greater synergism between surfactants in the system creates a dense layer around droplets and reduces the mobility of surfactants. Hence, this prevents droplets from coalescing. The interaction parameter between the employed surfactant mixtures versus the characteristic refinement time of the emulsions are displayed in Figures 5.9a and b.

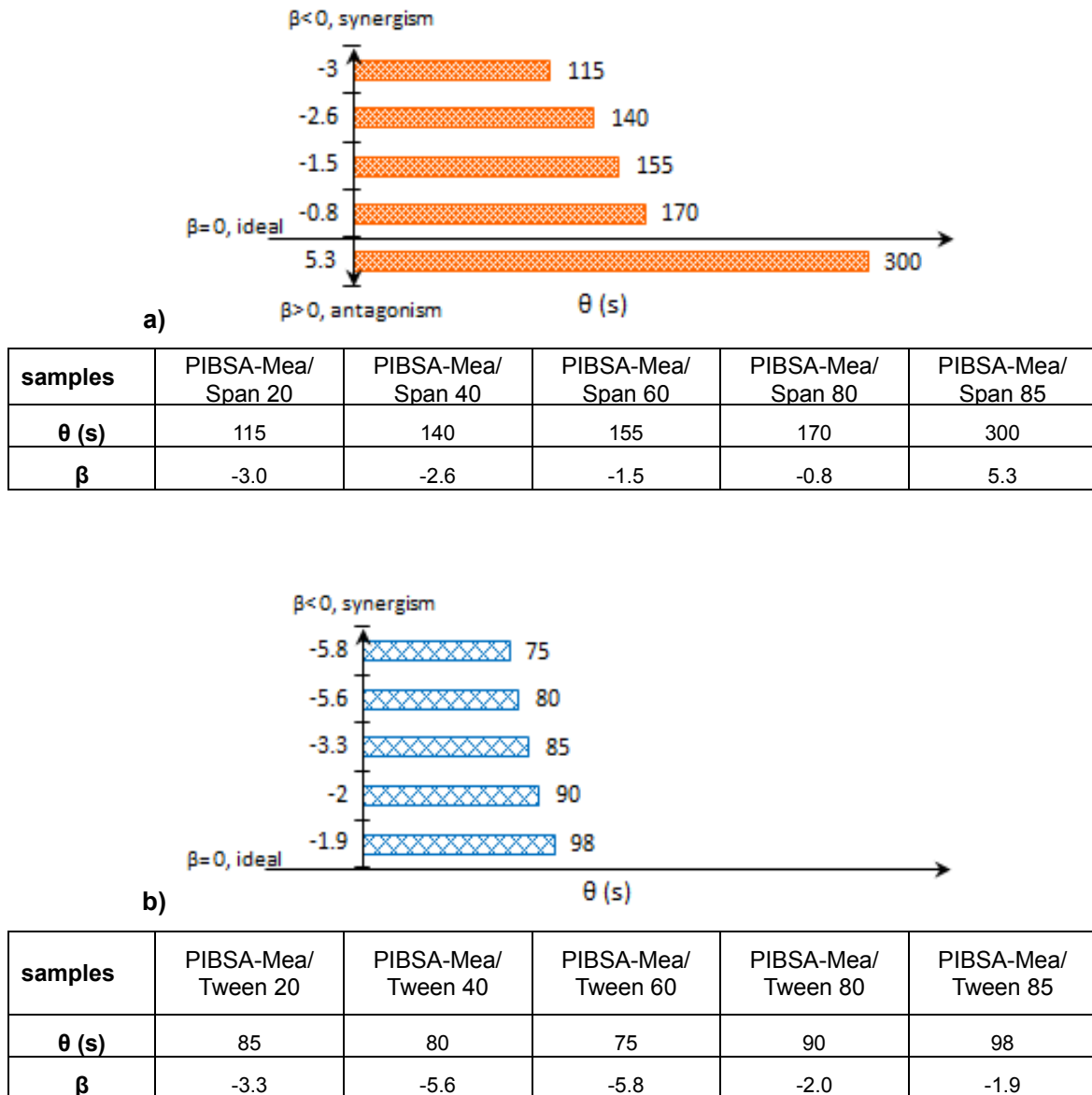


Figure 5.9: The interaction parameter (β) between (a) the PIBSA-Mea/Spans mixtures and (b) the PIBSA-Mea/Tweens, versus the characteristic refinement time (θ) of the emulsions

There is a clear correlation between the characteristic refinement time (θ) and the interaction parameter (β) for all the emulsions under investigation over the entire range of measured β values. However, the effect of β on refinement time was more pronounced for PIBSA-Mea/Spans mixtures. The β values of PIBSA-Mea/Tweens were always negative (synergetic mixtures) and therefore, the characteristic refinement times were similar.

5.2.3 Rheological properties

In this section, the rheological properties of HCEs (explosive type) are discussed. The surfactant mixtures under investigation were used to evaluate the effect of the structure of the co-surfactants exerted on the rheology of the emulsions. The stability of EEs is affected by crystallisation during storage or under high shear condition. However, in the range of stresses applied during the rheological measurement, no crystallisation or separation occurs. Studying the rheological properties of explosive emulsions could therefore provide a reliable means of predicting the pumpability of explosive emulsions for various technical applications (Masalova & Malkin, 2013). The main parameters influencing emulsion transportation in mines, such as pressure drop versus flow rate, are directly related to the rheological characteristics of the system. Reduction in the yield stress and other rheological parameters results in a decrease in pressure which prevents emulsion instability during the transportation process.

The rheological measurements were performed using a rotational dynamic rheometer Anton Paar MCR 301. The geometry of the measuring unit was 'bob and cup' with a sandblasted surface (Section 3.3.5). All rheological tests were conducted at 30 °C. It is important to note that the rheological behaviour of HCEs is dependent on factors such as droplet size, the nature of the employed surfactant, internal phase volume fraction, interfacial tension and others (Welch *et al.*, 2006). For the emulsions manufactured for the current study, the surfactant was varied in different formulations. Hence, the interfacial properties and the viscosity of the oil phases of the various samples were tested.

It should be noted that the rheological measurements of the emulsion systems under investigation were not the main focus of the current study. These were conducted to establish whether the rheological behaviour of such emulsions would alter with the use of the novel surfactant mixtures. Furthermore, it was expected that these measurements would assist in gaining insight into the pumpability of the emulsion formulations.

5.2.3.1 Flow behaviour

- **Oil phase viscosity**

Viscosity of the oil phases in the various prepared surfactant mixtures was measured using a shear rate ranging from 10-100 s⁻¹. Results are shown in Figure 5.10.

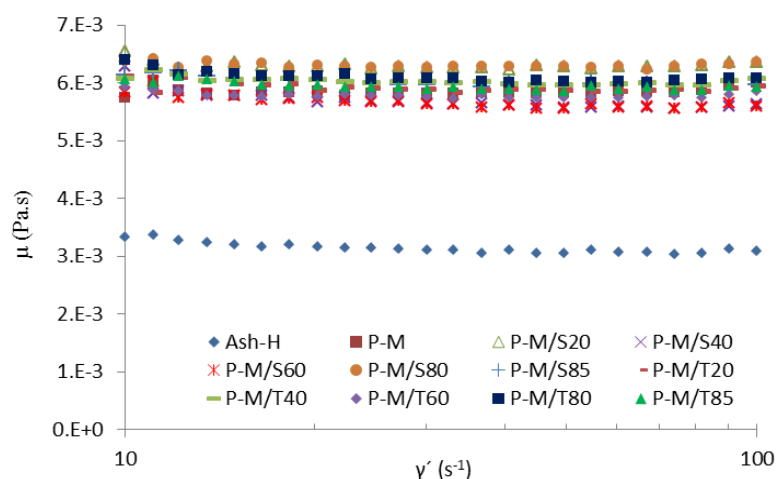


Figure 5.10: Rheological behaviour of the oil phases containing Ash-H oil and surfactant mixtures where P-M stands for PIBSA-Mea, S for Spans and T for Tweens

Newtonian behaviour was observed in all the oil phases tested. Viscosity of the oil phases containing the binary mixtures of surfactants was similar to the viscosity of the oil phase containing only the PIBSA-Mea surfactant. Hence, the effect of the viscosity of the oils on the rheological properties of the emulsions could be neglected (Table 5.9).

Table 5.9: Summary of the viscosity values for the oil phases used in the emulsions under investigation

Sample	μ (mPa.s)	Sample	μ (mPa.s)
Ash-H	3.14	PIBSA-Mea	5.85
PIBSA-Mea/ Span 20	6.30	PIBSA-Mea/ Tween 20	5.92
PIBSA-Mea/ Span 40	5.69	PIBSA-Mea/ Tween 40	6.03
PIBSA-Mea/ Span 60	5.67	PIBSA-Mea/ Tween 60	5.78
PIBSA-Mea/ Span 80	6.30	PIBSA-Mea/ Tween 80	6.10
PIBSA-Mea/ Span 85	6.01	PIBSA-Mea/ Tween 85	5.95

▪ Flow curve of the bulk emulsions

Due to the presence of densely packed and compressed drops, the rheological behaviour of EEs is complex. The shear thinning, elastic effect and appearance of yield stress are typical for this type of emulsion. At low shear rates, the viscosity is time-dependent for explosive emulsions. Two mechanisms of flow at low and high shear rates were observed by Masalova and Malkin (2007b). As shown in Figure 5.11 when the shear rate is low, larger droplets rolled over the smaller ones without causing any significant distortion in droplet shape. At high shear rates deformation of the droplets is the dominant flow mechanism (Masalova & Malkin, 2007).

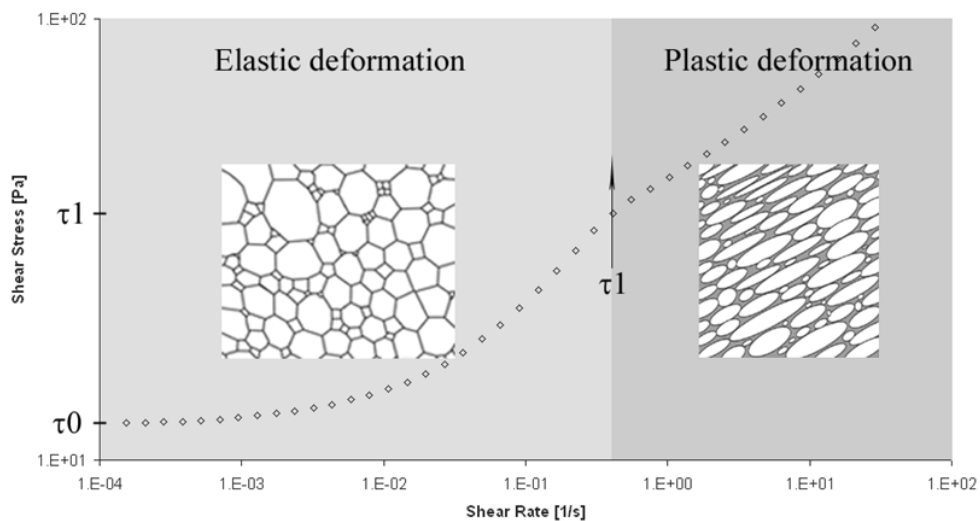


Figure 5.11: Two different mechanisms of flow occur during low and high shear rates for the EEs. At high shear rates, a more regular structure is accompanied by plastic deformations (right) and under conditions of low shear, drops maintain their shape and resist the stress elastically (left)

Figures 5.12 and 5.13 illustrate the flow curve obtained for the freshly-prepared samples. The test was performed in decreasing order of shear rate. There was no coalescence during flow. All the emulsions exhibited a marked non-Newtonian shear thinning behaviour and showed a distinct hump at moderate shear rates ($0.1-1 \text{ s}^{-1}$).

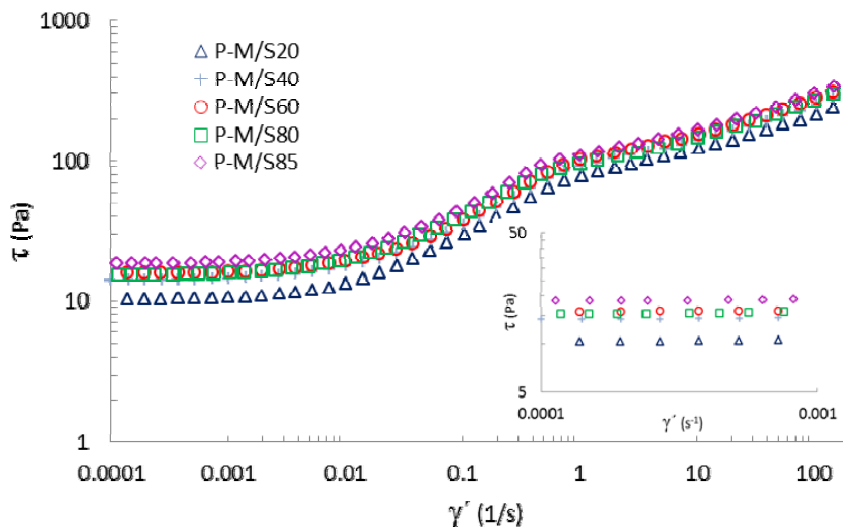


Figure 5.12: Flow curves for the explosive emulsions stabilised with PIBSA-Mea/Span mixtures

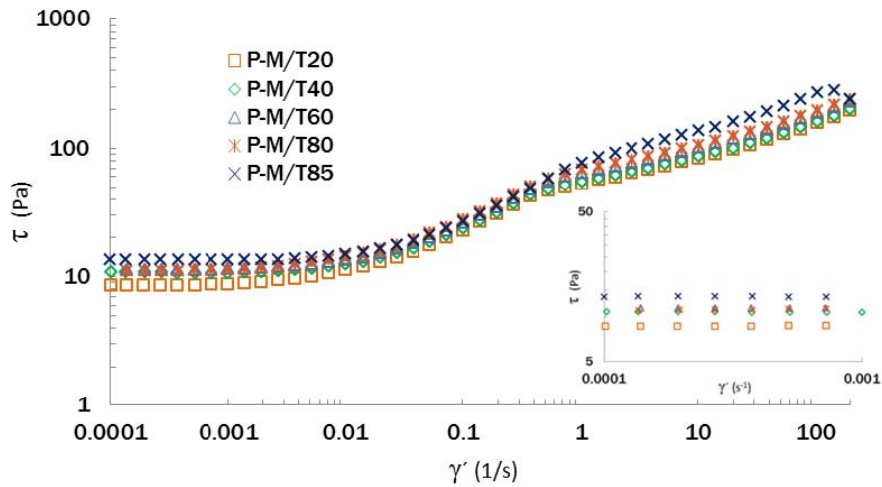


Figure 5.13: Flow curves for the explosive emulsions stabilised with PIBSA-Mea/Tween mixtures

Several models have been developed which satisfactorily describe flow properties of HCEs with two yield stresses, such as the Windhab and Foudazi models (Windhab, 1993; Foudazi *et al.* 2011). Of these, the Foudazi model is able to predict the entire range of flow curves for EEs, including the inflection point (hump). For the current study, flow curves for all emulsion samples under investigation were described by the use of Foudazi model (Equation 5.11).

$$\tau = \tau_{y0} + K\dot{\gamma}^{0.5} + (\tau_{y1} - \tau_{y0})[1 - \exp(-\dot{\gamma} / \dot{\gamma}^*)] \quad \text{Equation 5.11}$$

where τ_{y0} is the true yield stress, τ_{y1} is an asymptotic value of the yield stress value that corresponds to the transition (hump) in the flow behaviour at shear rate $\dot{\gamma}^*$, and K is an empirical constant.

This model showed excellent fitting of experimental results in the whole shear rate range, as shown by the dashed line in Figures 6.14 and 6.15 for PIBSA-Mea/Span 20 and PIBSA-Mea/Tween 20 emulsions, respectively. The relevant graphs can be found in Appendix D.

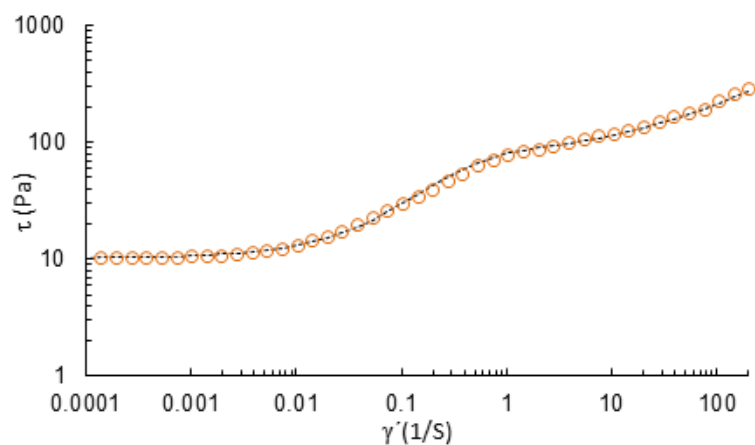


Figure 5.14: Fittings of Foudazi model (dash) on the flow curve of the PIBSA-Mea/Span 20 stabilised emulsion (dots)

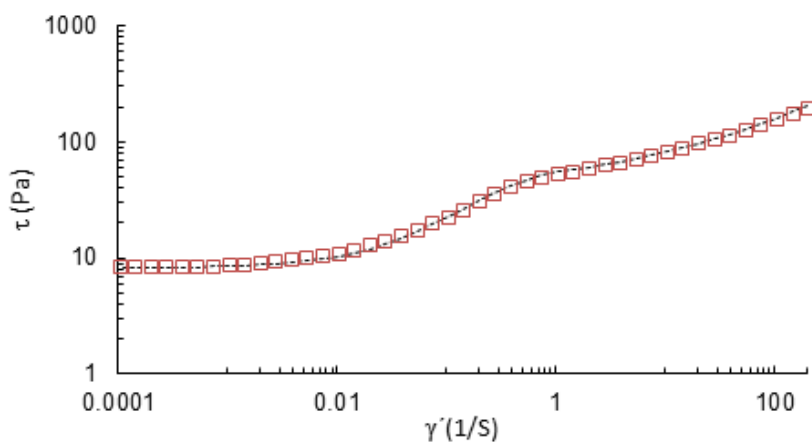


Figure 5.15: Fittings of Foudazi model (dash) on the flow curve of the PIBSA-Mea/Tween 20 stabilised emulsion (dots)

The summary of the coefficients obtained by the fitting of Foudazi model on experimental data for all samples is presented in Table 5.10. The root-mean-square error was used to measure the differences between flow curve, predicted by the model, and the experimental results.

Table 5.10: Summary of the coefficients obtained by fitting Foudazi equation on flow curve of the emulsion under investigation

Surfactant mixture	τ_{y1}	K	γ^{**}	τ_{y0} (Pa)	Error (%)
PIBSA-Mea	85	450	0.3	16.5	1.1
PIBSA-Mea/Span 20	70	210	0.35	10.1	0.5
PIBSA-Mea/Span 40	75	300	0.38	14.0	0.5
PIBSA-Mea/Span 60	80	400	0.32	15.0	0.7
PIBSA-Mea/Span 80	78	400	0.3	15.0	0.4
PIBSA-Mea/Span 85	80	1100	0.35	18.0	0.4
PIBSA-Mea/Tween 20	45	130	0.29	7.8	1.1
PIBSA-Mea/Tween 40	47	140	0.3	10.2	0.4
PIBSA-Mea/ Tween 60	50	240	0.35	10.4	0.8
PIBSA-Mea/ Tween 80	60	185	0.35	10.5	0.6
PIBSA-Mea/ Tween 85	75	400	0.45	13.1	0.6

It was observed that the yield stress in both low and high shear rate regimes increased in the formulations containing co-surfactants with longer alkyl tails and multitails. The presence of the unsaturated bond in the co-surfactants did not exert a marked effect on the rheological parameters of the emulsions under investigation. The yield stresses calculated for the PIBSA-Mea/Tweens stabilised emulsions was less than that of the PIBSA-Mea/Spans group of emulsions.

Using the Foudazi model is a suitable method to describe the flow behaviour of such systems with double yield stress. However, it is not applicable for calculation of pumping characteristics of emulsions, such as pressure drop versus flow rate, due to its complexity.

Based on a number of reports (Masalova, 2003; Malkin *et al.*, 2004) related to the calculation of pumping characteristics from rheological measurements, it has been found that the most suitable rheological model for calculation of pressure drop versus flow rate is the Hershel-Bulkley model. This has been proven for many emulsion explosives formulations by comparison of calculated values with direct measurements of pressure gradient and flow rate during the life trial experiment, where 50 tons of emulsions were transported through pipes with different diameters.

Figure 5.16a demonstrates an example of using the Herschel-Bulkley model (Equation 2.12) to describe flow curve of explosive emulsion sample. The Rabinowitsch-Weissenberg equation (Equation 5.13) was used to calculate pseudo-shear rate and $8V/D$ values using the coefficients of the Herschel-Bulkley model. A comparison of calculated and measured values of the pressure drop versus flow rate is presented in Figure 5.16b.

$$\tau = \tau_y + K\dot{\gamma}^n \quad \text{Equation 5.12}$$

where K and n are the fitting parameters, $\dot{\gamma}$ is shear rate and τ_y is the yield stress in low shear rate region.

$$\dot{\gamma}_{av} = \frac{4}{\tau_w^3} \int_0^{\tau_w} \tau^2 \dot{\gamma}(\tau) d\tau \quad ; \quad \tau_w = \Delta p D / 4L \quad ; \quad \dot{\gamma}_{av} = 8V / D \quad \text{Equation 5.13}$$

where $\dot{\gamma}(\tau)$ is the measured flow curve, $\dot{\gamma}_{av}$ is average shear rate, τ_w shear stress at the pipe wall, v is the average velocity, D is pipe diameter and L is the pipe length.

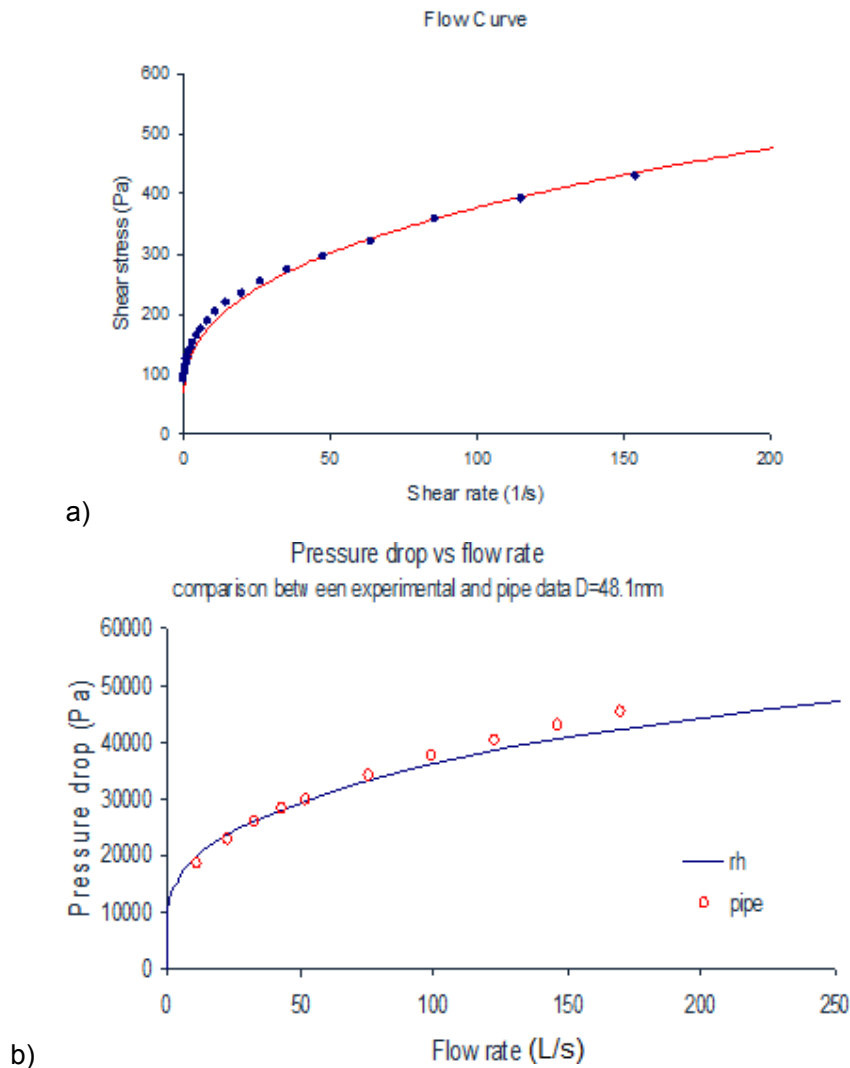


Figure 5.16: Flow curve of an EE fitted by Herschel-Bulkley model (left) and comparison between the experimental (dots) and calculated (line) pressure drop as a function of flow rate

In light of the above, the flow behaviour of the emulsion systems under study were described by the Herschel-Bulkley model in order to summarise the Herschel-Bulkley coefficients which could be used for estimation/comparison of the pumping characteristic for these new emulsion formulations.

As shown in Figure 5.17 and 5.18, the Herschel-Bulkley model showed a satisfactory fitting of flow curves over the upper and lower range of shear rates. The relevant graphs for the other emulsion samples can be found in Appendix D.

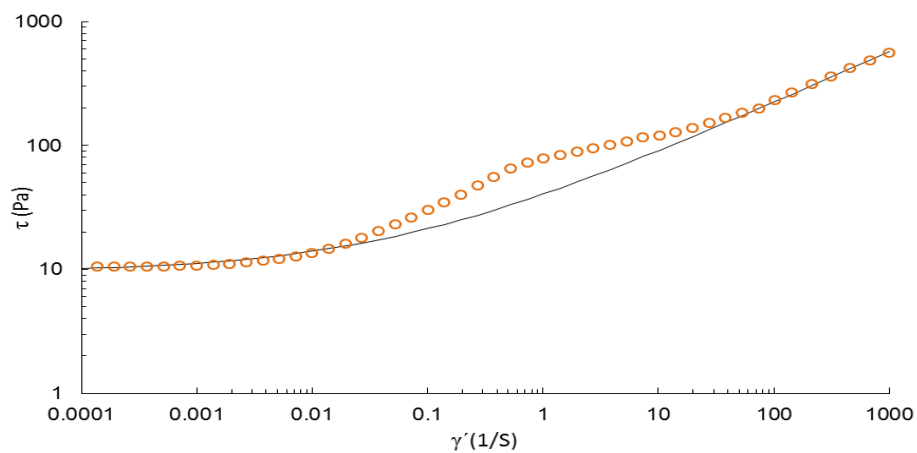


Figure 5.17: Flow curve of the PIBSA-Mea/Span 20 emulsion (dots) fitted by Herschel-Bulkley model (line)

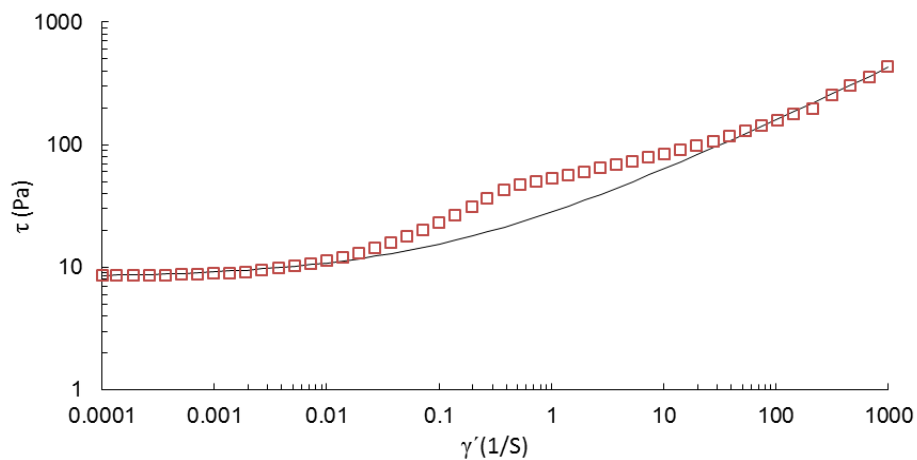


Figure 5.18: Flow curve of the PIBSA-Mea/Tween 20 emulsion (dots) fitted by Herschel-Bulkley model (line)

The summary of the yield stress coefficients obtained by the fitting of Herschel-Bulkley model on experimental data for all samples is presented in Table 5.11.

Table 5.11: Summary of yield stresses and co-efficient calculated for the emulsion formulations under investigation using Herschel-Bulkley equation

Surfactant mixture	Co-surfactant tail structure	τ_y	K	n
PIBSA-Mea	19 x C(CH ₃) ₂ -CH ₂	16.0	36	0.44
PIBSA-Mea/Span 20	11C	10.0	30	0.42
PIBSA-Mea/Span 40	15 C	13.5	33	0.42
PIBSA-Mea/Span 60	17 C	14.8	36	0.42
PIBSA-Mea/Span 80	17 C (C8=C9)	14.5	37	0.42
PIBSA-Mea/Span 85	3 x17 C (C8=C9)	18.0	48	0.47
PIBSA-Mea/Tween 20	11C	8.2	24	0.39
PIBSA-Mea/Tween 40	15 C	10.0	24	0.40
PIBSA-Mea/ Tween 60	17 C	10.4	27	0.42
PIBSA-Mea/ Tween 80	17 C (C8=C9)	10.5	27	0.43
PIBSA-Mea/ Tween 85	3 x17 C (C8=C9)	13.1	29	0.46

The average lower values of Herschel-Bulkley coefficients (τ_y , K and n) were obtained for the PIBSA-Mea/Tweens emulsions, compared to the PIBSA and PIBSA-Mea/Span emulsions. This means the use of water-soluble Tweens as co-surfactants could greatly improve the pumpability of explosive emulsions by reducing the required pressure drop to transfer the same amount of emulsion through a pipeline.

5.2.3.2 Viscoelastic behaviour

The HCEs are viscoelastic, comprised of both an elastic component represented by the storage modulus, and a viscous component, represented by the loss modulus. A strain amplitude sweep from 0.01 to 200% was conducted at a fixed oscillation frequency (1 Hz). Figures 5.19 and 5.20 show the evaluation of the storage modulus (G') of the emulsion formulations under investigation as a function of strain amplitude for both freshly prepared PIBSA-Mea/Spans and PIBSA-Mea/Tweens emulsions, respectively.

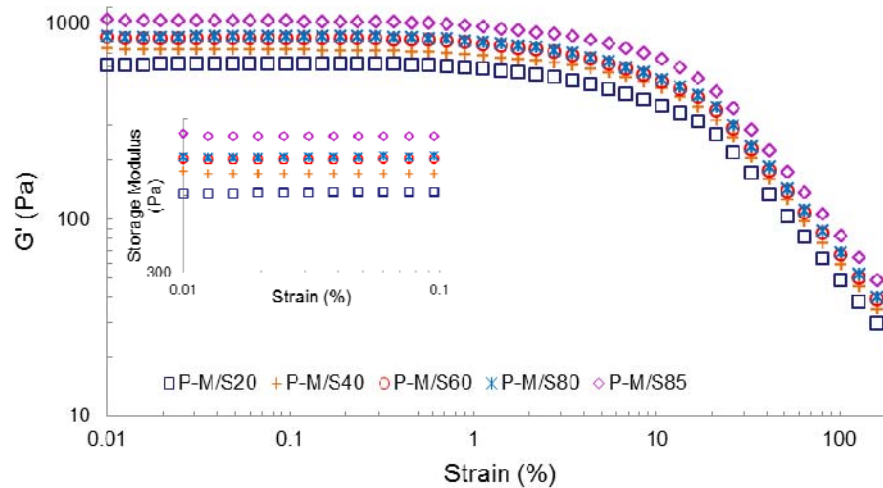


Figure 5.19: Storage modulus as a function of strain for the emulsions stabilised by PIBSA-Mea/Span mixtures ($D_{32} = 10 \mu\text{m}$)

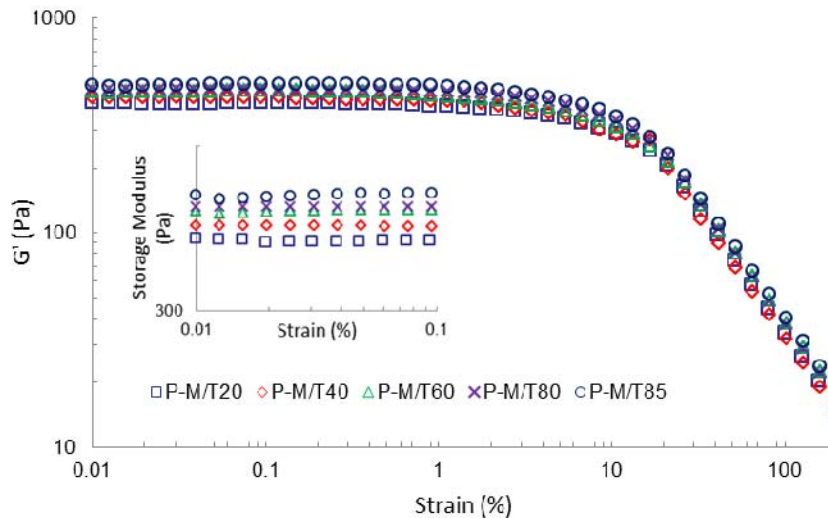


Figure 5.20: Storage modulus as a function of strain for the emulsions stabilised by PIBSA-Mea/Tween mixtures ($D_{32} = 10 \mu\text{m}$)

There were two characteristic regions observed in Figures 5.18 and 5.19, viz., the region when G' was independent of strain amplitude over a wide range of applied strains (up to 1%) represented by the plateau, and the region with a higher value of deformation, where the plateau disappears and the structure of the emulsions gradually deforms and breaks down (Bird *et al.*, 1987; Masalova *et al.*, 2011a).

Figure 5.21 and 5.22 illustrate the amplitude dependencies of G' and G'' for PIBSA-Mea/Span 80 and PIBSA-Mea/Tween 80 systems respectively (see Appendix D for the other

emulsions). The loss modulus (G'') showed a markedly lower value than did the storage modulus (by a factor of 10) in all samples under low strain. The G'' starts to increase after a certain strain amplitude and reaches a maximum at the crossover point where $G' = G''$ and beyond this point, the viscous nature of the emulsions dominate over their elastic nature.

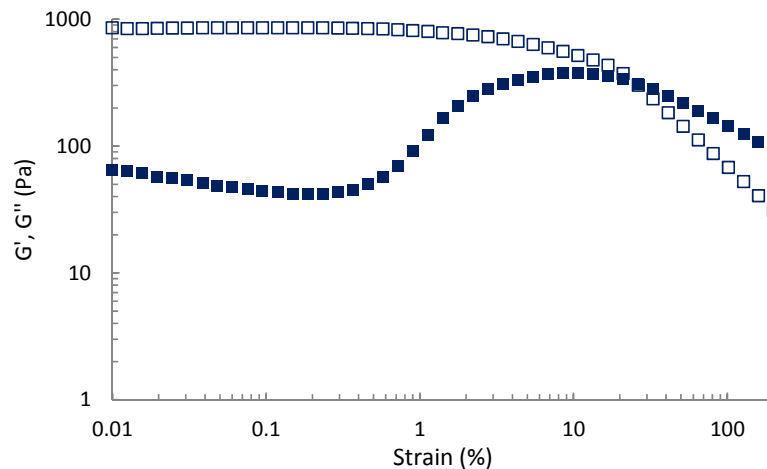


Figure 5.21: Storage modulus, G' (open) and loss modulus, G'' (filled) of the PIBSA-Mea/Span 80 emulsion as a function of strain amplitude

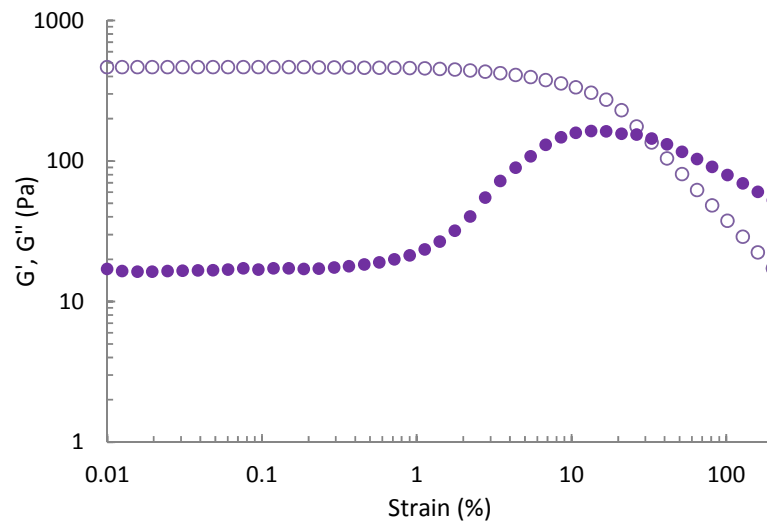


Figure 5.22: Storage modulus, G' (open) and loss modulus, G'' (filled) of the PIBSA-Mea/Tween 80 emulsion as a function of strain amplitude

A frequency sweep (angular frequency, $\omega = 0.1$ -100 rad/s) test at a constant strain (0.1% taken from the linear region of G' in amplitude sweep test) was performed (Figures 5.23 and 5.24).

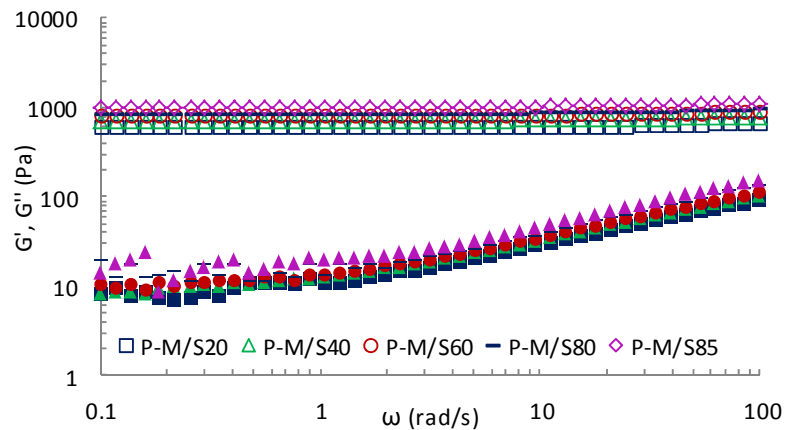


Figure 5.23: Storage modulus, G' (open) and loss modulus, G'' (fill) as a function of frequency for the emulsions stabilised by PIBSA-Mea/Span mixtures ($D_{32} = 10 \mu\text{m}$)

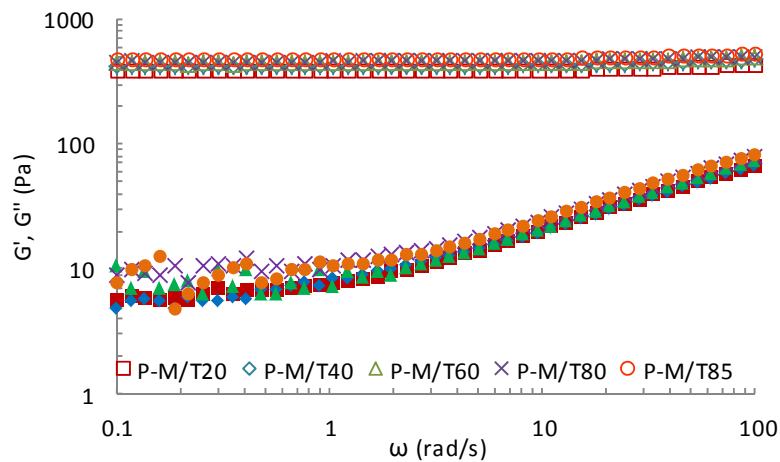


Figure 5.24: Storage modulus, G' (open) and loss modulus, G'' (fill) as a function of frequency for the emulsions stabilised by PIBSA-Mea/Tween mixtures ($D_{32} = 10 \mu\text{m}$)

The storage modulus remained constant over the entire range of measuring frequency. It was concluded that the elasticity/storage modulus of the explosive emulsions in this study was independent of frequency, as previously reported by Masalova *et al.* (2011a).

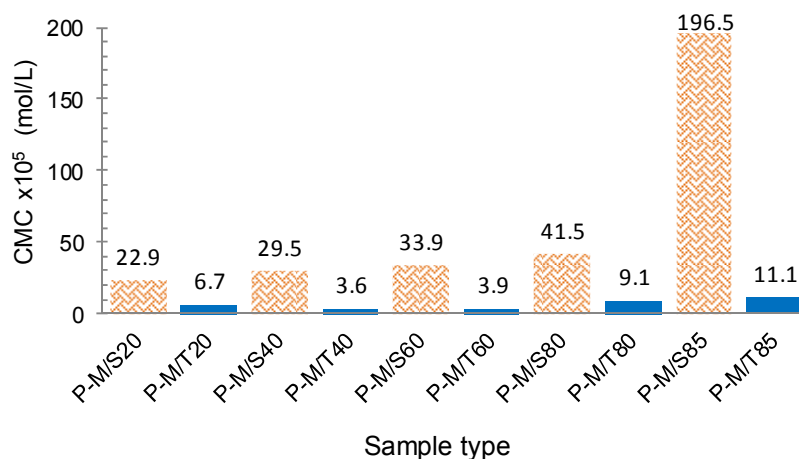
The storage moduli for all the emulsion samples obtained from both amplitude sweep and frequency sweep tests are listed in Table 5.12. The storage modulus for all the emulsion samples, from the amplitude sweep, is obtained by extrapolation of the plateau region of the graphs to zero strain (equilibrium storage modulus, G_0). The G_0 obtained from amplitude sweep is very similar to G_0 obtained from the frequency sweep for all the samples.

Table 5.12: Summary of equilibrium storage modulus (G_0) of the emulsion formulations under investigation obtained from amplitude sweep (AS) and frequency sweep (FS) tests

Surfactant mixture	G_0 (Pa) from AS	G_0 (Pa) from FS	Surfactant mixture	G_0 (Pa) from AS	G_0 (Pa) from FS
PIBSA-Mea	990	---	---	---	---
PIBSA-Mea/Span20	615	618	PIBSA-Mea/Tween 20	405	410
PIBSA-Mea/Span40	729	732	PIBSA-Mea/Tween 40	427	432
PIBSA-Mea/Span60	831	839	PIBSA-Mea/Tween 60	456	454
PIBSA-Mea/Span80	843	847	PIBSA-Mea/Tween 80	465	466
PIBSA-Mea/Span85	1021	1025	PIBSA-Mea/Tween 85	487	489

It can be seen that the equilibrium storage modulus (G_0) is more sensitive to surfactant structure for the PIBSA-Mea/Spans group, when compared with PIBSA-Mea/Tweens. The similar effect is observed in CMC values for both surfactant groups. This could be a consequence of the formation of the micellar structure in a continuous phase due to redundant quantities of the surfactants (Masalova *et al.*, 2011). The effect of surfactant tail structure on CMC values is more pronounced in PIBSA-Mea/Spans group, compared to PIBSA-Mea/Tweens.

The existence of reverse micelles in the continuous phase of explosive emulsions above CMC point was established with small-angle neutron scattering (SANS) measurements (Reynolds *et al.* 2000, 2001). CMC values of all surfactant mixtures under study are presented in Figure 5.25. A similar trend is observed for equilibrium storage moduli, G_0 (Table 5.12).

**Figure 5.25: CMC value for the Pibsa-Mea/Span (orange pattern) and Pibsa-Mea/Tween (blue fill) surfactant mixtures**

It is clearly seen that CMC values are higher for all samples in the PIBSA-Mea/Spans group than the PIBSA-Mea/Tween group. This could correspond to smaller amounts of micelles in the continuous phase for PIBSA-Mea/Spans, which has an effect on the equilibrium storage modulus. Consequently, the equilibrium storage modulus (G_0) of the PIBSA-Mea/Tweens stabilised emulsions were lower than the ones stabilised by PIBSA-Mea/Span mixtures.

5.2.4 Stability under high shear

Stability of emulsions under stress is of considerable importance, as it is essential that they are stable during the emulsification process and transport applications. For final application, explosive emulsions are transferred to deep underground mines and pumped through pipes to the target zone. It is expected that emulsions will keep their stability (not crystallise) during the pumping process where high shear pumping systems are involved. Hence it is essential to test any new emulsion formulations for their stability under high shear. To investigate the effect of the surfactant mixtures on stability of the HCEs under high shear, a double cylindrical pump, described in Chapter Three, was used. High shear conditions were simulated by passing the emulsion under 4 bar pressure through a small orifice (4mm hole diameter and 3 mm height), a number of times (NP= 3, 5, 7 and 10). This procedure was chosen as a standard test used by mining industries.

As a result of high shear, the droplet size continued to decrease as emulsion refinement continued. The evolution of the droplet size and the droplet size distribution under high shear for the emulsions undergoing a number of pumping cycles was obtained using the Malvern Mastersizer. The evolution of the droplet size and the droplet size distribution as a function of the pumping cycles for the HCEs stabilised with PIBSA-Mea/ Span 20 mixture is shown in Figure 5.26.

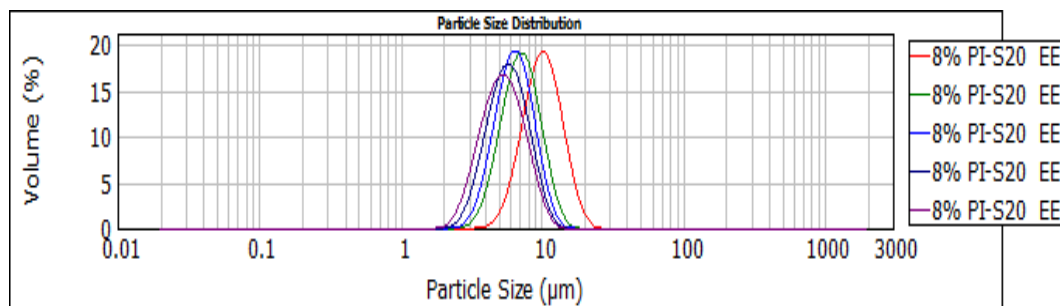


Figure 5.26: Histogram of drop size distribution of pumped emulsions stabilised by PIBSA-Mea/Span 20 mixture when NP =0 (red), 3 (green), 5 (blue), 7 (navy) and 10 (purple)

Most of the other samples followed similar trends, and results can be found in Appendix E. However, emulsions stabilised with only PIBSA-Mea, PIBSA-Mea/Span 85 and PIBSA-

Mea/Tween 85 mixtures showed marked crystallisation (Figures 5.28 and 5.29), particularly when NP exceeded five cycles. For this reason, accurate droplet size assessments were impossible for those mixtures and are not reported.

It is clear that droplet size was reduced when high shear was applied. For all the samples, the droplet size decreased exponentially as the number of pumping cycles increased. In all the samples under investigation there was a tendency to approach to a constant droplet size value, referred as the critical diameter (D_{crit}).

The following model was formulised (Yakhoub, 2009) and was used during the current study to fit the experimental results to determine D_{crit} :

$$D_{cal} = D_{crit} + e^{-(NP / \theta_D)}(D_0 - D_{crit}) \quad \text{Equation 5.14}$$

where D_0 was the initial droplet size before pumping, D_{crit} and θ_D were the fitting parameters and NP was the number of times passed through the pump orifice.

The critical droplet size (D_{crit}) of the shearing procedure was successfully determined using the model. The fitting graphs for the PIBSA-Mea/Span 40 and PIBSA-Mea/Tween 40 samples under high shear are illustrated in Figures 5.26. The data representing the fitting of other samples is provided in Appendix E.

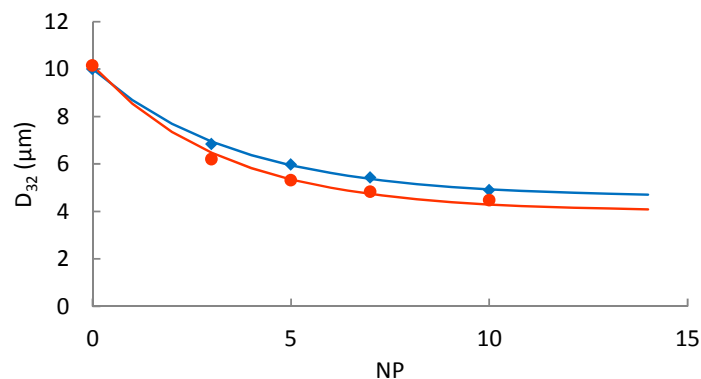


Figure 5.27: Droplet size (D_{32}) evolution as a function of pumping cycles (NP) for the PIBSA-Mea/Span 40 emulsion (orange circle) fitted by model (orange line) and the PIBSA-Mea/Tween 40 emulsion (blue square) fitted by model (blue line)

The droplet size reduction under high shear condition was slightly quicker for the PIBSA-Mea/Spans than the PIBSA-Mea/Tweens emulsions. The critical droplet size (D_{crit}) for the

pumped emulsions obtained from Equation 5.14 are listed in Table 5.13. These results clearly indicate the effect of co-surfactant type on the critical droplet size.

Table 5.13: Summary of critical droplet diameters of the explosive emulsions under investigation during the shearing process (D_0 , the initial droplet size of the emulsions equal to 10 μm)

Samples	D_{crit} (μm)	$(D_0 - D_{crit})/D_0$ %	Samples	D_{crit} (μm)	$(D_0 - D_{crit})/D_0$ %
PIBSA-Mea/ Span 20	4.1	0.59	PIBSA-Mea/ Tween 20	4.7	0.53
PIBSA-Mea/ Span 40	4.1	0.59	PIBSA-Mea/ Tween 40	4.7	0.53
PIBSA-Mea/ Span 60	4.0	0.6	PIBSA-Mea/ Tween 60	4.6	0.54
PIBSA-Mea/ Span 80	4.0	0.6	PIBSA-Mea/ Tween 80	4.5	0.55

In this investigation, the average droplet size of the emulsions, or D_{crit} , prepared with the PIBSA/Span mixtures decreased from 10 to 4.0 μm , while the D_{crit} of the PIBSA/Tween emulsions decreased to 4.7 μm . High shearing clearly decreased critical droplet size. Decrease of emulsion droplet size increases the viscosity of the emulsion. Additionally, an increase in viscosity reduces the pumpability of the emulsion when the emulsions flow through a pipe (Malkin *et al.*, 2004).

High shear conditions also accelerate crystallisation, as illustrated by the series of photomicrographs in Figures 5.28 for PIBSA-Mea and PIBSA-Mea/Spans stabilised emulsions and Figure 5.29 for PIBSA-Mea/Tweens stabilised emulsions.

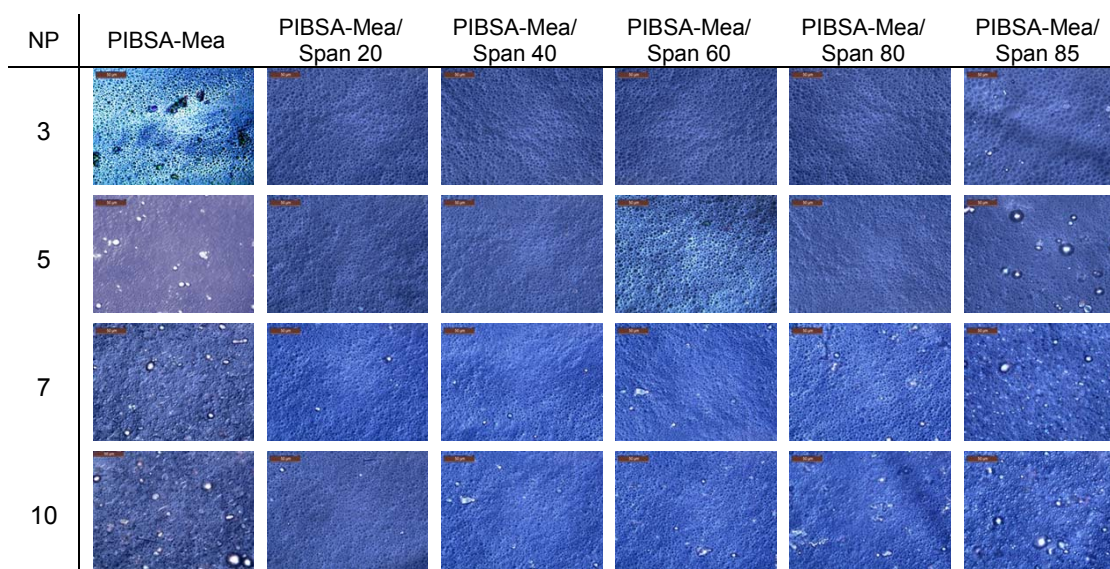


Figure 5.28: Photomicrographs of the PIBSA-Mea and PIBSA-Mea/Spans stabilised emulsions under different shear conditions. NP indicates the number of pumping cycles. Scale bar, 50 μm = 4 mm

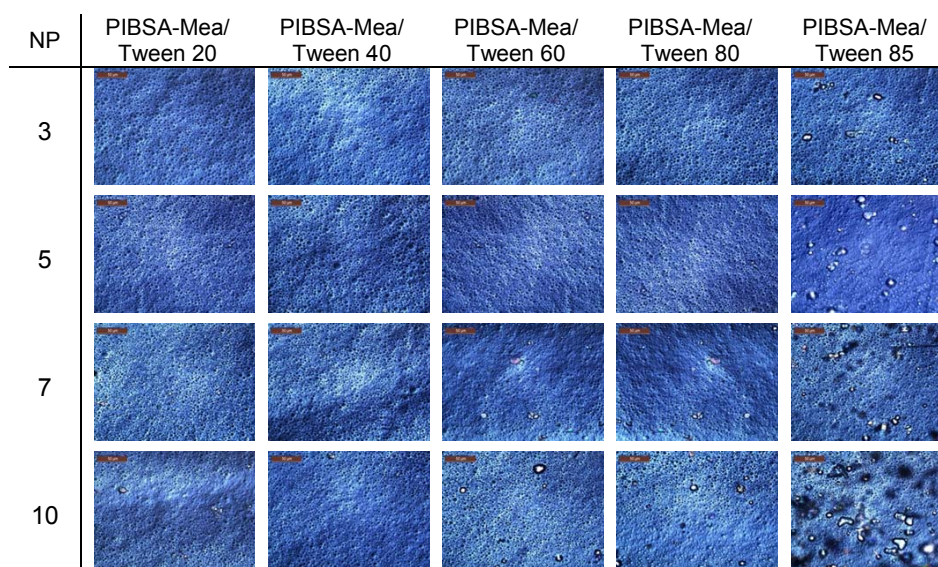


Figure 5.29: Photomicrographs of the PIBSA-Mea/Tweens stabilised emulsions under different shear conditions. NP indicates the number of pumping cycles. Scale bar, 50 μm = 4 mm.

Using only PIBSA-Mea to stabilise explosive emulsions do not provide acceptable emulsion stability under high shear conditions (Reynolds *et al.*, 2010). The addition of a co-surfactant to the system in most surfactant mixtures studied in the current investigation provided satisfactory stability under high shear associated with the pumping conditions tested. Small molecular weight Spans improved the high shear stability of the system, due to their high

mobility in the emulsion bulk. This enabled Spans to rapidly cover newly formed droplet surfaces under high shear conditions (Kovalchuk & Masalova, 2012).

Improvement of stability under high shear after addition of Tweens to the system may be attributable to the densely packed interfacial layer being resistant to applied forces, thus maintaining an integrated droplet surface. In addition, the marked affinity of Tween molecules to water is important. It is suggested that as soon as more water surfaces are formed under high shear (more free water becomes available), the kinetics of the system would be altered to favour Tween molecules. As such, these molecules would accumulate at the new interfaces rather than remaining as monomers and/or micelles in the bulk.

5.2.5 Ageing

Due to the presence of supersaturated drops in the system, the emulsions investigated during the current study were in an intrinsically metastable state. The stability of such emulsions is associated with the crystallisation of the aqueous phase. It should be noted that the ageing includes two steps:

- initiation of crystallisation nuclei in the explosive emulsions; and
 - spreading of crystals throughout the bulk of the emulsion
- (Becher, 1988; Kharatiyan, 2005; Masalova & Malkin, 2007c).

Below the crystallisation temperature (fudge point = 60° C), crystal nucleation of AN solution is a major concern. There are two possible mechanisms of crystallisation initiation. Crystals can start to form within the super-cooled droplets (homogeneous nucleation) or at interface (heterogeneous nucleation) (Somasundaran, 2006). In an explosive emulsion, homogeneous nucleation can occur due to impurities in AN powders as well as an external stimuli, such as high shearing. This may change the thermodynamics of the super-cooled system. On the other hand, heterogeneous nucleation occurs at interfacial film around the droplets and is affected by properties of the stabilising agent. Generally, in this type of emulsion, both types of crystal nucleation occur concurrently in the system. One type of crystal nucleation may predominate, however, depending on the formulation.

In the current study, for all the different emulsion formulations prepared, the same batch of AN with minimum impurities was used to minimise the influence of AN quality on crystal nucleation within droplets. Hence, factors which include the properties of the interface (White *et al.*, 2004; Masalova *et al.*, 2006,) and the micelle concentration (Kovalchuk & Masalova, 2012) exert a major effect on the emulsion stability during ageing.

The role of surfactant in preventing initiation and/or penetration of crystals through the HCE bulk with a metastable dispersed phase is very important. Surfactants can prevent nucleation of crystallisation by covering the droplet interface and creating a dense interfacial layer. Surfactants also form micelles in the continuous phase. These micelles create a mechanical barrier between drops, thus preventing the spreading of crystals through the entire system. It was therefore important during the current study to ascertain the effect/s of surfactant mixtures on the stability of the explosive emulsions during shelf life, prior to and after applying high shear. To do so, all samples were maintained under identical environmental conditions during ageing. During this time, transformation of the structures with regard to the crystallisation of the oxidiser was observed, using an optical microscope.

To ensure the absence of coalescence in the emulsions, the droplet size evolution was monitored by using a Malvern Mastersizer. Figures 5.30 and 5.31 illustrate the evolution of droplet size distribution of the PIBSA-Mea/Span 40 and PIBSA-Mea/Tween 40 emulsions before the initiation of crystallisation. The measurement of droplet size was not possible after the first crystals appeared in the bulk of emulsions.

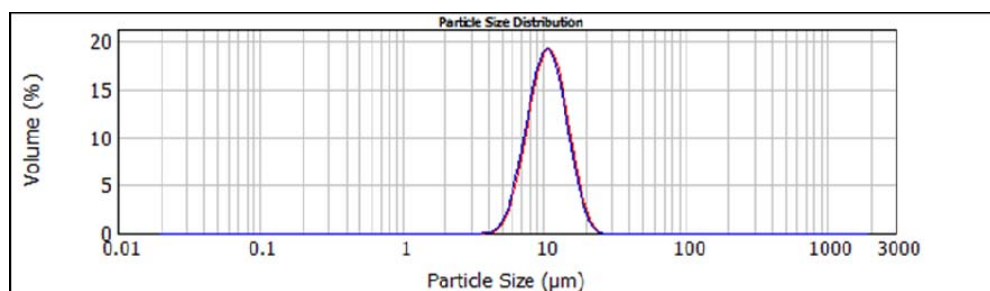


Figure 5.30: Droplet size distributions of PIBSA-Mea/Span 40 emulsion fresh (blue), after 10 days (green) and 20 days (red)

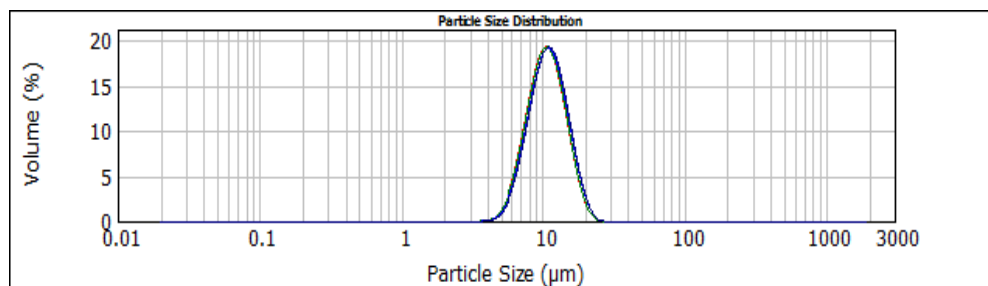


Figure 5.31: Droplet size distributions of PIBSA-Mea/Tween 40 emulsion fresh (green), after 10 days (red), 20 days (blue) and 30 days (navy)

No notable changes in droplet size were observed for any samples. Similar results have been reported in previous publications (Masalova & Malkin, 2007a; Tshilumbu *et al.*, 2013). The coalescence stability in such emulsions could relate to the steric and electrostatic effects induced by the presence of surfactant micelles in the inter-drop layer (Reynolds *et al.*, 2010). Therefore, the instability of the emulsions in the current study was discussed solely by the means of the crystallisation of the dispersed phase.

5.2.5.1 Ageing of un-pumped explosive emulsions

The microscopic observations of the commencement of crystallisation (t_{cr}) of emulsions stabilised by various surfactant mixtures are presented in Figure 5.32. Methodology to describe the definition of the start of crystallisation (the time required for crystallisation to initiate, t_{cr}) included a microscopic observation of the emulsions. This was conducted by taking 6 different samples from each emulsion container. The start of crystallisation was recorded as the time (days) when an average of 5 to 10 crystals in any emulsion was observed.

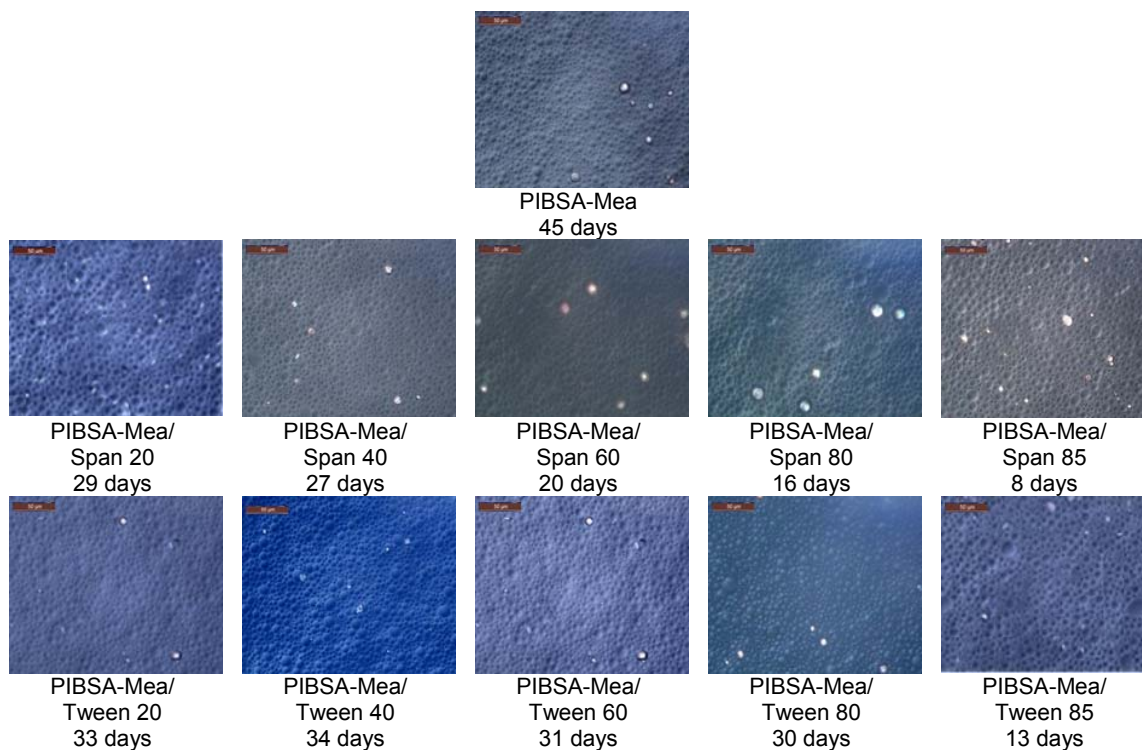


Figure 5.32: Photomicrographs of ageing in un-pumped emulsions samples containing different surfactant mixtures at t_{cr} . Scale bar, 50 μm = 6 mm

Figure 5.33 shows the starting day of crystallisation recorded for the emulsions.

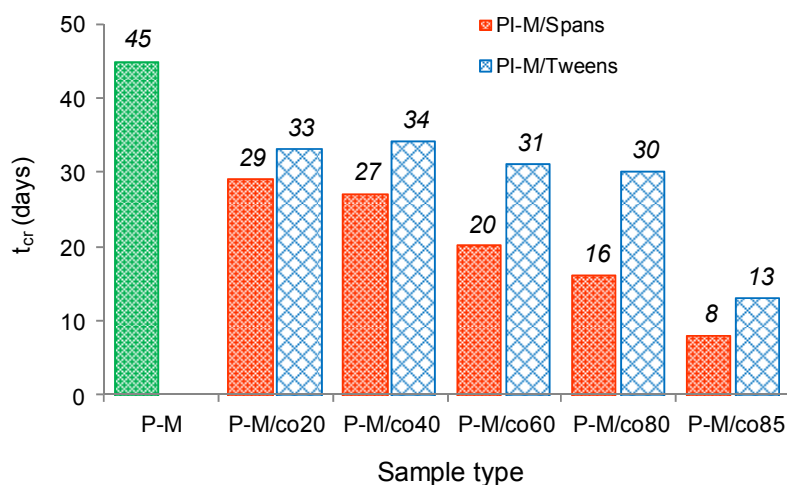


Figure 5.33: Time period required for commencement of crystallisation in different un-pumped emulsions (P-M denotes PIBSA-Mea and P-M/co denotes the mixtures of PIBSA-Mea/ co-surfactants - Spans or Tweens)

The overall stability of the samples containing Tweens as co-surfactants was superior to that recorded for the emulsions stabilised by Spans. However, the stability of an emulsion containing only PIBSA-Mea showed the best resistance to crystallisation during shelf life, due to the robust steric effects created by large numbers of PIBSA micelles in the inter-droplets layer (Shen & Duhamel, 2008). When co-surfactants are added to the system, mixed micelles form with different properties than PIBSA micelles alone. Therefore, the steric effect of the mixed micelles could be less influential.

The time frame related to the crystallisation kinetics until an emulsion is fully crystallised is greatly dependent on the emulsion formulation. To provide insight into the kinetics of crystallisation for the emulsions under study, the microphotographs of the emulsions after 45 days of manufacturing and the interaction parameters of their surfactant mixtures (β) are presented in Figure 5.34.

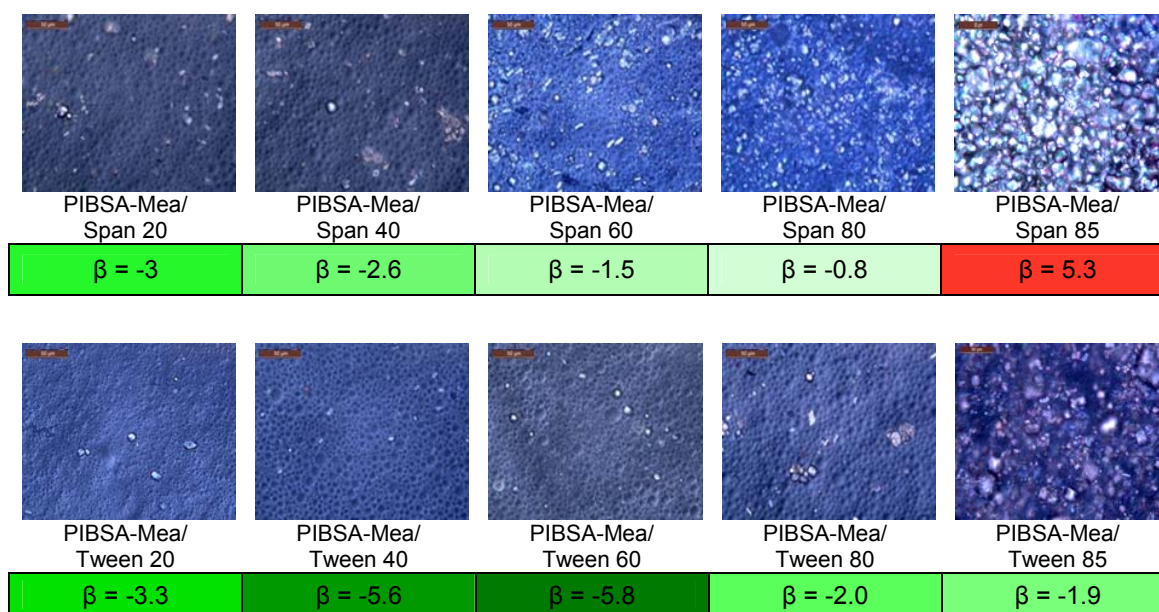


Figure 5.34: Photomicrographs of ageing in the un-pumped emulsions samples after 45 days. Scale bar, 50 μm = 6 mm

A more rapid rate of crystallisation was observed in the PIBSA-Mea/Span emulsions when compared to the PIBSA-Mea/Tweens. A decrease in synergism between PIBSA-Mea and Span co-surfactants resulted in a systematic decrease in ageing stability. This could be caused by a weakening of the interfacial structure and therefore it becomes increasingly less resistant to the intergrowth of crystals.

Emulsions prepared with Tween co-surfactants were more stable than were the other emulsions, because of the higher degree of synergism between PIBSA and Tweens compared to PIBSA-Mea/Spans, except Tween 85. The high rate of crystallisation in PIBSA-Mea/Tween 85 emulsions could be due to incompatibility in mixed micelles composed of bulky Tween 85 with three oleate tails and PIBSA.

The slower stability kinetics noted for PIBSA-Mea/Tween mixtures where the interaction parameter was identical to that of PIBSA-Mea/Spans could be due to the formation of higher numbers of micelles of PIBSA and Tween mixtures in the continuous phase. Such a condition would prevent the spreading the crystals in the emulsion bulk.

However, in the emulsions stabilised by PIBSA-Mea/Tweens after 40 to 50 days from the start of crystallisation, a separation of the phases occurred (Figure 5.35).



Figure 5.35: The white creamy paste structure of fully crystallised PIBSA-Mea/Spans emulsions (right) and the phase separated structure including AN agglomerates of the fully crystallised PIBSA-Mea/Tweens emulsions (left)

A possible explanation is that when the crystals formed in the emulsion, more water molecules were freed. These could then dissolve the Tweens molecules. In addition, Tweens could transport a fraction of the PIBSA molecules associated with Tweens to the water phase. This could alter the thermodynamics of the interface and cause phase separation. In PIBSA-Mea/Spans emulsions, a white creamy paste was observed within a 10-20 day time period after onset of crystallisation, and no separation of the two phases occurred.

5.2.5.1 Ageing of the pumped explosive emulsion

There is a time difference between the transportation/pumping of emulsion to the blasting point and detonation time. Therefore, the pumped emulsions are required to maintain stability for up to 2-3 weeks before blasting. In order to simulate this process, the pumped emulsion which had undergone five pumping cycles was chosen as the reference sample. The same aforementioned procedure that was used to monitor the stability of un-pumped emulsions was applied for the pumped samples.

The ageing of emulsions after undergoing five pumping cycles is illustrated in Figure 5.36 (10 days ageing) and 5.37 (20 days ageing). The PIBSA-Mea, PIBSA-Mea/Span 85 and PIBSA-Mea/Tween 85 samples crystallised under high shear and were not considered for further ageing control.

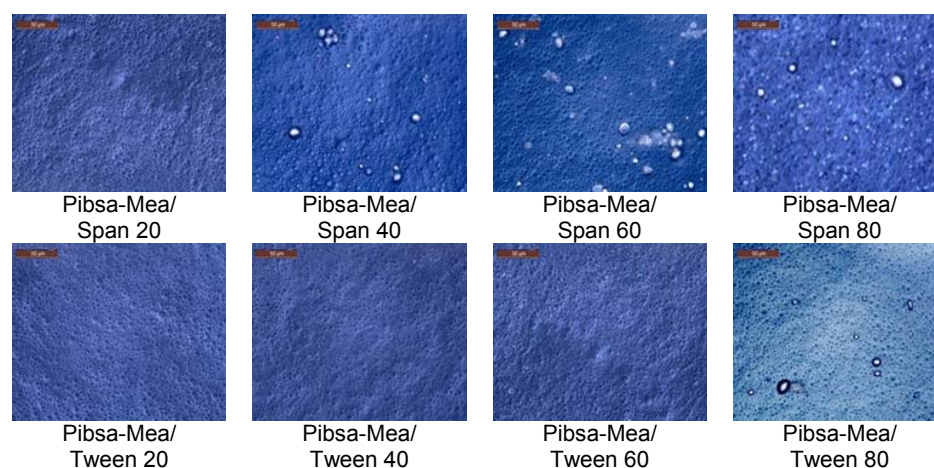


Figure 5.36: Photomicrographs showing the appearance of various pumped emulsions (NP=5) after ageing 10 days. Scale bar, 50 μ m= 6 mm

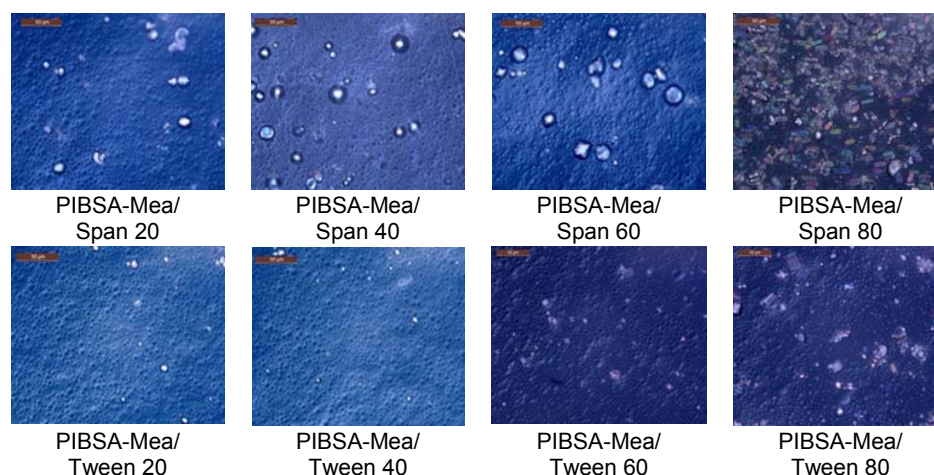


Figure 5.37: Photomicrographs showing the appearance of various pumped emulsions (NP=5) after ageing 20 days. Scale bar, 50 μ m= 6mm

It can be seen that a combination of PIBSA with Tween co-surfactants provides higher shear/crystallisation stability than do the other combinations. This is particularly important for technological applications of HCEs with a supersaturated aqueous phase.

The rapid crystallisation observed in the PIBSA-Mea/Span mixtures could be attributed to the replacement of PIBSA-Mea with highly mobile Span molecules surrounding newly-formed droplet surfaces. This would increase the probability of multilayer formation by Span molecules at the interfacial layer. It could be assumed that the initiation of crystallisation may be induced by such opaque multi-layers (Opawale & Burgess, 1998; Drelich *et al.*, 2010; Kovalchuk & Masalova, 2012).

CHAPTER SIX: SUMMARY AND CONCLUSION

The primary focus of this study was the effects of synergetic compatibility between various novel binary surfactant mixtures at interface on processing, rheological properties, pumpability and stability with regard to crystallisation of highly concentrated emulsions (HCE) with a super-cooled dispersed phase, with respect to co-surfactant structure.

In previous studies, various parameters, including viscosities of the two emulsion phases, concentration of internal phase, oxidiser type and concentration, and surfactant type and concentration were shown to be effective regarding stability with regard to crystallisation of explosive emulsions. However, very little is known about the relation between interfacial properties, particularly synergetic compatibility of surfactant mixtures and stability of such emulsions, where instability arises from crystallisation in the metastable dispersed phase.

The findings of the experimental investigations of the current study are summarised and as follows:

First, a feasibility study was conducted to find the other possible formulations to stabilise HCEs. Two groups of surfactants, including Pluronics (two types) and water-soluble Tweens (two types), as well as their mixtures with PIBSA and SMO (Span 80), were introduced into the emulsion formulations. In this stage of the investigation, presented in Chapter 4, the stability of samples was examined in terms of coalescence of the droplets. The reason for this was that the internal phase was ~60 wt% in oxidiser aqueous phase, which is not in super-cooled state at ambient temperature. It was not possible to produce HCEs when using Pluronics surfactants, either on their own or in combination with PIBSA or Tweens. Span 80/Tweens and Span 80/Pluronic PE3100 mixtures formed highly concentrated emulsions, but the emulsions were unstable to coalescence. The combination of PIBSA-Mea with Tween surfactants stabilised the emulsions and the rate of coalescence was negligible within the limits of our investigation.

Then, one of the stable formulations stabilised by a mixture of PIBSA and Tween 80 was used to form explosive emulsion (EE) with a super-cooled aqueous solution of ammonium nitrate as a dispersed phase. The emulsification process and stability of the manufactured emulsion on shelf and under high shear conditions was compared to the standard industrial emulsion stabilised by PIBSA/Span 80. Quicker refining and higher stability to crystallisation on shelf and under high shear conditions was achieved by replacing Span 80 with a Tween

80 co-surfactant. The results obtained from the abovementioned comparison study stimulated further investigation of the interfacial behaviour of both novel and standard formulations in various concentrations/ratios of surfactant/co-surfactant systems. The efficiency of PIBSA/Tween 80 in reducing interfacial tension was higher when compared to Tween 80 and PIBSA alone, while interfacial behaviour of the PIBSA/Span 80 mixture was similar to individual Span 80. An increase in the PIBSA-Mea/SMO ratio also decelerated the rate of interfacial tension reduction opposite to PIBSA-Mea/Tween 80. It was concluded that different types of interactions (synergism/ideal/antagonism) exist between these two surfactant mixtures.

Based on the results obtained from the feasibility study, the final matrix of samples with variation of the co-surfactants structures (Spans 20, 40, 60, 80 and 85 and Tweens 20, 40, 60, 80 and 85) was defined. The binary surfactant mixtures of these co-surfactants with PIBSA-Mea as main surfactant were divided into four groups based on a systematic variation of their chemical structures:

- the different lengths of a hydrophobic tail, including 11 (Span 20 and Tween 20), 15 (Span 40 and Tween 40) and 17 (Span 60 and Tween 60) carbon atoms;
- the presence of a double bond in the hydrophobic tail (Span 80 and Tween 80);
- the number of hydrophobic tails (Span 85 and Tween 85); and
- the different head groups (Spans vs. Tweens).

Interfacial characteristics of the surfactant mixtures were examined. First, the interfacial tensions of individual surfactants and their mixtures over a wide range of surfactant concentrations were measured (above and below critical micelle concentration), using a Kruss K100 tensiometer. Then, a non-ideal regular theory developed by Rosen was applied to estimate the degree of synergism (β) between the surfactant mixtures.

Results obtained in this investigation show that mixing co-surfactants with different chemical structures and hydrophobicity allows their compatibility with the basic surfactant to be varied. The combination of the hydrophilic nature of Tween molecules as the co-surfactants with PIBSA-Mea created a more packed layer (greater synergism) than that formed with Spans with the same hydrophobic tail structure. In the PIBSA-Mea/saturated alkyl tail Span mixtures, the synergism reduced with increasing tail length of the Spans, while the opposite was true for PIBSA/saturated tail Tweens. The presence of multitailes and unsaturated tails in co-surfactant structures in both Spans and Tweens mixtures reduced the degree of

synergism. In fact, adding multitailes Span 85 to PIBSA resulted in an antagonistic effect between surfactant and co-surfactant at the interface.

Results generated based on the interfacial analysis were used to interpret the outcomes of the shear effect during both the emulsification process and under high shear conditions. This was followed by an investigation of the rheological properties of the emulsions. Finally, the complete stability of the emulsions with regards to crystallisation of the supersaturated dispersed phase was studied and related to the interfacial characteristics of the surfactant mixtures.

It was confirmed that the synergetic compatibility between surfactant and co-surfactant plays an important role in emulsion stability as regards crystallisation and affects the emulsification process, as well as rheological properties of the emulsion.

Emulsion samples were manufactured using a Hobart N50 mixer at 80 °C (above crystallisation point of the oxidiser). The average droplet size (D_{32}) of the emulsion samples was measured during emulsification process, using a Malvern Mastersizer. It was found that the PIBSA-Mea/Tweens emulsions required less refining time to attain the target droplet size ($D_{32}= 10 \mu\text{m}$) and therefore, less energy input to manufacture similar droplet sizes when compared with PIBSA-Mea/Spans. This was mainly attributed to higher adsorption efficiency, lower water-oil interfacial tensions and efficient condensed interfacial film (higher synergism) of the PIBSA-Mea/Tween surfactant mixtures.

There was a clear correlation between the characteristic refinement time (θ) of the emulsions and the degree of synergism (β) of the surfactant mixtures. However, the effect of β on refinement time was more pronounced for PIBSA-Mea/Spans samples. In mixtures of PIBSA-Mea/Tweens, the β values were always negative (synergetic mixtures) and therefore, the characteristic refinement time values were similar.

The rheological properties of the emulsions including viscoelasticity and flow properties were obtained by using an MCR 301, Paar Physica rheometer through oscillation and rotational modes. Elastic modulus was obtained from the constant plateau zone in amplitude sweep as well as frequency sweep for the emulsions. The elastic moduli obtained from the both tests were similar. The flow behaviour of these emulsions was found to be non-Newtonian, characterised by shear thinning behaviour and the existence of double yielding point (yield pseudo-plastic).

It was found that the structure of co-surfactants influenced the rheological properties of explosive emulsions. Both the elastic modulus and the yield stress values were lower for PIBSA-Mea/Tweens systems when compared with PIBSA-Mea/Spans with the same tail structure. Increasing the hydrophobic tail length and the number of tails of co-surfactants caused an increase of characteristic rheological parameters (yield stress and storage modulus) for both groups of emulsions, while the effect of co-surfactants with unsaturated tails was negligible.

Pipeline transportation of the emulsion systems under investigation is an important characteristic. Flow curves of the emulsions were fitted by Herschel-Bulkley model in order to investigate the pumping characteristic of the novel formulations under study. Lower values of coefficients of the model were obtained for the explosive emulsions stabilised by using PIBSA-Mea/Tweens mixtures when compared with the emulsions stabilised by PIBSA-Mea/Spans. This means less energy (low pressure gradient) is required to pump the explosive emulsions stabilised by PIBSA-Mea/Tweens mixtures to maintain the same emulsion flow rate.

Simulation of high shear condition was performed using an industrial designated double piston-pumping instrument, where the fresh emulsions were forced under 4 bars of pressure applied into the piston-shaft out of the tube of the piston a through small orifice diameter (4 mm) set as the outlet. High shearing resulting from the emulsion pumping process played an important role in determining whether the droplets of such emulsion types (highly concentrated) crystallised, coalesced or just refined as they were pushed through the small orifice diameter. The effect of such high shear on the shelf life of the emulsions after pumping was also investigated. Furthermore, the microscopic structure and droplet size distribution of all the pumped emulsions were examined after pumping and with time.

No recordable signs of coalescence were observed in all samples under study within our experimental window. Adding co-surfactant to the emulsion formulation improved high shear stability for most of the emulsion samples. However, a superior shear stability was observed for the PIBSA-Mea/Tweens group when compared with the PIBSA-Mea/Spans group. Small molecular weight Spans improved the high shear stability of the system due to their higher mobility in the emulsion bulk when compared with PIBSA-Mea-only emulsion stabilisation, while the improvement in high shear stability resulting from adding Tweens to the system may be attributable to the densely packed interfacial layer being resistant to applied forces and also the high affinity of Tween molecules to water. When the emulsions droplets break into smaller drops, more water surfaces will be available. Therefore, Tween molecules would

quickly cover the new interfaces rather than remaining in the bulk, hence improving the stability of the emulsions under high shear.

Another consequence of high shearing was to accelerate crystallisation in the emulsion. The addition of a co-surfactant to the system in most of the surfactant mixtures studied (except Span 85 and Tween 85) in the provided satisfactory stability under high shear associated with the pumping conditions tested. However, a rapid crystallisation of PIBSA-Mea/Span systems when compared with PIBSA-Mea/Tweens over time was observed. It was concluded that the effect of the co-surfactant head group's chemical structure (type of co-surfactant family) is very important for technological applications of EEs.

The stability of the emulsions in terms of crystallisation (ageing) of the supersaturated dispersed phase was investigated over time using an optical Leica microscope equipped with a digital camera. Results revealed that the average stability of the PIBSA-Mea/Tween emulsions in terms of initiation and also crystallisation kinetics was higher than for PIBSA-Mea/Spans stabilised emulsions.

The interfacial properties of the surfactant mixtures at the aqueous-oil interface and the amount of their reverse mixed micelles in the oil phase affect the crystallisation initiation and crystal growth in the bulk of EEs. Therefore, it could be concluded that the higher stability could be due to more densely-packed interfaces created by PIBSA/Tween mixtures, as well as greater amounts of micelles in these emulsion systems when compared with PIBSA-Mea/Spans with similar tail structures.

There was a direct correlation between the synergetic compatibility and the shelf-life stability of emulsions for each group of surfactant mixture. However, the effect of synergism on improving the stability of EE was more strongly demonstrated based on the PIBSA-Mea/Spans range of samples.

From results obtained in the current study, it was established that the synergism between the surfactant and co-surfactant is one of the major factors which effect stability of the explosive emulsions. This is influenced by the structure of the surfactants. Therefore, the study of interfacial properties in relation to the structure of co-surfactant molecules could play an important role in understanding emulsion instability related to crystallisation of an oversaturated dispersed phase. Such a study could be used as a valuable starting-point for future design of unique and novel optimised surfactant systems, which could greatly benefit

the mining industry in terms of maximum emulsion explosives stability, pumpability and detonating properties.

In addition, using the information obtained from the formulations selected for the current study, it is apparent that it is entirely feasible to partially replace PIBSA with the water-soluble Tween family of surfactants. The Tweens are environmentally friendly, low-cost compounds and provided the emulsions of this study with an improved stability and pumpability for different technological applications. The latter would include suitable emulsification during production (quick refinement and low energy consumption), adequate long-term storage time and easier pumping.

At the end, it should be mentioned that currently used SMO (Span 80) is not the best co-surfactant from family of Span surfactants, in combination with PIBSA-Mea. In fact Span 20 and Span 40 provide better stability in comparison with SMO, in combination with PIBSA.

- **Recommendations for future research**

The following aspects were not covered in this thesis and could be identified as foci for future research:

- Investigation of the optimal ratio between PIBSA and co-surfactants to stabilise explosive emulsion.
- Investigation of the interfacial rheology of explosive emulsions in the presence of different surfactant mixtures and its effect on the emulsion properties.
- Introduction of the other water-soluble surfactants in combination with PIBSA or other oil-soluble surfactants.

BIBLIOGRAPHY

Abe, M. & Scamehorn, J.F. 2004. *Mixed surfactant systems*. 2nd ed. New York: Marcel Dekker.

Adam, N.K. 1924. The structure of surface films on water. *The Journal of Physical Chemistry*, 29:87-101.

Adya, A.K. & Neilson, G.W. 1991. Structure of a 50 mol kg⁻¹ aqueous solution of ammonium nitrate at 373 K by the isotopic difference method of neutron diffraction. *Journal of the Chemical Society, Faraday Transactions*, 87:279-286.

Aomari, N., Gaudu, R., Cabioc'h, F. & Omari, A. 1998. Rheology of water in crude oil emulsions. *Colloids and Surfaces A: Physicochemical and Engineering Aspects*, 139:13-20.

Aronson, M.P., Ananthapadmanabhan, K., Petko, M.F. & Palatini, D.J. 1994. Origins of freeze-thaw instability in concentrated water-in-oil emulsions. *Colloids and Surfaces A: Physicochemical and Engineering Aspects*, 85:199-210.

Aronson, M.P. & Petko, M.F. 1993. Highly concentrated water-in-oil emulsions: influence of electrolyte on their properties and stability. *Journal of Colloid and Interface Science*, 159:134-149.

Atkins, P.W. 1994. *Physical chemistry*. New York: W.H. Freeman Limited.

Babak, V., Langenfeld, A., Fa, N. & Stébé, M. 2001. Rheological properties of highly concentrated fluorinated water-in-oil emulsions. In Koutsoukos, P. (ed). *Trends in colloid and interface science XV*. Berlin, Heidelberg: Springer.

Bampffield, H.A. & Cooper, J. 1988. Emulsion Explosives. Becher P. (ed.). vol. 3. *Encyclopedia of emulsion technology*. New York: Marcel Dekker.

Barnhard, P. & Bahr, L.G. 1983. *Explosive emulsion composition*. U.S. Patent No. 4394199 A. Washington, DC: Patent and Trademark Office.

Becher, P. (ed). 1988. *Encyclopedia of emulsion technology*. New York: Marcel Dekker.

Bengoechea, C., Cordobés, F. & Guerrero, A. 2006. Rheology and microstructure of gluten and soya-based o/w emulsions. *Rheologica Acta*, 46:13-21.

Bergeron, V. 1999. Forces and structure in thin liquid soap films. *Journal of Physics: Condensed Matter*, 11:R215-R238.

Bhattacharyya, D.N., Seshan, S., Campbell, J.S. & Sen, S. 1983. Water-in-oil emulsion explosives and a method for the preparation of the same. U.S. Patent No. 4409044 A. Washington, DC: Patent and Trademark Office.

Binet, R., Cloutier, J.R., Edmonds, A.C.F., Holden, H.W. & McNicol, M.A. 1982. Explosive compositions based on time-stable colloidal dispersions. U.S. Patent No. 4357184 A.

Washington, DC: Patent and Trademark Office.

Bird, R.B., Armstrong, R.C. & Hassager, O. (eds). 1987. *Dynamics of polymeric liquids: fluid mechanics*. John Wiley and Sons Inc: New York.

Bluhm, H. F. 1969. Ammonium nitrate emulsion blasting agent and method of preparing same. *U.S. Patent No. 3447978 A*. Washington, DC: Patent and Trademark Office.

Boer, W. G. 2003. Adduct of polyalk(en)yl succinic anhydride and a urea, thiourea, guanidine, nitroguanidine, methylolurea, methylurea, triuret, biuret, semicarbazide and derivatives. *U.S. Patent No. 6630596 B2*. Washington, DC: Patent and Trademark Office.

Bouyer, E., Mekhloufi, G., Rosilio, V., Grossiord, J.L. & Agnely, F. 2012. Proteins, polysaccharides, and their complexes used as stabilisers for emulsions: alternatives to synthetic surfactants in the pharmaceutical field? *International Journal of Pharmaceutics*, 436:359-378.

Boyd, J., Parkinson, C. & Sherman, P. 1972. Factors affecting emulsion stability, and the HLB concept. *Journal of Colloid and Interface Science*, 41:359-370.

Bressy, L., Hébraud, P., Schmitt, V. & Bibette, J. 2003. Rheology of emulsions stabilised by solid interfaces. *Langmuir*, 19:598-604.

Brösel, S. & Schubert, H. 1999. Investigations on the role of surfactants in mechanical emulsification using a high-pressure homogenizer with an orifice valve. *Chemical Engineering and Processing: Process Intensification*, 38:533-540.

Butler, J.V. 1932. The thermodynamics of the surfaces of solutions. *Proceedings of the Royal Society A*, 135:348-375.

Buzza, D.M.A. & Cates, M.E. 1994. Uniaxial elastic modulus of concentrated emulsions. *Langmuir*, 10:4503-4508.

Campana, M., Webster, J.R.P., Gutberlet, T., Wojciechowski, K. & Zarbakhsh, A. 2013. Surfactant mixtures at the oil-water interface. *Journal of Colloid and Interface Science*, 398:126-133.

Cechanski, M. 1997. Polyolefin modified by an alkanolamine and hydrocarbon halide. *U.S. Patent No. 5639988 A*. Washington, DC: Patent and Trademark Office.

Cescon, L.A. & Millet, N.J. 1985. Stable nitrate/emulsion explosives and emulsion for use therein. *U.S. Patent No. US4555278 A* 1985-11-26. Washington, DC: Patent and Trademark Office.

Chattopadhyay, A.K. 1996a. Emulsion explosive. *U.S. Patent No.5500062 A*. Washington, DC: Patent and Trademark Office.

Chattopadhyay, A. K. 1996b. Explosives. *U.S. Patent No. 5567910 A*. Washington, DC: Patent and Trademark Office.

- Chattopadhyay, A.K., Ghaicha, L., Oh, S.G. & Shah, D.O. 1992. Salt effects on monolayers and their contribution to surface viscosity. *The Journal of Physical Chemistry*, 96:6509-6513.
- Choi, S.J. & Schowalter, W.R. 1975. Rheological properties of nondilute suspensions of deformable particles. *Physics of Fluids*, 18:420-427.
- Chow, M.C. & Ho, C.C. 1996. Properties of palm-oil-in-water emulsions: effect of mixed emulsifiers. *Journal of the American Oil Chemists' Society*, 73:47-53.
- Clay, R.B. 1978. Ammonium nitrate oxidiser. *U.S. Patent No. 4111727 A*. Washington, DC: Patent and Trademark Office.
- Clint, J.H. 1975. Micellization of mixed nonionic surface active agents. *Journal of the Chemical Society, Faraday Transactions 1: Physical Chemistry in Condensed Phases*, 71:1327-1334.
- Coolbaugh, T. & Mahamat, H. 2003. Explosive emulsion compositions containing modified copolymers of isoprene, butadiene, and/or styrene. *U.S. Patent No. 20030024619 A1*. Washington, DC: Patent and Trademark Office.
- Cooper, J. & Baker, A.S. 1989. Oxidiser dispersed in organic liquid; electroconductivity; storage stability. *U.S. Patent No. 20030024619 A1*. Washington, DC: Patent and Trademark Office.
- Crook, E.H., Fordyce, D.B. & Trebbi, G.F. 1963. Molecular weight distribution of nonionic surfactants. I. Surface and interfacial tension of normal distribution and homogeneous p,t-octylphenoxyethoxyethanols (OPE'S). *The Journal of Physical Chemistry*, 67:1987-1994.
- Daniels, R. 2011. *Galenic principles of modern skin care products*. Available: <http://www.skin-care-forum.basf.com/en/articles/skin/galenic-principles-of-modern-skin-care-products/2001/04/15?id=81fb2fb5-f040-4e82-9f6f-8f4b20e9e05f&mode=Detail> [Date accessed: 12/10/2014]
- Davies, J.T. 2012. *Interfacial phenomena 2e*. London: Academic Press.
- Defay, R. & Prigogine, I. 1951. *Tension superficielle et adsorption*. Paris: Desoer.
- Derjaguin, B. 1934. Untersuchungen über die reibung und adhäsion, IV. *Kolloid-Zeitschrift*, 69:155-164.
- Derkach, S.R. 2009. Rheology of emulsions. *Advances in Colloid and Interface Science*, 151:1-23.
- Dimitrova, T.D. & Leal-Calderon, F. 2004. Rheological properties of highly concentrated protein-stabilized emulsions. *Advances in Colloid and Interface Science*, 108–109:49-61.
- Din, K.U., Sheikh, M.S. & Dar, A.A. 2010. Analysis of mixed micellar and interfacial behavior of cationic gemini hexanediyl-1,6-bis(dimethylcetylammmonium bromide) with conventional ionic and nonionic surfactants in aqueous medium. *The Journal of Physical Chemistry B*,

114:6023-6032.

Drelich, A., Gomez, F., Clause, D. & Pezron, I. 2010. Evolution of water-in-oil emulsions stabilized with solid particles: influence of added emulsifier. *Colloids and Surfaces A: Physicochemical and Engineering Aspects*, 365:171-177.

Dynarowicz-Łątka, P. & Kita, K. 1999. Molecular interaction in mixed monolayers at the air/water interface. *Advances in Colloid and Interface Science*, 79:1-17.

Edamura, K., Torii, A. & Sakai, H. 1988. Water-in-oil emulsion explosive composition. *U.S. Patent No. 4732626 A*. Washington, DC: Patent and Trademark Office.

Egly, R.S. & Neckar, A.E. 1964. Ammonium nitrate-containing emulsion sensitizers for blasting agents. *U.S. Patent No. 3161551 A*. Washington, DC: Patent and Trademark Office.

Elena, J. & Emilio, A. 2007. Surfactant aggregates: experimental and theoretical characterization of mixed systems: *Encyclopedia of surface and colloid science*, 2nd ed. New York: CRC Press.

Elworthy, P.H. & Florence, A.T. 1969. Stabilization of oil-in-water emulsions by non-ionic detergents: the effect of polyoxyethylene chain length. *Journal of Pharmacy and Pharmacology*, 21:70S-78S.

Fainerman, V.B., Aksenenko, E.V., Krägel, J. & Miller, R. 2013. Viscoelasticity moduli of aqueous C14EO8 solutions as studied by drop and bubble profile methods. *Langmuir*, 29:6964-6968.

Fennema, O. R. 1996. *Food chemistry*, 3rd ed. New York: Marcel Dekker.

Finkle, P., Draper, H.D. & Hildebrand, J.H. 1923. The theory of emulsification. *Journal of the American Chemical Society*, 45:2780-2788.

Flourya, J., Desrumauxa, A., Axelosb, M. & Legrandc, J. 2003. Effect of high pressure homogenisation on methylcellulose as food emulsifier. *Journal of Food Engineering*, 58:227-238.

Forsberg, J.W. 1989. Salt compositions for explosives. *U.S. Patent No. 4708753 A*. Washington, DC: Patent and Trademark Office.

Foudazi, R., Masalova, I. & Malkin, A.Y. 2011. Flow behaviour of highly concentrated emulsions of supersaturated aqueous solution in oil. *Rheologica Acta*, 50:897-907.

Foudazi, R., Masalova, I. & Malkin, A.Y. 2010a. Effect of interdroplet interaction on elasticity of highly concentrated emulsions. *Applied Rheology*, 20:45096-45105.

Foudazi, R., Masalova, I. & Malkin, A.Y. 2010b. The role of interdroplet interaction in the physics of highly concentrated emulsions. *Colloid Journal*, 72:74-92.

Foudazi, R., Masalova, I. & Malkin, A.Y. 2012. The rheology of binary mixtures of highly concentrated emulsions: Effect of droplet size ratio. *Journal of Rheology* 56:1299-1314.

- Fowkes, F.M. 1962. Ideal two-dimensional solutions. II. A new isotherm for soluble and "gaseous" monolayers. *The Journal of Physical Chemistry*, 66:385-389.
- Fredrickson, A.G. 1964. *Principles and applications of rheology*. New Jersey: Prentice-Hall.
- Fried, V., Hameka, H.F. & Blukis, U. 1975. *Physical chemistry*. London: Macmillan.
- Frumkin, A.N. 1925. Electrocapillary curve of higher aliphatic acids and the state equation of the surface layer. *Zeitschrift für Physikalische Chemie* 116:466-488.
- Fu, Z., Liu, M., Xu, J., Wang, Q. & Fan, Z. 2010. Stabilization of water-in-octane nano-emulsion. Part I: Stabilized by mixed surfactant systems. *Fuel*, 89:2838-2843.
- Gaines, J. & George, L. 1966. Thermodynamic relationships for mixed insoluble monolayers. *Journal of Colloid and Interface Science*, 21:315-319.
- Ganguly, S., Mohan, V.K., Bhasu, V.C.J., Mathews, E., Adisheshaiah, K.S. & Kumar, A.S. 1992. Surfactant-electrolyte interactions in concentrated water-in-oil emulsions: FT-IR spectroscopic and low-temperature differential scanning calorimetric studies. *Colloids and Surfaces*, 65:243-256.
- Genes, P., Francoise, B., Quere, D. 2004. *Capillarity and wetting phenomena*. New York: Springer.
- Ghaicha, L., Leblanc, R.M. & Chattopadhyay, A.K. 1993. Influence of concentrated ammonium nitrate solution on monolayers of some dicarboxylic acid derivatives at the air/water interface. *Langmuir*, 9:288-293.
- Ghaicha, L., Leblanc, R.M., Villamagna, F. & Chattopadhyay, A. K. 1995. Monolayers of mixed surfactants at the oil-water Interface, hydrophobic interactions, and stability of water-in-oil emulsions. *Langmuir*, 11:585-590.
- Ghosh, S. & Rousseau, D. 2011. Fat crystals and water-in-oil emulsion stability. *Current Opinion in Colloid & Interface Science*, 16:421-431.
- Goodrich, F.C. 1957. Molecular interaction in mixed monolayers. In: Schulman, J.H., (ed). *2nd International Congress on Surface Activity*, London: Butterworth.
- Grace, H.P. 1982. Dispersion phenomena in high viscosity immiscible fluid systems and application of static mixers as dispersion devices in such systems. *Chemical Engineering Communications*, 14:225-277.
- Grassi, M., Lapasin, R. & Pricl, S. 1996. A study of the rheological behavior of scleroglucan weak gel systems. *Carbohydrate Polymers*, 29:169-181.
- Griffin, W.C. 1954. Calculation of HLB Values of non-ionic surfactants. *Journal of the Society of Cosmetic Chemists*, 5:249-256.
- Gullapalli, R.P. & Sheth, B.B. 1999. Influence of an optimized non-ionic emulsifier blend on properties of oil-in-water emulsions. *European Journal of Pharmaceutics and*

Biopharmaceutics, 48:233-238.

Hales, R.H., Cranney, D.H., Hurley, E.K. & Preston, S.B. 2004. Emulsion phase having improved stability. *U.S. Patent No. 6808573 B2*. Washington, DC: Patent and Trademark Office.

Hamaker, H.C. 1937. The london-van der waals attraction between spherical particles. *Physics* 4: 1058-1072.

Haque, M.E., Das, A.R. & Moulik, S.P. 1995. Behaviors of sodium deoxycholate (NaDC) and polyoxyethylene tert-octylphenyl ether (Triton X-100) at the air/water interface and in the bulk. *The Journal of Physical Chemistry*, 99:14032-14038.

Hartley, G. 1936. *Aqueous solutions of paraffin-chain salts; a study in micelle formation*. Paris: Hermann & Cie.

Hemar, Y., Hocquart, R. & Lequeux, F. 1995. Effect of interfacial rheology on foams viscoelasticity, an effective medium approach. *Journal de Physique II France*, 5: 1567-1576.

Hobson, D., Psaila, A. & Di Biase, S. 2007. Ethoxylated surfactants for water in oil emulsions. *U.S. Patent No. 20070119529 A1*. Washington, DC: Patent and Trademark Office.

Holland, P.M. & Rubingh, D.N. 1992. *Mixed surfactant systems*. Washington, DC: American Chemical Society.

Hua, X. & Rosen, M.J. 1982. Synergism in binary mixtures of surfactants: I. Theoretical analysis. *Journal of Colloid and Interface Science*, 90:212-219.

Huibers, P.D.T. & Shah, D.O. 1997. Evidence for synergism in nonionic surfactant mixtures: enhancement of solubilization in water-in-oil microemulsions. *Langmuir*, 13:5762-5765.

Hunter, R.J. 1993. *Introduction to modern colloid science*. Oxford: Oxford University Press.

Ishii, F., Takamura, A. & Ogata, H. 1988. Compatibility of intravenous fat emulsions with prodrug amino acids. *Journal of Pharmacy and Pharmacology*, 40:89-92.

Israelachvili, J. 1994. Self-assembly in two dimensions: surface micelles and domain formation in monolayers. *Langmuir*, 10:3774-3781.

Israelachvili, J.N. 2010. *Intermolecular and surface forces*. California: Elsevier Inc.

Israelachvili, J.N., Mitchell, D.J. & Ninham, B.W. 1976. Theory of self-assembly of hydrocarbon amphiphiles into micelles and bilayers. *Journal of the Chemical Society, Faraday Transactions 2: Molecular and Chemical Physics*, 72:1525-1568.

Jackson, N.E. & Tucker, C.L. 2003. A model for large deformation of an ellipsoidal droplet with interfacial tension. *Journal of Rheology*, 47:659-682.

Jafari, S.M., Assadpoor, E., He, Y. & Bhandari, B. 2008. Re-coalescence of emulsion

droplets during high-energy emulsification. *Food Hydrocolloids*, 22:1191-1202.

Jiao, J. & Burgess, D. 2003. Rheology and stability of water-in-oil-in-water multiple emulsions containing Span 83 and Tween 80. *AAPS Pharmaceutical Science*, 5:62-73.

Johnston, D.S., Coppard, E., Parera, G.V. & Chapman, D. 1984. Langmuir film balance study of the interactions between carbohydrates and phospholipid monolayers. *Biochemistry*, 23:6912-6919.

Kang, W., Xu, B., Wang, Y., Li, Y., Shan, X., An, F. & Liu, J. 2011. Stability mechanism of W/O crude oil emulsion stabilized by polymer and surfactant. *Colloids and Surfaces A: Physicochemical and Engineering Aspects*, 384:555-560.

Karbstein, H. & Schubert, H. 1995. Developments in the continuous mechanical production of oil-in-water macro-emulsions. *Chemical Engineering and Processing: Process Intensification*, 34:205-211.

Kharatiyan, E. 2005. Time effects in evolution of structure and rheology of highly concentrated emulsion. Doctoral thesis, Cape Peninsula University of Technology, Cape Town.

Khristov, K., Taylor, S.D., Czarnecki, J. & Masliyah, J. 2000. Thin liquid film technique-application to water-oil-water bitumen emulsion films. *Colloids and Surfaces A: Physicochemical and Engineering Aspects*, 174:183-196.

Klbrn: *Measurement of surface tension*. Available: <http://www.kibron.com/surface-tension/measurement-techniques>. [Date accessed: 01/03/2014].

Kim, J.: *Interaction between Polymer-Grafted Particles*. Available: <http://home.unist.ac.kr/~jukim/?mid=research>. [Date accessed: 05/10/2014]

Kolb, G., Viardot, K., Wagner, G. & Ulrich, J. 2001. Evaluation of a new high-pressure dispersion unit (HPN) for emulsification. *Chemical Engineering & Technology*, 24:293-296.

Kopeliovich, D.: *Stabilization of colloids*. Available: http://www.substech.com/dokuwiki/doku.php?id=stabilization_of_colloids [Date accessed: 01/03/2014]

Kovalchuk, K. & Masalova, I. 2012. Factors influencing the crystallisation of highly concentrated water-in-oil emulsions: A DSC study. *South African Journal of Science*, 108:1-5.

Kovalchuk, K., Masalova, I. & Malkin, A.Y. 2010. Influence of electrolyte on interfacial and rheological properties and shear stability of highly concentrated W/O emulsions. *Colloid Journal*, 72:806-814.

Krawczyk, M.A., Wasan, D.T. & Shetty, C. 1991. Chemical demulsification of petroleum emulsions using oil-soluble demulsifiers. *Industrial & Engineering Chemistry Research*, 30:367-375.

- Kraynik, A.M. & Reinelt, D.A. 1996. Linear elastic behavior of dry soap foams. *Journal of Colloid and Interface Science*, 181:511-520.
- Kuhl, T.L., Leckband, D.E., Lasic, D.D. & Israelachvili, J.N. 1994. Modulation of interaction forces between bilayers exposing short-chained ethylene oxide headgroups. *Biophysical Journal*, 66:1479-1488.
- Kunieda, H., Solans, C., Shida, N. & Parra, J.L. 1987. The formation of gel-emulsions in a water/nonionic surfactant/oil system. *Colloids and Surfaces*, 24:225-237.
- Lacasse, M.D., Grest, G.S., Levine, D., Mason, T.G. & Weitz, D.A. 1996. Model for the elasticity of compressed emulsions. *Physical Review Letters*, 76:3448-3451.
- Langenfeld, A., Schmitt, V. & Stébé, M.J. 1999. Rheological behavior of fluorinated highly concentrated reverse emulsions with temperature. *Journal of Colloid and Interface Science*, 218:522-528.
- Leal-Calderon, F., Thivilliers, F. & Schmitt, V. 2007. Structured emulsions. *Current Opinion in Colloid & Interface Science*, 12:206-212.
- Lissant, K.J. 1966. The geometry of high-internal-phase-ratio emulsions. *Journal of Colloid and Interface Science*, 22:462-468.
- Lissant, K.J., Peace, B.W., Wu, S.H. & Mayhan, K.G. 1974. Structure of high-internal-phase-ratio emulsions. *Journal of Colloid and Interface Science*, 47:416-423.
- Dannenfelser, R.M., Liu, R. & Li, S. 2008. Micellization and drug solubility enhancement: *Water insoluble drug formulation*. 2nd ed. Liu, R. (ed.). 255-306, New York: CRC Press.
- Lobo, L. & Svereika, A. 2003. Coalescence during emulsification: 2. Role of small molecule surfactants. *Journal of Colloid and Interface Science*, 261:498-507.
- Lu, D. & Rhodes, D.G. 2000. Mixed composition films of Spans and Tween 80 at the air-water interface. *Langmuir*, 16:8107-8112.
- Lucassen-Reynders, E.H. 1973. Interactions in mixed monolayers. I. Assessment of interaction between surfactants. *Journal of Colloid and Interface Science*, 42:554-562.
- Maeda, H. 1995. A simple thermodynamic analysis of the stability of ionic/nonionic mixed micelles. *Journal of Colloid and Interface Science*, 172:98-105.
- Maheshwari, R. & Dhathathreyan, A. 2004. Influence of ammonium nitrate in phase transitions of Langmuir and Langmuir-Blodgett films at air/solution and solid/solution interfaces. *Journal of Colloid and Interface Science*, 275:270-276.
- Malkin, A., Masalova, I., Pavlovski, D. & Slatter, P. 2004. Is the Choice of Flow Curve Fitting Equation Crucial for the Estimation of Pumping Characteristics? *Applied Rheology*, 14:89-95.
- Malkin, A., Masalova, I., Slatter, P. & Wilson, K. 2004. Effect of droplet size on the

rheological properties of highly-concentrated w/o emulsions. *Rheologica Acta*, 43:584-591.

Malkin, A.I.A., Malkin, A.Y. & Isayev, A.I. 2006. *Rheology: concepts, methods, and applications*. Toronto: ChemTec Publication.

Malkin, A.Y. & Masalova, I. 2007. Shear and normal stresses in flow of highly concentrated emulsions. *Journal of Non-Newtonian Fluid Mechanics*, 147:65-68.

Masalova, I. 2003. Industry Report: Comparison of measured and calculated pressure drop versus flow rate of explosive emulsions, *AEL Mining Service*.

Masalova, I., Foudazi, R. & Malkin, A.Y. 2011a. The rheology of highly concentrated emulsions stabilized with different surfactants. *Colloids and Surfaces A: Physicochemical and Engineering Aspects*, 375:76-86.

Masalova, I., Kovalchuk, K. & Malkin, A.Y. 2011b. IR Studies of interfacial interaction of the succinic surfactants with different head groups in highly concentrated W/O emulsions. *Journal of Dispersion Science and Technology*, 32:1547-1555.

Masalova, I. & Malkin, A.Y. 2007a. A new mechanism of aging of highly concentrated emulsions: Correlation between crystallization and plasticity. *Colloid Journal*, 69:198-202.

Masalova, I. & Malkin, A.Y. 2007b. Peculiarities of rheological properties and flow of highly concentrated emulsions: the role of concentration and droplet size. *Colloid Journal*, 69:185-197.

Masalova, I. & Malkin, A.Y. 2007c. Rheology of highly concentrated emulsions - concentration and droplet size dependencies. *Applied Rheology*, 17:42250-42259.

Masalova, I. & Malkin, A.Y. 2008. Master curves for elastic and plastic properties of highly concentrated emulsions. *Colloid Journal*, 70:327-336.

Masalova, I. & Malkin, A.Y. 2013. The engineering rheology of liquid explosives as highly concentrated emulsions. *Chemical Engineering Research and Design*, 91:204-210.

Masalova, I., Malkin, A.Y., Ferg, E., Kharatiyan, E., Taylor, M. & Haldenwang, R. 2006. Evolution of rheological properties of highly concentrated emulsions with aging -emulsion-to-suspension transition. *Journal of Rheology*, 50:435-451.

Masalova, I., Malkin, A.Y., Slatter, P. & Wilson, K. 2003. The rheological characterization and pipeline flow of high concentration water-in-oil emulsions. *Journal of Non-Newtonian Fluid Mechanics*, 112:101-114.

Masalova, I., Taylor, M., Kharatiyan, E. & Malkin, A.Y. 2005. Rheopexy in highly concentrated emulsions. *Journal of Rheology*, 49:839-849.

Mason, T. G. 1999. New fundamental concepts in emulsion rheology. *Current Opinion in Colloid & Interface Science*, 4:231-238.

Mason, T.G., Bibette, J. & Weitz, D.A. 1996. Yielding and flow of monodisperse emulsions.

Journal of Colloid and Interface Science, 179:439-448.

Mason, T.G., Lacasse, M.D., Grest, G.S., Levine, D., Bibette, J. & Weitz, D.A. 1997. Osmotic pressure and viscoelastic shear moduli of concentrated emulsions. *Physical Review E*, 56:3150-3166.

McBain, J.W. 1913. Mobility of highly-charged micelles. *Transactions of the Faraday Society* 9:99-101.

McClements, D.J. 2005. *Food emulsions: principles, practice, and techniques*. CRC Press NC.

McKenna, B. M. 2003. *Texture in food*. New York: CRC Press.

McKenzie, L.F. 1991. Stabilized emulsion explosive and method. *U.S. Patent No. 5076867 A*. Washington, DC: Patent and Trademark Office.

McKenzie, L.F. & Lawrence, L.D. 1990. Alkanolamine-modified polyisobutenyl succinic anhydride as emulsifier; storage stability. *U.S. Patent No. 4931110 A*. Washington, DC: Patent and Trademark Office.

Meller, A. & Stavans, J. 1996. Stability of emulsions with nonadsorbing polymers. *Langmuir*, 12:301-304.

Mittal, K.L. 1975. *Ultracentrifugal technique in the study of emulsions. Colloidal dispersions and micellar behavior*. Washington, DC: American Chemical Society.

Mohan, S. & Narsimhan, G. 1997. Coalescence of protein-stabilized emulsions in a high-pressure homogenizer. *Journal of Colloid and Interface Science*, 192:1-15.

Motomura, K., Yamanaka, M. & Aratono, M. 1984. Thermodynamic consideration of the mixed micelle of surfactants. *Colloid and Polymer Science*, 262:948-955.

Mudeme, S., Masalova, I. & Haldenwang, R. 2010. Kinetics of emulsification and rheological properties of highly concentrated explosive emulsions. *Chemical Engineering and Processing: Process Intensification*, 49:468-475.

Myers, D. 2005. *Fluid surfaces and interfaces. Surfactant science and technology*. 3th ed. New Jersey: John Wiley & Sons Inc.

Nagarajan, R. 2001. Molecular packing parameter and surfactant self-assembly: The neglected role of the surfactant tail. *Langmuir*, 18:31-38.

Nagarajan, R. & Ruckenstein, E. 1991. Theory of surfactant self-assembly: a predictive molecular thermodynamic approach. *Langmuir*, 7:2934-2969.

Narsimhan, G. & Goel, P. 2001. Drop coalescence during emulsion formation in a high-pressure homogenizer for tetradecane-in-water emulsion stabilized by sodium dodecyl sulfate. *Journal of Colloid and Interface Science*, 238:420-432.

Nguyen, A.D. 1991. Dry particles. *U.S. Patent No. 4997494 A*. Washington, DC: Patent and

Trademark Office.

Nixon, J. & Beerbower, A. 1969. Properties of high internal phase emulsions, effect of emulsifier parameters. *American Chemical Society, Division of Petroleum Chemistry*, 14:49-59.

Oldroyd, J.G. 1955. The effect of interfacial stabilizing films on the elastic and viscous properties of emulsions. *Proceedings of the Royal Society of London A.*, 232:567-577.

Omura, T. & Nanba, T. 2003. High internal aqueous phase water-in-oil type emulsion cosmetic composition. *U.S. Patent No. 20030064046 A1*. Washington, DC: Patent and Trademark Office.

Opawale, F.O. & Burgess, D.J. 1998. Influence of interfacial properties of lipophilic surfactants on water-in-oil emulsion stability. *Journal of Colloid and Interface Science*, 197:142-150.

Otsubo, Y. & Prud'homme, R.K. 1994. Rheology of oil-in-water emulsions. *Rheologica Acta*, 33:29-37.

Pal, R. 2000. Linear Viscoelastic behavior of multiphase dispersions. *Journal of Colloid and Interface Science*, 232:50-63.

Particle Sciences Drug Development Services Group: 2010. *Surfactants*. Available: <http://www.particlesciences.com/news/technical-briefs/2010/surfactants.html> [Date accessed: 01/10/2014]

Peltonen, L., Hirvonen, J. & Yliruusi, J. 2001. The behavior of sorbitan surfactants at the water–oil interface: straight-chained hydrocarbons from pentane to dodecane as an oil phase. *Journal of Colloid and Interface Science*, 240:272-276.

Peltonen, L.J. & Yliruusi, J. 2000. Surface pressure, hysteresis, interfacial tension, and CMC of four sorbitan monoesters at water–air, water–hexane, and hexane–air interfaces. *Journal of Colloid and Interface Science*, 227:1-6.

Perrin, P., Monfreux, N. & Lafuma, F. 1999. Highly hydrophobically modified polyelectrolytes stabilizing macroemulsions: relationship between copolymer structure and emulsion type. *Colloid and Polymer Science*, 277:89-94.

Petsev, N. 2004. Theory of emulsion fluctuation. In *Emulsions: structure, stability and interactions*. Petsev, D.N. (ed.) Interface Science and Technology series. 4: 313-350, Amsterdam: Elsevier.

Pickering, S.U. 1907. CXCVI.-Emulsions. *Journal of the Chemical Society, Transactions*, 91:2001-2021.

Pilpel, N. & Rabbani, M.E. 1988. Interfacial films in the stabilization of sunflower oil in water emulsions with nonionics. *Journal of Colloid and Interface Science*, 122: 266-273.

Pitt, A.R., Morley, S.D., Burbidge, N.J. & Quickenden, E.L. 1996. The relationship between

surfactant structure and limiting values of surface tension, in aqueous gelatin solution, with particular regard to multilayer coating. *Colloids and Surfaces A: Physicochemical and Engineering Aspects*, 114:321-335.

Pons, R., Erra, P., Solans, C., Ravey, J.C. & Stebe, M.J. 1993. Viscoelastic properties of gel-emulsions: their relationship with structure and equilibrium properties. *The Journal of Physical Chemistry*, 97:12320-12324.

Pons, R., Solans, C., Stebé, M.J., Erra, P. & Ravey, J.C. 1992. Stability and rheological properties of gel emulsions. *Progress in Colloid and Polymer Science*, 89: 110-113.

Pons, R., Solans, C. & Tadros, T.F. 1995. Rheological behavior of highly concentrated oil-in-water (o/w) emulsions. *Langmuir*, 11:1966-1971.

Ponton, A., Clément, P. & Grossiord, J.L. 2001. Corroboration of Princen's theory to cosmetic concentrated water-in-oil emulsions. *Journal of Rheology*, 45:521-526.

Prieve, D.C., Hoggard, J.D., Fu, R., Sides, P.J. & Bethea, R. 2008. Two independent measurements of debye lengths in doped nonpolar liquids. *Langmuir*, 24:1120-1132.

Princen, H.M. 1979. Highly concentrated emulsions. I. Cylindrical systems. *Journal of Colloid and Interface Science*, 71:55-66.

Princen, H.M. 1983. Rheology of foams and highly concentrated emulsions: I. Elastic properties and yield stress of a cylindrical model system. *Journal of Colloid and Interface Science*, 91:160-175.

Princen, H.M. 1986. Osmotic pressure of foams and highly concentrated emulsions. I. Theoretical considerations. *Langmuir*, 2:519-524.

Princen, H.M., Aronson, M.P. & Moser, J.C. 1980. Highly concentrated emulsions. II. Real systems. The effect of film thickness and contact angle on the volume fraction in creamed emulsions. *Journal of Colloid and Interface Science*, 75:246-270.

Princen, H.M. & Kiss, A.D. 1989. Rheology of foams and highly concentrated emulsions: IV. An experimental study of the shear viscosity and yield stress of concentrated emulsions. *Journal of Colloid and Interface Science*, 128:176-187.

Radeva, T. 2001. *Physical chemistry of polyelectrolytes*. New York: Marcel Dekker.

Rakshit, A.K., Zograf, G., Jalal, I.M. & Gunstone, F.D. 1981. Monolayer properties of fatty acids: II. Surface vapor pressure and the free energy of compression. *Journal of Colloid and Interface Science*, 80:466-473.

Rawle, A. 2011. *Basic principles of particle size analysis*. Available:<http://www.malvern.co.uk> [Date accessed: 30/05/2014]

Reinelt, D.A. & Kraynik, A.M. 1990. On the shearing flow of foams and concentrated emulsions. *Journal of Fluid Mechanics*, 215:431-455.

Reynolds, P.A., Gilbert, E.P., Henderson, M.J. & White, J.W. 2009a. Structure of high internal phase aqueous-in-oil emulsions and related Inverse micelle solutions. 3. Variation of surfactant. *The Journal of Physical Chemistry B*, 113:12231-12242.

Reynolds, P.A., Gilbert, E.P., Henderson, M.J. & White, J.W. 2009b. Structure of high internal phase aqueous-in-oil emulsions and related inverse micelle solutions. 4. Surfactant mixtures. *The Journal of Physical Chemistry B*, 113:12243-12256.

Reynolds, P.A., Gilbert, E.P. & White, J.W. 2000. High internal phase water-in-oil emulsions studied by small-angle neutron scattering. *The Journal of Physical Chemistry B*, 104:7012-7022.

Reynolds, P.A., Gilbert, E.P. & White, J.W. 2001. High internal phase water-in-oil emulsions and related microemulsions studied by small-angle neutron scattering. 2. The distribution of surfactant. *The Journal of Physical Chemistry B*, 105:6925-6932.

Reynolds, P.A., Henderson, M.J. & White, J.W. 2004. A small angle neutron scattering study of the interface between solids and oil-continuous emulsions and oil-based microemulsions. *Colloids and Surfaces A: Physicochemical and Engineering Aspects*, 232:55-65.

Reynolds, P.A., McGillivray, D.J., Gilbert, E.P., Holt, S.A., Henderson, M.J. & White, J.W. 2002. Neutron and X-ray reflectivity from polyisobutylene-based amphiphiles at the air-water interface. *Langmuir*, 19:752-761.

Reynolds, P.A., McGillivray, D.J., Mata, J.P., Yaron, P.N. & White, J.W. 2010. The stability of high internal phase emulsions at low surfactant concentration studied by small angle neutron scattering. *Journal of Colloid and Interface Science*, 349:544-553.

Roberts, G.S., Sanchez, R., Kemp, R., Wood, T. & Bartlett, P. 2008. Electrostatic charging of nonpolar colloids by reverse micelles. *Langmuir*, 24:6530-6541.

Rosen, M.J. & Gu, B. 1987. Synergism in binary mixtures of surfactants. 6. Interfacial tension reduction efficiency at the liquid/hydrophobic solid interface. *Colloids and Surfaces*, 23:119-135.

Rosen, M.J. & Kunjappu, J.T. 2012. *Surfactants and interfacial phenomena*. New Jersey: John Wiley and sons Inc.

Rosen, M.J., Zhu, Z.H., Gu, B. & Murphy, D.S. 1988. Relationship of structure to properties of surfactants. 14. Some N-alkyl-2-pyrrolidones at various interfaces. *Langmuir*, 4:1273-1277.

Rubingh, D.N. 1979. Mixed micelle solutions. In: Mittal, K.L. (ed.) *Solution chemistry of surfactants*. New York: Springer.

Russel, W.B., Saville, D.A. & Schowalter, W.R. 1989. *Colloidal dispersions*. Cambridge: University Press.

Sadoc, J.F. & Rivier, N. 1999. *Foams and emulsions*. Dordrecht: Kluwer Academic

Publishers.

Santana, R.S., Fasolin, L.H. & Cunha, R.L. 2012. Effects of a cosurfactant on the shear-dependent structures of systems composed of biocompatible ingredients. *Colloids and Surfaces A: Physicochemical and Engineering Aspects*, 398:54-63.

Santhanalakshimi, J. & Maya, S. 1997. Solvent effect on reverse micellization of Tween 80 and Span 80 in pure and mixed organic solvents. *Proc. Indian Acad. Sci. (Chem. Sci.)*, 109:27-38.

Sarmoria, C., Puvvada, S. & Blankschtein, D. 1992. Prediction of critical micelle concentrations of nonideal binary surfactant mixtures. *Langmuir*, 8:2690-2697.

Scamehorn, J.F. 1986. ACS Symposium Series: An Overview of Phenomena Involving Surfactant Mixtures. Phenomena. In: *Mixed surfactant systems*. Washington DC: American Chemical Society.

Schick, M.J. 1987. *Nonionic surfactants: physical chemistry*. New York: Marcel Dekker.

Schlaepfer, A.U.M. 1918. XLIII.-Water-in-oil emulsions. *Journal of the Chemical Society, Transactions*, 113:522-526.

Schultz, S., Wagner, G., Urban, K. & Ulrich, J. 2004. High-pressure homogenisation as a process for emulsion formation. *Chemical Engineering & Technology*, 27:361-368.

Schulz, M.B. & Daniels, R. 2000. Hydroxypropylmethylcellulose (HPMC) as emulsifier for submicron emulsions: influence of molecular weight and substitution type on the droplet size after high-pressure homogenisation. *European Journal of Pharmaceutics and Biopharmaceutics*, 49:231-236.

Schuster, D. 1996. *Encyclopedia of emulsion technology*. New York: Marcel Dekker.

Seekkuarachchi, I.N., Tanaka, K. & Kumazawa, H. 2005. Formation and characterization of submicrometer oil-in-water (O/W) emulsions, using high-energy emulsification. *Industrial & Engineering Chemistry Research*, 45:372-390.

Shen, Y. & Duhamel, J. 2008. Micellization and adsorption of a series of succinimide dispersants. *Langmuir*, 24:10665-10673.

Shiao, S.Y., Chhabra, V., Patist, A., Free, M.L., Huibers, P.D.T., Gregory, A., Patel, S. & Shah, D.O. 1998. Chain length compatibility effects in mixed surfactant systems for technological applications. *Advances in Colloid and Interface Science*, 74:1-29.

Shinoda, K. 1967. The correlation between the dissolution state of nonionic surfactant and the type of dispersion stabilized with the surfactant. *Journal of Colloid and Interface Science*, 24:4-9.

Shinoda, K. 1969. The comparison between the PIT system and the HLB-value system to emulsifier selection. In: *Proceedings of the 5th International Congress of Surface Activity*,

Barcelona, Spain. 275-283.

Shinoda, K. & Friberg, S. 1975. Microemulsions: colloidal aspects. *Advances in Colloid and Interface Science*, 4:281-300.

Shinoda, K., Saito, H. & Arai, H. 1971. The effect of the size and the distribution of the oxyethylene chain lengths of nonionic emulsifiers on the stability of emulsions. *Journal of Colloid and Interface Science*, 35:624-630.

Siddiqui, S.W. 2014. The effect of oils, low molecular weight emulsifiers and hydrodynamics on oil-in-water emulsification in confined impinging jet mixer. *Colloids and Surfaces A: Physicochemical and Engineering Aspects*, 443:8-18.

Solans, C., Esquena, J., Azemar, N., Rodriguez, C. & Kunieda, H. 2004. Highly concentrated (gel) emulsions: Formation and properties. In: Petsev, D.N. (ed.) *Interface science and technology. Emulsions: structures Stability and interactions*, 4:511-555.

Somasundaran, P. (ed). 2006. *Encyclopedia of surface and colloid Science*. Vol. 7. New York: CRC Press, Taylor and Francis.

Stang, M., Schuchmann, H. & Schubert, H. 2001. Emulsification in high-pressure homogenizers. *Engineering in Life Sciences*, 1:151-157.

Sudweeks, W.B. & Jessop, H.A. 1979. Organic fuel continuous phase, aqueous inorganic oxidizer discontinuous phase, with fatty acid amide or ammonium salt emulsifier. *U.S. Patent No. 4141767 A*. Washington, DC: Patent and Trademark Office.

Sudweeks, W.B. & Jessop, H.A. 1980. Emulsion blasting composition. *U.S. Patent No 4216040 A*. Washington, DC: Patent and Trademark Office.

Swarbrick, J. & Boylan, J.C. 1991. *Encyclopedia of pharmaceutical technology: Economic characteristics of the R&D-intensive pharmaceutical industry to fermentation processes*. New York: Marcel Dekker.

Szymczyk, K. 2012. Composition of multicomponent surfactant systems at the water–air interface. *Journal of Surfactants and Detergents*, 15:647-656.

Szymczyk, K. & Jańczuk, B. 2007. The properties of a binary mixture of nonionic surfactants in water at the water Air interface. *Langmuir*, 23:4972-4981.

Tadros, T.F. 2006. *Applied surfactants: principles and applications*. Weinheim: Wiley-VCH.

Takamura, A., Ishii, F., Noro, S.I., Tanifuji, M. & Nakajima, S. 1984. Study of intravenous hyperalimentation: Effect of selected amino acids on the stability of intravenous fat emulsions. *Journal of Pharmaceutical Sciences*, 73:91-94.

Takamura, A., Minowa, T., Noro, S. & Kubo, T. 1979. Effects of Tween and Span group emulsifiers on the stability of o/w emulsions. *Chemical & Pharmaceutical Bulletin*, 27:2921-2926.

Talmon, Y. & Prager, S. 1978. Statistical thermodynamics of phase equilibria in microemulsions. *The Journal of Chemical Physics*, 69:2984-2991.

Tan, D.: *Saponification Part 1: Chemistry behind soap and detergent*. Available: <http://aceyourchemistry.blogspot.com/2013/04/saponification-part-1-chemistry-behind.html> [Date accessed: 02/11/2013]

Tcholakova, S., Denkov, N.D. & Danner, T. 2004. Role of surfactant type and concentration for the mean drop size during emulsification in turbulent flow. *Langmuir*, 20:7444-7458.

Tesch, S. & Schubert, H. 2002. Influence of increasing viscosity of the aqueous phase on the short-term stability of protein stabilized emulsions. *Journal of Food Engineering*, 52:305-312.

Tomic, E. 1973. Emulsion type explosive composition containing ammonium stearate or alkali metal stearate. *U.S. Patent No. 3770522 A*. Washington, DC: Patent and Trademark Office.

Tropea, C., Yarin, A.L. & Foss, J.F. 2007. *Handbook of experimental fluid mechanics*. Berlin: Springer.

Tshilumbu, N.N., Ferg, E.E., & Masalova, I. 2010. Instability of highly concentrated emulsions with oversaturated dispersed phase. Role of a surfactant. *Colloid Journal*, 72: 569–573.

Tshilumbu, N.N., Kharatyan, E. & Masalova, I. 2013. Effect of nanoparticle hydrophobicity on stability of highly concentrated emulsions. *Journal of Dispersion Science and Technology*, 35:283-292.

Varadaraj, R., Bock, J., Valint, P., Zushma, S. & Thomas, R. 1991. Fundamental interfacial properties of alkyl-branched sulfate and ethoxy sulfate surfactants derived from Guerbet alcohols. 1. Surface and instantaneous interfacial tensions. *The Journal of Physical Chemistry*, 95:1671-1676.

Venter, P.N. & Kruger, F. 1996. Emulsion explosive. *U.S. Patent No. US6478904 B1*. Washington, DC: Patent and Trademark Office.

Villamagna, F., Chattopadhyay, A.K. & Chung, L.M. 1993. Sensitizer and use. *U.S. Patent No. 2093309 A1*. Washington, DC: Patent and Trademark Office.

Villamagna, F., Chattopadhyay, A.K. & Lee, M.C. 1995a. Low density foam. *U.S. Patent No. 5456729 A*. Washington, DC: Patent and Trademark Office.

Villamagna, F., Whitehead, M.A. & Chattopadhyay, A.K. 1995b. Mobility of surfactants at the water-in-oil emulsion interface. *Journal of Dispersion Science and Technology*, 16:105-114.

Wade, C. 1973. Water-in-oil emulsion explosive containing entrapped gas. *US Patent No. 3715247 A*. Washington, DC: Patent and Trademark Office.

Wade, C.G. 1978. Water-in-oil emulsion explosive composition. *U.S. Patent No. 4110134 A*. Washington, DC: Patent and Trademark Office.

- Walstra, P. 1993. Principles of emulsion formation. *Chemical Engineering Science*, 48:333-349.
- Walstra, P. 2002. *Physical chemistry of foods*. New York: Marcel Dekker.
- Walstra, P. & Smulders, P.E.A. 1998. *Emulsion formation. Modern aspects of emulsion science*. Cambridge: The Royal Society of Chemistry.
- Wan, L. & Lee, P. 1974. Studies on surface film of sorbitan esters at the air/water interface. *Canadian Journal of Pharmaceutical Sciences*, 9:82-85.
- Webber, R.M. & Engineers, A.I.O.C. 1999. *Relation between Laplace pressure and the rheology of high internal phase emulsions*. American Institute of Chemical Engineers.
- Welch, C.F., Rose, G.D., Malotky, D. & Eckersley, S.T. 2006. Rheology of high internal phase emulsions. *Langmuir*, 22:1544-1550.
- White, W.J., Reynolds, P.A., Hawley, A. & Perriman, A. 2004. Interfacial structure of block copolymers at the oil/water interface. In: Holloway, M.A., Banwell, G.M. & Sharrad, C. (eds). Research School of Chemistry- Annual Report. Canberra: Institute of Advanced Studies- Australian National University.
- Windhab, E. 1993. Bericht: IV. Tagung Lebensmittel rheology.
- Wu, X., Van De Ven, T.G.M. & Czarnecki, J. 1999. Colloidal forces between emulsified water droplets in toluene-diluted bitumen. *Colloids and Surfaces A: Physicochemical and Engineering Aspects*, 149:577-583.
- Xiao, X., Hu, J., Charych, D.H. & Salmeron, M. 1996. Chain length dependence of the frictional properties of alkylsilane Molecules self-assembled on mica studied by atomic force microscopy. *Langmuir*, 12:235-237.
- Yakhoub, H. 2009. Effect of high shearing on rheological/structural properties of highly concentrated w/o emulsions. M.Tech. Thesis. Cape Peninsula University of Technology, Cape Town.
- Yaron, P.N., Scott, A.J., Reynolds, P.A., Mata, J.P. & White, J.W. 2011. High internal phase emulsions under shear. Co-surfactancy and shear stability. *The Journal of Physical Chemistry B*, 115:5775-5784.
- Yates, D.E. & Dack, S.W. 1987. Immiscible oxidizer phase dispersed in fuel phase containing hydrophilic, lipophilic modifier. *U.S. Patent No. 4710248 A*. Washington, DC: Patent and Trademark Office
- Young, T. 1804. The Bakerian Lecture: Experiments and calculations relative to physical optics. *Philosophical Transactions of the Royal Society of London*, 94:1-16.
- Yuan, Y. & Lee, T.R. 2013. Contact angle and wetting properties. In: Bracco, G. & Holst, B. (eds). *Surface science techniques*. Berlin: Springer.

Zana, R. 1995. Aqueous surfactant-alcohol systems: a review. *Advances in Colloid and Interface Science*, 57:1-64.

Zank, J., Reynolds, P.A., Jackson, A.J., Baranyai, K.J., Perriman, A.W., Barker, J.G., Kim, M.H. & White, J.W. 2006. Aggregation in a high internal phase emulsion observed by SANS and USANS. *Physica B: Condensed Matter*, 385–386:776-779.

Zhou, Q. & Rosen, M.J. 2003. Molecular interactions of surfactants in mixed monolayers at the air/aqueous solution interface and in mixed micelles in aqueous media: the regular solution approach. *Langmuir*, 19:4555-4562.

Zograf, G. 1982. Physical stability assessment of emulsions and related disperse systems: a critical review. *Journal of the Society of Cosmetic Chemists*, 33:345-358.

APPENDICES

APPENDIX A: CHOICE OF SURFACTANT

Interfacial Tension

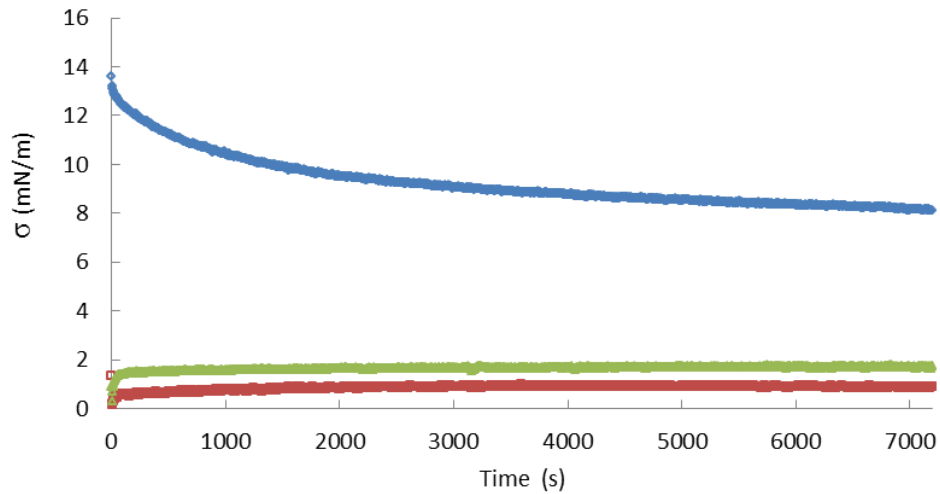


Figure A.1: Determination of the interfacial tension for PIBSA-Mea (blue), Pluronic PE 3100 (red) and PIBSA-Mea/PE 3100 (10/1) mixture (green)

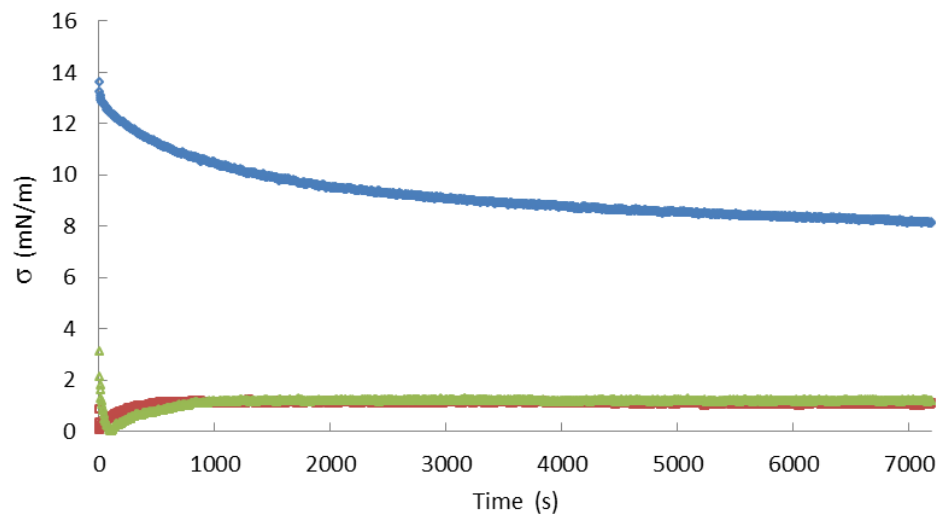


Figure A.2: Determination of the interfacial tension for PIBSA-Mea (blue), Pluronic PE 6100 (red) and PIBSA-Mea/PE 6100 (10/1) mixture (green)

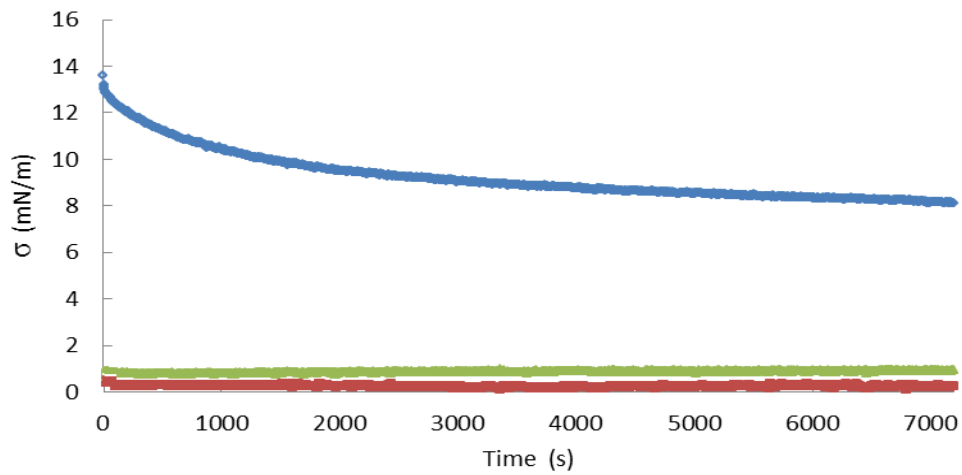


Figure A.3: Determination of the interfacial tension for PIBSA-Mea (blue), Tween20 (red) and PIBSA-Mea/Tween 20 (10/1) mixture (green)

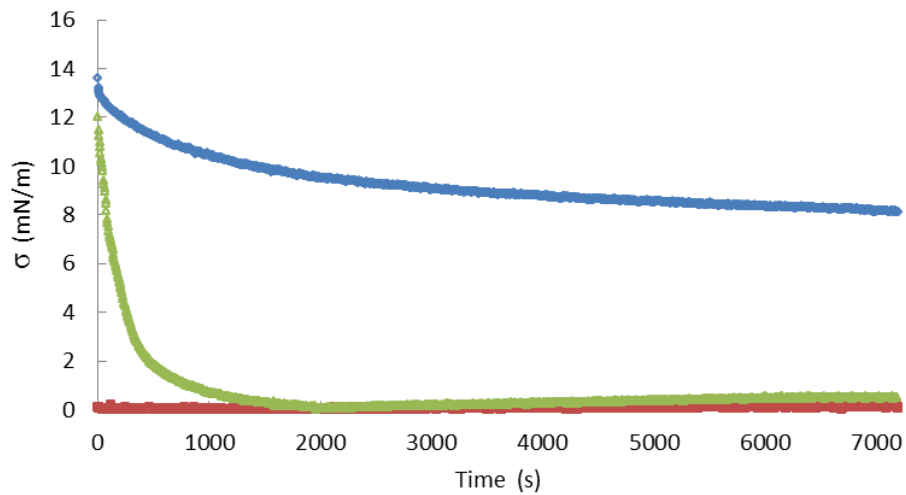


Figure A.4: Determination of the interfacial tension for PIBSA-Mea (blue), Tween80 (red) and PIBSA-Mea/Tween 80 (10/1) mixture (green)

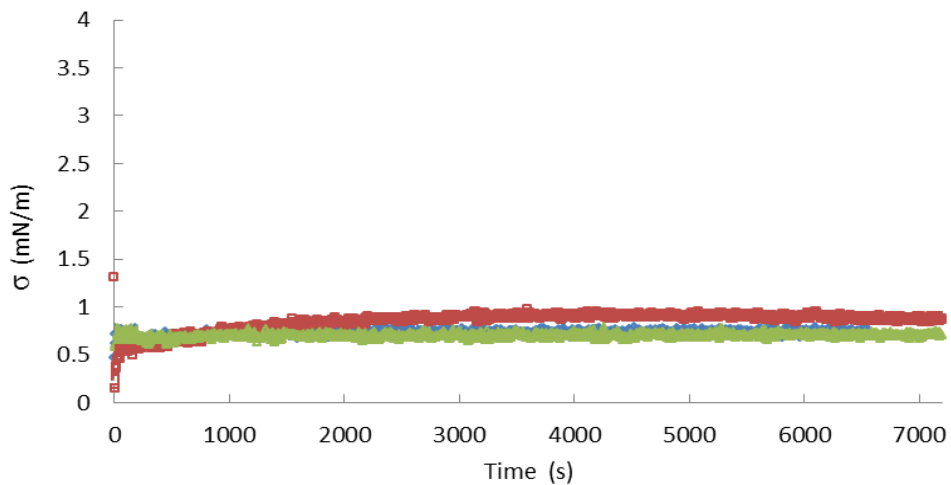


Figure A.5: Determination of the interfacial tension for SMO (blue), Pluronic PE 3100 (red) and Span 80/PE 3100 (10/1) mixture (green)

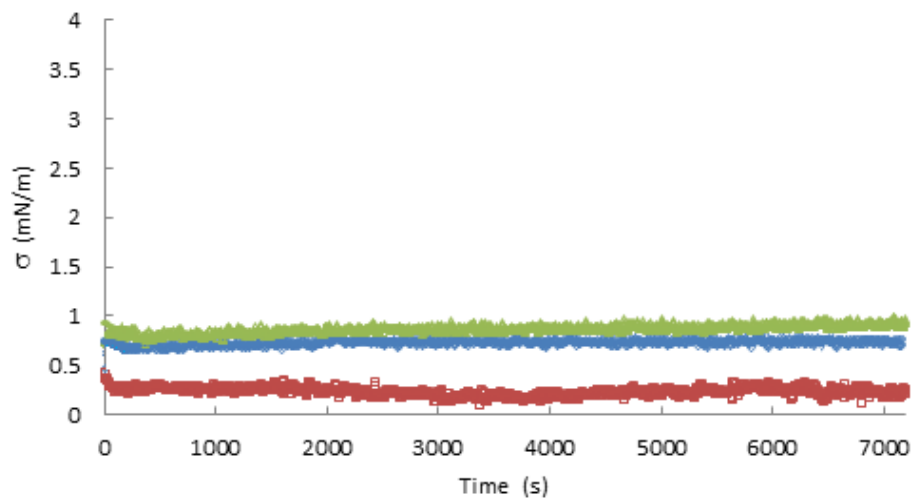


Figure A.6: Determination of the interfacial tension for SMO (blue), Tween20 (red) and Span 80/Tween 20 (10/1) mixture (green)

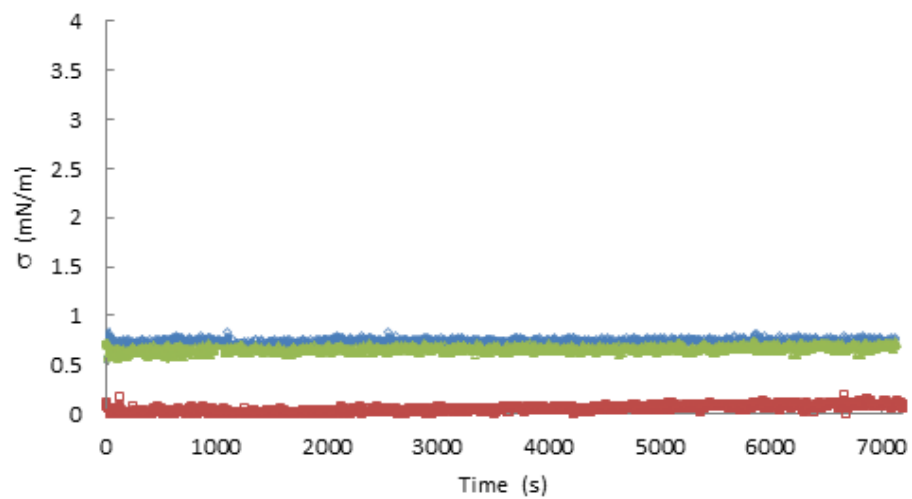


Figure A.7: Determination of the interfacial tension for SMO (blue), Tween80 (red) and Span 80/Tween 80 (10/1) mixture (green)

Evolution of droplet size over time

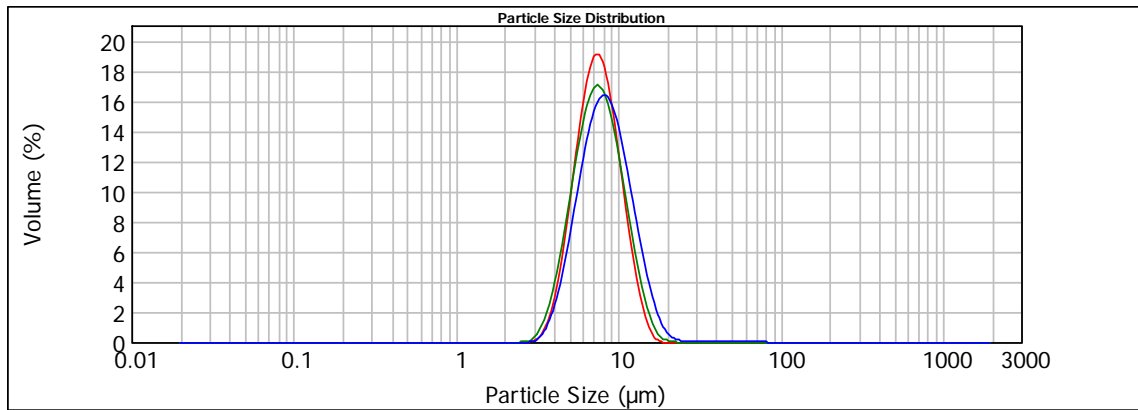


Figure A.8: Evolution of droplet size with time for the PIBSA-Mea/Tween 20 emulsion fresh (red), after three days (green) and after 10 days (blue)

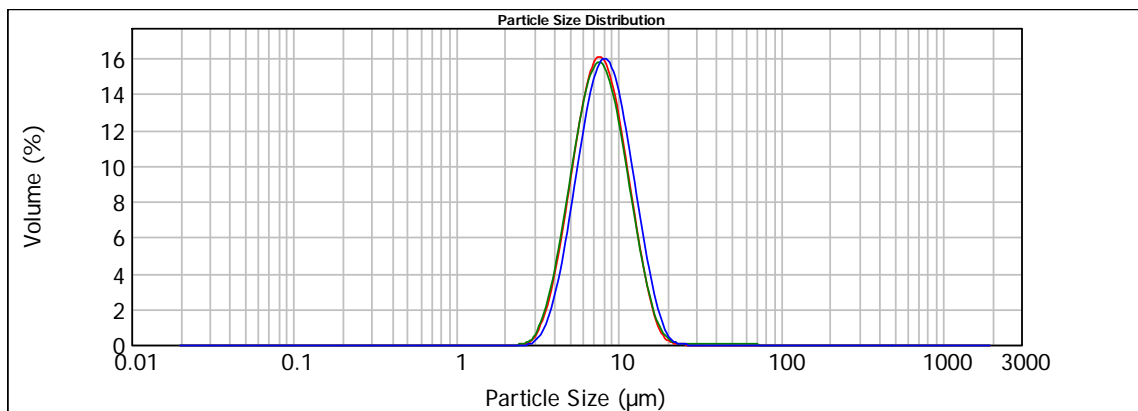


Figure A.9: Evolution of droplet size with time for the PIBSA-Mea/Tween 80 emulsion fresh (red), after 3 days (green) and after 10 days (blue)

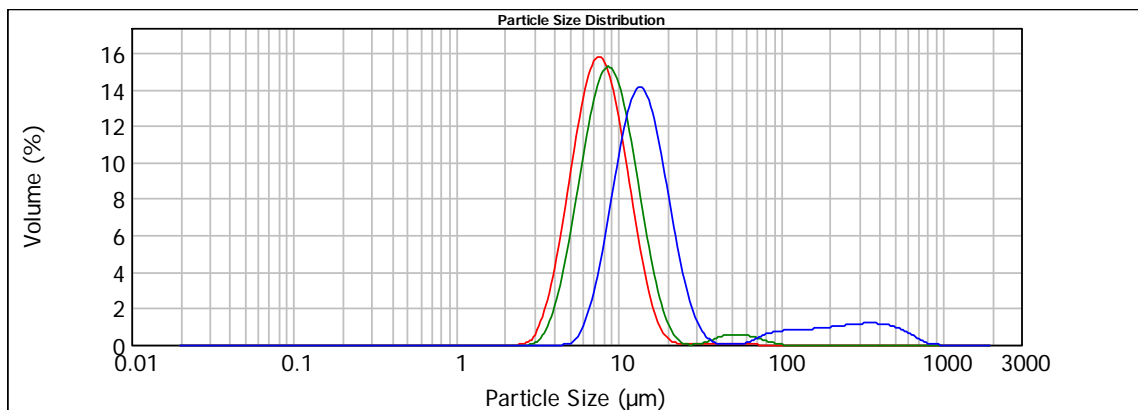


Figure A.10: Evolution of droplet size with time for the SMO/Pluronic PE3100 emulsion fresh (red), after 3 days (green) and after 10 days (blue)

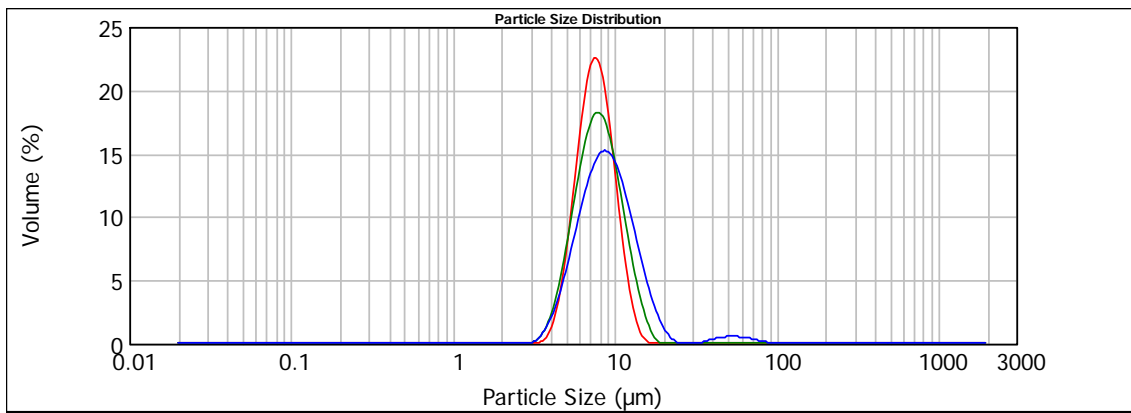


Figure A.11: Evolution of droplet size with time for the SMO/Tween 20 emulsion fresh (red), after three days (green) and after 10 days (blue)

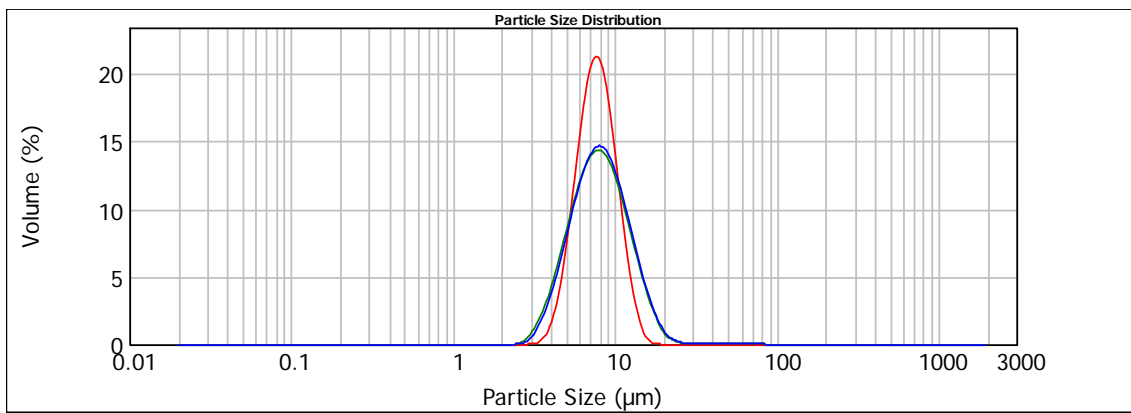


Figure A.12: Evolution of droplet size with time for the SMO/Tween 80 emulsion fresh (red), after three days (green) and after 10 days (blue)

APPENDIX B: EFFECT OF SURFACTANT STRUCTURE ON INTERFACIAL PROPERTIES

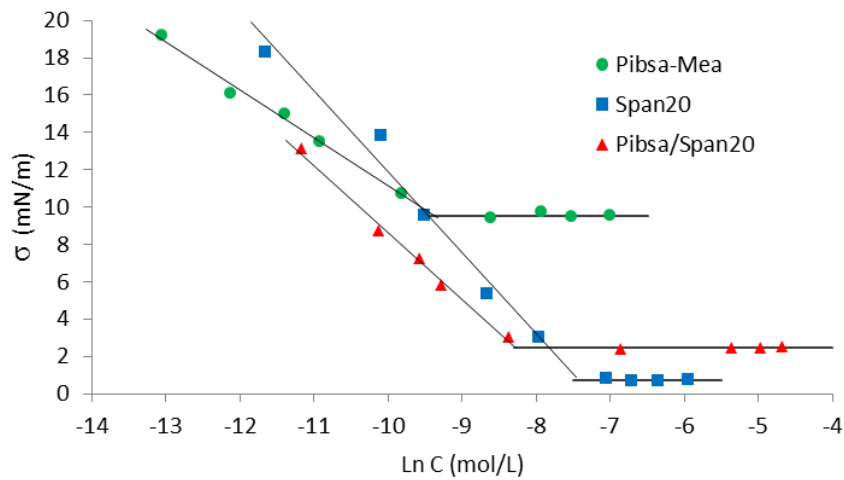


Figure B.1: Determination of CMC value of Span 20 surfactant and PIBSA-Mea/Span 20 mixture

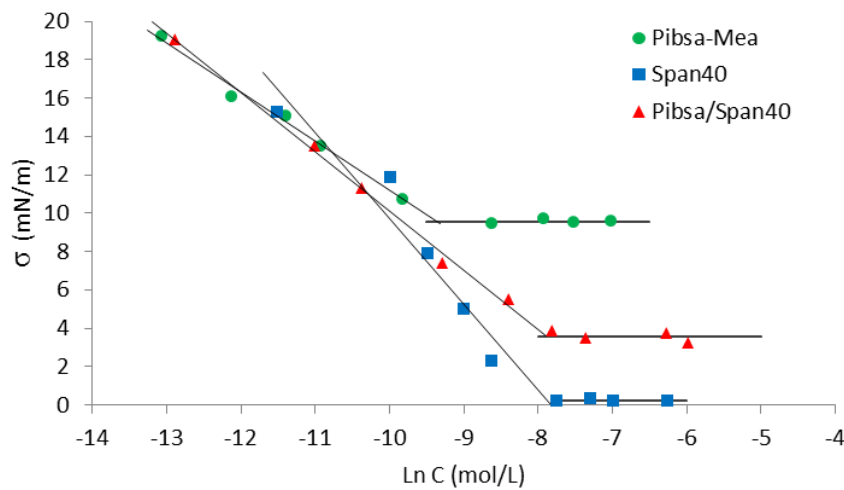


Figure B.2: Determination of CMC value of Span 40 surfactant and PIBSA-Mea/Span 40 mixture

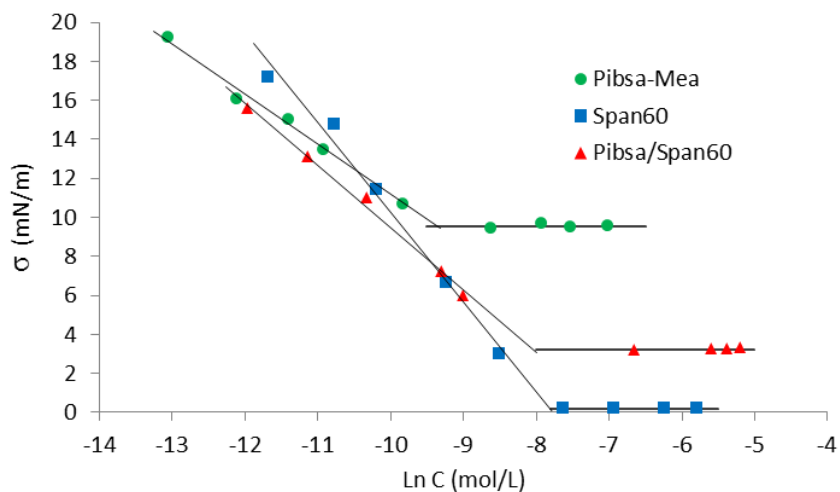


Figure B.3: Determination of CMC value of Span 60 surfactant and PIBSA-Mea/Span 60 mixture

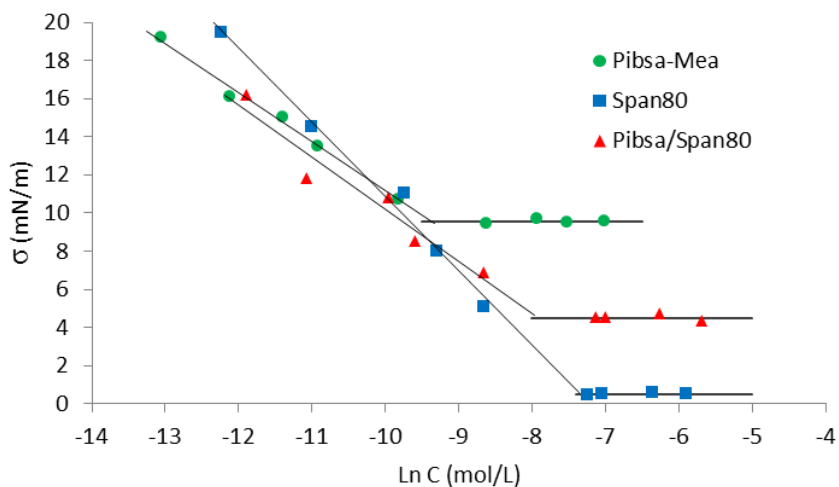


Figure B.4: Determination of CMC value of Span 80 surfactant and PIBSA-Mea/Span 80 mixture

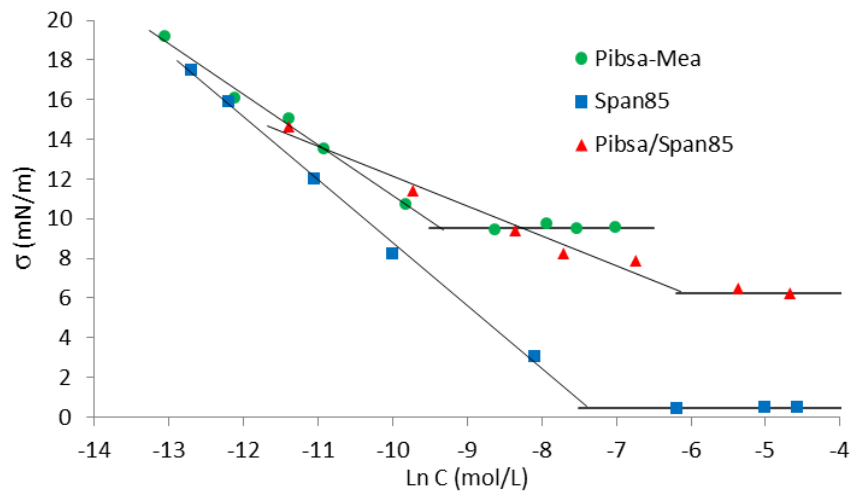


Figure B.5: Determination of CMC value of Span 85 surfactant and PIBSA-Mea/Span 85 mixture

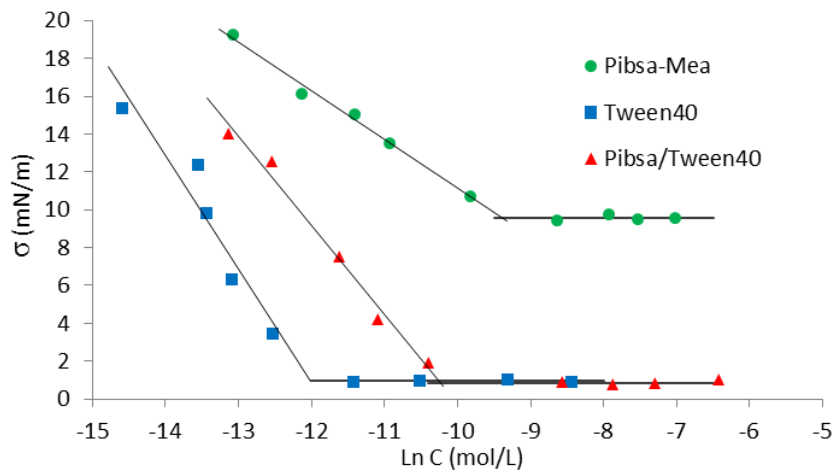


Figure B.6: Determination of CMC value of Tween 40 surfactant and PIBSA-Mea/Tween 40 mixture

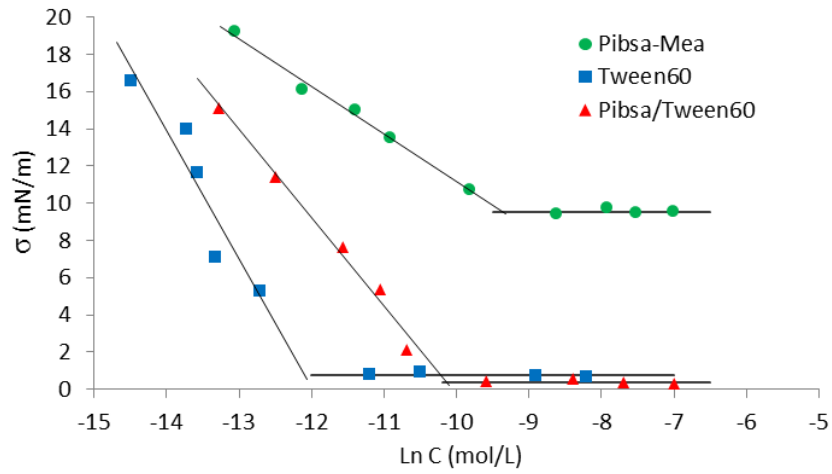


Figure B.7: Determination of CMC value of Tween 60 surfactant and PIBSA-Mea/Tween 60 mixture

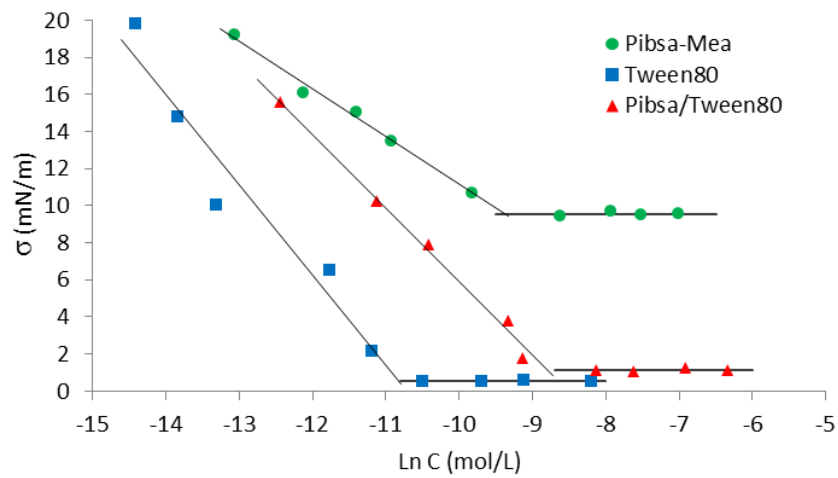


Figure B.8: Determination of CMC value of Tween 80 surfactant and PIBSA-Mea/Tween 80 mixture

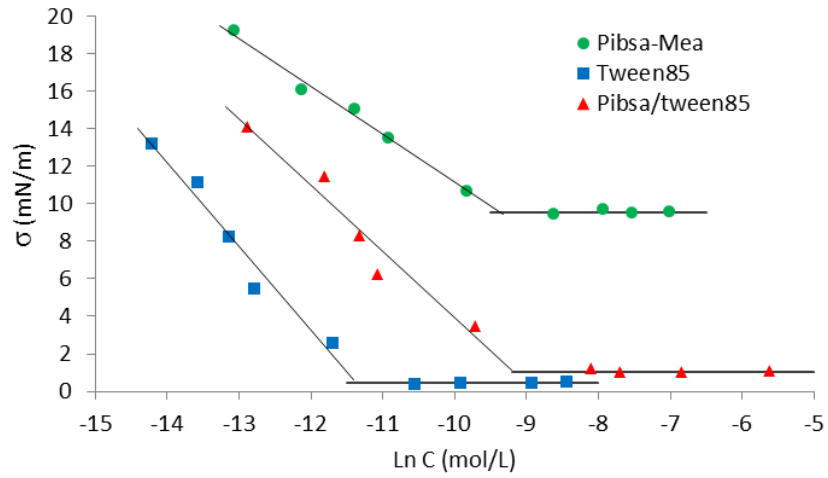


Figure B.9: Determination of CMC value of Tween 85 surfactant and PIBSA-Mea/Tween 85 mixture

APPENDIX C: EFFECT OF SURFACTANT STRUCTURE ON REFINEMENT TIME

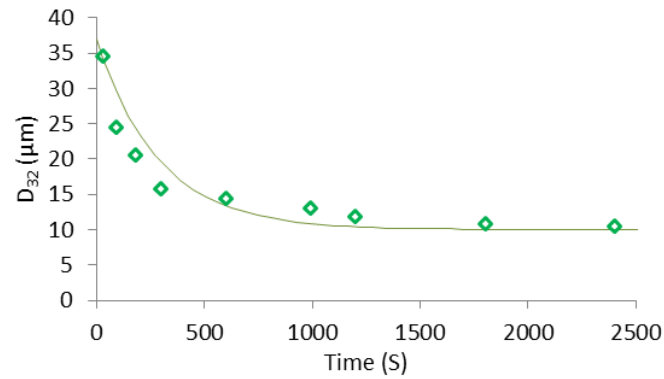


Figure C.1: Droplet size evolution as a function of refining time for the pure PIBSA-Mea emulsion (dots) fitted by model (line)

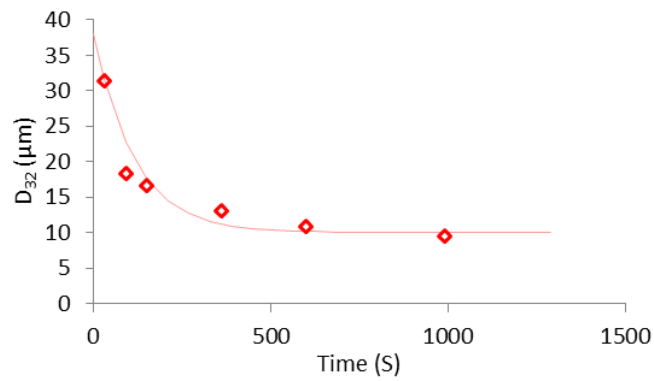


Figure C.2: Droplet size evolution as a function of refining time for the PIBSA-Mea/Span 20 emulsion (dots) fitted by model (line)

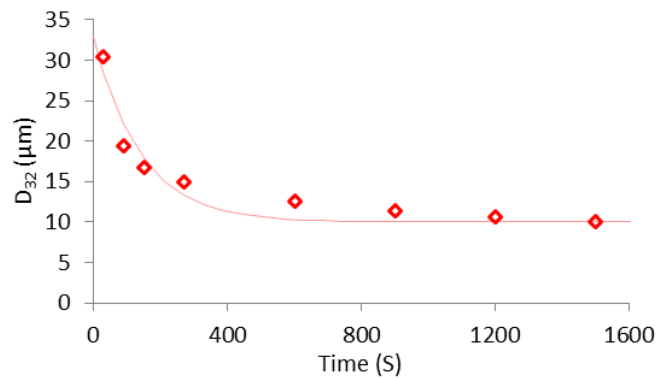


Figure C.3: Droplet size evolution as a function of refining time for the PIBSA-Mea/Span 40 emulsion (dots) fitted by model (line)

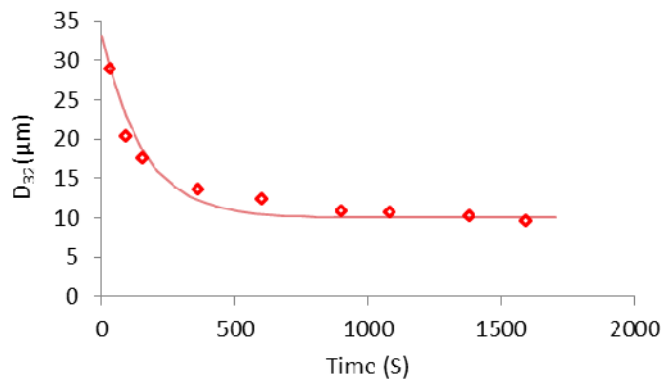


Figure C.4: Droplet size evolution as a function of refining time for the PIBSA-Mea/Span 60 emulsion (dots) fitted by model (line)

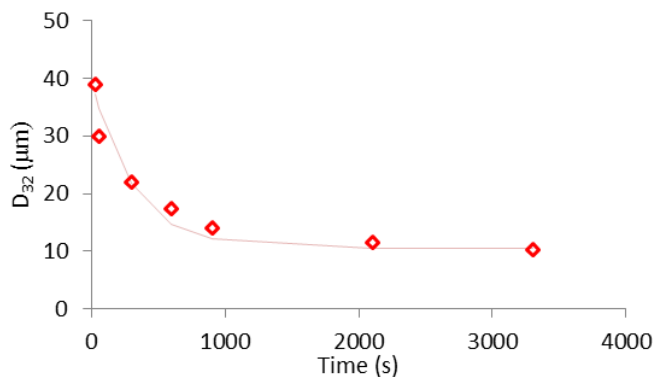


Figure C.5: Droplet size evolution as a function of refining time for the PIBSA-Mea/Span 85 emulsion (dots) fitted by model (line)

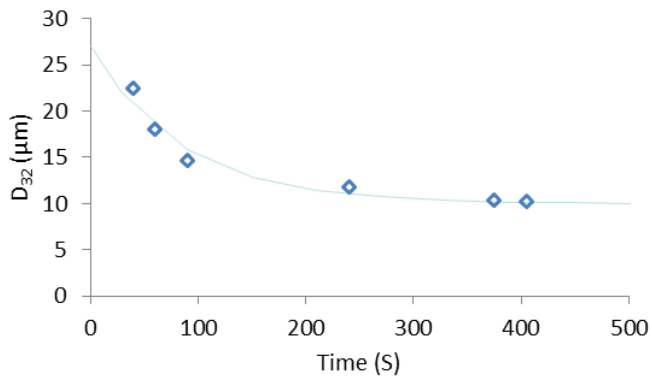


Figure C.6: Droplet size evolution as a function of refining time for the PIBSA-Mea/Tween 20 emulsion (dots) fitted by model (line)

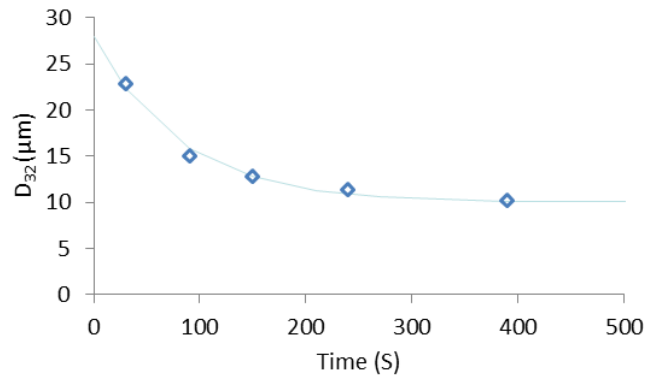


Figure C.7: Droplet size evolution as a function of refining time for the PIBSA-Mea/Tween 40 emulsion (dots) fitted by model (line)

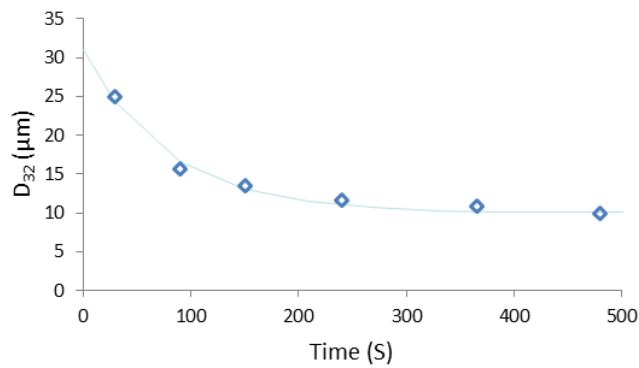


Figure C.8: Droplet size evolution as a function of refining time for the PIBSA-Mea/Tween 60 emulsion (dots) fitted by model (line)

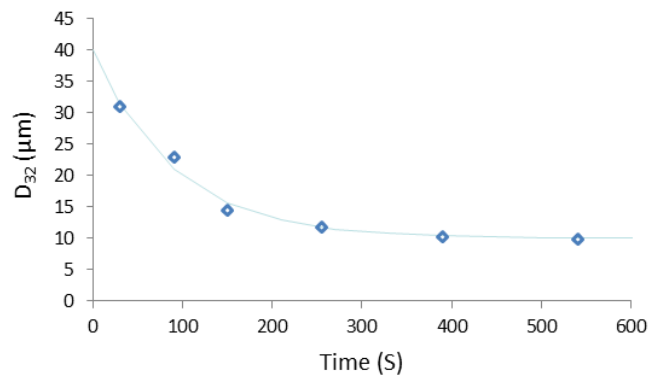


Figure C.9: Droplet size evolution as a function of refining time for the PIBSA-Mea/Tween 80 emulsion (dots) fitted by model (line)

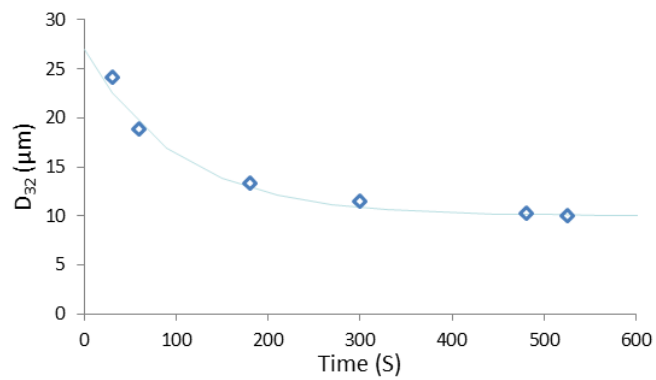


Figure C.10: Droplet size evolution as a function of refining time for the PIBSA-Mea/Tween 85 emulsion (dots) fitted by model (line)

APPENDIX D: EFFECT OF SURFACTANT STRUCTURE ON RHEOLOGICAL PROPERTIES OF THE EMULSIONS

Determination of yield stress of the fresh emulsions using Foudazi model

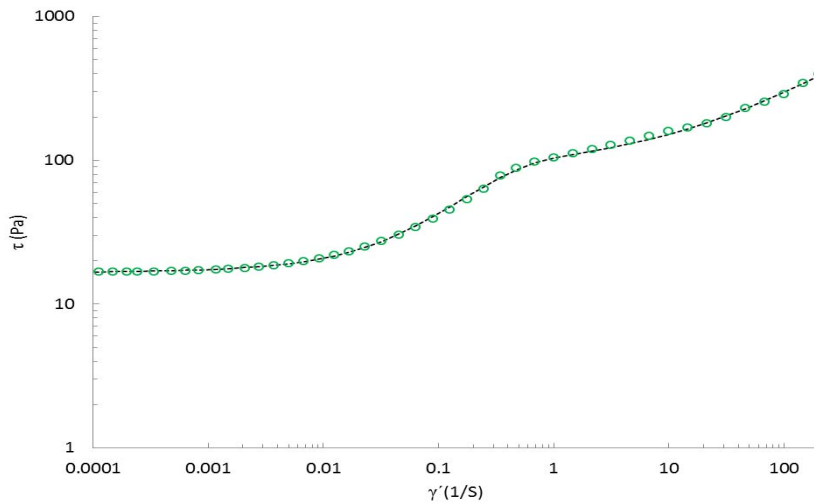


Figure D.1: Fittings of Foudazi model (dash) on the flow curve of the PIBSA-Mea stabilised emulsion (dots)

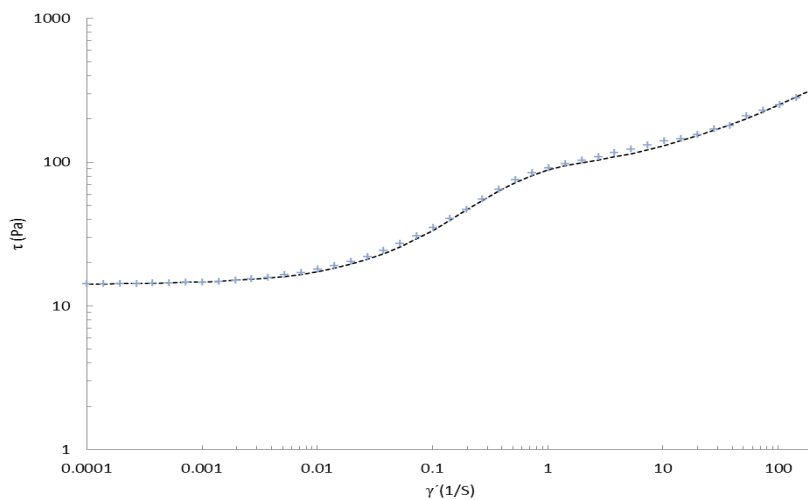


Figure D.2: Fittings of Foudazi model (dash) on the flow curve of the PIBSA-Mea/Span 40 stabilised emulsion (dots)

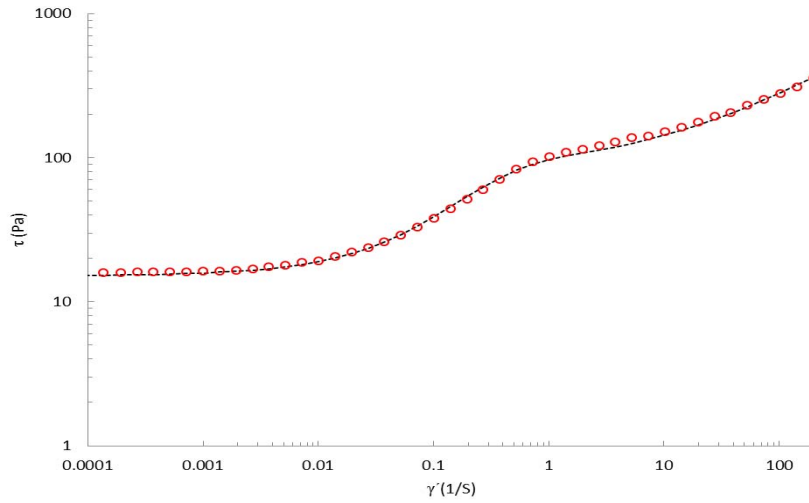


Figure D.3: Fittings of Foudazi model (dash) on the flow curve of the PIBSA-Mea/Span 60 stabilised emulsion (dots)

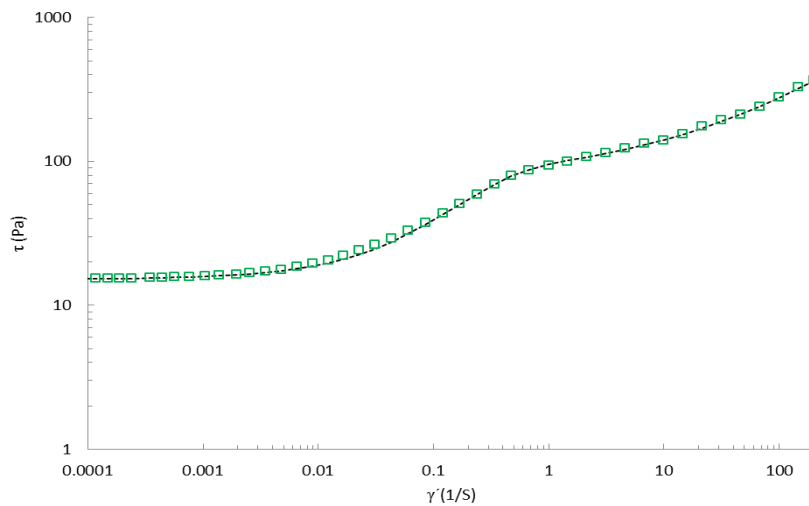


Figure D.4: Fittings of Foudazi model (dash) on the flow curve of the PIBSA-Mea/Span 80 stabilised emulsion (dots)

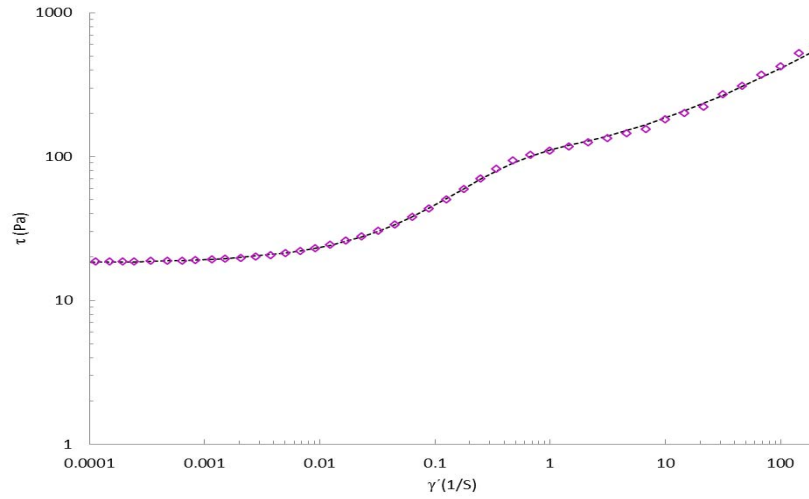


Figure D.5: Fittings of Foudazi model (dash) on the flow curve of the PIBSA-Mea/Span 85 stabilised emulsion (dots)

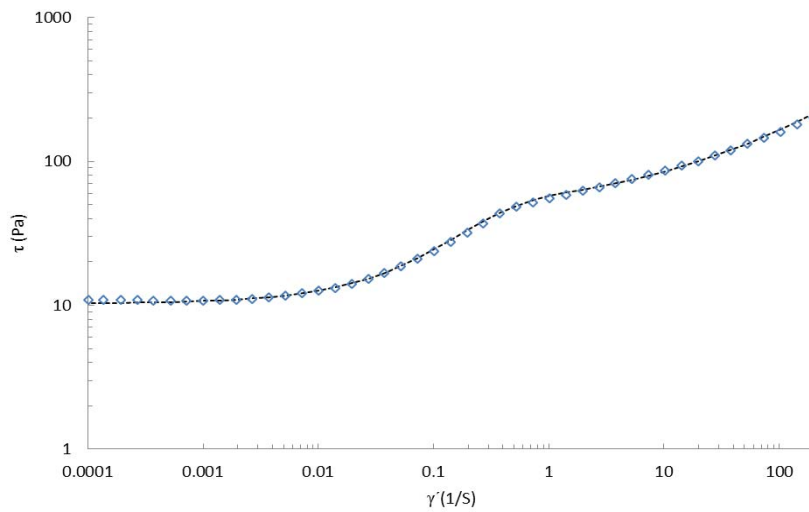


Figure D.6: Fittings of Foudazi model (dash) on the flow curve of the PIBSA-Mea/Tween 40 stabilised emulsion (dots)

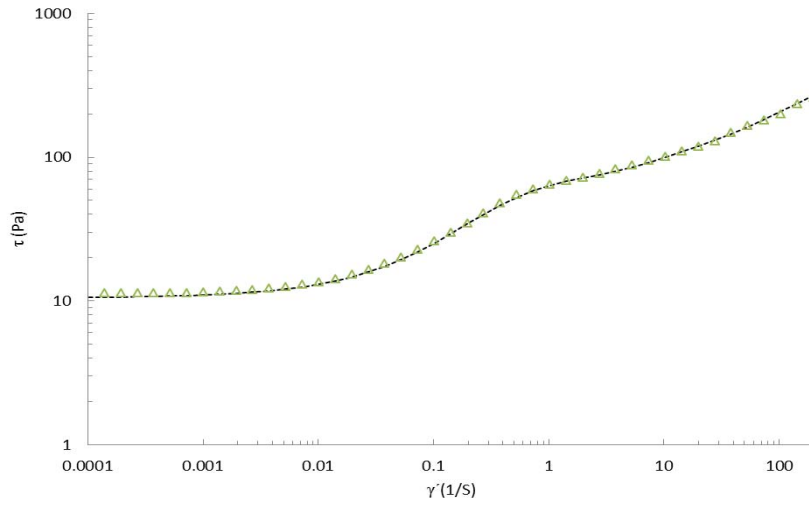


Figure D.7: Fittings of Foudazi model (dash) on the flow curve of the PIBSA-Mea/Tween 60 stabilised emulsion (dots)

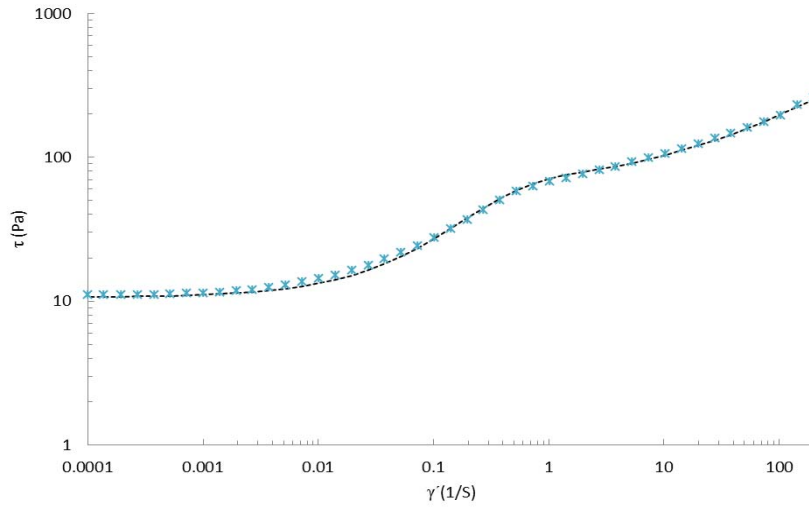


Figure D.8: Fittings of Foudazi model (dash) on the flow curve of the PIBSA-Mea/Tween 80 stabilised emulsion (dots)

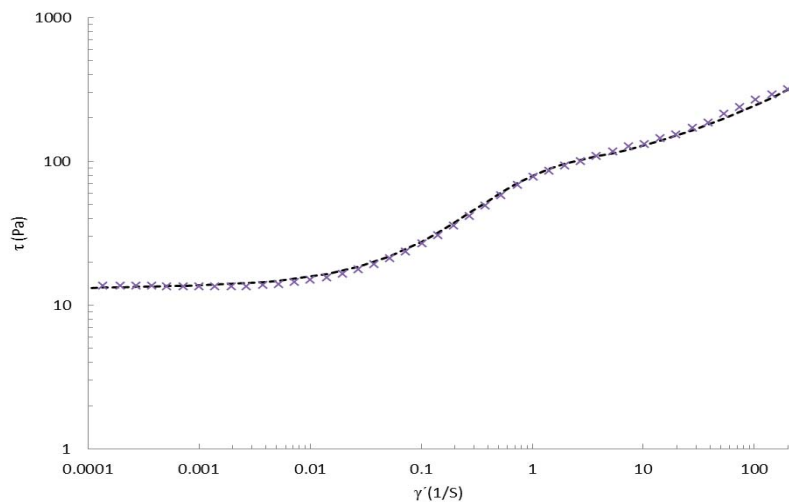


Figure D.9: Fittings of Foudazi model (dash) on the flow curve of the PIBSA-Mea/Tween 85 stabilised emulsion (dots)

Viscoelasticity

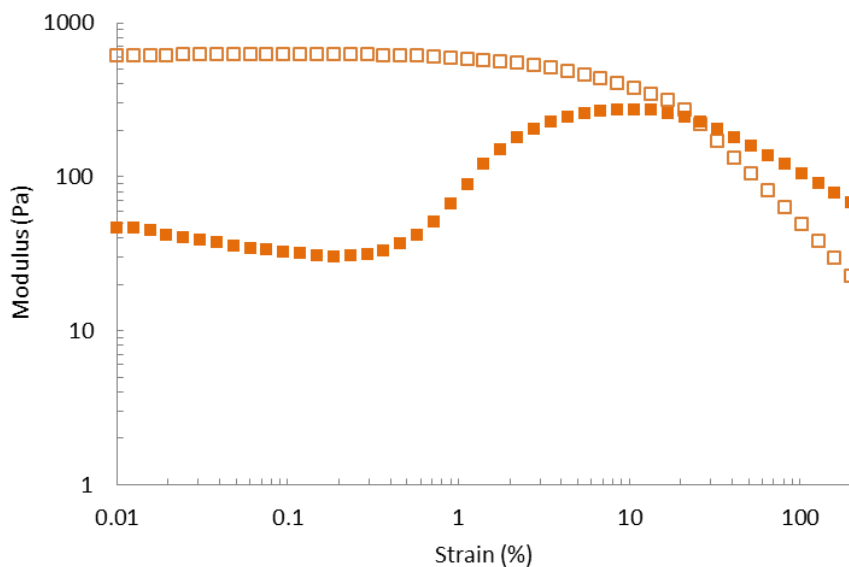


Figure D.10: Storage modulus (open) and loss modulus (filled) of the PIBSA-Mea/Span 20 emulsion

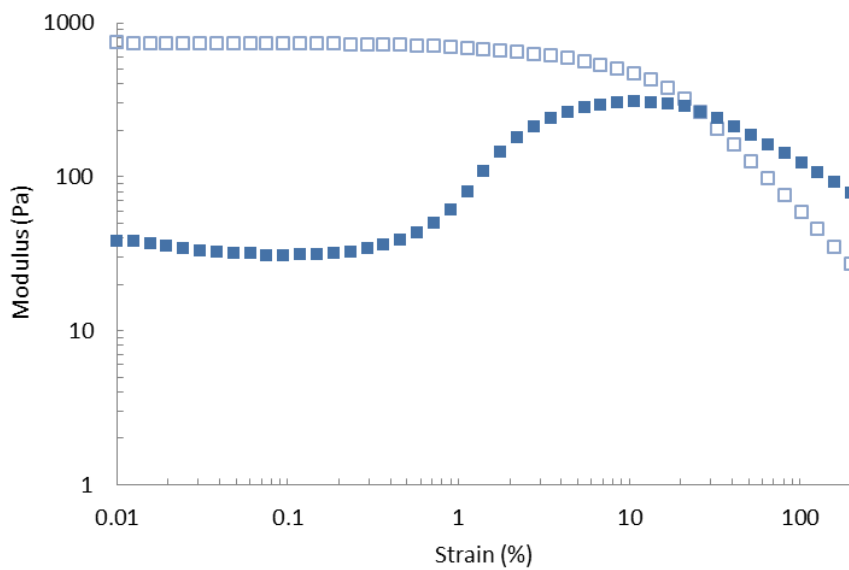


Figure D.11: Storage modulus (open) and loss modulus (filled) of the PIBSA-Mea/Span 40 emulsion

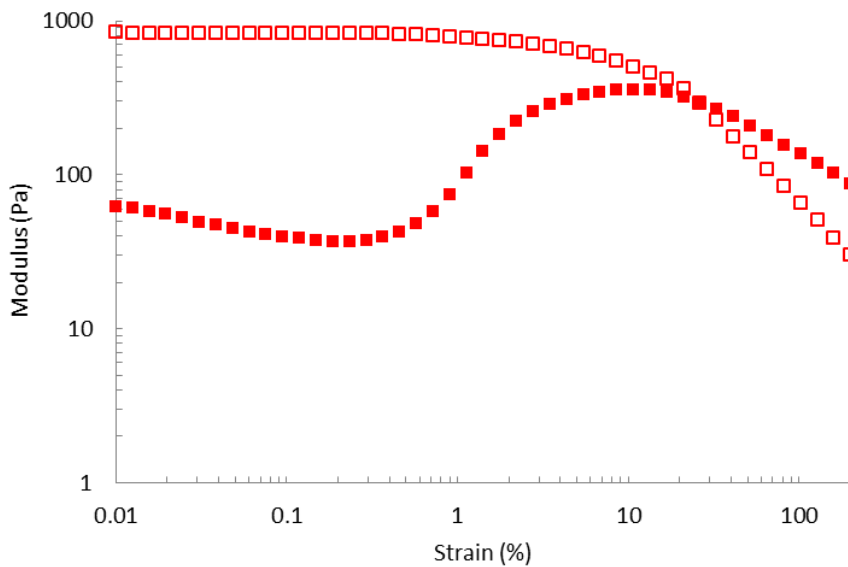


Figure D.12: Storage modulus (open) and loss modulus (filled) of the PIBSA-Mea/Span 60 emulsion

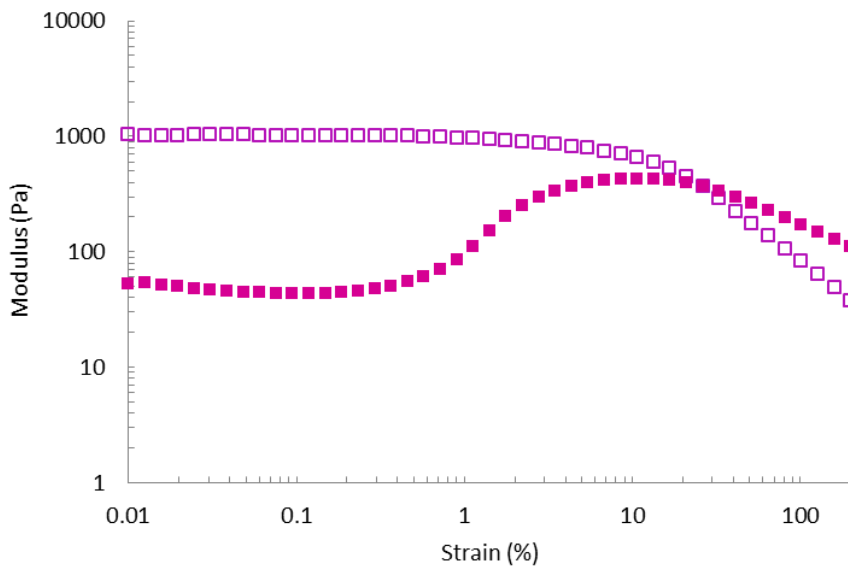


Figure D.13: Storage modulus (open) and loss modulus (filled) of the PIBSA-Mea/Span 85 emulsion

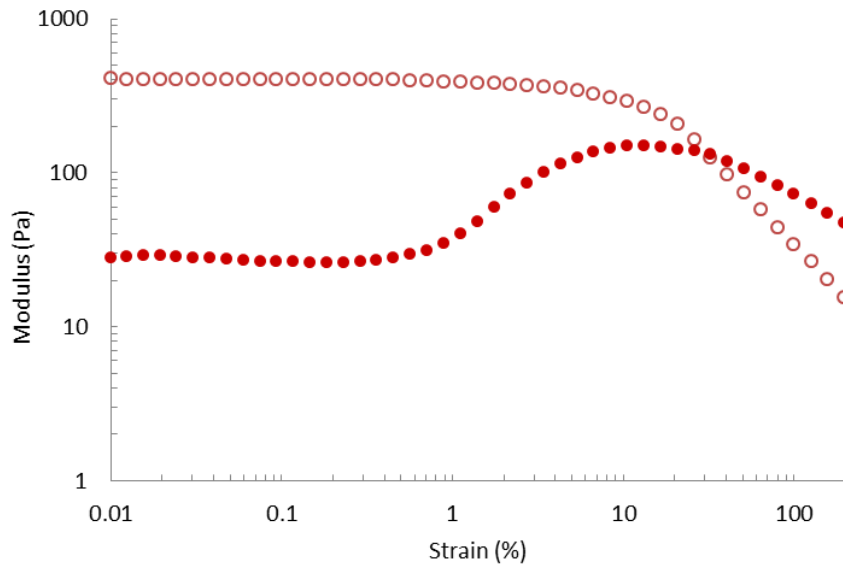


Figure D.14: Storage modulus (open) and loss modulus (filled) of the PIBSA-Mea/Tween 20 emulsion

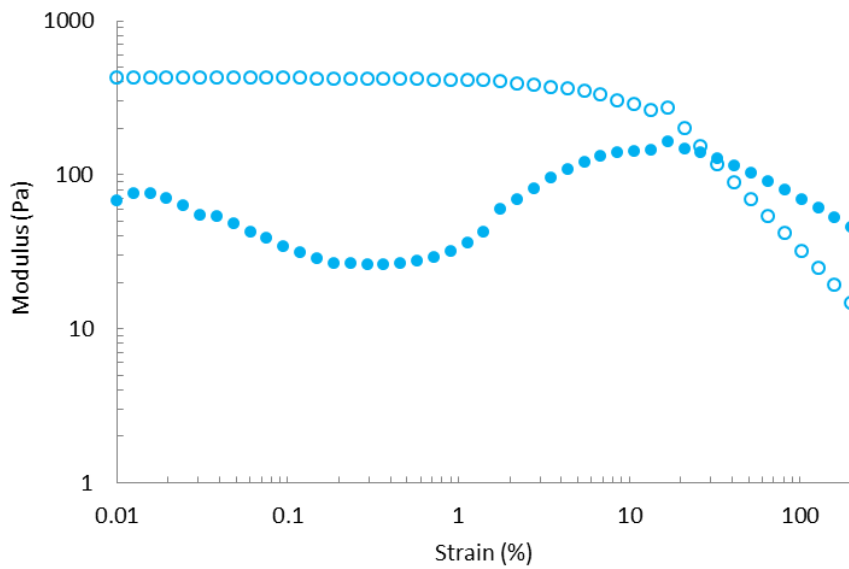


Figure D.15: Storage modulus (open) and loss modulus (filled) of the PIBSA-Mea/Tween 40 emulsion

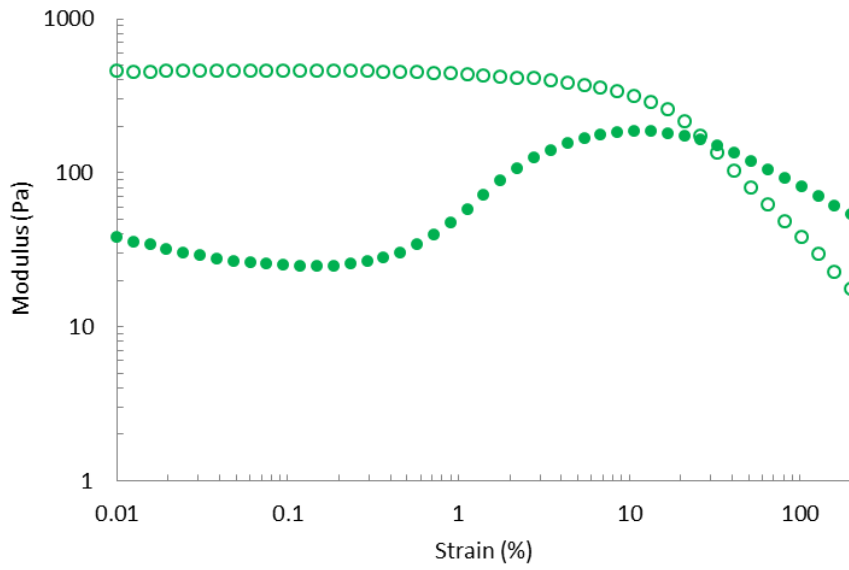


Figure D.16: Storage modulus (open) and loss modulus (filled) of the PIBSA-Mea/Tween 60 emulsion

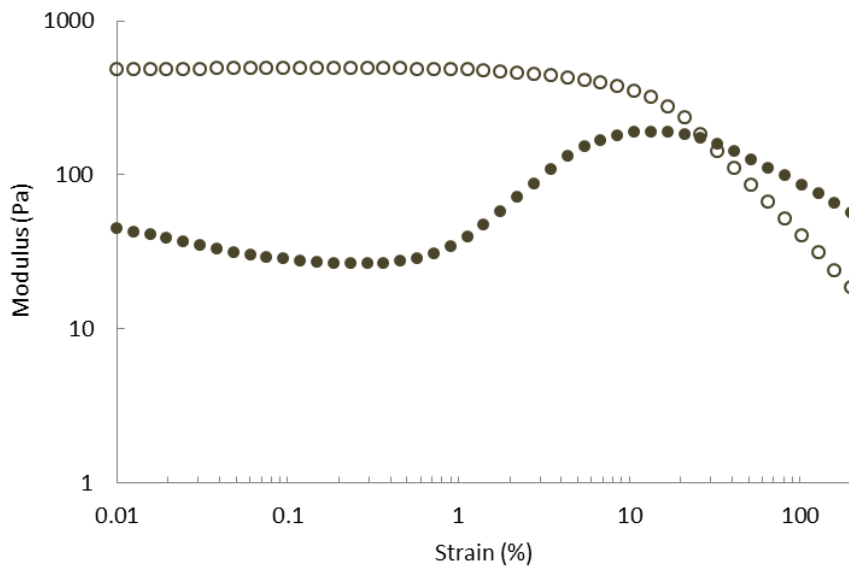


Figure D.17: Storage modulus (open) and loss modulus (filled) of the PIBSA-Mea/Tween 85 emulsion

APPENDIX E: EFFECT OF SURFACTANT STRUCTURE ON SHERA STABILITY OF THE EMULSIONS UNDER HIGH SHEAR CONDITION

Droplet size distribution (DSD) as a function of pumping cycles (NP)

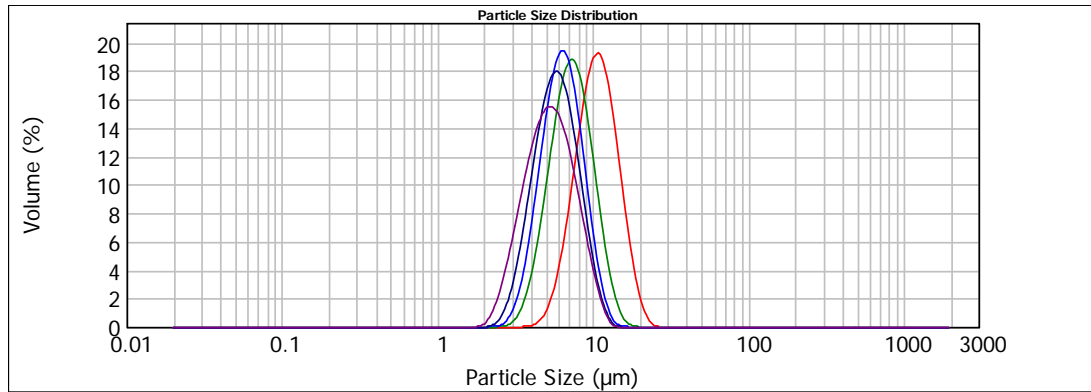


Figure E.1: Droplet size distributions of PIBSA-Mea/Span 40 emulsion under 0 (red), 3 (green), 5 (blue), 7 (navy), 10 (violet) pumping cycles

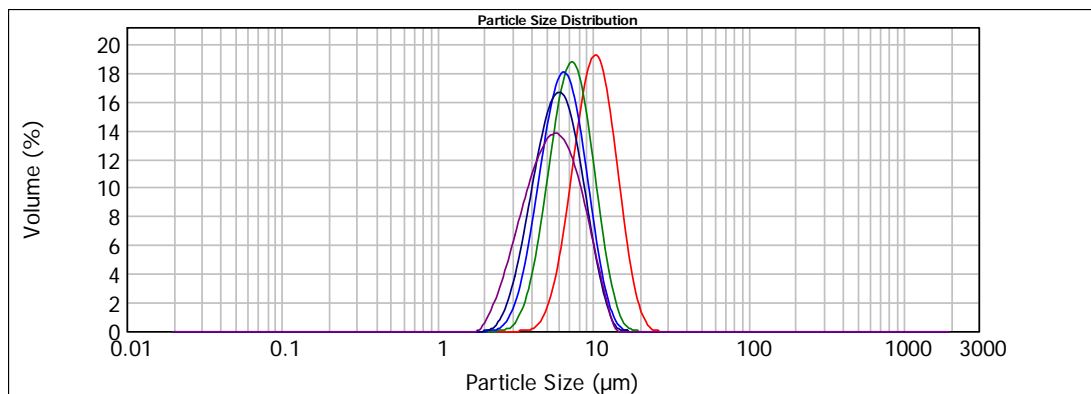


Figure E.2: Droplet size distributions of PIBSA-Mea/Span 60 emulsion under 0 (red), 3 (green), 5 (blue), 7 (navy), 10 (violet) pumping cycles

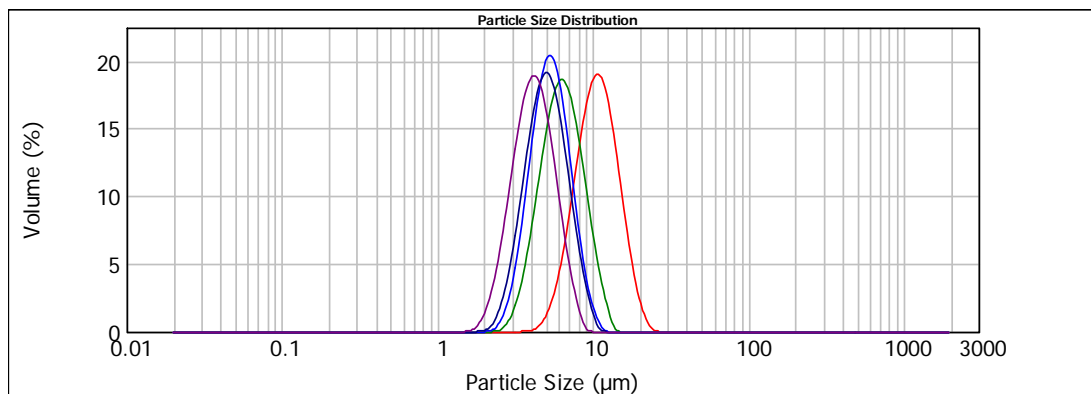


Figure E.3: Droplet size distributions of PIBSA-Mea/Span 80 emulsion under 0 (red), 3 (green), 5 (blue), 7 (navy), 10 (violet) pumping cycles

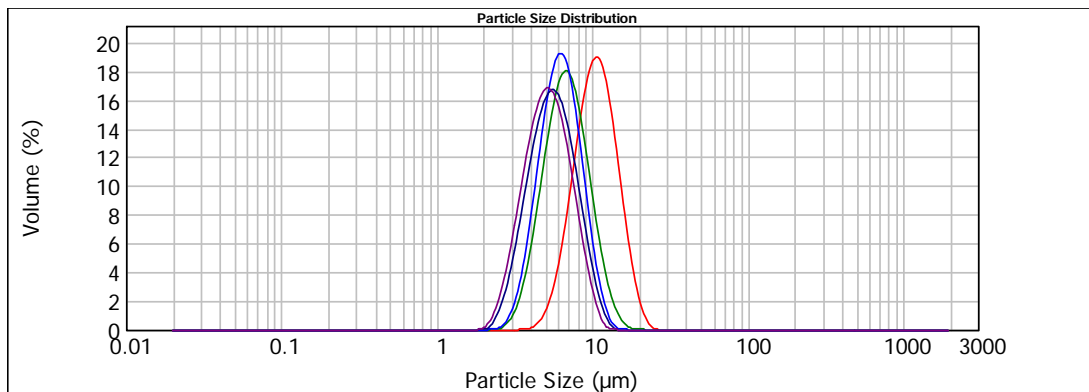


Figure E.4: Droplet size distributions of PIBSA-Mea/Tween 20 emulsion under 0 (red), 3 (green), 5 (blue), 7 (navy), 10 (violet) pumping cycles

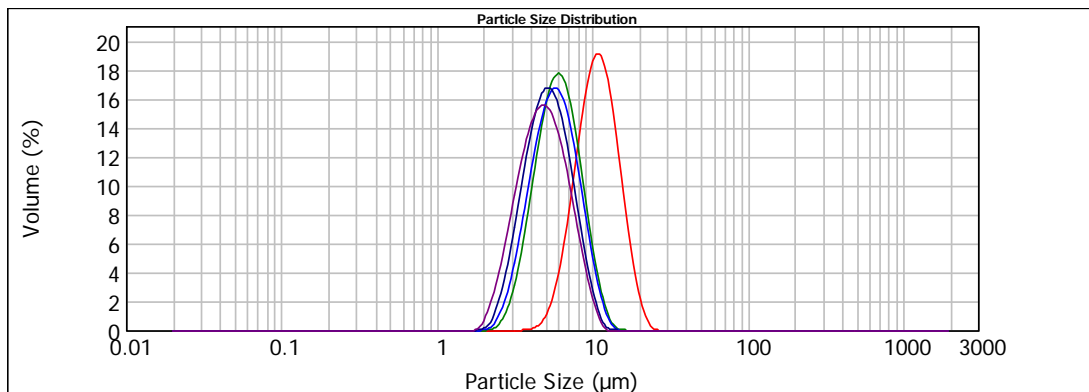


Figure E.5: Droplet size distributions of PIBSA-Mea/Tween 40 emulsion under 0 (red), 3 (green), 5 (blue), 7 (navy), 10 (violet) pumping cycles

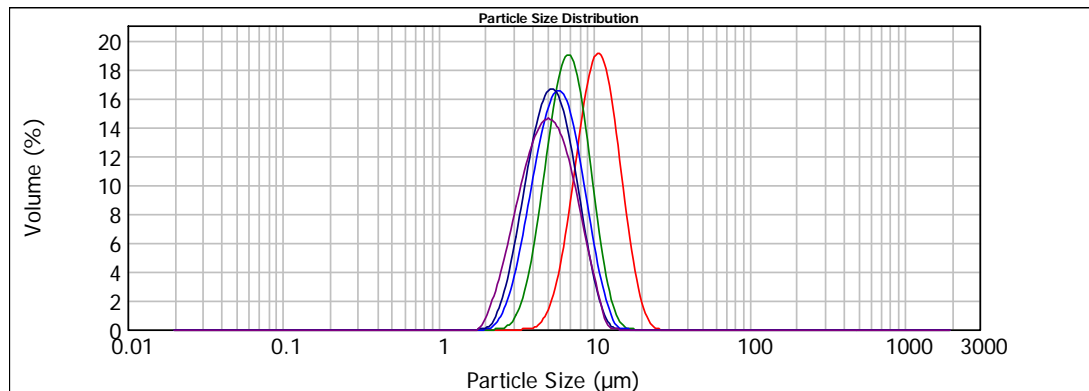


Figure E.6: Droplet size distributions of PIBSA-Mea/Tween 60 emulsion under 0 (red), 3 (green), 5 (blue), 7 (navy), 10 (violet) pumping cycles

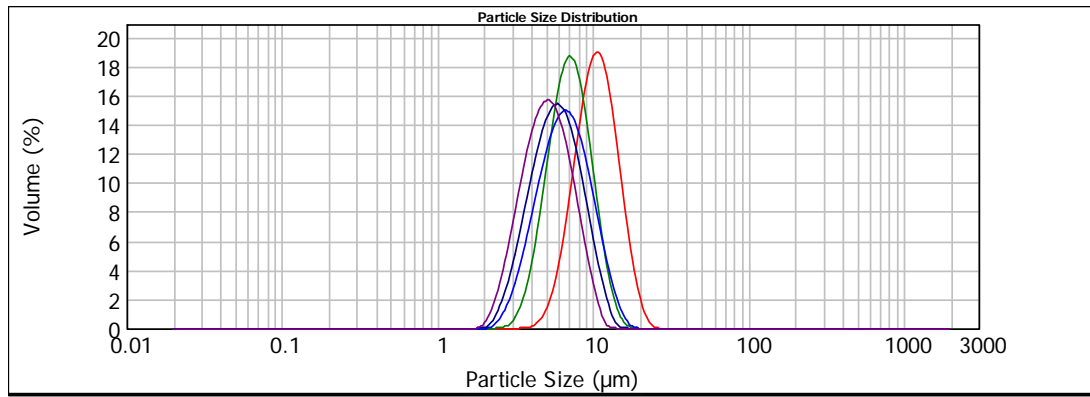


Figure E.7: Droplet size distributions of PIBSA-Mea/Tween 80 emulsion under 0 (red), 3 (green), 5 (blue), 7 (navy), 10 (violet) pumping cycles

Evolution of droplet size under high shear (pumping) with pumping cycles (NP)

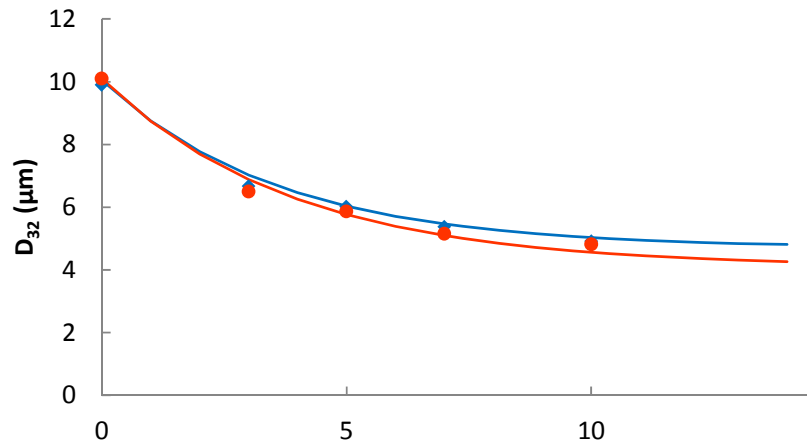


Figure E.8: Droplet size evolution as a function of pumping cycles for the PIBSA-Mea/Span 20 emulsion (orange circle) fitted by model (orange line) and the PIBSA-Mea/Tween 20 emulsion (blue square) fitted by model (blue line)

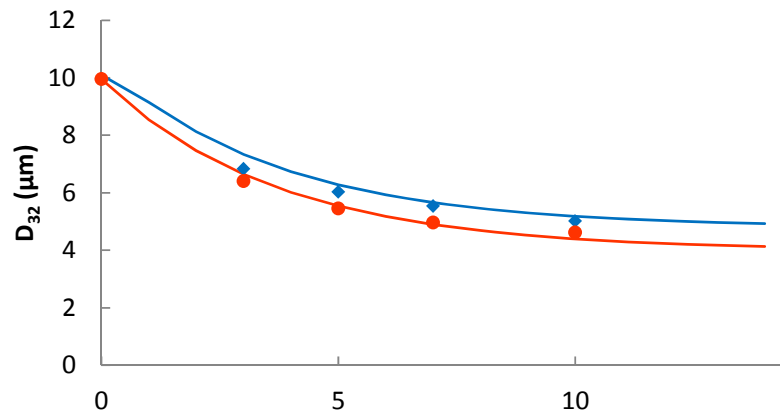


Figure E.9: Droplet size evolution as a function of pumping cycles for the PIBSA-Mea/Span 60 emulsion (orange circle) fitted by model (orange line) and the PIBSA-Mea/Tween 60 emulsion (blue square) fitted by model (blue line)

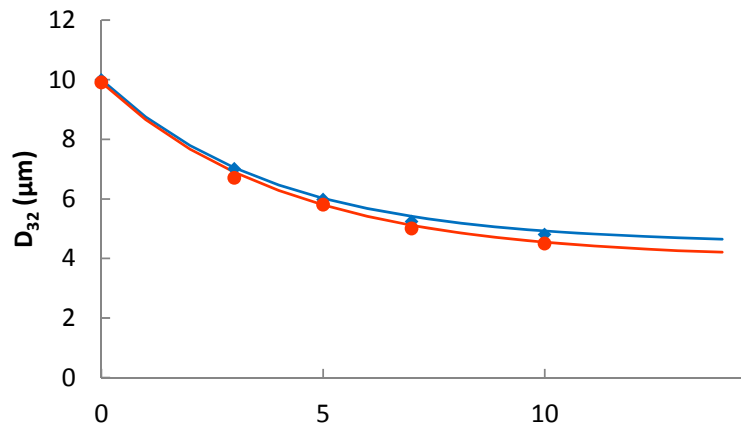


Figure E.10: Droplet size evolution as a function of pumping cycles for the PIBSA-Mea/Span 80 emulsion (orange circle) fitted by model (orange line) and the PIBSA-Mea/Tween 80 emulsion (blue square) fitted by model (blue line)